THE UNIVERSITY
of EDINBURGH

Defining and exploiting the developmental origin of MLL-AF4-driven infant Acute Lymphoblastic Leukaemia

Vasiliki Symeonidou

Doctor of Philosophy

The University of Edinburgh

2019

Declaration

I declare that this thesis was composed by myself that the work contained herein is my own except where otherwise stated in the text, and that this work has not been submitted for any other degree or professional qualification except as specified.

Vasiliki Symeonidou
Edinburgh, December 2019

Acknowledgements

I would like to thank my supervisor Prof. Katrin Ottersbach for giving me the opportunity to do a Ph.D. in her lab and for her support; what a great journey this has been! I would also like to thank my Ph.D. committee, Profs Kamil Kranc, Lesley Forrester and Keisuke Kaji. Dr. Simon Tomlinson and his group as well as Dr. Stephen Clegg for their support during my first steps in the Bioinformatics arena. I would like to thank Dr. Andrew Finch for performing the lipidomics experiments, analysing the accompanied data and helpful discussions. I would also like to thank the SCRM flow cytometry team - Fiona Rossi, Clare Cryer, Andrea Corsinotti and Bindy Heer - many times they have gone out of their way to help and support me and for this I am most grateful. I would also to thank Dr. Linh My Huynh for help with the cloning aspects of my work and Benedetta Carbone for her support for the CRISPR-Cas9 work. I would also like to thank Prof. Pablo Menendez for giving me the opportunity to spend time in his lab and learning from their experience, following from this I would like to thank Drs Talia Velasco and Clara Bueno for their help with the human foetal liver transduction experiments and MLL-AF4 lentiviral particles production.

Abstract

Infant MLL-AF4-driven pro-B Acute Lymphoblastic Leukaemia (ALL) is the most common leukaemia in infants. This devastating disease, which arises *in utero*, renders the infant patients with an aggressive disease and with a 5-year survival rate of less than 50%. It has long been speculated that along with the fusion protein, the foetal origin of the disease is one of the main contributing factors to its aggressive nature. The first aim of this work was to identify if and how this was the case. Towards this end, multiple RNA sequencing experiments were performed comparing foetal and neonatal/adult populations in both humans and mice. This allowed for the identification of the transcriptional differences between foetal and neonatal/adult cells. The results showed that the foetal derived cells were characterised by a proliferative and oncogenic nature whereas neonatal/adult cells had a mature and immune cell-like profile. From this it can be concluded that the foetal nature of the leukaemia-initiating cell could support the aggressive nature of the infant disease.

To address the question of whether the foetal characteristics were maintained in the transcriptome of the blasts, the transcriptional profile of the foetal cells was compared to that of blasts derived from infant patients. Interestingly, there was a large commonality between the two. To further investigate whether the common genes were critical for the disease, 21 were selected and functional assays performed using the SEM cell line. With this approach, several genes were identified deletion of which had a tremendous impact on the survival of the SEM cells. The genes that were shown to be critical for the SEM cells included *PLK1*, *BUB1B*, *HSPD1*, *ELOVL1*, *CCNB1*, *NUTF2* and *TPX2*. Of particular interest was *PLK1* because there is an inhibitor (Volasertib) available that is currently in phase III clinical trials. Inhibition of PLK1 using Volasertib in the SEM cells resulted in cell cycle arrest, which led to apoptosis. Another gene of interest was *ELOVL1*, because its knockout effect appears to be unique to the infant disease. Knockout of *ELOVL1* in SEM resulted in apoptosis and

investigation into the lipidome of the knockout cells identified a dramatic decrease in lipids that contain very long fatty acid chains. Additionally, using overexpression assays, *DACH1* was shown to decrease the proliferation potential of the SEM cells. From this data it can be concluded that the foetal origin of the disease could be used as a means to identify novel therapeutic targets.

A further aim of this work was to investigate and understand the early disease stages. For this, an additional RNA sequencing experiment was performed. This experiment used an Mll-AF4 expressing mouse model to characterise the transcriptional profile of a pre-leukemic population. Of particular interest was *Skida1* which was shown to be upregulated in the Mll-AF4 expressing cells. Intriguingly, *SKIDA1* was also upregulated in the blasts of infants with MLL-AF4 driven ALL compared to blasts derived from paediatric patients with the same disease and healthy controls. Interestingly, *Skida1* belongs to the same family of proteins as *DACH1*. Intriguingly, while *SKIDA1* was upregulated in the infant patients, *DACH1* was not expressed at all. These findings suggest that this family of proteins could play an important role for the infant disease.

This has been a proof of concept study where it was shown that by defining the transcriptome of the cell of origin of the disease and by identifying early molecular aberration caused by MLL-AF4 it was possible to identify novel disease targets.

Lay Summary

Leukaemia is a cancer of the blood and like the majority of cancers it is caused by mutations. Typically, an accumulation of multiple mutations is required for the leukaemia to develop which leads to the production of abnormal cancer cells called blasts. In general, it takes time for an individual cancer or leukaemia to develop and therefore these diseases are predominantly associated with aging.

Unfortunately, there is a unique set of leukaemias that run a different course and these type of leukaemias affect infants. These leukaemias are caused by a single very potent mutation where one part of one gene (called MLL) breaks and fuses with part of another gene (AF4). The leukaemias that arise by such events are called MLL-AF4-driven and occur while the infant is still in their mother's womb (*in utero*). Unfortunately, infants with this disease have an extremely poor prognosis because the disease is very aggressive and, owing to the fact that we do not completely understand the underling biology of this disease, there are few therapeutic targets.

It has long been speculated that the foetal origin of these types of leukaemias is what makes them unique and very different from adult leukaemias. We know that the cells of the developing embryo (foetal cells) are very different from adult cells, as they need to support the needs of a rapidly growing organism. They have acquired specific features, for example, we know that these cells divide a lot more than other cells. Although, we do have some knowledge of how these cells are different, we still do not have the complete picture. The first aim of this work was to investigate how foetal cells are different from adult ones. Interestingly, it was observed that the foetal cells not only divide a lot more than adult cells but also that they have a very oncogenic nature. This oncogenic nature can form a supportive environment for the initial mutation to flourish and lead to this aggressive infant disease.

Having identified these unique features of the foetal cells, the next step was to ensure that they are present in the blasts of the infant patients. Interestingly, some of them were, indeed, present suggesting that this environment seems to play a role not only in the disease initiation but also in its maintenance. To ensure that this was true, experiments were performed where the specific features were removed from the cells. This was achieved by removing a gene from a model of the infant disease. With this approach, it was observed that the removal of some of these features had a tremendous impact on the disease, as it dramatically decreased the survival of the disease model cells. Intriguingly, none of these features have been associated with the infant disease prior to this study.

In summary, this study was able to define the foetal nature of the leukaemia initiating cells thereby adding to our comprehension of the underlying biology of this unique disease. Additionally, features were identified in the blasts of infant patients that were residue of the foetal cell of origin of the disease and removal of these features in a disease model resulted in a tremendous decrease in the survival of those cells. Therefore, this study serves to present a new approach for the identification of novel therapeutic targets for infant patients with MLL-AF4 driven acute leukaemia.

Abbreviations

ALL	Acute Lymphoblastic Leukaemia
alphaMEM	Minimum Essential Medium Eagle - Alpha Modification
AML	Acute Myeloid Leukaemia
BCR	Breakpoint cluster region
BFP	Blue fluorescent protein
BM	Bone marrow
CAR-T	chimeric antigen receptor T-cell
Cas9	CRISPR associated protein 9
CLP	Common lymphoid progenitor
CMP	Common myeloid progenitor
CNS	Central nervous system
CRISPR	clustered regularly interspaced short palindromic repeats
DE	Differentially expressed
DMEM	Dulbecco's Modified Eagle Medium
DMSO	Dimethyl sulfoxide
DNA	Deoxyribonucleic acid
DS	Double stranded
E	Embryonic day

EB	Elution buffer
EDTA	Ethylenediaminetetraacetic acid
ELOVL	Elongation of very long chain fatty acids
EtOH	Ethanol
FACS	Fluorescent activated cell sorting
FL	Foetal liver
FLT3L	FMS-like tyrosine kinase 3 ligand
FPKM	Fragments Per Kilobase of transcript per Million
FSC	Foetal Calf Serum
GeCKO	Genome-Scale CRISPR Knock-Out
GEO	Gene expression omnibus
GFP	Green fluorescent protein
GO	Gene ontology
GSEA	Gene set enrichment analysis
hESCs	Human embryonic stem cells
HexCer	hexosyl ceramides
HSC	Haematopoietic stem cell
HSPC	Haematopoietic stem and progenitor cell
iALL	infant ALL
IL2	Interleukin 2

IL7	Interleukin 7
IMDM	Iscove's Modified Dulbecco's Media
KO	Knockout
LB	Lysogeny broth
LDAC	low dose cytarobine
LFC	Log fold change
LMPP	Lymphoid primed multipotent progenitors
LT-HSC	Long term HSC
MA4+	MLL-AF4+
MACS	Magnetic activated cell sorting
MBD	Menin biding domain
MDB	Membrane desalting buffer
MEP	Megakaryocyte erythroid progenitor
MLL	Mixed Lineage Leukaemia
MLL-R	Mixed lineage leukaemia - Rearrangement
MNC	Mononucleated cells
MPP	Multipotent progenitors
padj	Adjusted p value
pALL	paediatric ALL
PB	Base pair

PBS	Phosphate-buffered saline
PC	Post conception
PC	phosphatidylcholines
PCA	Principal component analysis
Pen/Strep	Penicillin/Streptomycin
PHD	Plant homology domain
RCR	Polymerase chain reaction
RD	Repression domain
RIN	RNA integrity number
RNA	Ribonucleic acid
RPKM	Reads Per Kilobase of transcript per Million
RPM	Rotations per minute
RPMI	Roswell Park Memorial Institute
RT-qPCR	Real-time quantitative PCR
SCF	Stem cell factor
sgRNA	single guide RNA
SM	sphingomyelin
SNL	Speckled nuclear localisation
ST HSC	Short term HSC
TG	Triglyceride

TIDE	Tracking of Indels by Decomposition
TrXG	Thrithorax
VLFAs	Very long fatty acids
WBC	White blood cells

Contents

List of figures

List of tables

Chapter 1 Introduction

1.1 Haematopoiesis

1.1.1 Overview of haematopoiesis

Blood is a fascinating tissue. In homeostasis, it comprises a plethora of different cell types that establish innate and acquired immunity, haemostasis and oxygen transport. This beautifully synchronised cell production machinery depends on haematopoietic stem cells (HSCs), which lie at the apex of the haematopoietic hierarchy, and their ability to self-renew and produce the entire collection of differentiated progeny.

1.1.2 Haematopoietic hierarchy

It was early in the 19th century that biologists observed under the microscope the existence of two different lineages in the bone marrow, lymphoid and myeloid. It was also at the same time, that it was speculated that those lineages share a common origin, a cell that would later become known as the haematopoietic stem cell (HSC) (Watcham et al., 2019, Doulatov et al., 2012). The existence of HSCs and their ability to give rise to all the different blood cell types was proven to be true in the seminal work of Till, McCulloch and Becker in the early 1960s (Becker et al., 1963, Till and McCulloch, 1961). They performed pioneering experiments, using repopulation assays and X-ray induced chromosomal lineage tracing, to establish that the haematopoietic system derives from multipotent HSCs rather than from multiple lineage specific/committed stem cells (Becker et al., 1963, Till and Mc, 1961). These early findings laid the foundation for the study of blood in both homeostasis and disease.

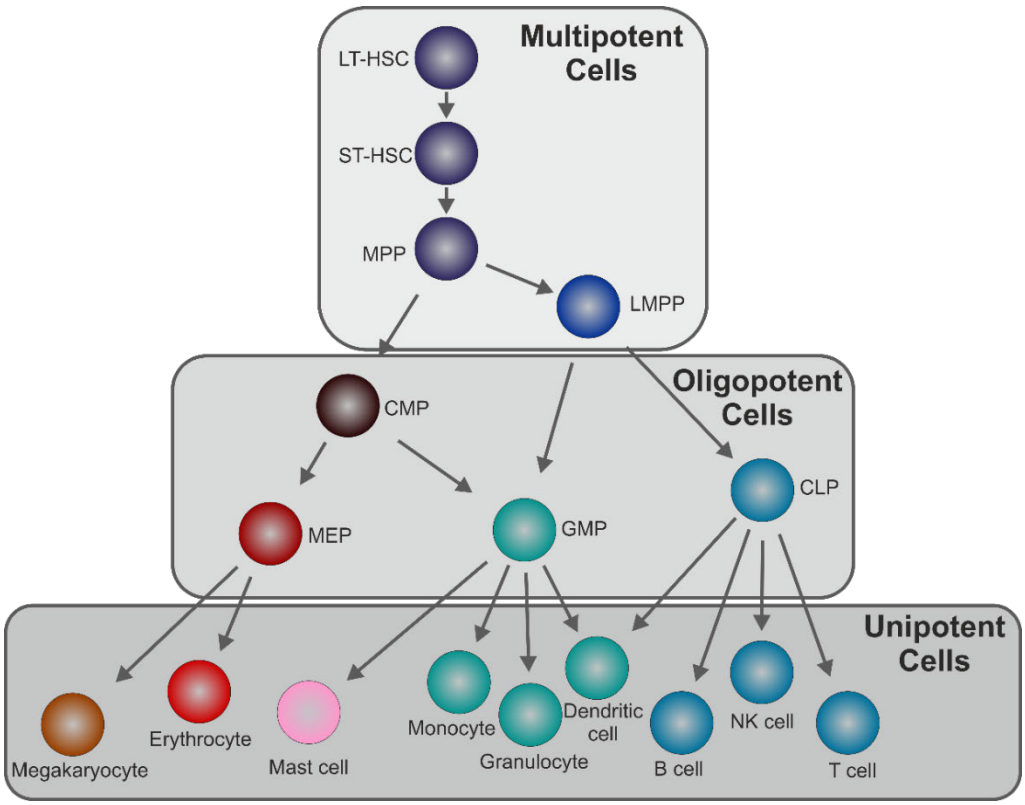

Figure 1.1| The haematopoietic hierarchy (Adapted from Watcham *et al*., 2019). The haematopoietic hierarchy depicted as a tree, where the top branch comprises multipotent cells, the middle oligopotent cells and at the bottom of the tree are located the terminally differentiated cells (unipotent cells).

The classical view of the haematopoietic hierarchy is a tree, with HSCs at the top and the terminally differentiated cells at the bottom (Fig. 1.1). In a nutshell, our lifelong blood production relies on HSCs which, on one hand, self-renew or generate daughter cells and on the other hand, undergo multi-step differentiation in order to generate all the progeny which will go on to provide the terminally differentiated cells (Doulatov et al., 2012). Although it was once thought to be a relative uniform population, we now know that the HSC pool is highly heterogeneous (Laurenti and Gottgens, 2018). This heterogeneity is attributed to variation in the self-renewal and differentiation properties of HSCs (Laurenti and Gottgens, 2018). Self-renewal is assessed by the repopulation potential of the cells in irradiated recipients. In line with this, long-term HSCs (LT-HSCs) have the highest repopulation potential, which equates to a successful primary and secondary transplantation (Jordan and Lemischka,

1990, Dykstra et al., 2007). HSCs that can give rise to all the cells in the haematopoietic hierarchy but with progressively shorter repopulation periods are either short-term HSCs or multipotent progenitors (MPPs) (Oguro et al., 2013, Kiel et al., 2005, Kent et al., 2009, Sieburg et al., 2006, Guenechea et al., 2001, Muller-Sieburg and Sieburg, 2006). The lymphoid-primed multipotent progenitors (LMPPs) have also been shown to have limited repopulation potential (Adolfsson et al., 2005, Boiers et al., 2013). In addition to variation in self-renewal potential, HSCs also differ in their lineage output potential. Different subgroups of HSCs show bias towards one lineage over others (Dykstra et al., 2007, Muller-Sieburg et al., 2004, Sanjuan-Pla et al., 2013, Yamamoto et al., 2013).

Lineage commitment is a multistep process where multipotent cells choose their fate in response to extracellular signals (van Galen et al., 2014, Laurenti and Gottgens, 2018). The first step in lineage commitment, which occurs in the multipotent cells, is loss of the capacity to self-renew, this can be observed in MPPs and LMPPs (Morrison et al., 1997, Adolfsson et al., 2005). While MPPs have the capacity to differentiate towards all the lineages, LMPPs lack the ability to generate erythrocytes and megakaryocytes. Both these populations possess only transient repopulation capacity in mice (Morrison et al., 1997, Adolfsson et al., 2005). Oligopotent cells such as common myeloid progenitors (CMPs), granulocyte-monocyte progenitors (GMPs), common myeloid progenitors (CMPs) and megakaryocyte-erythroid progenitors (MEPs) will further commit to produce the terminally differentiated and mature cells, which are unipotent. The mechanism by which cell fate decisions are executed involves a cascade of activation/de-activation of transcriptional and epigenetic regulators. This cascade is initiated by extracellular signals dictating cell fate choices and it is thought to occur as early as within the HSC compartment (Lee et al., 2017, Laurenti and Gottgens, 2018)

1.1.3 Ontogeny of the haematopoietic system

Ontogeny of the haematopoietic system begins in the developing embryo and is highly conserved, though not identical, in vertebrates. As the anatomy of the developing embryo changes, different anatomical sites are employed in the establishment of the haematopoietic system. The use of multiple sites for foetal haematopoiesis is highly conserved. In both humans and mice, developmental haematopoiesis occurs in two waves, a first primitive and a second definite.

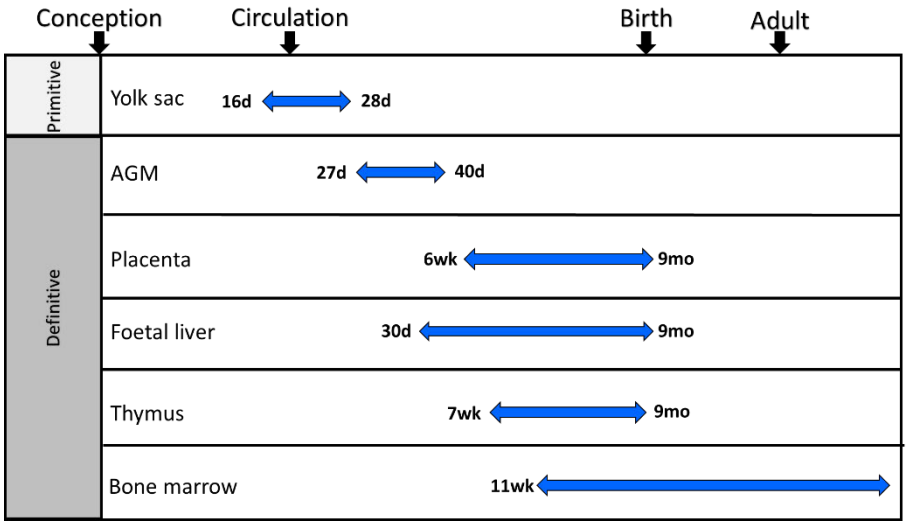

Figure 1.2 | Ontogeny of the human haematopoietic system (Adapted from Rowe *et al*., 2016). Ontogeny of the human haematopoietic system is a multi-step process that occurs in multiple anatomical sites, including the yolk sac, AGM, placenta, foetal liver, thymus and bone marrow.

The first transient wave of haematopoiesis originates outside the embryo in the yolk sac. In humans, this occurs around 16-18 days post conception (pc) with the appearance of large primitive nucleated erythrocytes and some occasional primitive macrophages and megakaryocytes (Fukuda, 1973, Luckett, 1978, Oberlin et al., 2002). Initiation of the second and definitive wave is marked by the appearance of intra-aortic haematopoietic clusters on the ventral wall of the aorta within the aorta-gonad-mesonephros (AGM) region around day 27 pc (Tavian et al., 1996, Tavian et al., 1999). It was in the AGM

and in particular, in the dorsal aorta where the first definitive HSCs/progenitors were isolated. The first CD34+CD45+ cells emerge in the pre-umbilical region of the dorsal aorta and by day 33 pc they reach several hundred (Marshall et al., 1999, Ivanovs et al., 2011, Ivanovs et al., 2017). As blood circulation has been established by this point (21 days pc), the next step in the haematopoietic ontogeny is the establishment of foetal liver haematopoiesis. In the liver around 27-29 days pc Tavian *et al.* observed seeding of growing numbers of CD34+CD45+ cells (Tavian et al., 1999). Recently, Oberlin *et al.* identified the existence of two phenotypically and functionally different HSCs in the human foetal liver embryo, one being more primitive than the other. Interestingly, the more primitive population exhibited a greater capacity for self-renewal, proliferation and differentiation (Oberlin et al., 2010). Liver colonisation occurs 30-33 days after conception (Migliaccio et al., 1986). It is speculated, that the liver remains the predominant niche where HSC expansion and differentiation takes place until birth after which the bone marrow (BM) takes over (Charbord et al., 1996). In addition, stem and progenitor cells have also been identified in the placenta following 9 weeks of gestation (Robin et al., 2009, Muench et al., 2017). In a recent study, it was shown that even though B-lymphopoiesis takes places in both the foetal liver and bone marrow; it is in the foetal bone marrow that B-progenitors predominantly expand. In addition, they identified a Pro B progenitor which was defined as CD34+CD10-CD19 which has not been identified in adult bone marrow (O'Byrne et al., 2019).

Colonisation of the BM with HSCs and progenitor cells marks the end of the embryonic period. This is closely associated with the development of the BM niche. The BM niche can only be established following osteogenesis and vascularisation of the bones, which allows for the seeding of the BM with HSCs and haematopoietic progenitors (Ivanovs et al., 2017). Following birth, the BM is responsible for the lifelong production of blood cells.

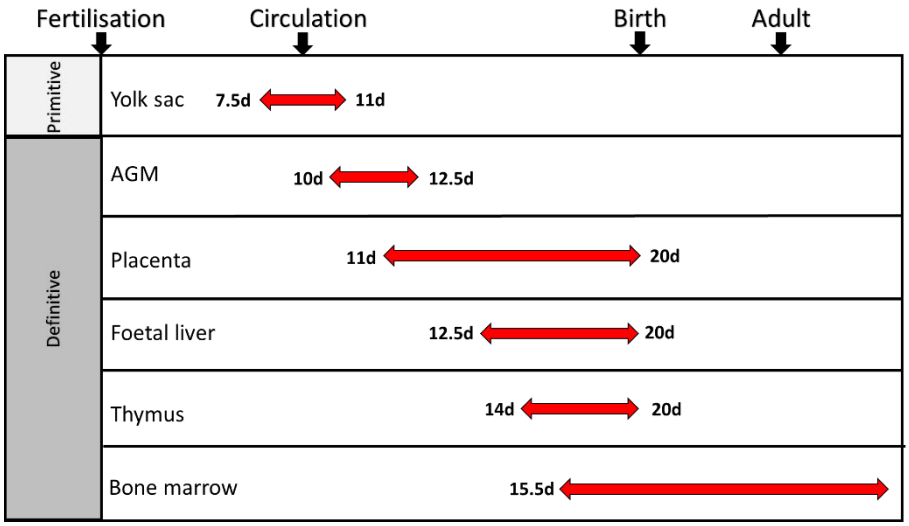

Figure 1.3 | Ontogeny of murine haematopoietic system (Adapted from Rowe *et al.*, 2016). Ontogeny of the murine haematopoietic system is a multi-step process that occurs in multiple anatomical sites, including the yolk sac, AGM, placenta, foetal liver, thymus and bone marrow.

In mice, the sequence of anatomic locations where haematopoiesis evolves is the same as with the human; however, due to the differences in the gestation period the timelines differ. In mice, the earliest primitive erythroid cells emerge in the yolk sac blood islands at embryonic day (E) 7.5 and, as with the human, these cells are essential for the oxygenation of the growing embryo (Silver and Palis, 1997). Following a transient definitive wave produced by the yolk sac, the first long term transplantable HSC emerge in the AGM around E 10.5 (Medvinsky et al., 1993, Medvinsky and Dzierzak, 1996). In addition to the AGM, the placenta and the early umbilical cord and vitelline artery are also implicated in the development of HSCs and are considered sources of haematopoietic stem cells (Ottersbach and Dzierzak, 2005, de Bruijn et al., 2000, Gekas et al., 2005). Additionally, HSCs can be found in the liver and it is in the liver where they rapidly expand and, as with the human, the liver remains the major site for haematopoiesis until birth which the BM takes over (Micklem et al., 1972, Muller et al., 1994, Fleischman et al., 1982, Yoder, 2004, Kikuchi and Kondo, 2006).

1.1.4 Developmental changes in the haematopoietic system

It is fascinating that the entire adult haematopoietic system relies on HSCs generated before birth, at least in mice. Lineage tracing has been instrumental in deciphering the direct relationship between foetal and adult HSCs (Samokhvalov et al., 2007, Gothert et al., 2005, Pei et al., 2017). Interestingly, even though they share a common origin, foetal and adult blood cells possess a multitude of different characteristics.

Starting at the apex of the haematopoietic hierarchy, it has been shown that foetal HSCs are highly proliferative and have a higher self-renewal capacity as compared to their adult counterparts (Micklem et al., 1972, Ivanovs et al., 2011, Rebel et al., 1996). In particular, in humans, foetal derived HSCs replicate every 3.5 - 4 weeks as opposed to the much slower replication of adult HSCs, which occurs every 40 weeks (Ivanovs et al., 2011, Catlin et al., 2011). In addition, the less purified CD34+CD38- haematopoietic stem and progenitor cell (HSPC) compartment showed the same trend of proliferation, with the foetal cells being more proliferative than adult cells when compared with repopulation assays (Holyoake et al., 1999). Notta *et al.* showed that the cloning efficiency of the CD34+ and CD34+CD38- compartments was highest for cells derived from the foetal liver, then from cord blood and finally from adult bone marrow. In this study, they measured cloning efficiency using methylcellulose assays and by observing whether a single cell gave rise to colonies from one or multiple lineages (Notta et al., 2016). Interestingly, Benz *et al.* showed that there is a higher proportion of myeloid-biased HSCs in the adult haematopoietic system, which is not what they observed in the foetal liver where all lineages were equally represented (Benz et al., 2012, Cheshier et al., 1999).

In addition, to their proliferation and differentiation potential, foetal and adult HSCs have different requirements to maintain their stem cell nature. In particular, it has been shown that adult HSCs require stem cell factor (SCF)

for their maintenance; however, SCF is redundant for the generation and maintenance of foetal ones (Bowie et al., 2007). *Etv6* is also critical for the maintenance of adult but not foetal HSCs (Hock et al., 2004b). Conditional deletion of *C/EBPa* only affects adult HSCs by enhancing their proliferation potential, and this over-proliferative state has been linked to increased expression of *N-myc*, which is normally repressed by *C/EBPa* in adult HSCs (Ye et al., 2013). Additionally, *Gfi1* is only critical for adult haematopoiesis as *Gfi1* knock-out mice develop normally, but when HSCs from adult mice are transplanted into irradiated recipients, they show reduced repopulation activity (Hock et al., 2004a). *Bmi1* is required for self-renewal of adult HSCs but not foetal (Park et al., 2003). Epigenetic regulators also influence foetal and adult HSCs differently. In particular, Polycomb repressive complex factors *Ezh1* and *Ezh2* exert opposing roles in adult and foetal HSCs. While loss of the former mainly affects adult HSCs, loss of the latter predominantly impacts foetal HSCs (Hidalgo et al., 2012, Mochizuki-Kashio et al., 2011). Genes that have been shown to be essential for maintaining the high self-renewal potential of foetal but not adult HSCs include *Lin28b*, *Hmga2*, and *Sox17* (Copley et al., 2013, Yuan et al., 2012, He et al., 2011, Kim et al., 2007). Foetal and adult HSCs have very different roles and this is reflected in the high self-renewal potential of foetal cells but also in the highly quiescent state of adult HCSs (Bowie et al., 2006, Cheshier et al., 1999).

A recent study applied quantitative proteomics to characterise and compare the proteome of murine foetal and adult HSPCs. As expected, foetal-derived HSPCs upregulated proteins related to cell cycle and proliferation. Adult HSPCs were shown to express proteins that are involved in the defence against viruses, bacterial and oxidative stress, but these proteins were not present in foetal cells. Additionally, they observed that interferon-α (INF-α) stimulation exerts different effects on foetal and adult HSPCs (Jassinskaja et al., 2017).

Significant differences can also be observed in the differentiated cells derived from foetal and adult cells. One example is the variation in lymphopoiesis that

can be observed across development. In particular, it has been shown first in mice and later in humans that B-1a B-cells arise only from embryonic progenitors, while conventional B-2 B-cells arise from both foetal and adult HSCs (Kantor et al., 1992, Griffin et al., 2011, Bueno et al., 2016, Hayakawa et al., 1985). Additionally, marginal zone B cells arise from embryonic progenitors (Yoshimoto et al., 2011). Another example is differences observed in erythroid cells. Different globins are observed in foetal versus adult erythroid cells, and while primitive erythroid cells circulate in a nucleated state, this is not true for definitive erythroid cells which enucleate prior to entering the circulation (Kingsley et al., 2004). Foetal macrophages (monocytic cells) also differ from their adult counterparts. In particular, the former have been shown to secrete high amounts of proteins acting on tissue remodelling and angiogenesis, whereas the latter express chemokines, scavenger receptor and tissue degrading enzymes (Klimchenko et al., 2011, Copley and Eaves, 2013).

As we have seen, the cellular context in foetal and adult haematopoiesis is very different. In essence, it seems that foetal and adult HSPCs have fundamentally different regulation and behaviour, which potentially cascades downstream along the haematopoietic hierarchy. Of course, we can imagine that these differences are not only critical for haematopoiesis, but they could also play a determining role in haematological malignancies such as leukaemia.

1.2 Haematological malignancies

Haematological malignancies refer to diseases that affect the haematopoietic hierarchy by influencing the homeostatic processes of blood production. In general, there are two main groups: 1) non-malignant diseases (such as anaemia and myelodysplastic syndromes) and 2) malignant diseases (such as acute lymphoblastic leukaemia and acute myeloid leukaemia). The focus of this work has been acute lymphoblastic leukaemia (ALL), which affects the lymphoid lineages as opposed to acute myeloid leukaemia (AML) that disturbs the myeloid lineage. ALL is more prevalent in children while AML predominates in adults. This is probably due to the differences in the cellular make-up and/or microenvironment during which the leukaemic transformation occurs (Babovic and Eaves, 2014).

1.3 Epidemiology of paediatric leukaemias

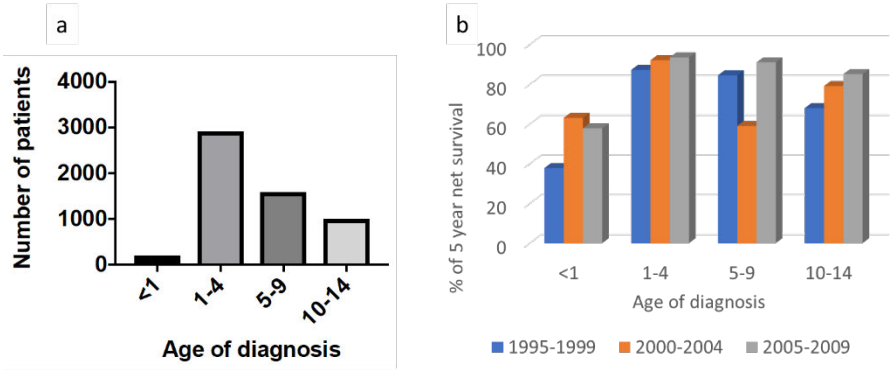

Figure 1.4 | Epidemiology of paediatric leukaemias (Data obtained from Bonaventure *et al.*). a) Incidence of paediatric leukaemia 1995-2009, UK data. b) 5-year net survival rate of paediatric patients with ALL 1995-2009, UK data.

Leukaemias are the most common malignancies in children aged 0-14, and the majority of the paediatric patients are burdened with ALL, which accounts for approximately 81% of the cases (Fig. 1.4a) (Bonaventure et al., 2017). Paediatric ALL can be caused by perturbations in either B or T cells; however, the most common type of ALL observed in paediatric patients is precursor-B cell ALL. Paediatric ALL, once lethal, now, with the advancements of medicine, the cure rates are extremely high (Greaves, 2018). A recent study showed that the 5-year survival rate of children aged 1-14 diagnosed with ALL was above 90% (Fig. 1.4b) (Bonaventure et al., 2017). Long-term survival without recurrence of disease is the primary clinical indicator of therapeutic success for patients with leukaemia (Good et al., 2018). However, Bonaventure *et al.* observed that infants with the same disease suffer from a much worse prognosis. In this study, they attribute the lower survival rates of infants with ALL to the presence of rearrangements at the Mixed Lineage Leukaemia (MLL) gene (Bonaventure et al., 2017).

1.4 The Mixed Lineage Leukaemia gene

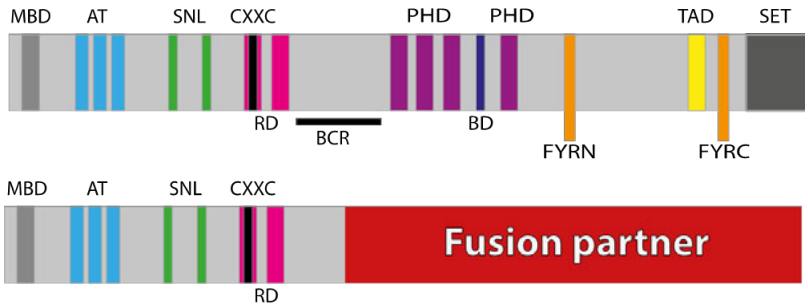

Figure 1.5 | The mixed lineage leukaemia gene (Adapted from Winters and Bernt, 2017). The top schematic depicts a simplified version of wild type MLL and the bottom the truncated MLL with the fusion partner. In the majority of MLL-R the PHD fingers, bromodomain, activation domain (TA) and SET domain are lost. (BCR= breakpoint cluster region)

The Mixed Lineage Leukaemia (*MLL*) gene is a member of the highly conserved lysine (K) methyltransferase (KMT) 2 family of proteins (Krivtsov et al., 2017). It is the mammalian homologue of the *Drosophila* thrithorax gene, which is a member of an evolutionarily conserved family of proteins, the *thrithorax* group (TrxG) (Tkachuk et al., 1992). *MLL*, which at that point was known as *ALL1*, was first described in two back to back Cell papers in 1992 (Gu et al., 1992, Tkachuk et al., 1992).

1.4.1 *MLL* structure and function

MLL is a large nuclear protein with multiple domains that is encoded on human chromosome 11q23 and consists of 37 exons (Tkachuk et al., 1992, Krivtsov et al., 2017). Structurally, it contains, starting at the N-terminal portion of the protein, a domain that is critical for the interaction of *MLL* with *Menin/LEDGF* (Hughes et al., 2004, Milne et al., 2005, Yokoyama and Cleary, 2008). Following from the menin-binding domain (MDB), there are three AT hook motifs, which are essential for DNA binding, two speckled nuclear localization motifs (SNL1 and SNL2) and two repression domains (RD1 and RD2)

(Tkachuk et al., 1992, Yano et al., 1997). The first repression domain displays homology to the DNA methyltransferase 1 (*DNMT1*) gene and is known as MT-domain (MT) (Ma et al., 1993). The homology region includes the CxxC zinc finger motif that binds unmethylated CpG containing DNA (Birke et al., 2002, Ma et al., 1993). The latter has been reported to exert transcription repression activity (Zeleznik-Le et al., 1994). Near the centre of *MLL* is the plant homology domain (PHD) comprising of four PHD fingers with an interspersed bromodomain between finger 3 and 4. The third PHD finger has been shown to bind to lysine 4 in histone 3 (H3K4), which is critical for *MLL*-depended transcription activity (Chang et al., 2010). The PHD domains are critical for the function of *MLL*, which could either be that of a transcriptional activator or repressor. CYP33/PPIE isomerase is the molecular switch that allows for the dual role of *MLL*. In particular, when one of the subdomains of PHD (PHD3/4) is docked to the bromodomain, it allows this domain to read di-/tri-methylated H3K4 (me2/3) signatures within chromatin, and binding to this histone mark is required for *MLL* transcriptional activation. However, when the same domain binds to CYP33/PPIE, this causes a conformational change which has as a result the disconnection from the bromodomain and instead the binding to the methyl DNA binding domain (Fair et al., 2001, Hom et al., 2010, Park et al., 2010, Milne et al., 2010, Chang et al., 2010). Finally, at the carboxy-terminus, *MLL* contains a transcription activation domain (TA) and a SET (Su(var)3-9, enhancer of zeste thrithorax) domain which confers the H3K4 methyltransferase activity (Nakamura et al., 2002, Milne et al., 2002).

The full-length *MLL* protein is post-translationally cleaved into MLL^N and MLL^C fragments by taspase1 at two conserved cleavage sites (CS1 and CS2) (Hsieh et al., 2003b, Hsieh et al., 2003a). Following cleavage, the two fragments reassemble through interaction of FYRN with the FYRC domain in order to form a stable complex with correct nuclear sublocalization (Hsieh et al., 2003b). *MLL* is part of a large protein complex; MLL^N associates with Menin and *LEDGF*, and this protein complex has been associated with increased transcription of differentiation/regulatory genes as well as cyclin-dependent

kinase inhibitors (Hughes et al., 2004, Milne et al., 2005). MLL^C interacts with *RbBP5*, *Ash2L*, *WDR5* and *DPY30* in order to achieve a potent and stable structural platform for activation of the catalytic activity of the SEM domain (Dou et al., 2006, Patel et al., 2009). Additionally, MLL^C recruits acetyltransferases MOF and CREB, which has been shown to be important for transcription activation of target genes (Dou et al., 2005, Ernst et al., 2001).

In homeostasis, *MLL* is critical for mammalian development, morphogenesis and homeobox gene expression (Yu et al., 1998, Yu et al., 1995). Regarding homeobox gene expression, Yu *et al.* observed that Mll expression is critical for maintenance of Hox gene expression but not for their initiation (Yu et al., 1998), while Milne *et al.* and Nakamura *et al.* provided evidence that *Mll* positively regulates expression of the *HOXA* cluster genes via its H3K4 methyltransferase activity (Milne et al., 2002, Nakamura et al., 2002).

Mll heterozygous (+/-) mice showed growth retardation, skeletal deformities and displayed haematopoietic abnormalities (Yu et al., 1995). *Mll* homozygous (-/-) deletion was embryonic lethal, with abnormal expression of Hox genes and a decrease in foetal haematopoietic cells due to a decrease in haematopoietic precursors. In addition, haematopoietic precursors had reduced clonogenic potential, as observed by colony-forming unit (CFU) assays of foetal haematopoietic cells, but with no specific effect on the lineage output (Yu et al., 1995, Yagi et al., 1998, Hess et al., 1997). Ernst *et al.* showed, using chimeric embryos and repopulation assays, that *Mll* is essential for definitive haematopoiesis. In the absence of *Mll*, they observed a block in HSC development and differentiation. This block occurred at the early stages of haematopoiesis, as AGM-derived *Mll*-deficient cells had no HSC activity and did not contribute to foetal liver haematopoiesis (Ernst et al., 2004). McMahon *et al*. further validated this using a different Mll KO mouse model, in this study they observed embryonic lethality between E12.5 and 16.5 and a dramatic reduction in liver-derived HSC. Further to this mouse model, they also developed a conditional Vav-Cre-mediated mouse model, which ablates Mll only in the haematopoietic system. They observed that even though the

haematopoietic system in the bone marrow was largely unaffected, when the *Mll*-deficient cells were transplanted into lethally irradiated recipients, their reconstitution potential was compromised (McMahon et al., 2007). These data suggest that *Mll* is essential for foetal haematopoiesis but is not required postnatally in order to maintain normal steady state. However, it is critical for both pre and postnatal regulation of stem cell self-renewal. Jude *et al.* also investigated the role of *Mll* in the adult haematopoietic system. Using an inducible knockout system, they observed that *Mll* expression was also essential for maintenance of adult HSCs and progenitors while committed lymphoid and myeloid cells remained unaffected. (Jude et al., 2007).

1.5 *MLL*- rearranged leukaemias

MLL rearrangements (MLL-R) result in the production of chimeric proteins in which the amino terminus of *MLL* is fused with the carboxy-terminal portion of a partner gene. This is of particular interest as the fusions occur in frame and results in the generation of aberrant fusion proteins that are frequently involved in acute leukaemia. Interestingly, truncated MLL^N without a fusion partner was not sufficient to transform cells whereas when lacZ (a gene encoding the enzyme β- galactosidase) was fused to MLL^N this was sufficient to cause leukaemia (Dobson et al., 2000). From this, they suggested that *MLL* fusions could lead to leukaemogenesis even if the fusion partner had no functional/pathogenic role.

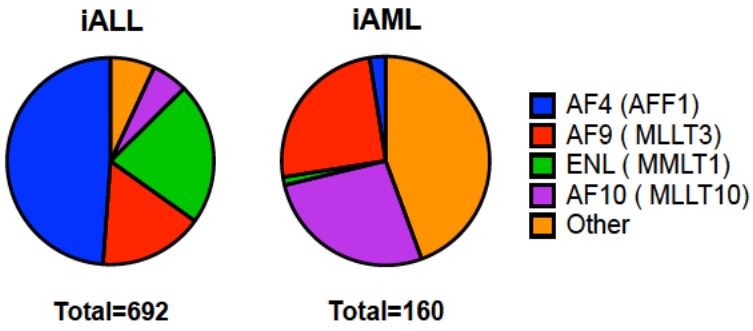

Figure 1.6 | Incident of the most common MLL fusion partners in infant leukaemias, infant ALL (iALL) and infant AML (iAML). Data obtained from Meyer *et al.*

Patients diagnosed with MLL-R leukaemias are usually infants and have a dismal prognosis (Pui et al., 2002). There is an extraordinary variety of fusion partners, as more than 84 *MLL* fusion partners have been described in the literature (Meyer et al., 2018). However, the most common ones are *AF4 (AFF1)*, *AF9 (MLLT3)*, *ENL (MLLT1)* and *AF10 (MLLT10),* which together comprise the majority of diagnosed ALL cases (Fig. 1.6). In two seminal papers, the distinct gene expression pattern and H3K79 profile of MLL-R leukaemias were described and, for the first time, MLL-R leukaemias were

defined as a unique entity very different from other non MLL-R ALL acute leukaemias (Armstrong et al., 2002, Krivtsov et al., 2008). MLL-R rearrangements are present in 75% of infants with ALL while they are only present in 1% of paediatric patients. MLL rearrangements are also present in infants with AML but the incidence is much lower (Fig. 1.6). The most common MLL-R is MLL-AF4, which is present in the majority of infants with ALL and these patients suffer from a particular poor prognosis.

1.6 AF4

AF4 (ALL1-Fused Gene from Chromosome 4 Protein) is a member of the ALF4 family comprising four paralogous nuclear proteins including AF4, AF5q31, *LAF4*, and *FMR2*. Even though *AF4* is the most common translocation partner gene in *MLL*-R, *LAF4* and *AF5q31* have also been reported (Meyer et al., 2018). *AF4* has been shown to play a critical role in lymphoid development as AF4 knockout in mice results in severe impairment of the maturation of B- and T-cell populations; however, it does not affect other haematopoietic compartments even though it is expressed in cells of other haematopoietic lineages (Isnard et al., 2000).

At the molecular level, *AF4* has been shown to act as a positive regulator of post-transcription elongation factor b (*pTEFb*). *PTEFb*, is a heterodimer of Cyclin Dependent Kinase 9 (*CDK9*) and Cyclin T1 or T2 and is capable of phosphorylating the carboxy- terminal domain (CTD) of RNA polymerase II (*RNAPII*). The interaction of *Af4* and *pTEFb* facilitates transcription elongation, which results in transcriptional activation (Bitoun et al., 2007).

1.7 MLL-AF4-driven infant ALL

Infant leukaemia is defined as leukaemia diagnosed in a patient before their first birthday and is very rare. As mentioned earlier, the most common leukaemia in infants is MLL-AF4-driven ALL and patients with this rearrangement have an extremely poor prognosis.

1.7.1 The unique biology of MLL-AF4 infant ALL

Infant MLL-AF4-driven ALL occurs in an immature B - lineage precursor, which lacks CD10 expression and frequent co-expresses lymphoid and myeloid markers. From this, it has been suggested that these leukaemias arise from a very immature lymphoid-primed progenitor that can intrinsically differentiate towards both the lymphoid and myeloid lineage (Brown, 2013, Basso et al., 1994, Bardini et al., 2015). The patients are burdened with aggressive clinical features including high white blood cell (WBC) counts, hepatosplenomegaly, central nervous system (CNS) involvement and leukaemia cutis (skin infiltration with leukaemic blasts) (Hilden et al., 2006, Brown, 2013). Poor response to prednisone and enhanced chemoresistance is also common amongst infant patients. Even though patients achieve complete remission quickly, they frequently relapse within one year of therapy (Pieters et al., 2019). These unique disease features led to the belief that the disease arises *in utero*, which would explain why it manifests so quickly after birth.

There is substantial evidence supporting the *in utero* origin of the disease. The first evidence came from studies conducted in identical twins with MLL-R-driven leukaemia, where both twins shared the same fusion sequence. The only plausible explanation for this was that the fusion occurred *in utero* in one twin and then metastasised to the other twin via the shared blood circulation due to the monochorionic placenta (Ford et al., 1993). To further support the

in utero origin of the disease, the same group performed retrospective analysis of blood spots (Guthrie cards) taken at birth from infant patients. They observed that the fusions were present at birth in all the patients (Gale et al., 1997). Further to this, in a recent study, they identified the foetal liver derived stem and progenitor cell compartment (CD34+CD38-) as the cell of origin of the disease (Agraz-Doblas et al., 2019).

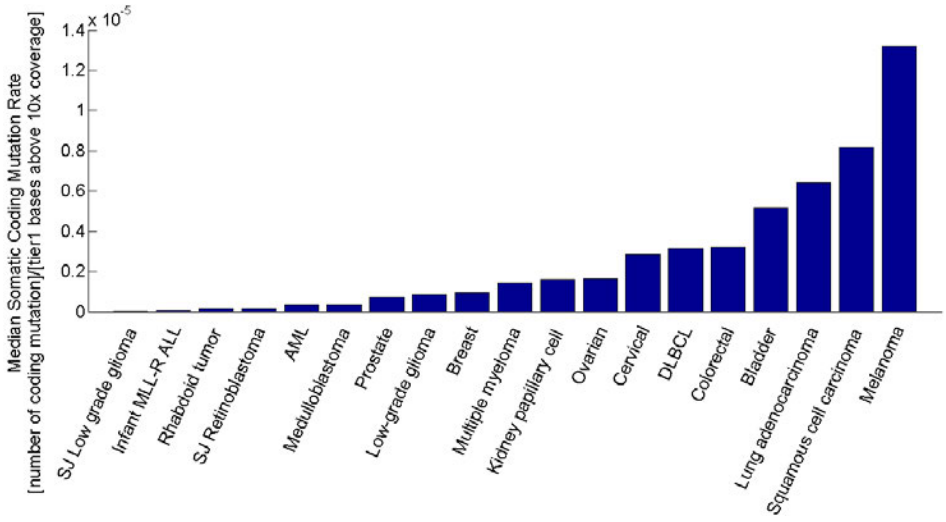

Figure 1.7 |The mutational landscape in a variety of cancers. (Data obtained from Andersson e*t al.*, 2015). Infants with MLL-R have one of the lowest numbers of somatic mutations amongst cancers. They only have a slightly higher number of mutations when compared to SJ Low grade glioma, which is also predominantly observed in young patients.

At the molecular level, these patients have a silent mutational landscape suggesting that no other co-operating mutations are required for the transformation to occur (Fig. 1.7) (Andersson et al., 2015, Agraz-Doblas et al., 2019). In these studies, they observed that there are some mutations present, in particular, in the PI3K-RAS signalling pathway; however, these mutations were sub-clonal and they were not always present in relapse. From this data, it has been concluded that in infants with this disease the fusion itself is the main disease driver.

Of particular interest is the location of the chromosomal breakpoint, which in the majority of patients can be found between exon 9 and intron 11 of MLL. It should be noted that, in the majority of infants, the MLL-AF4 breakpoint is located within MLL intron 11 (Meyer et al., 2018). This has been attributed to specific molecular features that are present in this region, including a DNA topoisomerase II cleavage site, an apoptotic cleavage site, a strong DNase I hypersensitive site and an RNA polymerase II binding site (Stanulla et al., 1997, Aplan et al., 1996, Strissel et al., 1998, Scharf et al., 2007). Therefore, it has been suggested that the high incidence of DNA double strand breaks in this location could be due to either the specifics of the chromatin structure or linked to transcriptional processes (Meyer et al., 2018, Scharf et al., 2007). Patients with breakpoints within intron 11 have a worse prognosis as compared to patients with upstream breakpoints.

One very interesting aspect of MLL-AF4 epidemiology is that it can be found in two very different clinical settings. One setting is infants with *de novo* ALL, but it can also be found in adults with leukaemias secondary to chemotherapy treatment with topoisomerase II poisons. From this, it has been suggested that maternal exposure to environmental DNA topoisomerase II inhibitors such as dietary flavonoids could contribute to the risk of MLL-AF4 infant leukaemia; however, evidence for this is weak (Alexander et al., 2001, Spector et al., 2005).

1.7.2 MLL-AF4-driven leukaemogenesis

MLL-AF4 fusion occurs when the N terminal portion of *MLL* fuses with AF4 to create a chimeric protein. The fusion proteins contain the N terminal portion of *MLL* including the *MENIN* binding and CXXC domains; however, the downstream PHD fingers and SET domain are replaced with *AF4*. The MLL/MENIN complex further binds to *LEDGF*, which via its PWWP domain allows binding to nucleosomes (Yokoyama and Cleary, 2008). The PWWP

domain binds to di-/trimethylated histone H3 lysine 36 (H3K36me2/3), and this has been associated with gene activation (Barski et al., 2007),while the CXXC domain of *MLL* binds unmethylated CpGs which are enriched in active promoters (Birke et al., 2002). Therefore, *MLL* binds at two sites, via CXXC and PWWP domains, and this has been shown to be critical for stable target binding (Eidahl et al., 2013). Additionally, there is an interaction with PAFc (polymerase associated factor complex) (Muntean et al., 2010, Milne et al., 2010). These interactions have been deemed critical for leukaemogenesis as they recruit MLL-AF4 to gene targets (Okuda et al., 2014, Yokoyama and Cleary, 2008, Yokoyama et al., 2005, Muntean et al., 2010, Milne et al., 2010).

Truncated *MLL* is not sufficient to initiate leukaemia and because the SET domain is lost, *MLL* fusion proteins rely on the fusion partner in order to activate transcription. Interestingly, *AF4* and other fusion proteins *AF9*, *AF10* and *ENL* form a complex that further associates with *pTEFb* and *DOT1L* and leads to aberrant gene expression via aberrant recruitment of *DOT1L* to the promoters of *MLL* target genes (Bitoun et al., 2007, Mueller et al., 2007, Mueller et al., 2009, Ballabio and Milne, 2012). *DOT1L* controls the levels of H3K79me2/3, which has been associated with gene activation (Guenther et al., 2008, Krivtsov et al., 2008). Additionally, in a recent study it was established that *AF4* associates with the SL1 domain of *MLL*, which results in activation of RNAPII-dependent transcription (Okuda et al., 2015). Therefore, MLL-AF4 fusion proteins use the N terminal domain to recognise their target genes and the fusion partner to stimulate transcription elongation, which leads to aberrant expression of target genes including *RUNX1*, *HOXA9* and *BCL2* (Benito et al., 2015, Wilkinson et al., 2013). Interestingly, Kerry *et al.* further showed that a subset of aberrantly activated genes exhibit a unique spreading pattern, and those genes were deemed essential for leukaemogenesis (Kerry et al., 2017). Overall, MLL-AF4 expressing blasts exhibit a persistent expression of *MLL* target genes and an increase in histone H3K79 methylation (Krivtsov et al., 2008)

1.7.3 Disease models

MLL-AF4 has proven difficult to model despite the fact that there is only one very potent disease driver. Several mouse models have been generated; however, we still do not have a mouse model that closely resembles the infant disease. The first mouse model generated was described in Chen *et al.*, where they fused the human *AF4* gene to mouse *MLL* locus. The mice in this study developed, after prolonged latency, mixed lymphoid/myeloid hyperplasia and the haematological malignancies observed were often B-cell lymphomas (Chen et al., 2006). The second attempt was done by Metzler *et al.* where they used conditional invertor technology in which a floxed *AF4* cDNA was inserted into the *MLL* locus in the opposite orientation to transcription. Upon Cre-recominase expression, *AF4* would flip around and be expressed in a chimeric mouse-human Mll-AF4 fusion protein. In their model, expression of Cre-recombinase was conditional to *Rag1*, *Lck* and CD19 expression. These mice developed B cell malignancies with a mature phenotype and only after a long latency (Metzler et al., 2006). Barrett *et al.* later used the same model but used VE-Cadherin Cre expression to allow expression of Mll-AF4 at the stage of the first definitive haematopoietic cells. Using this model, they identified a pre-leukaemic stage and established the LMPPs as the cell of origin of the disease; however, the mice developed B cell lymphomas after a long latency (Barrett et al., 2016). Another mouse model was generated, where Mll-AF4 expression was conditional to Mx1-Cre, and these mice developed acute B precursor cell leukaemia and AML, with a median latency of 131 days. Interestingly, blasts derived from the murine B cell precursor leukaemia were highly enriched in the gene expression and H3K79 profile of MLL-R patient samples (Krivtsov et al., 2008).

Substantial efforts have been made to model this disease using human cells. Montes *et al.* transduced human cord blood derived CD34+ cells with MLL-AF4 lentiviral particles and observed that MLL-AF4 conferred a proliferation and survival advantage *in vitro*; however, upon transplantation into NSG mice

MLL-AF4 was not sufficient to initiate leukaemia (Montes et al., 2011). The same group enforced expression of MLL-AF4 in human embryonic stem cells (hESCs), which led to an upregulation of HOXA cluster genes. Upon differentiation, the MLL-AF4-expressing hESCs favoured an endothelial fate over a haematopoietic one (Bueno et al., 2012). However, Tan *et al.* showed that MLL-AF4-expressing induced pluripotent stem cells exhibit high repopulation potential and were able to fully reconstruct the human haematopoietic system in mice (Tan et al., 2018).

The best model that we currently have was described in a recent study and involved fusion of the N terminus of human *MLL* with the murine *Af4*. The benefit of this approach was that they achieved higher viral titers and therefore higher transduction efficiencies. By transducing human CD34+ cord blood and bone marrow cells with MLL-Af4 retroviral particles and then transplanting them into NSG mice, they were able to initiate a pro-B ALL *in vivo*. The mice developed leukaemia by week 22 and the blasts were predominantly CD34+CD10-CD19+, which is a hallmark of the infant disease. Additionally, they performed molecular profiling of the blasts, and indeed a large part of the molecular signature of the disease was recapitulated in the blasts. In particular, MLL-Af4 was able to co-immunoprecipitate with *DOT1L* and super elongation complex (SEC) components, and the use of *DOT1L* inhibitors blocked the disease. However, it should be noted that the blasts did not display HOXA cluster upregulation, which is another hallmark of the disease. Interestingly, when they transplanted murine haematopoietic stem and progenitor cells (HSPCs) expressing MLL-Af4 they observed that the mice developed AML. The murine leukaemia phenotype was not influenced by culturing the cells prior to the transplantation in lymphoid or myeloid conditions (Lin et al., 2016). Using the same system, the same group investigated the interaction between fusion proteins and the microenvironment. They observed that the MLL-Af4 oncogenic activity was lineage-depended, suggesting that the lymphoid context is critical for MLL-Af4 leukaemogenesis. Additionally, they observed that under myeloid conditions these cells became unstable, vulnerable and prone to loss of self-renewal potential and lineage switching (Lin et al., 2017).

Much controversy exists around the importance of the reciprocal protein AF4-MLL for the infant disease. It was recently shown that AF4-MLL was expressed in 45% of the infant patients and that these patients had a significantly better prognosis. Interestingly, they also observed a close correlation between the reciprocal fusion and HOXA cluster expression (Agraz-Doblas et al., 2019, Trentin et al., 2009). In an effort to understand the role of AF4-MLL, Bursen *et al.* transduced murine Lin-Sca+ cells with AF4-MLL and transplanted them into mice, which subsequently developed pro-B ALL, B/T biphenotypic leukaemia or mixed lineage leukaemia but with long latency. In a human setting, Kumar *et al.* used siRNA to knock down expression of AF4-MLL and also MLL-AF4 in two patient-derived leukaemia cell lines (SEM and RS4;11). They observed that loss of AF4-MLL did not affect survival, proliferation or growth of the cell lines; however, knockdown of MLL-AF4 resulted in cell cycle arrest and apoptosis (Kumar et al., 2011). However, this study was criticised for lack of specificity of the AF4-MLL siRNA that could lead to false negative results. Using primary cells, Prieto *et al.* observed that AF4-MLL transduction of human CD34+ cells exerts an enhancement effect upon transplantation albeit with no leukaemogenic potential (Prieto et al., 2017). Wilkinson *et al.* provided further evidence for the interaction of the two fusion proteins and the critical role of RUNX1 in this interaction (Wilkinson et al., 2013).

1.7.4 Therapeutic approaches

Infants with MLL-AF4-driven ALL suffer from a dismal prognosis. In order to identify optimum treatments for these patients, large collaborative efforts have been established, including Interfant-06 (Driessen et al., 2017, Pieters et al., 2019). In this international clinical trial, patients were treated with intensive multiagent chemotherapy, followed by consolidation with myeloid-style or lymphoid-style chemotherapy. This was because the blasts of infants express both lymphoid and myeloid markers and a lineage switch has also been observed, where the patient relapse to AML following treatment (Pieters et al., 2019). This was followed with either further chemotherapy or allogenic haematopoietic stem cell transplant. Unfortunately, the latest data from this study were disappointing as no improvements were observed regarding the outcome of the infant patients (Pieters et al., 2019). This data suggest that the molecular biology of the disease is unique and therefore requires novel therapeutic approaches.

Toward this end, of particular interest are demethylating agents and histone deacetylase inhibitors, which target the abnormal epigenetic profile of the disease especially H3K79 methyltransferase *DOT1L* inhibitors (Bhatla et al., 2012, Garrido Castro et al., 2018, Stumpel et al., 2012). Multiple small inhibitors of *DOT1L* showed promising results in preclinical models; however, further clinical evidence are required to establish the suitability of this treatment for infant patients (Daigle et al., 2013, Daigle et al., 2011).

The critical role of the MLL-MENIN interaction presents another interesting therapeutic target, and several small molecules have been identified with promising results *in vitro* and *in vivo* (Grembecka et al., 2012, Borkin et al., 2015). *BRD4*, which is a member of the BET bromodomain-containing proteins, has also been considered an interesting therapeutic target as removal of *BRD4* was shown to cause a rapid downregulation of proto-oncogene *MYC*; however, the specificity of such a compound is in question as

it appears that it targets the myeloid lineage as opposed to MLL-R (Delmore et al., 2011).

HDAC inhibition has also been reported of being capable of reversing gene-expression profiles associated with chemotherapy resistance in infant MLL-R ALL (Stumpel et al., 2012). Multiple compounds have been identified to exert promising results in xenograft models of the disease including romidepsin and panobinostat, however, further studies are required to ensure safety and efficiency of these compounds (Cruickshank et al., 2017, Garrido Castro et al., 2018).

Another promising avenue is targeting the microenvironment interactions. One example of such treatment is the use of CXCR4 inhibition that when used in combination with other treatments (for example FLT3 inhibitor lestaurtinib) can lead to better outcome (Sison et al., 2013).

In addition, immunotherapies directed against B-cell antigens such as blinatumomab (an anti-CD19 monoclonal antibody) and chimeric antigen receptor T (CAR-T) cells have shown high antileukaemic potential in infant case reports (von Stackelberg et al., 2016, Maude et al., 2018). However, downregulation of the CD19 antigen and lineage switching has been observed in infants treated with B-lineage specific therapy (Rayes et al., 2016, Mejstrikova et al., 2017, Gardner et al., 2016).

1.8 Motivation and aims

Following from the latest Interfant publication it is clear that the prognosis of patients with MLL-AF4-driven ALL has not improved. It is also clear that lack of improvement could be attributed to the unique biology of the disease that is not completely understood. What makes infant leukaemia a distinct entity is its *in utero* origin. Therefore, it has long been speculated that the foetal origin of the disease is a key contributor to the aggressive disease phenotype. As mentioned earlier, several studies investigated differences between foetal and adult haematopoietic stem and progenitor cells; however, none of the studies correlated their finding with the MLL-AF4-driven infant ALL.

Therefore, the first aim of this study was to further define a foetal and neonatal/adult transcriptional signature in both humans and mice and use this approach to corroborate how the foetal origin could affect the disease phenotype. Additionally, I used this approach to identify genes that were expressed at similar levels between foetal-derived cells and blasts and therefore could be a residue of the foetal cell of origin. I speculated that these genes might be of importance for the pathogenesis of the disease and could therefore serve as novel therapeutic targets.

Additionally, following on from Barrett *et al*. where, using an Mll-AF4 expressing mouse model, they captured a pre-leukaemic stage and pinpointed LMPPs as the cells of origin of the disease, I aimed to identify genes that were expressed in LMPPs at the early stages of the disease and identify novel disease targets.

Having identified novel disease targets using the aforementioned approaches, my final aim was to investigate whether these targets could exert an effect on the disease phenotype.

1.8.1 Summary of aims

- Define the transcriptional profile of murine foetal and bone marrow derived LMPPs.
- Compare the transcriptional profile of murine foetal derived LMPPs expressing Mll-AF4 with controls.
- Define the transcriptional prolife of human foetal liver and cord blood derived HSC/MPPs.
- Compare the transcriptional profile of human foetal liver derived HSC/MPPs with LMPPs and investigate which is the potential cell of origin of the disease.
- Identify genes the expression of which was conserved across species and establish a list of such genes. Investigate expression of these genes in the blasts of infants with MLL-AF4 driven ALL.
- Identify genes that could serve as novel therapeutic targets and use *in vitro* approaches to investigate the effect.

Chapter 2 Materials & methods

2.1 Sample collection and processing

2.1.1 Collection of human foetal tissues (first and second trimester – 9 to 20 weeks gestational age)

Foetal tissues were obtained from second trimester foetuses undergoing elective surgical termination following informed consent from the patient.

Dissection of the foetal livers was conducted by a member of the RAA/FT/001 study and the liver was placed in PBS. The liver was mechanically disrupted in order to create a single cell suspension and then passed through a 40µm cell filter (Becton-Dickinson). The single cell suspension was washed with PBS with 10% FCS and 1mM EDTA (washing buffer), the samples were washed by centrifugation at 500xg for 5 minutes and the supernatant was removed.

The pellet was resuspended in 40ml of washing buffer (for livers obtained from 16 to 20 weeks of gestation, the pellet was resuspended in 80ml of washing buffer). In order to separate the mononucleated cells (MNC), the Ficoll™ (Sigma-Aldrich, Haverhill, England) gradient separation method was used. 20ml of the cell suspension were layered over 10ml of Ficoll™ and the samples were centrifuged for 30 minutes at 1500rpm (with no breaks). Following centrifugation, the MNC layer, which was visible, was collected with a Pasteur pipette and washed with at least 30ml of washing buffer at 300xg for 10 minutes. The cell pellet was either further processed for enrichment or was cryopreserved in freezing medium (FSC with 10% DMSO and 1% P/S).

Cord blood samples obtained from the Scottish cord bank in Glasgow and the Cambridge stem cell biobank were already CD34 enriched and thus no further processing was required.

2.1.2 Collection of murine tissues

Heterozygous Mll-AF4loxP knock-in (Metzler et al 2006) and heterozygous VEC-Cre transgenic (Chen et al 2009) mice were crossed in order to produce Mll-AF4+ VEC-Cre+ and Mll-AF4- VEC-Cre+ embryos. Additionally, I obtained E14.5 embryos from wild-type C57BL6/N crosses and adult bone marrow from adult C57BL6/N mice (8-10 weeks old).

After dissection of the E14.5 embryos, the liver was macroscopically identified and placed in a 1.5ml tube containing PBS where it was mechanically disrupted with a syringe into a single cell suspension. Bone marrow was obtained by removing and crushing the long bones (femur and tibia) of the adult mice. In order to ensure single cell suspension, the samples were passed through a 50μM filter (Wolf Laboratories). The samples were washed once with either PBS for the foetal liver or complete medium (PBS, 10% FSC, 1% Pen/strep) for the bone marrow and placed on ice until the staining step.

2.2 Genotyping

Genotyping of the embryos for the Mll-AF4loxP knock-in and VEC-Cre transgenic timed mattings was performed in order to ensure the appropriate genotypes of each mouse embryos.

For DNA extraction the HotSHOT method was used, where 1/5 of the embryo's head was used (Truett et al., 2000). Specifically, the tissue was initially placed in an alkaline lysis buffer (0.04% disodium EDTA and 0.25% NaOH in water) and heated to 95°C at 1000rpm for 20 minutes. This was followed by addition of a lysis neutralisation reagent (4% 1M Tris-HCl in water). 1µl of the HotSHOT mixture was mixed with 12.5µl Kapa2G PCR mixture (Merck), 9µl of water and 1.25µl of (10nM) each primer.

Target	Forward primer	Reverse primer
Vec-Cre	GCC TGG CGA TCC CTG AAC ATG	CCC AGG CTG ACC AAG CTG AG
Mll-AF4	ATG ATG CCA CTG TGC TGT GT	TCG CCT TCT TGA CGA GTT CT

The above were placed in a thermal cycler and the following PCR conditions were used:

Initial denaturation	92°C for 2 min	
Denaturation	95 °C for 15 s	30 cycles for Mll-AF4 35 cycles for Vec-Cre
Annealing	58 °C for 15 s	
Extension	72 °C for 5 s	
Final extension	72 °C for 10 s	
Infinite hold	4 °C	

The PCR products were visualised on a 1% agarose (Sigma-Aldrich) gel using GelRed™ (Biotium). In addition to the samples a 1000bp DNA ladder (Invitrogen) and also a positive and negative control were used in every gel, the gels were run for 20 minutes at 120V and visualised with a gel documentation system (Gene Flash, SYNGENE).

2.3 Magnetic-activated cell sorting and flow cytometric cell sorting and analysis

2.3.1 Magnetic-activated cell sorting (MACS)

Magnetic-activated cell sorting (MACS) was used for enrichment of human foetal liver samples for CD34 using Miltenyi Biotec CD34 MicroBeadKit – Ultra Pure Human (Miltenyi Biotec). Following single cell suspension and Ficoll separation, foetal liver-derived MNCs were resuspended in 300µl of FACS buffer and 100µl of FcR Blocking Reagent and 100µl of CD34 MicroBeads UltraPure were added to the sample. The samples were incubated at 2-8°C for 30 minutes, in the dark. Following incubation, the samples were washed at 300xg for 10 minutes and the pellet was resuspended in 500µl of FACS buffer. The cell suspension was transferred into a LS MACS column attached to a magnet (which has been previously primed by allowing 3ml of FACS buffer to go through) and 3 x 3ml of buffer were added for washing the column afterwards. The flow through contained the unlabelled cells whereas the labelled cells were retained inside the column by the magnet. Finally, the column was removed from the separator and placed inside a falcon tube. 5ml of buffer were added to the column and the column was immediately flushed by firmly pushing the plunger into the column. The labelled cells obtained in the final step were washed and processed in accordance with the downstream application that they were going to be used for.

2.3.2 Cell staining for flow cytometric analysis and sorting

General staining protocol:

Cells were initially washed with FACS buffer (PBS, 2% FCS and 1% P/S). The pellet was then resuspended in approximately 100µl of FACS buffer for 1 million cells. 5µl of Fc blocker agent (BD) was added and the samples were incubated for 10 minutes. Following the end of the 10-minute incubation period, the appropriate antibody cocktail (see below) was added to the samples and the samples were incubated for 20 minutes at 4°C, in the dark. 1ml of FACS buffer was added to the samples and the samples were washed by centrifugation for 5 minutes at 2000 rpm where possible at 4°C. The pellet was resuspended at 200µl and the appropriate viability dye added. It should be noted that the appropriate compensation controls (single stained and fluoresce-minus-one) were used when setting up an experiment and for complicated sorting strategies with every experiment.

2.3.3 Flow cytometric analysis and sorting

Samples were analysed using a 4 laser FACSAria (Beckton Dickinson) and a 3 laser NovoCyte (Acea Biosciences). Samples were sorted on either a FACSDiva or FACSAria (Beckton Dickinson).

2.3.4 Analysis of flow cytometry data

Data was analysed with FlowJo software (Tree Star). Gating strategies are as described in this chapter and also in the results.

2.3.5 Sorting of murine LMPP

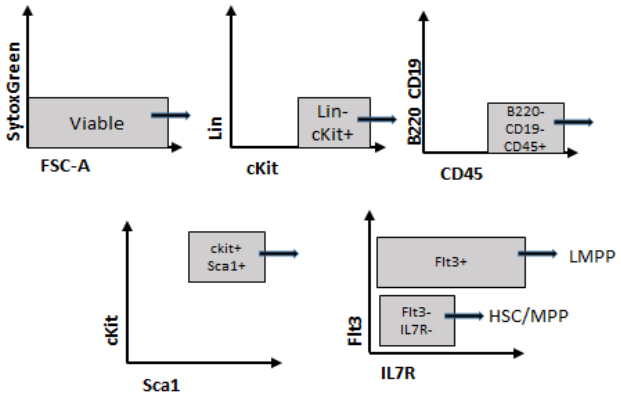

Figure 2.1 | Schematic representation of murine LMPP sorting strategy Viable cells were gated on cells→ singlets

It should be noted that this protocol was established by Charlotta Böiers (Boiers et al., 2013). Following dissection of E14.5 foetal liver and bone marrow, a single cell suspension was created, the samples were washed with complete medium (CM) (PBS, 10% FSC and 1% P/S) and LMPPs were sorted for Lin-Sca1+c-kit+CD45+B220-CD19-Flt3+. A master mix of appropriate antibodies was created (Table 2.1) and added to the samples and controls. The samples were incubated at 4°C for 20 minutes and then washed with CM. A second staining step was required for the Flt3 and as such the samples were incubated with StAV-Qd655 for a further 20 min at 4°C. The samples were washed twice with CM and finally the viability dye SytoxGreen (Thermo Fisher Scientific) was added at a concentration of 1:1000. The stained pellet was resuspended in 300µl of FACS buffer and the samples were sorted using the Cell Sorter BD FACS ARIA II or BD FACS Fusion. Controls included an unstained control as well as single stains and fluorescence-minus-one (FMO) controls for all antibodies. The sorted cells were collected in CM at 4°C. After sorting, the samples were centrifuged at 500xg for 5 minutes at 4°C in a fixed angle centrifuge and the pellets immediately processed for the downstream application.

Antibody / fluorophore	Clone	Provider
IL7R-PE	A7T34	eBioscience
Sca1-PB	E13-161.7	Biolegent
ckit-APCeF780	2B8	eBioscience
CD45-AF700	30-F11	eBioscience
Flt3-biotin	A2F10	eBioscience
B220-PECy7	RA3-6B2	Biolegend
CD19-PECy7	1D2	Biolegend
StAV-Qd655		Life technologies
CD3e-APC*	I45-2C11	BD
Ter119-APC*	TER119	eBioscience
F4/80-APC*	2BM8	eBioscience
Nk1.1-APC*	PK136	BD
Gr1-APC*	RB6-8C5	BD
SytoxGreen		Life technologies

Table 2.1 | List of antibodies for the murine LMPP sort *antibodies used for lineage cocktail

2.3.6 Sorting of human HSC/MPP and LMPP

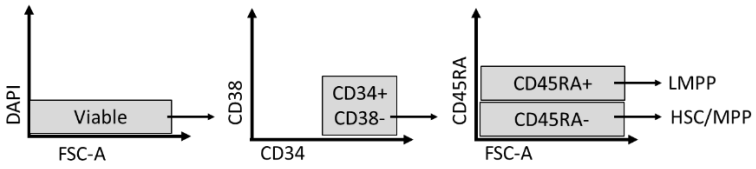

Figure 2.2 | Schematic representation of human LMPP sorting strategy Viable cells were gated on cells→ singlets

Human foetal liver and cord blood derived samples were initially enriched for CD34 using magnetic-activated cell sorting. The CD34 enriched populations were further sorted for haematopoietic stem and progenitor cells (HSC/MPPs) CD34+CD38-CD45RA- and LMPPs CD34+CD38-CD45RA+. It should be noted that human cord blood samples were also enriched for CD34. The samples were resuspended in approximately 100µl of FACS buffer for 1 million cells and 5µl of Fc blocker agent (Becton Dickinson) added and the samples were incubated for 10 minutes. A master mix of appropriate antibodies (Table 2.2) was created and the samples were then stained and incubated for 20 minutes at 4 °C, in the dark. The samples were washed with 1ml of FACS buffer and the pellet was resuspended in 300µl of buffer. DAPI (Biolegend) was used as a viability dye. Following sorting, the cells were processed in an appropriate manner for downstream applications.

Antibody / fluorophore	Clone	Provider
CD34 FITC	581	Biolegend
CD38 PE	HIT2	Biolegend
CD45RA APC	HI100	Biolegend

Table 2.2| List of antibodies for the human LMPP sort

2.3.7 Cell Tracer

Cell Tracer™ Far Red Cell Proliferation kit (Thermo Fisher Scientific) was used for *in vitro* cell proliferation analysis.

The following protocol has been optimised for cell concentrations of $1x10^6$ cells/mL and the dye was used at a 1μM concentration.

$1x10^6$ cells were washed with PBS and the supernatant was removed. The dye, which was diluted into 1ml of PBS, was added to the cells. The cells were incubated for 20 minutes at room temperature, in the dark. 7ml of FACS buffer were added to the cells and the cells incubated for 5 minutes and then washed. Following the final washing, 1/3 of the cells were resuspended in FACS buffer for immediate analysis (day 0 of analysis) while the remaining 2/3 were placed in culture medium and cultured for 4 days (day 4 of analysis). Cells were cultured in SEM medium (RPMI (Gibco) and 10% FCS) at 37°C with 5% CO_2. Following the 4 days incubation, the cells were washed and resuspended in FACS buffer for flow cytometric analysis. It should be noted that during analysis acquisition flow rate was less than 150 events per second. It should also be noted that for the day 0 time point the cells were incubated for at least 10 minutes prior to the analysis in order to allow the CellTrace™ reagent to undergo acetate hydrolysis. The viability dye for this experiment was Sytox Orange (Life Technologies) used at 1:1000.

2.3.8 Zombie NIR™ Fixable Viability Kit

The Zombie fixable viability dye (Biolegend) was used to stain live cells for treatments that would lyse the cells such as analysis of the cell cycle.

The following protocol has been optimised for cell concentrations of $1x10^6$ cells and the dye was at 1:100 dilution (stock solution was diluted with 100µl of DMSO).

$1x10^6$ cells were washed with PBS. 1µl of the dye was diluted in 100µl of PBS. The cells were resuspended in 100µl of PBS containing the dye and the cells were incubated at room temperature for 15 minutes, in the dark. Following incubation, the cells were washed with FACS buffer and resuspended in FACS buffer ready for the cell cycle analysis.

2.3.9 Cell cycle analysis

Cell cycle analysis was conducted in order to observe differences in the number of cells present in the different phases of the cell cycle between treatments. It should be noted that in order to ensure that all the cells analysed for the cell cycle were viable, I either used the Zombie NIR™ Fixable Viability Kit or the cells were sorted and immediately analysed. The buffer for the cell cycle was made by our Flow Cytometry facility and contained 5µg/ml Dapi (Thermo Fisher Scientific) in 1% IGEPAL (Merck). One volume of cell cycle buffer was added to the cells that were resuspended in either PBS or FACS buffer. The mixture was incubated for 1 minute and then immediately analysed. It should be noted that during acquisition with the flow cytometric analyser, I always acquired less than 150 events per second.

2.3.10 Competition assay

The competition assay was used to assess the proliferation/viability potential of cells. In particular, it was used to assess the effect of specific sgRNAs on the phenotype of the SEM cells. For the competition assay, I mixed in a 1:1

ratio wild-type SEM cells with Cas9-GFP SEM cells and then transduced the cells with the sgRNA of interest. It should be noted that in all the competition assays I always used a positive and negative control. In order to assess the impact of the sgRNA I performed flow cytometric analysis of the cells at different time points (days 2, 6 and 12).

2.3.11 Migration assay

The migration assay was performed with the CRISP/R Cas9 SEM cells to assess whether sgRNAs could affect the migration potential of cells. For the assay, I generated SEM Cas9-sgRNAs cell lines, including one line for the negative control. All the cell lines were passaged at least once before sorting $1x10^5$ SEM-Cas9-sgRNA cells for the assay. Following sorting, the cells were washed and resuspended in culture media and incubated overnight at 37°C with 5% CO_2. The following morning the cells were centrifuged, and all the media was carefully removed. A transwell (Corning, 8μm pore) was placed in a standard 24-well plate. The cells were resuspended in RPMI with no FCS in order to starve them and they were placed on top of the transwell. In order to create the migration gradient, 600μl of migration media (RPMI with 10% FSC and 100ng/ml CXCL12 -Thermo Fisher Scientific) were added to the lower well of the 24-well plate. The cells were allowed to migrate for 5 hours at 37°C and 5% CO_2. Following incubation, the cells were washed and resuspended in 200μl FACS buffer. For the analysis of the migration assay, the cells migrated were counted using a Novocyte flow cytometer (Acea Biosciences) where the number of live cells was counted in 150μl of buffer.

2.4 Clonogenic assays

2.4.1 Methylcellulose assay for murine lymphoid potential

2000 cells were resuspended in 300µl of IMDM (Life Technologies). The cells were then transferred to 3ml of methylcellulose (M3630, Stem Cell Technologies) with cytokines (20ng/mL Scf, Il7 and Flt3L) and mixed vigorously by vortexing. The mixture was left to settle for at least 5 minutes and 1ml of the methylcellulose containing the cells was dispensed into a 35mm plate. The three technical replicates (three plates) were placed in a 35mm petri dish along with an extra petri dish containing sterile water. The cells were incubated at 37°C with 5% CO_2 for 10 days. After 10 days, the number of colonies was counted. For re-plating, 2000 cells were re-plated into a new CFU assay where the cells were incubated at 37°C with 5% CO_2 for 10 days.

2.4.2 Methylcellulose assay for human myeloid potential

MethoCult™ H4034 Optimum (Stem Cell Technologies) was used for the assessment of the myeloid potential of human stem and progenitor cells. 3ml of MethoCult™ H4034 Optimum used for each sample where 2000 cells were resuspended into 300µl of IMDM (Life Technologies). The cells were then transferred to 3ml methylcellulose and mixed vigorously by vortexing. The mixture was left to settle for at least 5 minutes and 1ml of the methylcellulose containing the cells was dispensed into a 35mm plate. The three technical replicates (three plates) were placed in a 35mm petri dish with an extra petri dish containing sterile water. The plates were incubated at 37°C, in 5% CO_2 for 14 days. After 14 days, the number of colonies was counted.

2.4.3 Clonogenic assay for human lymphoid potential

For the B cell differentiation assay, I used the MS5 stroma cell line which supports differentiation of stem cells towards the B cell lineage. MS5 cells were grown in alphaMEM (Life Technologies) supplemented with 10% FSC, 1% L-Glutamine (Life Technologies), 1% HEPES (Life Technologies), 1% 2-mercaptoethanol (Life Technologies) and 1% penicillin/streptomycin (pen/strep). MS5 were thawed 72 hours prior to passaging and re-plated 24 hours prior to initiation of the differentiation.

For the differentiation, 25000 MS5 cells were plated in a 24-well plate, 24 hours prior to the initiation of the differentiation. On the day of the experiment, the MS5 cells were confluent. For the differentiation assay, I used 1000 -10000 haematopoietic stem and progenitor cells. The differentiation media contained the MS5 medium supplement with recombinant human cytokines including Flt3L (10ng/mL), SCF (20ng/ml), interleukin-2 (IL2) (10ng/ml), interleukin-7 (IL7) (5ng/mL) (Miltenyi Biotec). During differentiation, half of the medium was replaced every 4 days and the plates were incubated at 37°C, in 5% CO_2 for 14. At the end of the differentiation period, the cells were analysing using flow cytometry for lymphoid and myeloid markers using the following antibodies (Table 2.3). DAPI was used as a viability dye (1:1000).

Antibody / fluorophore	**Clone**	**Provider**
CD19 PE	HIB19	Biolegend
CD33 APC Cy7	P67.6	Biolegend
CD10 APC	HI10a	Biolegend

Table 2.3 | List of antibodies for assessing lymphoid and myeloid potential.

2.5 RNA extraction

2.5.1 RNA extraction from small cell numbers

RNA extraction of small cell numbers (800 – 50000 cells) was performed using the NucleoSpin RNA XS kit (Macherey-Nagel). Cell pellets were lysed with 100µl of RA1 containing 2µl TCEP (where TCEP is a reducing agent) and the samples were vigorously vortexed. 100µl of 70% EtOH were added to the homogenised lysate and the samples were vortexed again. The samples were transferred into NucleoSpin® RNA XS columns and the tubes centrifuged for 30 sec at 11000xg, which allowed binding of the RNA to the column. The next step was to desalt the silica membrane by the addition of 100µl of Membrane Desalting Buffer (MDB) followed by centrifugation for 30 sec at 11000xg. The next step was the digestion of DNA, which was achieved by addition of 25µl of rDNase reaction mixture (3µl of rDNase and 27µl Reaction buffer for rDNase) on top of the membrane, followed by incubation for 15 minutes at room temperature. The next step was inactivation of the rDNase with 100µl of RA2 buffer, followed by a 2-minute incubation at room temperature and centrifugation for 30 sec at 11000xg. This was followed by two washing steps. For the first wash step, 400µl of RA3 buffer were added to the column, which was followed by spinning at 11000xg for 30 seconds. For the second wash, 200µl RA3 buffer were added, followed by spinning at 11000xg for 2 minutes. One final spin was conducted in order to ensure that the column was completely dry. Finally, 12µl of RNase-free water was added to the centre of the column and the column was spun down at 11000xg for 30 seconds.

2.5.2 RNA extraction from large cell numbers

RNA extraction from large cell numbers (>50000 cells) was performed using the RNA mini kit (Qiagen). Cell pellets were disrupted by the addition of 600µl of RLT buffer and the lysates homogenised with vigorous vortexing and pipetting. 600µl of 70% EtOh was added to the cell lysates and the lysates were further vortexed and mixed well by pipetting. 700µl of the samples were transferred into an RNease spin column and the samples centrifuged for 15 seconds at 8000xg. This step was repeated one more time to allow the entire lysate to be loaded onto the column, after which the flow through was discarded. 350µl of RW1 buffer were added to the spin columns and the samples were spun down at 8000xg for 15 seconds. It should be noted that a DNase (Qiagen) step was incorporated into the standard RNA extraction protocol. For each reaction, 10µl of DNase I (27.27 Kunitz units) solution were added to 70µl of buffer RDD (Qiagen) and the solution was added directly to the columns and incubated for 15 minutes at room temperature. 350µl of buffer RWI were added to the RNeasy spin column and the column was centrifuged for 15 sec at 10000rpm. Two more washing steps followed with RPE buffer, one with 500µl and spinning at 8000xg for 15 seconds and the second with 500µl RPE with spinning at 8000xg for 2 minutes. Another spinning step was incorporated in order to ensure that the column was dry. For the final step, 30µl of RNase-free water were added to the centre of the column and the RNA was eluted by centrifugation at 8000xg for 30 seconds.

2.6 DNA extraction

2.6.1 DNA extraction

DNA extraction was performed with the DNeasy Blood and Tissue kit (Qiagen). 1-2x10^6 cells were centrifuged at 300xg for 5 minutes and the pellet was resuspended in 200µl PBS to which 20µl of proteinase K were added. 200µl of buffer AL were further added to the mixture and the samples incubated for 10 min at 56ºC. 200µl of ethanol were added and the samples mixed thoroughly. The mixture was transferred into a DNeasy Mini spin column and centrifuged at 6000xg for 1 min, after which the flow through was discarded. 500µl of AW1 buffer were added to the columns and the columns centrifuged at 6000xg for 1 minute, after which the flow through was discarded. 500µl of AW2 buffer were added to the columns, the columns centrifuged at 20000xg for 3 minutes and the flow through again discarded. The columns were further centrifuged for 1 minute at 6000xg. Finally, 200µl buffer AE were added directly onto the DNease membrane, the columns incubated for 1 minute at room temperature and then centrifuged at 6000xg for 1 minute.

2.6.2 Gel extraction

DNA was extracted using the QIAquick gel extraction kit (Qiagen). Initially, the DNA band containing the product of interest was excised from the agarose gel and the gel slice weighed. 3 volumes of buffer QG were added to 1 volume of gel and the mixture was incubated at 50ºC for 10 min or until the gel slice was completely dissolved. Once the gel slice was completely dissolved, 1 gel volume of isopropanol was added, and the mixture placed in a QIAquick spin column and centrifuged at 17900xg for 1 minute and the flow through discarded. 500µl of buffer QG were added and the column was centrifuged at

17900x g for 1 minute and the flow through discarded. 750µl of buffer PE were added and the column was centrifuged at 17900x g for 1 minute and the flow through discarded. The column was further centrifuged at 17900x g for 1 minute and the flow through discarded. 50µl of buffer EB were added and the column was incubated for 1 minute at room temperature before it was further centrifuged at 17900x g for 1 minute.

2.6.3 PCR product purification

PCR product purification was achieved using a PCR purification kit (Qiagen). 5 volumes of buffer PB were added to 1 volume of PCR sample. The mixture was transferred into a QIAquick column which it was centrifuged at 17900xg for 1 minute and the flow through discarded. 750µl of buffer PE were added, the column centrifuged at 17900x g for 1 minute and the flow through discarded. The column was further centrifuged at 17900x g for 1 minute and the flow through discarded. 50µl of buffer EB was added and the column incubated for 1 minute at room temperature before it was further centrifuged at 17900x g for 1 minute.

2.7 RNA and DNA quantification

2.7.1 RNA quantification with Agilent High Sensitivity DNA Screen Tape

The Agilent Tapestation system allows electrophoresis of RNA samples. 2µl of RNA samples or RNA ladder (Agilent) were mixed with 1µl of High Sensitivity RNA Screen Tape sample buffer (Agilent) and vortexed using IKA vortexer (Agilent) at 2000 rpm for 1 minute and spun down. To achieve denaturation of the samples, they were placed in a thermal cycler at 72°C for 3 minutes and then at 4 ºC for 2 minutes. Finally, the samples were loaded onto the Tapestation for analysis.

2.7.2 DNA quantification with Agilent High Sensitivity DNA Screen Tape

The Agilent Tapestation system allows electrophoresis of DNA samples. 2µl of DNA samples or DNA ladder were mixed with 2µl of High Sensitivity D1000 sample buffer and vortexed for 1 minute. The mixed samples were spun down and loaded onto the Tapestation for analysis alongside a ladder.

2.7.3 DNA quantification with Qubit

Qubit RNA HS (Thermo Fisher Scientific) and Qubit dsDNA HS (Thermo Fisher Scientific) assays were also used for the quantification of RNA and DNA. For each assay, the appropriate standards were set up and the samples were prepared according to the manual. Briefly, the appropriate amount of sample (usually 2µl) was added to the working solution (1µl of Qubit RNA/DNA reagent in 200µl of Qubit RNA/DNA buffer), the samples were vortexed and incubated

for 2 minutes. After incubation, the samples were analysed using the Qubit 2.0 Fluorometer. In order to determine the amount of RNA/DNA the following formula was used:

Concentration of sample = QF value × (200 x X),

where: QF value = the value given by the Qubit® fluorometer

X = the number of microliters of sample added to the assay tube

2.7.4 DNA and RNA quantification using Nanodrop

Nanodrop 2000 (Thermo Fisher Scientific) was also utilised for the measurement of both RNA and DNA, specifically for larger samples. The Nanodrop was initially cleaned and the appropriate blank was utilised (water for RNA and elution buffer for DNA) and 1µl of sample was placed in the spectrophotometer for further measurement.

2.8 Library preparation for RNA sequencing

The SMARTer Stranded Total RNA-Seq Kit - Pico Input Mammalian v1 and v2 was used for the generation of indexed cDNA libraries from approximately 1ng of high-quality RNA that were compatible with next-generation sequencing (NSG) and in particular the Illumina platform Hiseq4000. The preparation of libraries using the SMARTer Stranded RNA seq pico input protocol can be divided into seven different steps: 1) first-strand cDNA synthesis, 2) addition of Illumina Adapters and barcodes, 3) library purification with AMPure beads, 4) depletion of Ribosomal cDNA, 5) final PCR amplification and 6) library purification with AMPure beads and 7) library validation.

1. First-strand cDNA synthesis

Following RNA extraction, 1 ng of RNA was mixed with 1µl SMART Pico Oligos Mix, 4µl 5X first Strand buffer and nuclease-free water, and the reaction mixture was placed in a thermal cycler at 94°C for 4 minutes. Following incubation, the samples were placed immediately on ice for 2 minutes. The first step of first strand cDNA synthesis was fragmentation of RNA into fragments of the appropriate size for Illumina sequencing platforms.

Following RNA fragmentation, the first strand master mix (4.5µl Template Switching Oligo Mix, 0.5µl RNase Inhibitor, 2µl SMARTScribe Reverse Transcriptase) was added to the mixture and the mixture was placed in a preheated hot-lid thermal cycler at 42°C for 90 minutes followed by 70°C for 10 minutes, after which the samples were stored at 4°C until the next step.

2. Addition of Illumina adapters and indexes

The second step was the addition of Illumina adapters since each sample/library should have a different adapter in order to be distinguished during the analysis. After the first strand cDNA synthesis, 2µl Nuclease-free water, 25µl 2X SeqAmp PCR buffer, 1µl Seq Amp DNA polymerase, 1µl Forward PCR primer HT and 1µl Reverse PCR primer HT were added to the

tube. The samples were mixed and briefly spun down before being placed in a preheated hot-lid thermal cycler using the following program.

94°C 1 minute

98°C 15sec
55°C 15sec
68°C 30sec
5 cycles

68°C 2 minutes

4°C forever

3. Purification of the RNA-sequencing library using AMPure beads

This step allowed for the purification of cDNA by binding of the cDNA to the AMPure beads, which are magnetic. During this step, fragments less than 100bp were removed.

45µl of AMPure beads were added to the 50µl sample mixture, the beads and the sample were incubated for 10 minutes in order for the DNA to bind to the beads. After the incubation, the tubes were placed on a magnetic stand for several minutes (until the solution was clear and the sample with beads sitting at one side of the tube). Once the supernatant was clean, it was removed and the beads were washed twice with 70% ethanol and then allowed to dry. Once the beads were dry, 18µl of nuclease-free water were added and the beads incubated with the water for rehydration. The tubes were again placed on the magnetic stand until the solution was completely clear. 16µl of the supernatant were transferred to a new tube, which is the sample.

4. Depletion of Ribosomal cDNA with ZapR and R-probes

During this step, the library fragments that have been generated during the previous step are “cleaned” from fragments originating from rRNA. This was

achieved by hybridisation of the rRNA with R-probes, which were then cut by ZapR.

To the libraries, that have been previously generated, 2μl 10X ZapR Buffer, 1μl R-probes (previously incubated in a thermal cycler at 72°C for 2 minutes) and 1.25μl ZapR were added. The tubes were incubated in a pre-heated hot-lid thermal cycler at 37°C for 60 minutes, followed by 10 minutes at 72°C after which the samples were stored at 4°C until the next step.

5. Final RNA-seq library amplification

During the previous step, the library fragments derived from rRNA were cleaved thus leaving only the library fragments of interest. During this step, those library fragments were amplified, and since the barcodes have already been added, a single pair of primers was used to amplify all the libraries.

In order for the library amplification to occur, 26μl Nuclease-free water, 50μl 2X SeqAmp PCR buffer, 2μl Seq Amp DNA polymerase and 2μl PCR2 primer mix were added to the mixture and the samples placed in a thermal cycler using the following program:

94°C 1 minute

98°C 15sec ┐
55°C 15sec ├ 15 cycles
68°C 30sec ┘

4°C forever

6. Purification of final RNA-seq library using AMPure beads

The final step of this protocol is the purification of the final RNA-seq libraries using the AMPure beads as described in step 3. However, it should be noted that I used 100μl of beads.

7. Quantification of the libraries using Agilent Tapestation and Qubit.

Following quantification, the libraries were pooled together into one sample of 10nM. The libraries were sequenced on a HiSeq4000 Next-Generation-Sequencing platform.

It should be noted that for the human samples 100bp Paired-end RNA-sequencing was performed with illumina NextSeq sequencing instrument (HiSeq 4000), while for the murine samples 75bp Paired-end RNA-seq was performed with illumina NextSeq sequencing instrument (HiSeq 4000).

2.9 Cell lines and plasmids

The following cell lines were used:

1) SEM K2 (SEM) cells were cultured in RPMI (Gibco), 1% pen/strep and 10% FCS. SEM cell line was established from a five-year old patient during relapse, this patient did present with MLL-AF4-driven leukaemia at infancy.

2) HEK 293 (HEK) cells were cultured in GMEM (Gibco), 10% FCS, 200mM L-Glutamine (Thermo Fisher Scientific), 1% Penicilin/Strepromyocin, 1% Non-essential amino acids (Thermo Fisher Scientific). The human embryonic kidney 293 cells (HEK) were originally obtained from human embryonic kidney cells that were grown in tissue culture and were immortalised.

3) MS5 cells were cultured in alphaMEM (Gibco), 1% pen/strep, 2mM L-glutamine, 10mM HEPES (Thermo Fisher Scientific), 50µM 2-mercaptoethanol (Thermo Fisher Scientific). The MS5 stromal cell line was derived from murine bone marrow stromal cells.

The following plasmids were used:

Plasmid	Notes for use
pEF1a-MLL-AF4-PGK-eGFP	Lentiviral MLL-AF4 expressing vector
pEF1a-PGK-eGFP	Empty vector for MLL-AF4 experiments
pEFS-NS-Cas9-P2A-eGFP	Lentiviral Cas9 vector
U6-gRNA-P2A-BFP	Lentiviral gRNA vectror
pCMV-DACH1-P2A-gGFP	PiggyBac DACH1 expressing vector
pCMV-rtTA-P2A-BFP	PiggyBac control vectror for DACH1 experiments
pCMV-hyPBase	Hyperactive piggyBac transposase used along with the DACH1 and control vector to allow integration into the genome
psPAX2	2nd generation lentiviral packaging plasmid
pMD2.G	VSV-G envelope expressing plasmid

2.10 Transfection

2.10.1 Transection via nucleofection

Transfection of SEM cells was achieved via nucleofection, using the SF kit (Lonza). 24 hours prior, the nucleofection cells were passaged in a 1:4 ratio. On the day of the nucleofection, cells were counted and $1x10^6$ cells were placed in a 15ml falcon and centrifuged for 5 minutes at 2000rpm. While the samples were spinning, the nucleofection solution was prepared, which contained 100µl of SF solution and 4mg of the plasmid of interest. Following centrifugation, the supernatant was removed and the nucleofection solution (containing the plasmid) was added to the cells. The cells with the solution were transferred into a nucleofection cuvette and the samples were immediately transfected using the DJ100 pulse of a Lonza 4D nucleofector (Lonza). Following nucleofection, 500µl of medium were added to the cuvette and the entire content was transferred to a 6-well plate and 1.5ml of fresh medium (RPMI+10% FCS) were added, before the cells were incubated at 37°C with 5%CO_2.

2.10.2 Transfection with PEI for lentiviral particle production

This protocol was used for the preparation of the MLL-AF4 lentiviral particles and it was performed in the lab of Pablo Menendez.

Prior to the transfection, $2x10^6$ HEK cells were seeded in a 10cm dish with 10ml of HEK cell culture media so that the confluency of the cells on the day of the experiments was around 40-50%.

On the day of the transfection, a plasmid master mix was prepared comprising the viral packaging plasmid pPax2 (8µg), the viral envelop pMD2.4 (4 µg) and the plasmid of interest, 2µg for MLL-AF4 or empty vector, if multiple plates were used then multiple master mixes were prepared. To each tube containing the plasmid mix, 500µl of DMEM (Thermo Fisher Scientific) and 35µl PEI (1µg/µl) (Sigma-Aldrich) were added and the mixture incubated for 20 minutes at room temperature. The DNA/PEI mixture was added to the cells and 4 hours later fresh media was added. The viral supernatant was harvested 48 post-transfection; it was filtered using a 0.45-micron syringe filter (Millipore) and stored at -80ºC.

2.10.3 Transfection with Fugene for lentiviral particle production

Prior to the transfection, $135x10^5$ HEK cells were seeded on a 6-well plate with 2ml of HEK cell culture media. This achieved 40-50% confluence on the day of the transfection.

On the day of the transfection, the following mix was prepared: for each reaction 570 µl of OPTI-MEM serum reduced media (Life Technologies) was mixed with 30µl of Fugene (Promega). The mixture was vortexed and incubated for 5 minutes at room temperature. To the same mixture, the plasmids of interest were added: 2.5µg of plasmid of interest was mixed with 3.6µg psPAX2 and 1.4µg pMD.G. The mixture was vortexed and incubated at room temperature for 15 minutes. The DNA-Fugene mixture was added to the 293T cells in a drop-wise manner and the plate was gently swirled in order to ensure homogenous distribution. The cells were incubated at 37°C and 5% CO2 for 16 hours and the medium was replaced with 2ml of fresh HEK cell media. The supernatant was collected 48 after the first media change and was filtered using a 0.45-micron syringe filter (Millipore) and either stored at -80ºC or further processed with LentiX concentrator.

2.11 Virus concentration

The harvested supernatants containing lentiviral particles for MLL-AF4 and Cas9 were further concentrated. The former with ultracentrifugation and the latter with LentiX (Takara).

2.11.1 Ultracentrifugation

For the ultracentrifugation, the samples were centrifuged at 26000rpm for 2 hours at 4°C using the Beckton Dickinson UltraCentrifuge. This was done in the Menendez lab.

2.11.2 Lenti-X

The lentiviral particles for Cas9 were concentrated using the LentiX system, where, following filtering of the virus, 4.7ml of LentiX were used for 14ml of viral solution and the mixture was incubated for 24 hours at 4°C. Following the incubation, the samples were centrifuged for 2 hours at 1500rpm at 4°C. Following centrifugation, the supernatant was removed, and the pellet was resuspended in 140µl of GMEM and left overnight at 4°C. Finally, the 140µl were aliquoted into Eppendorf's.

2.12 Bacteria transformation and inoculation

Subcloning Efficiency DH5α^{TM} competent cells (Life Technologies) were used for the purposes of this project. Competent cells, which were stored at -80°C, were thawed on ice. For the transformation, 10ng of plasmid were added in a 50μl aliquot of competent cells. The competent cells with the plasmid were incubated for 30 minutes on ice. Following incubation, the cells were placed in a dry bath at 42°C for 30 seconds and then immediately placed on ice for 2 minutes. 200ml of pre-warmed SOC (Life Technologies) were added to the tube and the tubes were incubated at 37°C for 1 hours at 225-220 rpm. Following incubation, 200μl of the mixture were spread on LB agar plates with ampicillin (50 mg/ml) and the plates were left to dry for 5 minutes before being placed overnight at 37°C. After 8 hours, a single colony was picked and placed in LB with appropriate antibiotics and incubated at 37ºC overnight. It should be noted that I used 100ml of LB for a maxi/midi prep, while for miniprep I used 3ml of LB.

2.13 Plasmid DNA purification

2.13.1 HiSpeed plasmid Maxi/Midi kit

For the isolation of large amounts of DNA from competent cell pellets, the HiSpeed Maxi/Midi Kit was used following the manufacturer's instructions. Specifically, the LB culture containing the bacteria of interest was pelleted at 6000xg for 15 minutes at 4°C. The pellet was resuspended in 10ml of P1 buffer and was homogenised. 10ml of P2 were added and the tubes inverted a few times before incubating the mixture for 5 minutes at room temperature. 10ml of pre-chilled buffer P3 were added and the tubes inverted a few times in order for the components to mix and the mixture then incubated at room temperature

for 10 minutes. The lysate was filtered through a pre-equilibrated QIAfilter cartridge and washed with 60ml of buffer QC. The DNA was eluted with 15ml of buffer QF. The DNA was precipitated with the addition of 10.5ml isopropanol, which was incubated for 5 minutes with the eluate. The eluate - isopropanol mixture was placed in a QIAprecipitator and the mixture filtered. 2ml of 70% ethanol were also added to the QIAprecipitator and the ethanol filtered. The membrane of the QIAprecipitator was dried before attaching it to a 1.5ml syringe containing 1ml of TE buffer, which was eluted into a 1ml Eppendorf tube.

2.13.2 MiniPrep kit

For the isolation of small quantities of DNA from competent cells, the Qiagen MiniPrep protocol was used. 3ml of the bacteria were cultured in LB overnight. The following morning, they were pelleted by centrifugation at 8000rpm for 3 minutes at room temperature. The pellet was resuspended in 250µl buffer P1 and transferred into a micro centrifuge tube. 250µl of buffer P2 were added and the contents mixed through by inverting a few times. 350µl of N3 buffer were added and the tube was immediately mixed thoroughly. The tube was centrifuged for 10 minutes at 13000 rpm in a table top micro centrifuge. Following centrifugation, 800µl of the supernatant were transferred to a QIAprep 2.0 spin column and the column centrifuged for 60 seconds at 13000 rpm. The column was further washed with 500µl buffer PB and with 750µl buffer PE. The column was centrifuged for 1 minute in order to remove any residual wash buffer. Finally, the DNA was eluted by the addition of 50µl of buffer EB.

2.14 sgRNA design, cloning and validation

The sgRNA sequences were designed using Chop Chop and were further validated against GeCKO (Labun et al., 2019, Labun et al., 2016, Montague et al., 2014). (https://chopchop.cbu.uib.no/)

The sgRNA were 20 base sequences and to the top strand (+) was added the following sequence -caccG and to the bottom strand (-) was added the following sequence aaac C.

Initially, the backbone was linearised by digesting it with BsbI (NEB) for 3 hours at 37ºC, using the following:

Components	1x
Backbone (1.8µg/µl) Cutsmart Buffer (10x) BbsI dH_2O	0.83µl 5µl 1µl 43.17µl
Total	50µl

Following linearisation, the backbone was separated on a 1% w/v agarose gel. The linearised backbone was excised and column-purified using QIAquick gel extraction kit (Qiagen).

At the same time, the sgRNAs (Table 2.5) were annealed as follows:

Components	1x
Top strand oligo (100 µM) Bottom strand oligo (100 µM) T4 ligation buffer (NEB) 1	9µl 9µl 2µl
Total	20µl

The two oligos were annealed using a heat block starting at 95ºC and ramping down to 25ºC at 5 º/min. Following annealing, the ds-oligos were diluted with EB (Qiagen):

1st dilution: 180µl EB were added to the original annealing mixture (A)

2nd dilution: 137µl EB were mixed with 4 µl of A ds-oligo (B)

3rd dilution: 57µl EB were mixed with 3 µl of B

For the ligation of the backbone with the ds oligo the following were mixed on ice

Components	
Linearised backbone ds-oligo Ligase buffer (10x) T4 ligase H_2O	1µl (=3.7 fmol) 2µl (=14.2 fmol) 1µl 1µl 5µl
Total	10µl

The ligation mixture was left for 1-2h at room temperature. 5µl of the ligation mixture was used for bacteria transformation. Following appropriate purification method, the plasmid DNA was sent for sequencing to ensure correct insertion of the sgRNA. The oligo used for sequencing was: TACGATACAAGGCTGTTAGAGAG

In order to validate the "cutting efficiency" of the sgRNAs, I either had two sgRNAs for the same gene showing the same effect on the phenotype of the cells or I performed TIDE assay. (https://tide.deskgen.com/)

TIDE assay was used to determine the frequency of insertion and deletion in a pool of SEM Cas9-sgRNA transduced cells (Brinkman et al., 2014). For the TIDE assay, SEM Cas9 cells were transduced with sgRNA lentiviral particles and after 30 – 48 hours, genomic DNA was extracted from the transduced cells and from control SEM Cas9 Cells. The following were used for one reaction:

Components	Amount
Genomic DNA 50ng Forward primer (10µM) Reverse primer (10 µM) NEBNext® High-Fidelity 2X PCR Master Mix H_2o	X µl 2µl 2µl 25µl 21- X µl
Total	50µl

The above were placed in a PCR tube and in a thermal cycler at

95ºC 1 minute

95ºC 15sec
58ºC 15sec
72ºC 30sec
} 25 cycles

4ºC forever

Following the PCR reaction, the PCR product was purified using the QIAquick PCR purification kit (Qiagen). The purified PCR product was sent for standard capillary (Sanger) sequencing using one of the TIDE sequencing primers (Table 2.4). The sequencing data were uploaded on the TIDE assay tool. It should be noted that I used a test sample and a control sample. The control sample was used as a template to estimate the frequency of insertions and deletions and therefore the efficiency of the sgRNA.

Gene	Primer F	Primer R
BUB1B sg1	ACCATGAATAATCACCTTTCGG	CTGCACCACAGTGAAATGAAAT
ELOVL1 sg1	TCTCCTTTCCAGAGAGGTTCAG	GTGCTTTTTCCACCAAAGGTAG
SKIDA1 sg1	ACCTCATCATTAAAGGGAAGCA	CGGGGTATTTGCTAAAAATCTG

Table 2.4| TIDE primers used in this study

Gene	sgRNA sequence
APEX1 g1	GTAACGGGAATGCCGAAGCG
APEX1 g2	AATTGACCTTCGCAACCCCA
ASPM g1	AGACCAATTCGAAGCCACAA
ASPM g2	TTCGAAAAGATAGACACCTA
BUB1B g1	GCGGATCATGTCCACGCTTC
BUB1B g2	TCGTTGAGCTAAAACTCGTG
CCNB1 g1	AGGCGCAAAGCGCGTTCCTA
CCNF g1	CGGCCTTCATTGTAGAGGT
CCNF g2	GTGTGGACCGGTACCTGCGG
CENFP g1	AATGTCGCGGTGATTCATGG
CENPF g2	GTTTCAGCTTGACAGTCTCG
DLAT g1	TCTAGAAGCATACCTACCGG
DLAT g2	CTGTTGCGACGAGCGGGAGC
ELOVL1 g1	GTGGGGGGTAAAGATTGCCC
ENC1 g1	ACGATCCAACATTAGACGTG
ENC1 g2	CTGTTCCACACGTCTAATGT
HMMR g1	CGTGTTCTTCTACAGGAACG
HMMR g2	GGGTCATTGAATCGTTTCAA
HSPD1 g1	GGCTTCGAGAAGATTAGCAA
HSPD1 g2	GCTGAACGTCTTCAAGATTC
HSPD1 g3	CGGCTTGCAAAACTTTCAGA
TGA4 g1	AGTAGCCGAACAGCGTGTTG
TGA4 g2	CTCACCATCGGTTCGCCCCG
K F20A g1	AGAAACTACGACATCGTCAT
K F20A g2	CCCCTGCCGTCATGTCGCAA
LMNB1 g1	GCATGAAACGCGCTTGGTAG
LMNB1 g2	CGTAGTGTACGTACAACTAG
NUTF2 g1	TTACGTAAATTGCGCCTAGT
NUTF2 g2	AGTGGGCTGATGGTCCTGCG
RGL1 g1	CAGCCGAGAACTACTGATGA
RGL1 g2	CTGCGAGTCGAACCACTCAG
SK DA1 g1	TGAGCGTGCATTTGGCGGCG
SUV39H2 g1	TTCGGGGAAGACGAGTATCG
SUV39H3 g2	AATCACGTATCTCTTTGATC
TPX2 g1	CATCAACTTACAGGAGATGA
TPX2 g2	ACCGGTTCGTCCTCTTCCTA
TTLL12 g1	CATCATACACGAACAACCGT
TTLL12 g2	TCCCCAGCGTCGAAAACCTG
RPS19	TACCCCCAGCTTCCACAGCG
Negative control	GTAGCGAACGTGTCCGGCGT

Table 2.5 |sgRNA sequences used in this study

2.15 Transduction

2.15.1 Transduction of SEM cells

Transduction of SEM cells was achieved via spinoculation. Specifically, 2x 10^5 SEM cells were placed in a 12-well plate and transduced with lentiviral particles in the presence of polybrene at 1µg/ml (Sigma-Aldrich). SEM cells were then centrifuged at 2000 rpm for 45 minutes and, following centrifugation, 1.5ml fresh media was added.

2.15.2 Transduction of human primary cells

Human foetal liver derived CD34+ cells, approximately 1-2x10^6 cells, were transferred into a 12-well fibronectin coated plate (Corning) and transduced with concentrated virus in the presence of polybrene at 1µg/ml. The cells were left overnight with the virus and the following day fresh media was added.

2.16 Real-time quantitative PCR

2.16.1 cDNA synthesis

Following RNA extraction, cDNA synthesis was performed with iScript™ Advanced (BioRad) cDNA synthesis kit for RT-qPCR following manufacturer's instructions. For a single reaction, the following were added to a PCR tube: 4µl of 5x iScript Advanced reaction mix, 1µl of iScript Advanced Reverse transcriptase, the required amount of RNA template and the reaction mix was

topped up with water to 20µl. If multiple reactions were required, then a master mix for the 5x iScript Advanced reaction mix and iScript Advanced Reverse transcriptase would be prepared. The PCR tubes were placed in a thermal cycler for 20min at 46°C and the reverse transcription reaction terminated by incubating the samples for 1 minute at 95°C.

2.16.2 RT-qPCR

RT-qPCR was performed either using the SYBR Green or TaqMan technology. For SYBR Green, all the primer pairs were validated to ensure 1.8-2.0 efficiency. A master mix was generated for each primer pair as follows:

Component	Amount
cDNA (4ng/ml)	1µl
Forward primer (10nM)	0.5µl
Reverse primer (10nM)	0.5µl
LightCycler® 480 SYBR Green I Master (Roche) or TaqMan Fast advanced master mix (Thermo Fisher Scientific)	5µl
H_20	3µl
Total	10µl

Note: for TaqMan, instead of forward and reverse primer, 1µl of TaqMan assay was used.

Gene - Human	Forward Primer	Reverse Primer
MLL	AATGATCCGCGAGGAGATAGC	GCAGGGAAGAAAGGTGAAGACA
AF4	CTGCGTCTGGACCACTTTCT	ATGACTAGAGCCGAACCCCT
MEIS 1	ATGTGACAATTTCTGCCACCG	CCTGAACGAGTAGATGCCGTG
HOXA9	CCCCATCGATCCCAATAA	CACCGCTTTTTCCGAGTG
RUNX1C	AGCCTGGCAGTGTCAGAAGT	GGGACTCAATGATTTCTTTTACCA
GAPDH	AGCCACATCGCTCAGACAC	GCCCAATACGACCAAATCC
DACH1	TGGAACAAGTTCGCATCCTG	GGTCTAGAACTTGCGTTGGT
IRX1	TCTCAGCCTCTTCTCGC AGATG	GGTCCCCGTATTGGAAC TGGC
TBP	GCA GTG CCC AGC ATC ACT AT	GCA GTG CCC AGC ATC ACT AT
GFP	CAAGATCCGCCACAACATCG	GACTGGGTGCTCAGGTAGTG
	TaqMan Assay	
DACH1	Hs00974297_m1	
PLK1	Hs00983227_m1	
HSPD1	Hs01036753_g1	
ELOVL1	Hs00967955_g1	
BUB1B	Hs01084828_m1	
BACT	Hs01060665_g1	
SKIDA1	Hs01096520_s1	
Gene - Mouse	Forward Primer	Reverse Primer
Skida1	CGC TTA TTT TCG GAG CCT GC	TCT GGT GAC TCG GCT TTG AC
Sell	TAC ATT GCC CAA AAG CCC TTA T	CAT CGT TCC ATT TCC CAG AGT C
Dach1	CCT GGG AAA CCC GTG TAC TC	AGA TCC ACC ATT TTG CAC TCA TT
Mycn	TTGAGCGACTCAGATGATGAGG	AACACAGCGCTTGAGGATCA

Table 2.6 | Primers and TaqMan Assays used for this project

2.17 Statistics and star system

The statistical test used in each experiment is denoted in the caption with the exception of the RNA sequencing data. The normal distribution of the data was ensured using the Shapiro-Wilk normality test with the exception of the RNA sequencing data.

* $p \leq 0.05$

** $p \leq 0.01$

*** $p \leq 0.001$

**** $p \leq 0.0001$

2.18 RNA sequencing analysis pipeline

Raw reads were initially trimmed using Trimmomatic – this was done by the company that performed Next Generation Sequencing. For some of the sequenced libraries, further adaptor trimming was required and for this Trim Galore! (v0.4.5) was used.

(https://www.bioinformatics.babraham.ac.uk/projects/trim_galore/)

The quality of the data was assessed with FASTQC (v.0.11.5). (https://www.bioinformatics.babraham.ac.uk/projects/fastqc/).

The reads were aligned with Kallisto (v0.43.1) (human reads were aligned to GRCh38 and murine data were aligned to GRCm38) (Bray et al., 2016). Kallisto is a pseudoaligner that was developed by the Pachter lab and is a method for quantifying abundances of transcripts for RNA sequencing experiments.

The Bioconductor package Tximport (v.3.5) was used to import transcript-level abundance, estimated counts and transcript lengths and also to summarise them into matrices that are compatible with DeSeq2 (Soneson et al., 2015). For the Tximport, the abundance.h5 was used, which is the output from Kallisto.

The expression level of each gene and the differential expression analysis was performed using the DESeq2 (v.3.5) pipeline (Love et al., 2014). Genes were considered differentially expressed if they had an *adjusted p-value* of less than 0.05.

Gene Set Enrichment Analysis was performed using the GSEA Jana Desktop tool (Subramanian et al., 2005, Mootha et al., 2003).

Gene Ontology analysis was performed using Panther (Mi et al., 2019) .

Heatmaps were generated using Pheatmap.
(https://CRAN.R-project.org/package=pheatmap).

PCAs were generated using either DeSeq2 or pcaExplorer (v.3.6)
(http://bioconductor.org/packages/pcaExplorer/).

HISAT2 (v.2.1.0) was used for the genotyping of the Mll-AF4+ Vec-Cre+ and Mll-AF4-Vec-Cre+ RNA sequencing libraries. This was achieved be creating an index using the human AF4 cDNA sequence.

R version 3.4.3 was used (http://www.rstudio.org/)

Microarray data were analysed with GEO2R

(https://www.ncbi.nlm.nih.gov/geo/geo2r/)

2.19 Lipidome

For the lipidome experiment SEM-Cas9 cells were transduced with sgRNAs for *ELOVL1* and neg control. The transduced cells were sorted at day 2 and 4 following transduction using flow cytometry for live, GFP (Cas9) and BFP (sgRNAs). The sorted cells were span down at 2000rpm for 5 min, the supernatant was removed, and the pellets were stored at -80ºC.

Lipids were extracted in 100% isopropanol (MS grade) and extracts were cleared by centrifugation. 10 ul of lipid extract was loaded onto an Accucore C18 column (150 x 2.1 mm, Thermo Scientific) fitted with a guard column attached to a Thermo Ultimate 3000 BioRS HPLC. The column was equilibrated in 60% buffer A (50 % methanol, 50 % water, 10 mM ammonium acetate, 0.1 % v/v formic acid, 8 µM phosphoric acid) and 40% buffer B (100% isopropanol, 10 mM ammonium acetate, 0.1 % v/v formic acid, 8 µM phosphoric acid) and the following gradient at 500 µl/min was applied (time/%B): 0.3/40, 3.5/45, 7/75, 25/97. Lipids were eluted into a Q Exactive mass spectrometer (Thermo Scientific) in positive mode with a scan range of 150-2000 in MS1 and data-dependent Top5 MS2 (normalised collision energy 25, isolation window 0.8 Da). Other settings were as standard.

Data were processed using Compound Discoverer (Thermo Scientific) with lipid annotations matching an in-house mass list and with MS2 verifications matching an in-house MS2 spectral library.

Chapter 3 Defining the transcriptional profile of LMPPs in wild-type and Mll-AF4 expressing mouse models

3.1 Defining the transcriptional profile of foetal liver and bone marrow-derived LMPPs.

3.1.1 Introduction

Infant leukaemia is rare, however, in the majority of these few patients there is a common disease driver, the fusion between MLL and AF4. This t (4; 11) translocation results in the production of an aberrant fusion protein that is the only molecular abnormality identified in the majority of these patients. In addition to the fusion protein, it has long been speculated that the foetal origin of the disease is also a critical contributor to the aggressive disease phenotype.

To answer this question, Barrett *et al.* performed an investigation on the effects of Mll-AF4 expression in the foetal and adult murine haematopoietic system. In this study, using an Mll-AF4-expressing mouse model, they showed that foetal-derived cells are more prone to transformation by Mll-AF4 compared to their adult counterparts. In particular, they observed that when Mll-AF4 was expressed in E14.5 foetal liver there was a dramatic increase in the B lymphoid output. However, there was little enhancement observed when Mll-AF4 was expressed in adult bone marrow cells. This emphasises the critical contribution of the leukaemia-initiating cell in the disease phenotype. Additionally, in the same study they observed that the greatest impact was observed when the fusion was expressed in the LMPPs, suggesting that they are key contributors to this enhancement and potential cells of origin of the disease (Barrett et al., 2016, Malouf and Ottersbach, 2018).

Following from Barrett *et al.* it is clear that the foetal liver cells are more permissive to transformation by Mll-AF4 compared to adult bone marrow-derived cells. However, we have limited understanding of what makes foetal cells vulnerable to Mll-AF4 while adult cells seem to be more resistant. It has already been established that foetal and adult cells possess fundamentally different characteristics, and one key example is that foetal cells are much more proliferative (Ivanovs et al., 2011, Catlin et al., 2011, Holyoake et al., 1999, Jassinskaja et al., 2017). We can imagine that the difference in the proliferation potential of foetal and adult cells could be a key contributor to this disease. But is that all? Are there other key characteristics?

To answer this question, I performed an RNA sequencing experiment comparing foetal liver and adult bone marrow-derived LMPPs. The aim of this experiment was to define the transcriptional profile of these cells. This experiment will aid in understanding why foetal LMPPs are more prone to transformation by Mll-AF4 compared to their adult counterparts. Additionally, we will get a general idea of how the foetal origin of the disease might influence the disease phenotype.

3.1.2 Experimental design used to define the transcriptional profile of foetal liver and bone marrow-derived LMPPs

In order to define the transcriptional profile of the foetal liver and adult bone marrow-derived LMPPs an RNA sequencing experiment was performed (Fig. 3.1).

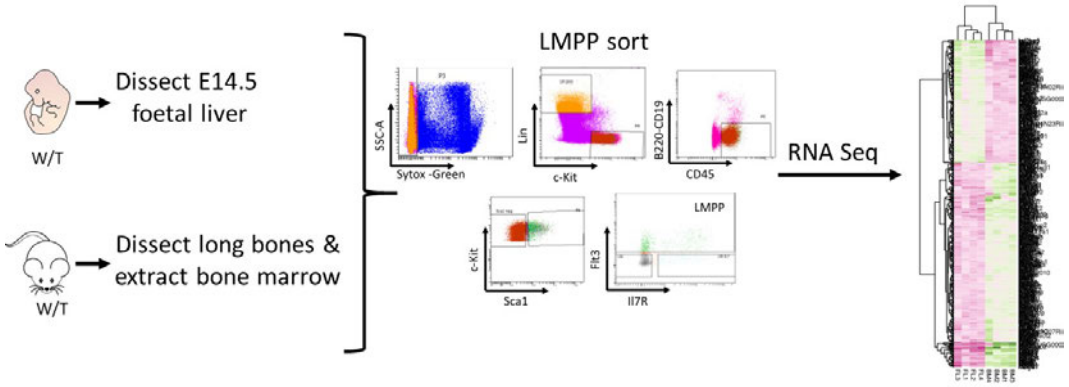

Figure 3.1| Experimental design used to define the transcriptional profile of foetal liver and adult bone marrow derived LMPPs. (Simplified version).

The steps used for this experiment were as follows: 1) dissection of E14.5 foetal liver and adult bone marrow, 2) sorting of LMPPs (Lin- B220- CD19- ckit+Sca1+CD45+ Flt3+), 3) RNA extraction, 4) validation of RNA quality and quantity (only samples with RIN ≥ 8 were used), 5) library preparation for RNA sequencing, 6) libraries/samples were sequenced with the HiSeq 4000 platform, 7) sequencing data quality control and analysis.

For the purposes of this experiment E14.5 foetal liver and adult bone marrow (8-10 weeks) LMPPs were sorted and RNA sequencing libraries were prepared. RNA samples used in this experiment were of the highest quality (RNA integrity number (RIN) ≥ 8) (Fig. 3.2). Four libraries were prepared per condition and these libraries were pooled together and send for sequencing. The Illumina HiSeq 4000 platform was used, and 75bp-paired end sequencing was performed.

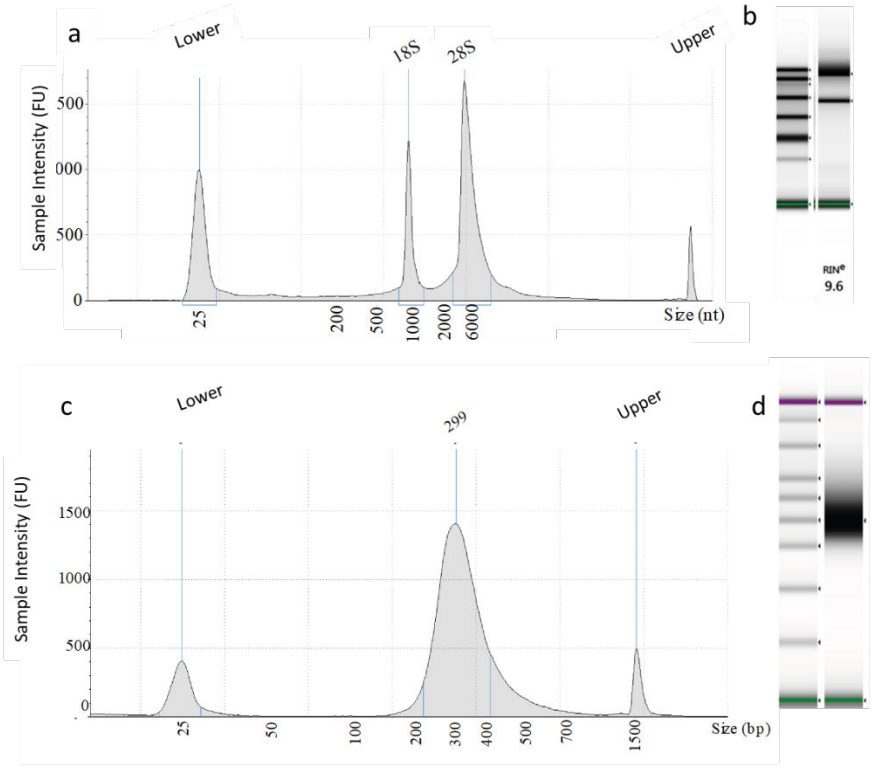

Figure 3.2| Quality control of RNA sequencing libraries - pre sequencing.

a) Electropherogram of one of the RNA samples used to prepare one of the libraries. The abundance of 18S and 28S ribosomal RNA peaks is measured and used to determine the RIN value. b) Gel view of the same RNA sample (second lane) and the ladder (first lane), the RIN of this sample was 9.6. c) Electropherogram of the library prepared using 1ng of the RNA sample. d) Gel view of the same library (second lane) and ladder (first lane).

3.1.3 Quality control of RNA sequencing data

Following an RNA sequencing experiment, the first step is quality control of the data. Initially, it is important to ensure that the raw reads of all the libraries are of good quality and this is a critical step for downstream application. In order to check the quality of the raw reads FASTQC was performed. Following success of FASTQC, the next step was to perform quality control of the libraries in order to ensure consistency between them.

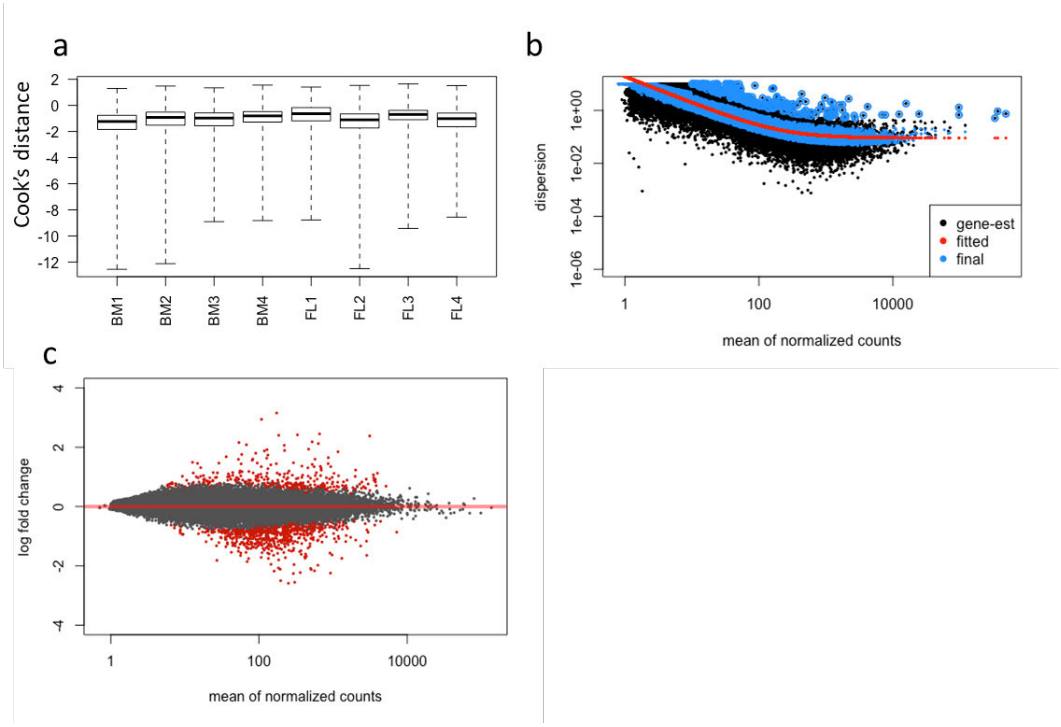

Figure 3.3| Quality control of the RNA sequencing libraries - post sequencing.

a) Boxplot of outliers, b) Dispersion plot, c) MA plot.

Towards this end, Cook's distance was computed for all the samples. Cook's distance measures the influence exerted by each sample on the log fold change (LFC) and how LFC would change if that sample was to be removed. This showed that there were no outliers amongst the samples (Fig. 3.3a). Next, the dispersion was quantified and with this approach it was ensured that there was only a small number of gene outliers (Fig. 3.3b). It can be observed that for the majority of the genes, the final dispersion estimates (blue points) follow the mean dispersion (red line) and only a small number of genes are outliers (larger blue circles at the top of the graph). Finally, by plotting the LFC versus the mean of normalised counts, it can be observed that only a fraction of the genes (dots) are differentially expressed (dots in red) while the majority of them are distributed around 0 on the y-axis (Fig. 3.3c).

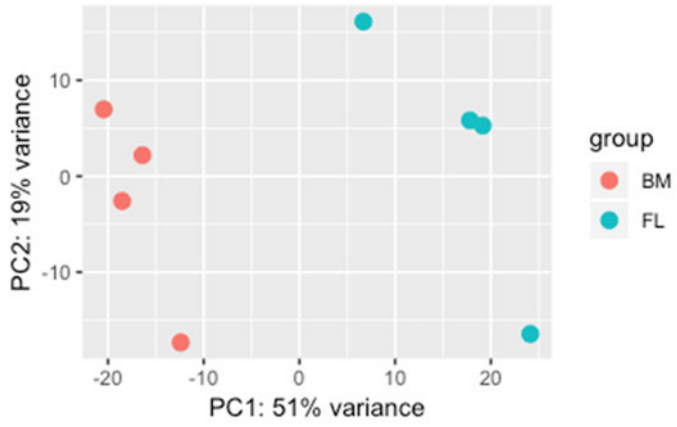

Figure 3.4| Principal component analysis of foetal liver and bone marrow-derived LMPPs.

a) PCA plot of the foetal liver (FL) and bone marrow (BM)-derived libraries reveals a clear clustering of the two population.

Another way to visualise the data is by performing principal component analysis (PCA). PCA revealed a consistency between the libraries of the same population. In particular, we can observe that the foetal liver (FL) and bone marrow (BM)-derived LMPPs form two different clusters, one cluster for each tissue of origin. There is a clear separation between the two clusters in PC1, with PC1 = 51% (Fig. 3.4). Differential expression analysis revealed 768 differentially expressed (DE) genes between the two populations, with 333 upregulated in the foetal liver and 435 in the bone marrow derived LMPPs (Appendix 1). It should be noted that genes were considered DE if the *padj* ≤0.05.

3.1.4 Genes differentially expressed between foetal liver and bone marrow-derived LMPPs

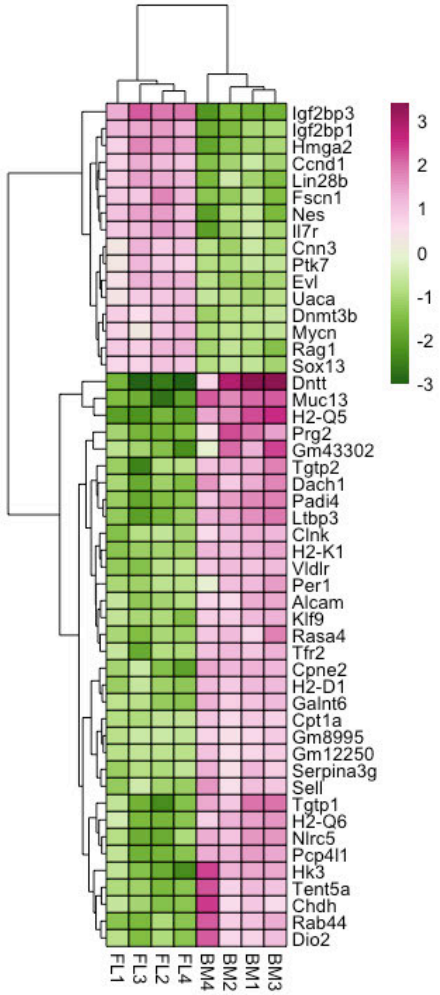

Figure 3.5| Heatmap of the top 50 differentially expressed genes between foetal liver (FL) and adult bone marrow (BM)-derived LMPPs.

The top 50 DE genes are shown in Fig. 3.5. *Lin28b* was upregulated in the foetal-derived LMPPs, while *Dntt* was upregulated in their bone marrow-derived counterparts. The expression pattern of these genes is a critical validation of this experiment as *Lin28b* is known to be uniquely expressed in foetal tissues, while *Dntt* has been to shown to be upregulated in adult tissues (Boiers et al., 2018, Copley et al., 2013).

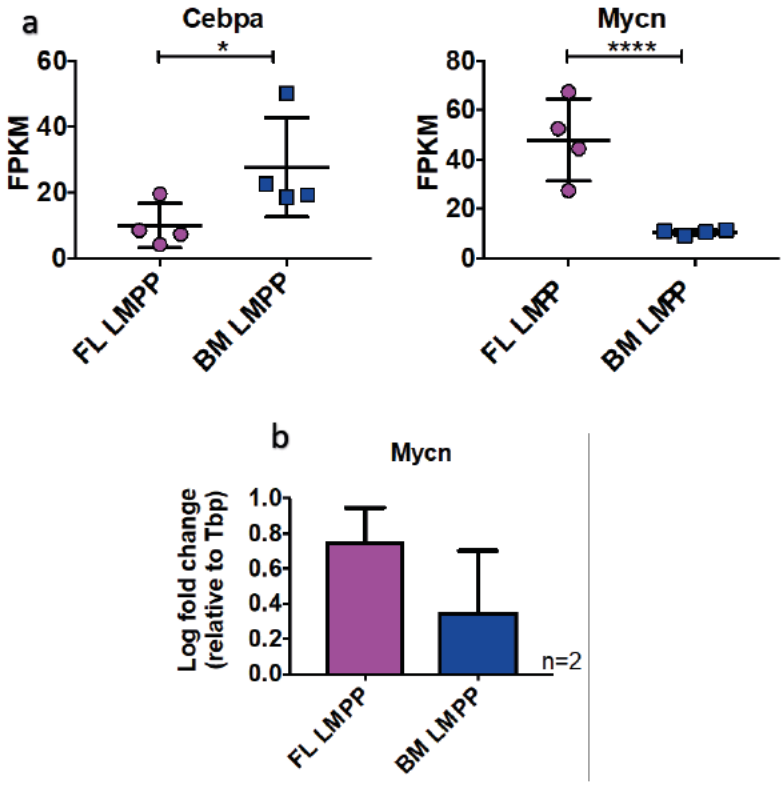

Figure 3.6|Expression of *Cebpa* and *Mycn* in foetal liver and bone marrow-derived LMPPs.

a) Expression of *Cebpa* and *Mycn* in the foetal liver (FL) and bone marrow (BM)-derived LMPPs. RNA sequencing data are shown as mean ±SD, each dot represents a sample. Fragments Per Kilobase of transcript per Million (FPKM). b) qPCR validation of *Mycn* expression. Data are shown as mean + SD.

Additionally, *Cebpa* was upregulated in the bone marrow-derived LMPPs, while *Mycn* was upregulated in the foetal-derived ones (Fig. 3.6). As mentioned earlier, *Mycn* is a downstream target of *Cebpa* and deletion of the latter resulted in expression of the former. Ye *et al.* established *Cebpa* to be of critical importance for the switch from foetal to adult HSCs (Ye et al., 2013). Therefore, the expression pattern of these genes provides further validation to this experiment.

Interestingly, investigation into the top 120 DE genes revealed that a large number of them have previously been linked with cancer or leukaemia were

upregulated in the foetal liver-derived LMPPs (Fig. 3.7a-b). Amongst those genes was *Lin28b*, which is an onco-foetal protein. *Lin28b* has been shown to be over-expressed in aggressive forms of Juvenile myelomonocytic leukaemia (JMML) and AML. Inhibition of this gene impaired leukaemia growth in AML suggesting that it is a potent oncogene (Helsmoortel et al., 2016, Zhou et al., 2017). Other onco-foetal proteins included the Insulin-like growth factor 2 mRNA-binding (IGF2BP) family. *Igf2bp1* has been shown to play a critical role in ovarian cancer and ETV6/RUNX1-driven leukaemia. In both cases downregulation of this gene resulted in growth impairment of the cancer/leukaemia cells (Muller et al., 2018, Stoskus et al., 2016). The second family member, *Igf2bp2* has been associated with colorectal cancer and AML (Ye et al., 2016, He et al., 2018). The last member of the family, *Igf2bp3*, has an established role in promoting lung tumourigenesis. (Zhao et al., 2017, Palanichamy et al., 2016). Intriguingly, *IGF2BP3* has been shown to be overexpressed in MLL-R B ALL. (Zhao et al., 2017, Palanichamy et al., 2016). The High-mobility group AT-hook family of proteins 1 and 2 (Hmga1 and 2) were also upregulated in the foetal liver-derived LMPPs. High expression of both genes has been linked with poor clinical outcome in leukaemia, the former with childhood B-ALL and the latter with AML (Roy et al., 2013, Marquis et al., 2018). Busch *et al.* studied the collective over-expression of *HMGA2*, *LIN28B* and *IGF2BP1* in an ovarian cancer cell model. From this study, it was concluded that this “oncogenic triangle” is critical for cancer initiation and could be used as a promising target for therapeutic treatment (Busch et al., 2016).

Boiers *et al.* showed that *IL7R*-expressing cells are more frequent in the haematopoietic progenitor compartment (CD34+CD45+) derived from human foetal liver as compared to cord blood and bone marrow (Boiers et al., 2018). This is also what has been observed in the present study. *IL7R* has been implicated in paediatric T-ALL and has recently been shown to be a promising therapeutic target for the same disease (Akkapeddi et al., 2019, Zenatti et al., 2011). Cyclin D1 (*Ccnd1*), which is a cell cycle regulator, has been found to be upregulated, amongst others, in hairy cell leukaemia (Bosch et al., 1995). *ID1* overexpression has been established in AML patients. Intriguingly,

deletion of this gene in mouse models resembling infant MLL-AF9-driven AML prolonged their survival whereas the opposite was observed when the same gene was deleted in mouse models representing adult MLL-AF9-driven AML (Man et al., 2016). This study serves as another example of how foetal and adult cells differ and how this can influence not only the disease phenotype but also response to treatment. Other genes upregulated in the foetal liver- derived cells included *Ptk7*, *Fgd5* and *Stc1*, which have been linked with cervical cancer, lung cancer, breast cancer and renal carcinoma, respectively (Sun et al., 2019, Li et al., 2014, Ma et al., 2015, Valla et al., 2017).

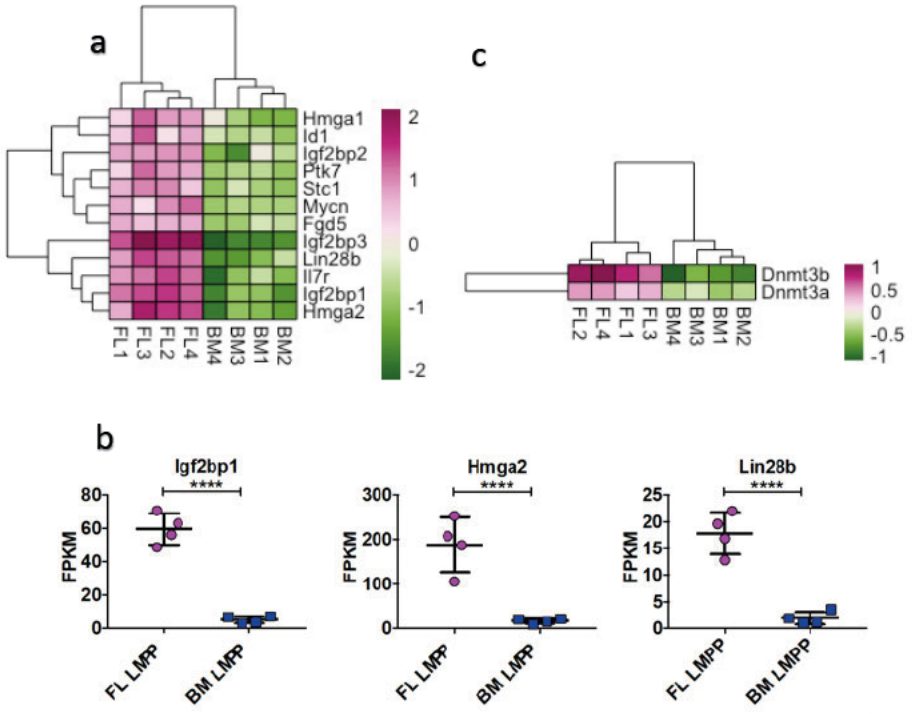

Figure 3.7| Expression of oncogenes upregulated in the foetal liver-derived LMPPs.

a) Heatmap of oncogenes upregulated in the foetal liver-derived LMPPs. b) Expression of genes associated with the "oncogenic triangle". RNA sequencing data are shown as mean ±SD, each dot represents a sample. c) Heatmap of *Dnmt3a* and *Dnmt3b* expression in foetal liver and bone marrow LMPPs.

Dnmt3a and *b* were also upregulated in foetal liver LMPPs (Fig. 3.7c). *Dnmt3a* mutations are frequent in patients with AML and the presence of these mutations has been associated with poor overall survival. These mutations can result in both loss or gain of function and in general affect translation. Mutations in *DNMT3A* do not cause dramatic alterations in the gene expression level or genomic instability and yet they play a critical role in the disease pathogenesis (Ley et al., 2010, Sandoval et al., 2019). *DNMT3B* over-expression has been recently linked with T-ALL and Burkitt's lymphoma were it was shown to exert a tumour promoter function (Poole et al., 2017).

Investigation of the top upregulated genes in the bone marrow-derived LMPPs revealed that some of them had an established tumour suppressor role (Fig. 3.8). *Padi4* and *Aatk* overexpression inhibited cancer cell growth in a number of cancer cell lines (Tanikawa et al., 2009, Haag et al., 2014). *Klf9*, *LNC2* and *TAP1* exerted a tumour suppressor role in colorectal cancer, whereas *Per1* played the same role in breast cancer (Brown et al., 2015, Kim et al., 2017, Ling et al., 2017, Yang et al., 2009). *MYCT1* overexpression led to inhibition of cell proliferation and increased apoptosis in AML cell lines HL-60 and KG-1a (Fu et al., 2018). *Dach1* was also upregulated in the bone marrow-derived LMPPs. Intriguingly, *DACH1* has been shown to act as a tumour suppressor in a number of different cancers. These cancers include hepatocellular carcinoma, lung adenocarcinoma, glioma cells, laryngeal squamous cell carcinoma, colorectal cancer, breast cancer, pancreatic cancer and renal cancer (Cao et al., 2017, Zhang et al., 2018, Liu et al., 2015, Chen et al., 2013, Watanabe et al., 2011, Xu et al., 2017, Bu et al., 2016, Chu et al., 2014).

Although a number of tumour suppressor genes were amongst the top upregulated in the bone marrow-derived LMPPs, some oncogenes were also part of the same list (Fig. 3.8). *Muc13* has been shown to be overexpressed in many cancers and it has been shown to be a promising therapeutic target for colon cancer (Sheng et al., 2017). Additionally, *Ltbp3* expression levels have been linked to the initiation of early metastatic events in a number of different cancers (Deryugina et al., 2018). *Aff3*, which is a member of the same family

as *AF4*, has been shown to be upregulated in breast cancer, and this resulted in resistance of the cancer cells to tamoxifen (Shi et al., 2018). *Itgb5* has also been found to a play role in breast cancer by increasing the tumorigenic potential of breast cancer cells (Bianchi-Smiraglia et al., 2013).

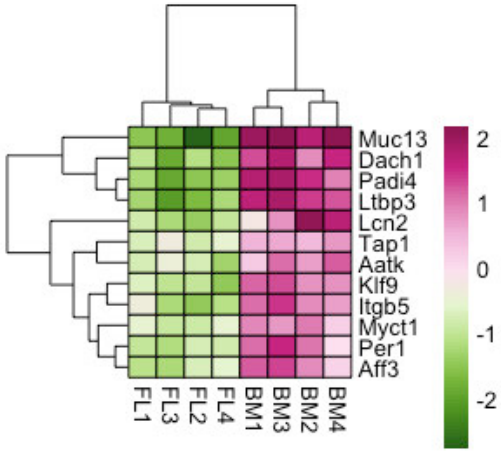

Figure 3.8 | Tumour suppressors and oncogenes upregulated in the bone marrow-derived LMPPs. Heatmap of tumour suppressor genes and oncogenes upregulated in the bone marrow-derived LMPPs.

Another gene that was upregulated in bone marrow LMPPs was *Sell* (Fig. 3.9). *Sell* (CD62L) is a cell adhesion molecule and has been recently described as a marker that can be used to identify human bone marrow-derived LMPPs (Lin-CD34+CD10-CD62L^{h}) (Kohn et al., 2012). Interestingly, in the same study they suggested that there is only a small number of Lin-CD34+CD10-CD62L^{h} in cord blood cells. A similar phenotype was observed in murine systems where it was suggested that CD62L could be used as an alternative to *Flt3* to define murine LMPPs (Cho and Spangrude, 2011). However, we can observe in figure 3.9 that *Sell* is highly expressed in bone marrow derived LMPPs but there is very low expression in their foetal liver-derived counterparts. This expression pattern and in accordance with the previous publications suggests a different role for *Sell* in foetal and adult-derived cells.

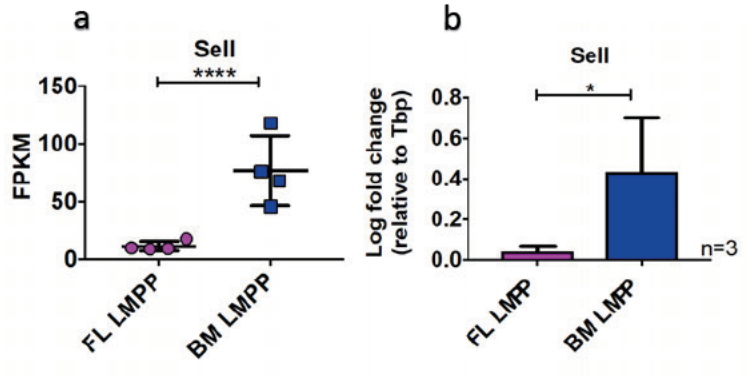

Figure 3.9| *Sell* expression in foetal liver and bone marrow-derived LMPPs

a) *Sell* expression in foetal liver (FL) and bone marrow (BM) LMPPs. RNA sequencing data are shown as mean ±SD, each dot represents a sample. d) qPCR validation of *Sell* expression in foetal liver (FL) and bone marrow (BM) LMPPs, data are shown as mean +SD, Student's t test was performed.

3.1.5 The transcriptional profile of murine foetal liver and bone marrow-derived LMPPs

To obtain a more general idea about the genes differentially expressed between foetal liver and bone marrow-derived LMPPs, gene ontology (GO) analysis was performed. This allowed grouping of genes DE between the two populations into functionally related processes (Fig. 3.10).

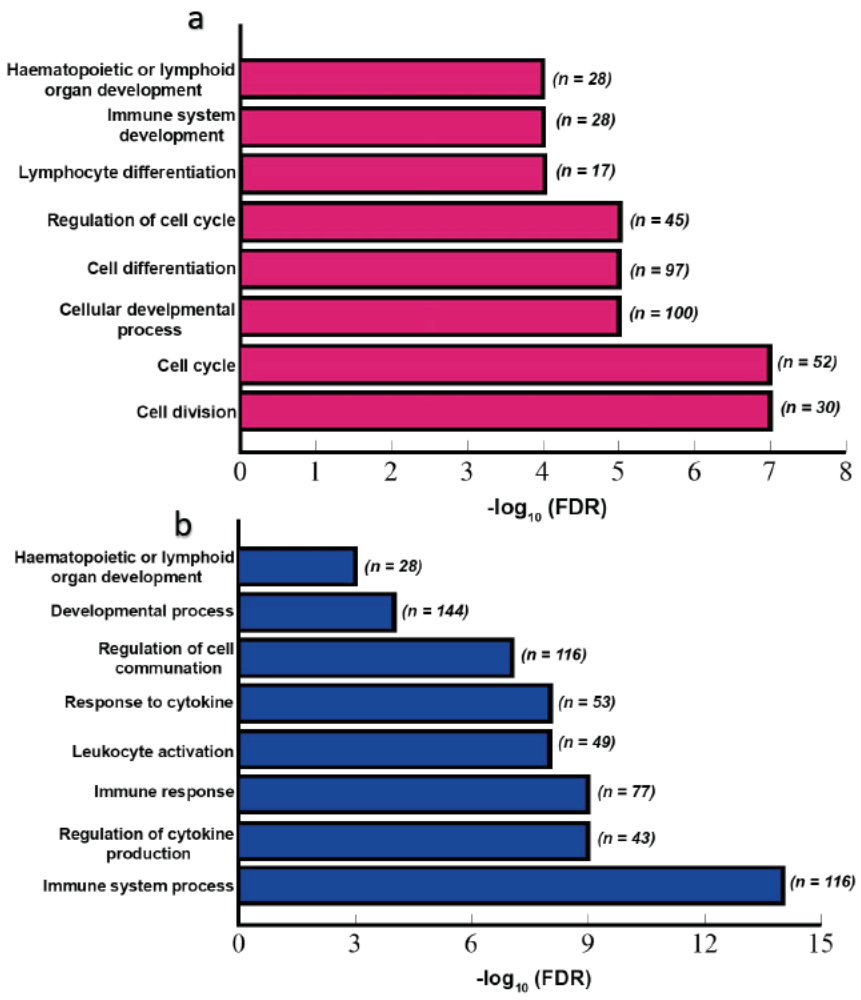

Figure 3.10| Gene ontology of genes differentially expressed between foetal and bone marrow-derived LMPPs.

a) Gene ontology (GO) of genes upregulated in foetal liver LMPPs. (n= number of genes upregulated that are related to the specific process). b) GO of genes upregulated in bone marrow LMPPs. (n= number of genes upregulated that are related to the specific process).

GO revealed that in the foetal liver-derived LMPPs the top upregulated processes were involved in cell cycle/ division and regulation thereof (Fig. 3.10a). Other processes included immune system development and haematopoietic or lymphoid organ development (Fig. 3.10a). On the other hand, bone marrow-derived LMPPs predominantly upregulated processes involved with the immune system (Fig. 3.10b). Intriguingly, the adult cells also upregulated some developmental processes suggesting that those cells still undergo developmental changes.

Surprisingly, the GO process related to haematopoietic and lymphoid organ development was present in both foetal and adult bone marrow-derived LMPPs (Fig. 3.10). In order to further investigate this, I identified the genes that make up this process in both populations (Fig. 3.11). There was no consistency in the genes as they were all members of different families of proteins, except for *Anxa1* and *Anxa2* that were upregulated in bone marrow LMPPs. To further validate this data, the expression of these genes was investigated in a previously published proteomics study where they compared E14.5 foetal liver and adult bone marrow Lin-Sca+c-kit+ cells (LSK) (Jassinskaja et al., 2017). It should be noted that I did not analyse this dataset but the data I show were obtained from an excel spreadsheet the authors provided/submitted with this paper. A number of genes were in common between the two studies (underlined genes) (Fig. 3.11). It should be noted that the majority of the genes that were not in common, were not present in the proteomics study as opposed to having a different expression pattern. From this data, we can observe a different requirement of foetal and adult haematopoietic or lymphoid organ development, which is a reflection of haematopoiesis in general.

GO biological process
Haematopoietic or
lymphoid organ development

FL LMPP		
Plcg2	Pld4	Gimap1
Fubp1	Id2	Il7r
Rag1	Hspa9	Satb1
Card11	Hdac9	Ikzf1
Tcf3	Itm2a	Lfng
Sirpa	Pipk42a	Zfp385a
Ccr9	Mef2c	Pabpc4
Tnfs11	Cd79b	tcf7
Ercc2	Cli3	
Enfa	Itf4	

BM LMPP		
H2-Ab1	Spn	Cebpa
Anxa2	Dnajb9	Bcl2l11
Cdk6	Cd74	Ptpn22
Prg4	Herc6	Sox6
Gata2	Pbx1	Vegfa
Bcl6	Anxa1	Tyro3
Angpt1	B2m	Dnase2a
Tnfaip3	Clec4e	Lmo2
Nkx2-3	Meis1	
Fech	Bcl2	

Figure 3.11| Genes that make up the GO process "Haematopoietic or lymphoid organ development" in foetal liver and bone marrow derived LMPPs.

First box represents genes upregulated in foetal liver (FL) derived LMPPs while the second box represents genes upregulated in bone marrow (BM) derived LMPPs. Underlined genes had similar expression pattern between the present study and the one performed by Jassinskaja *et al.*, 2017. It should be noted that I did not analyse this dataset but the data I show were obtained from an excel spreadsheet the authors provided/submitted with this paper.

Another way to obtain a general idea about the differentially expressed genes between the two populations is to perform gene set enrichment analysis (GSEA). GSEA, similar to GO, groups functionally related genes and allows identification of biological pathways and processes that differ between two populations. The top upregulated pathways in the foetal liver-derived LMPPs were involved in cell cycle, proliferation and growth (Fig. 3.12). In particular, G2M checkpoint was the top upregulated pathway, and this reflects the proliferative nature of the cells. E2F targets were also enriched, and E2F transcription factors have been deemed crucial for regulation of cell cycle progression and tumourigenesis (Bracken et al., 2004). The MTORC1 signalling pathway was also enriched in the same population, wish is a master growth regulator that promotes cellular growth and proliferation (Dowling et al., 2010).

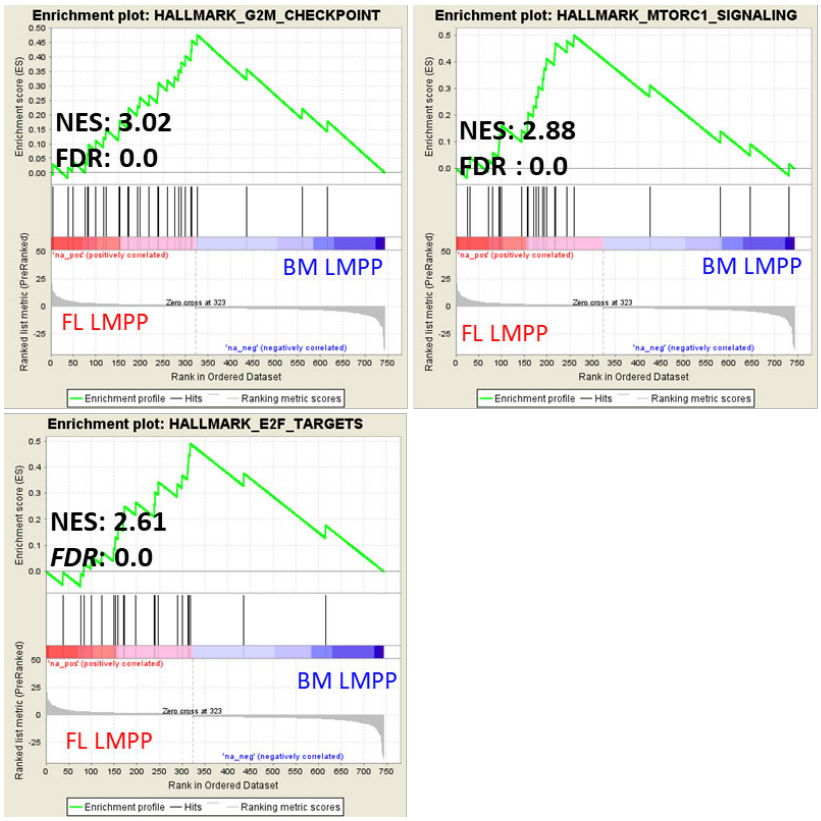

Figure 3.12| Gene set enrichment analysis of foetal liver derived LMPPs (FDR= false discovery rate, NES = normalised enrichment score).

The bone marrow-derived LMPPs showed an enrichment for immune system-related pathways. There was enrichment in interferon-gamma response, interferon-alpha response and TNFA signalling via NFKB. Jassinskaja *et al.* also identified multiple proteins of interferon-alpha signalling pathway to be upregulated in the bone marrow-derived LSK. All the pathways upregulated in the bone marrow-derived cells have established roles in the immune system. This suggests that bone marrow LMPPs have a more mature and immune cell-like transcriptional profile.

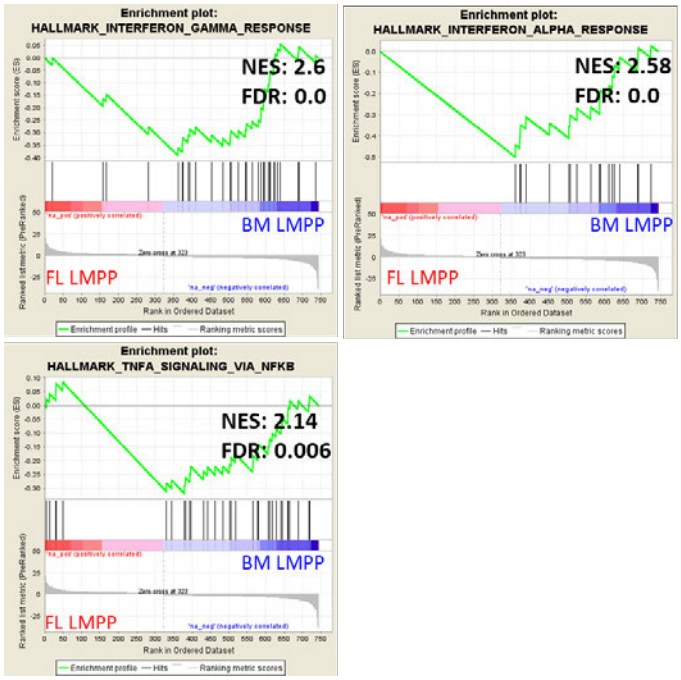

Figure 3.13| Gene set enrichment analysis of genes upregulated in the bone marrow derived LMPPs.

GO and GSEA results were consistent. Foetal liver LMPPs upregulated pathways involved in cell proliferation and growth, while bone marrow LMPPs upregulated pathways that are related to the immune system.

3.2 Molecular characterisation of the initial stages of transformation during the pre-leukaemic state

3.2.1 Introduction

It is well established that MLL-AF4-driven infant ALL arises *in utero* and multiple efforts have been made to capture the early disease stages. This will allow us to understand how MLL-AF4 co-operates with its environment in order to initiate and drive this aggressive infant leukaemia. Barrett *et al.,* using a mouse model where Mll-AF4 expression was conditional to VE-Cadherin (VEC) expression, conducted an investigation into the early disease stages in the developing embryo. In this study, they observed that Mll-AF4 expression in foetal cells led to an increase in B lymphoid output and self-renewal potential. These features were present from as early as the E11.5 AGM but were more pronounced in the E14.5 foetal liver. They also observed that LMPPs were the main contributor to the enhanced B lymphoid output. It should be noted that the median survival of these mice were 437 days and the mice developed B and T cell lymphomas as exemplified by surface markers B220 and CD3 respectively, therefore this mouse model in not representative of the aggressive infant disease. However, in this study, they were able to capture for the first time, a pre-leukaemia state, which was most prominent at E14.5 and define the LMPP as the potential cell of origin of the disease (Barrett et al., 2016).

Having captured a pre-leukaemic stage and identified a potential cell of origin, it would now be possible to examine the early stages of the disease initiation. In order to achieve this, an RNA sequencing experiment was performed where E14.5 Mll-AF4 expressing LMPPs were compared with control LMPPs. The aim of this was to identify early transcriptional changes that take place when Mll-AF4 is expressed.

3.2.2 Experimental design used to define the transcriptional changes induced by Mll-AF4 during the pre-leukaemic state

In order to define the transcriptional profile of Mll-AF4 expressing LMPPs, an RNA sequencing experiment was performed (Fig. 3.14).

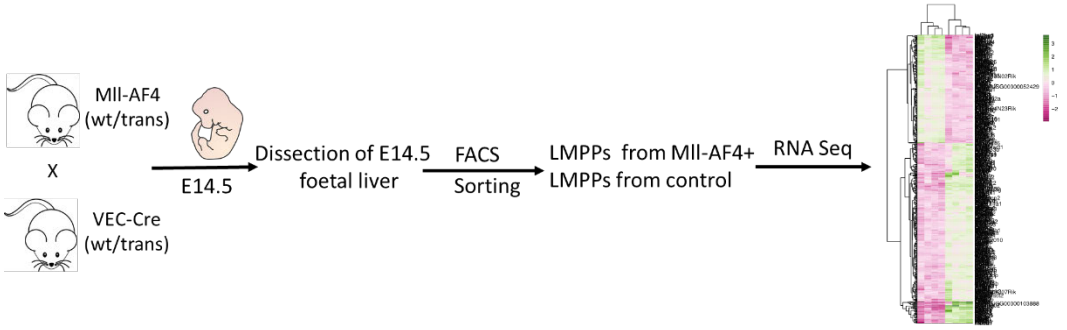

Figure 3.14 | Experimental design used to define the transcriptional prolife of Mll-AF4 expressing foetal liver LMPPs. (Simplified version)

The steps used for this experiment were as follows: 1) Crossing of Cre-conditional Mll-AF4 invertor mouse line with VE-Cadherin Cre-mouse line, 2) Harvesting of E14.5 embryos, 3) Embryo genotyping, 4) Sorting of LMPPs from Mll-AF4+Vec-Cre+ (Mll-AF4+) and Mll-AF4-Vec-Cre+ (control), 5) RNA extraction, 6) validation of RNA quality and quantity (only samples with RIN ≥ 8 were used), 7) library preparation for RNA sequencing, 8) libraries/samples were sequenced with the HiSeq 4000 platform, 9) sequencing data quality control and analysis.

For the purposes of this experiment, the Cre-conditional Mll-AF4 invertor mouse line was crossed with the VE-Cadherin (VEC)-Cre line (Metzler et al., 2006, Chen et al., 2009, Barrett et al., 2016). E14.5 embryos were harvested and genotyped in order to identify embryos that would express the fusion (Mll-AF4+VEC-Cre+) and controls (Mll-AF4-VEC-Cre+). The foetal livers were dissected from embryos with the desired genotype, LMPPs were sorted and RNA sequencing libraries were prepared (as described in the previous section). Four libraries were prepared per condition, pooled together and sent for sequencing. The Illumina HiSeq 4000 platform was used and 75bp-paired end sequencing was performed.

3.2.3 Quality control of the RNA sequencing data

In order to ensure that the correct population was sorted, the first step was to perform a lymphoid colony assay comparing Mll-AF4 expressing HSC/MPPs (haematopoietic stem cells/ multipotent progenitors) with LMPPs. We can observe in Fig. 3.15 that there was a greater number of B lymphoid colonies when LMPPs were plated as compared to HSC/MPPs, thus confirming previous results (Barrett et al., 2016). This difference was persistent between first and second plating.

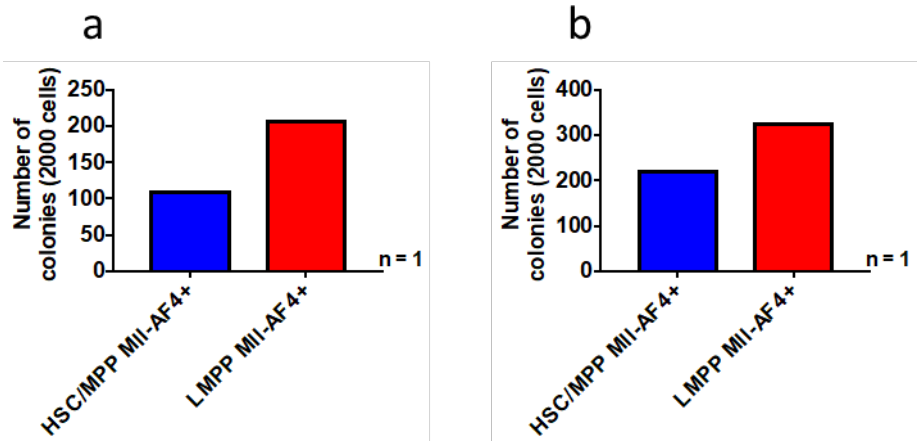

Figure 3.15 | Lymphoid colony assay using Mll-AF4 expressing HSC/MPPs and LMPPs.

a) Number of colonies obtained when 2000 Mll-AF4 expressing HSC/MPPs and LMPPs were plated on methylcellulose under lymphoid conditions, first plating. b) Number of colonies obtained when 2000 Mll-AF4 expressing HSC/MPPs and LMPPs were re-plated on methylcellulose under lymphoid conditions, second plating.

In accordance with the previous RNA sequencing experiment, the first step was to perform FASTQC in order to ensure that the raw reads were of good quality. Following success of the first step, the next step was to perform quality control of the libraries. Initial analysis indicated that one of the libraries was an outlier. Cook's distance was measured, which showed that for sample MA2 Cook's distance was larger compared to that of the other samples (3.16a). This suggests that inclusion of this sample in downstream analysis could lead to

distortion of any statistical tests. Further to this, PCA was performed where it was revealed that in PC1 there was a great difference between sample MA2 and the remaining seven samples (Fig. 3.16b). This data also suggests that sample MA2 is an outlier and this sample was removed from further analysis.

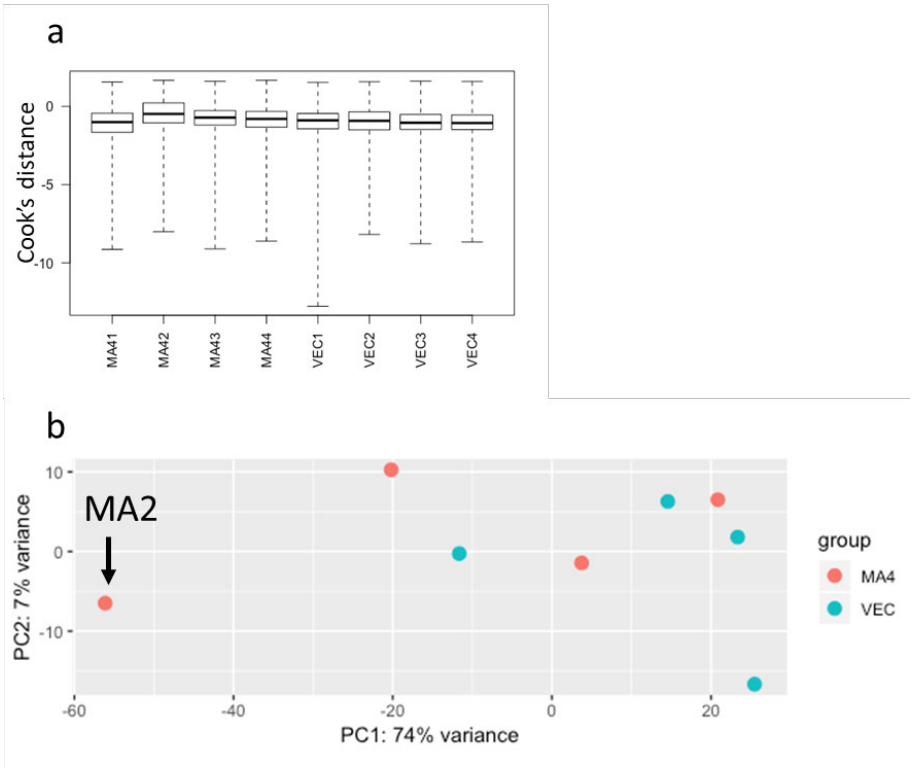

Figure 3.16 | Quality control reveals an outlier amongst the libraries.

a) Cook's distance identified MA2 as an outlier. b) PCA identified MA2 as an outlier.

Following removal of the outlier, quality control of the remaining libraries was performed were the consistency of the remaining libraries was ensured (Fig. 3.17). Even though preliminary quality controlled ensured consistency amongst the libraries, PCA analysis revealed that there was no clear clustering amongst the two populations (Fig. 3.18a).

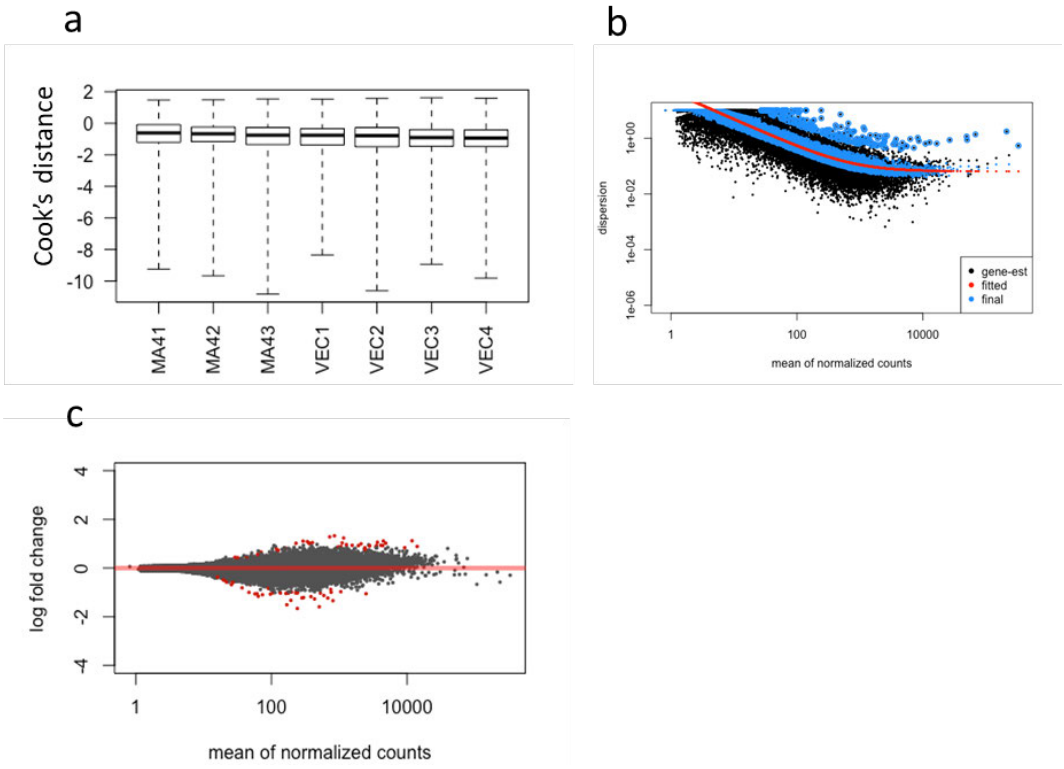

Figure 3.17| Quality control of the RNA sequencing libraries - post sequencing

a) Boxplot of outliers, b) Dispersion plot, c) MA plot.

In order to ensure that this was not due to a technical error during the library preparation and that the genotypes of the samples were correct, the RNA sequencing data were further genotyped using HISAT2. For the purposes of the transcriptional genotyping, the libraries were aligned to the human AF4 cDNA. In theory, the samples with Mll-AF4+VEC-Cre+ genotype will have greater number of aligned reads to AF4 as compared to Mll-AF4-VEC-Cre+ samples. Indeed, following transcriptional genotyping, the results showed that samples with the Mll-AF4+VEC-Cre+ genotype exclusively expressed AF4 (Fig. 318b), suggesting that there was no technical error. From this, it was concluded that there was a small difference between Mll-AF4 expressing and control LMPPs. Differential expression analysis revealed 53 genes DE

between the two populations (Appendix 2). As with the previous RNA sequencing experiment, genes were considered DE if *padj*≤0.05.

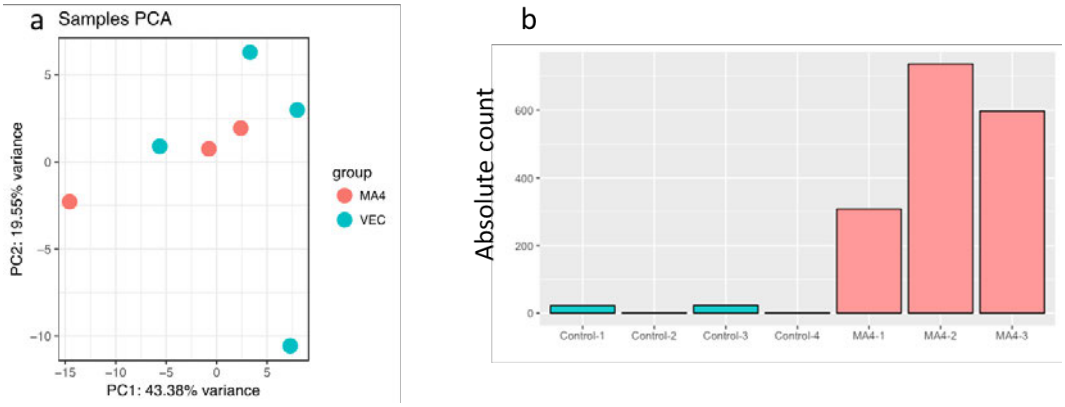

Figure 3.18| PCA plot and genotyping of the Mll-AF4 and control LMPPs RNA sequencing libraries

a) PCA plot of the 7 libraries reveals no clear clustering amongst the libraries Mll-AF4+VEC-Cre+ (MA4) and Mll-AF4-VEC-Cre+ (VEC) samples. b) Transcriptional genotyping of libraries using AF4, Mll-AF4-VEC-Cre+ (Control) and Mll-AF4+VEC-Cre+ (MA4) samples.

3.2.4 Genes differentially expressed between Mll-AF4 expressing and control LMPPs

The differential expression analysis revealed 53 genes differentially expressed between the Mll-AF4 expressing and control LMPPs. Interestingly, *Hoxa9* which has an established role in the disease was upregulated in the Mll-AF4 expressing LMPPs (padj = 0.057) (Fig. 3.19a).

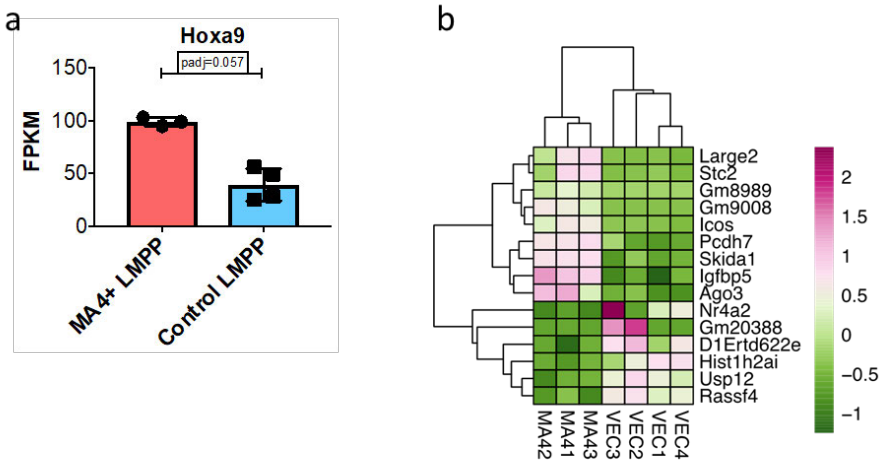

Figure 3.19 | Genes differentially expressed between Mll-AF4 expressing and control LMPPs

a) *Hoxa9* expression in Mll-AF4 expressing (MA4+) and control LMPPs. RNA sequencing data are shown as mean ±SD, and each dot represents a sample library. b) Heatmap of top 10 DE genes between Mll-AF4 (MA4) expressing and control (VEC) LMPPs.

In order to identify genes that are direct targets of the fusion, the genes differentially expressed were compared with data obtained from a previously published MLL-AF4 ChIP-Sequencing experiment. This MLL-AF4 ChIP-seq experiment was performed using the SEM cell line (Kerry et al., 2017). SEM is a cell line that was derived from the peripheral blood of a patient that was diagnosed with MLL-AF4-driven ALL at infancy, but the cell line was derived when the patient relapsed at the age of 5 years old. It should be noted that I did not analyse the ChIP-seq data and the data used were part of a

spreadsheet provided by the authors as part of their publication. Two genes were common in both datasets *Skida1* and *Ago3*. Both *Skida1* and *Ago3* were amongst the top 10 DE genes between Mll-AF4 expressing and control LMPPs (Fig. 3.19-20).

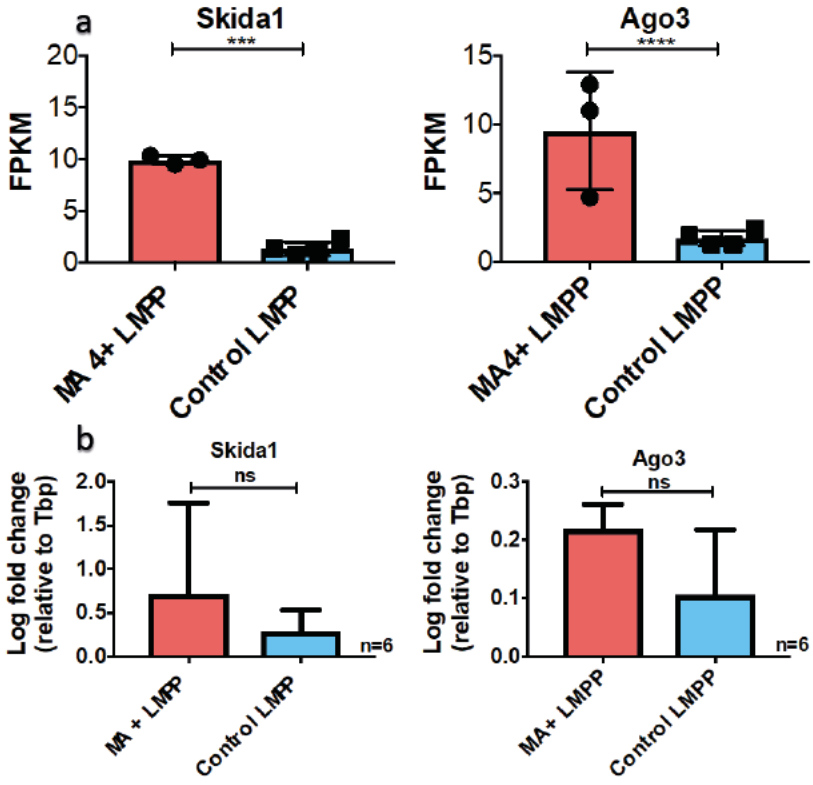

Figure 3.20| *Skida1* and *Ago3* expression in Mll-AF4 expressing (MA4+) and control LMPPs.

a) *Skida1* and *Ago3* expression in Mll-AF4 expressing (MA4+) and control LMPPs. RNA sequencing data are shown as mean ±SD, each dot represents a sample. b) qPCR validation of *Skida1* and *Ago3* expression in MA4+ and control LMPP. Data are shown as mean +SD, Student's t test was performed.

To further validate this data, expression of those genes was investigated in samples from infant patients with MLL-AF4-driven ALL. Munoz-Lopez A *et al*. published a microarray dataset where they compared the transcriptome of blasts derived from infant patients with that of healthy cord-blood derived controls (Munoz-Lopez et al., 2016). In this study, they used three different populations as healthy controls including HSC/MPPs (CD34+CD38-CD19-

CD33-), myeloid progenitor cells (CD34+CD33+) and B-cell progenitors (CD34+CD19+). In order to compare the infant blasts with the healthy controls, the three healthy population were considered as one. Interestingly, *SKIDA1* was upregulated in the infant patients compared to the healthy controls, however, *AGO3* was not (Fig. 3.21).

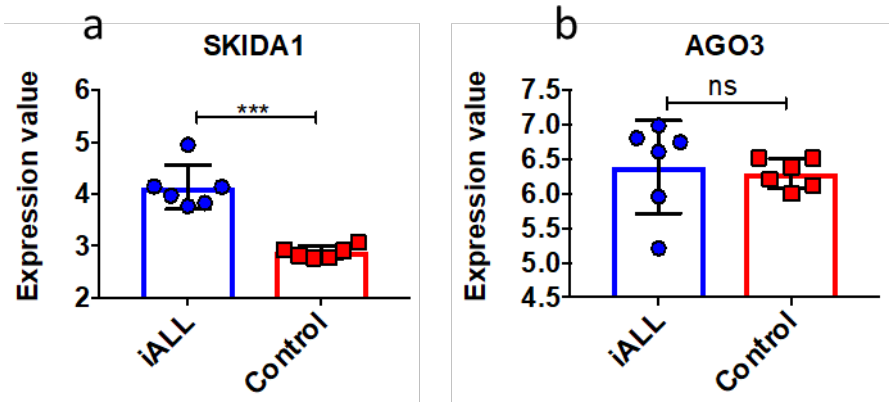

Figure 3.21 | Expression of *SKIDA1* and *AGO3* in the blasts of infant patients with MLL-AF4 driven ALL and healthy controls. (Microarray data) (Data obtained from (Munoz-Lopez et al., 2016).

a) Expression of *SKIDA1* in blasts of infant patients with MLL-AF4 driven ALL (iALL) and healthy controls (Control). b) Expression of *AGO3* in blasts of infant patients with MLL-AF4 driven ALL (iALL) and healthy controls (Control). Microarray data are shown as mean ±SD, and each dot represents a sample.

Following from this, I investigated expression of the two genes in a different dataset published by the same group (Agraz-Doblas et al., 2019). In this study, they performed RNA sequencing of the blasts of 27 infant patients with MLL-AF4-driven ALL and 5 healthy controls. The healthy controls in this study were foetal liver derived CD34+CD19+ cells. Excitingly, *SKIDA1* was differentially expressed between the infant blasts and the healthy controls (Fig. 3.22a). However, *AGO3* was not differentially expressed. It should be noted that I did not analyse this dataset and the authors provided the data I present here. Additionally, I also investigated *SKIDA1* expression in the Andersson *et al*. dataset (Andersson et al., 2015). In this study they performed RNA sequencing of the blasts of 17 infant and 5 paediatric patients with MLL-AF4-driven ALL. I performed differential expression analysis between the infant and

paediatric (> 2 years) patients, and *SKIDA1* was one of the genes differentially expressed between the two populations (Fig. 3.22b).

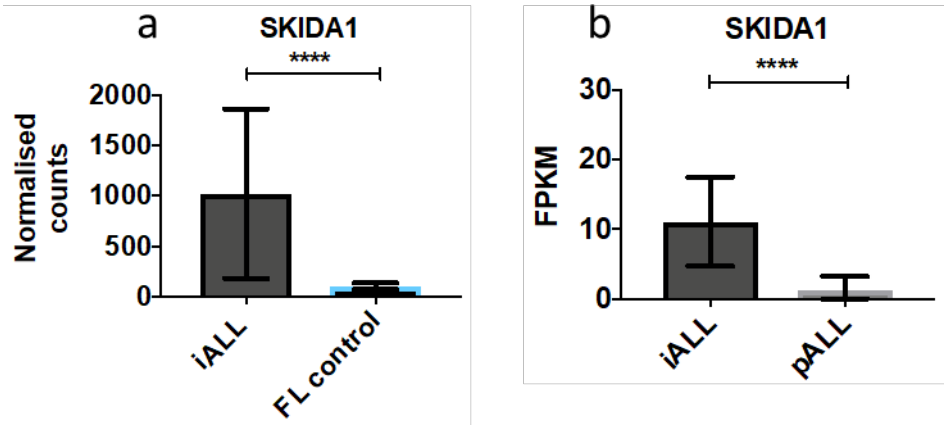

Figure 3.22| Expression of *SKIDA1* in the blasts of infant, paediatric patients with MLL-AF4 driven ALL and healthy controls.

a) *SKIDA1* expression in blasts of infants with MLL-AF4-driven ALL (iALL) and foetal liver (FL control) derived CD34+CD19+ cells, data obtained from (Agraz-Doblas et al., 2019); data are shown as mean ±SD. It should be noted that I did not analyse this dataset and the authors provided the data I present here. b) *SKIDA1* expression in blasts of infant (iALL) and paediatric (pALL) patients with MLL-AF4 driven ALL. Data obtained from Andersson *et al*., 2015. RNA sequencing data are shown as mean ±SD.

SKIDA1 expression pattern is intriguing and suggests that it might play a role in the disease initiation and maintenance. Interestingly, *SKIDA1* upregulation has previously been associated with cancer and leukaemia. In particular, *SKIDA1* (also known as *C10orf140*) expression was positively correlated with *HOXA9* expression in AML patients (Chen et al., 2019). Additionally, *SKIDA1* upregulation has been associated with ovarian cancer and colon adenocarcinoma (Pharoah et al., 2013, Cortes-Ciriano et al., 2017). *SKIDA1* (Ski/Dach domain-containing protein 1) is a member of the Dachshund (DACH) family of proteins. Interestingly, another member of this family, *Dach1* was upregulated in the bone marrow- derived LMPPs compared to the foetal liver derived ones (described in the previous section). While *SKIDA1* expression has been positively correlated with cancer and leukaemia, the opposite is true for *DACH1*, which has been shown to act as tumour

suppressor. The inverse role of these two genes suggests that this family of proteins could play a critical role in the infant disease.

SKIDA1 and *DACH*1 expression was investigated in the SEM cell line where it was shown that expression of both genes was very low, with *DACH1* expression being lower than *SKIDA1* (Fig. 3.23a). To further investigate the role of *SKIDA1* in MLL-AF4-driven ALL, a CRISPR-Cas9 approach was used to achieve a gene knockout. In particular, a SEM-Cas9 expressing cell line was generated which was transduced with sgRNA lentiviral particles targeting *SKIDA1*. The high efficiency of the gene knock-out was ensured using TIDE (Tracking of Indels by decomposition) assay (Fig. 3.23b). However, knockout of *SKIDA1* did not influence the survival of the SEM cells. One key point about these findings is that the SEM cell line was established from a five-year old patient during relapse, although this patient did originally present with MLL-AF4-driven leukaemia at infancy. Therefore, the SEM cell line might not be an accurate representation of the infant disease, which could explain why *SKIDA1* expression was low. However, it could also be that *SKIDA1* is not important for the disease.

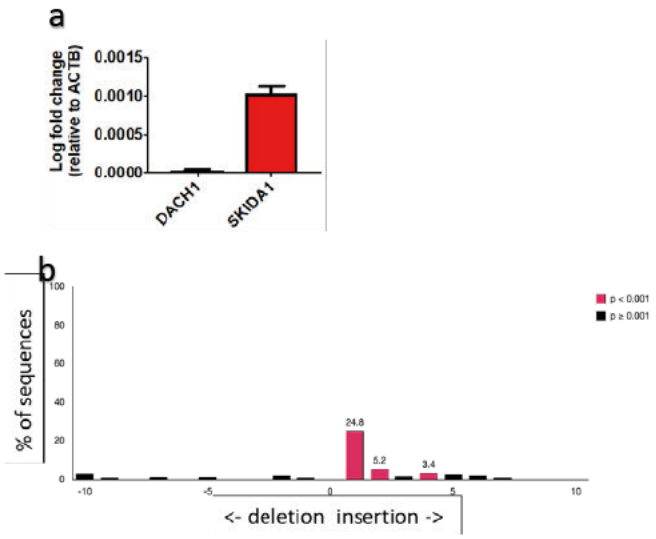

Figure 3.23| Investigation into the role of SKIDA1 in MLL-AF4-driven ALL.

a) qPCR of *DACH1* and *SKIDA1* expression in the SEM cell line. Data are shown as mean +SD, n=1. b) TIDE assay of SKIDA1 sgRNA.

3.3 Discussion

Infant MLL-AF4-driven ALL is a devastating disease with a unique underlying biology, which we do not completely understand. The uniqueness of this disease has been attributed to the foetal origin of the leukaemia-initiating cell. Although, it has long been established that foetal and adult cells are fundamentally different, it was Barrett *et al.* that first established how these differences influence MLL-AF4-driven ALL. In particular, in this study they showed that foetal derived cells are more prone to transformation by Mll-AF4 compared to their adult counterparts. To investigate the underlying reasons for this, the transcriptional profile of foetal liver and adult bone marrow LMPPs was compared.

The transcriptional landscape of foetal-derived LMPPs revealed the proliferative and oncogenic nature of these cells. On the other hand, bone marrow-derived cells upregulated both tumour suppressors and oncogenes, suggesting a more “balanced” nature. From this data, it is clear that the foetal nature of the leukaemia-initiating cell could be a critical factor in the initiation of this aggressive disease. We can imagine that the environment that supports rapid growth of the embryo if hijacked by MLL-AF4 could lead to an aggressive disease.

Having identified the potential role of the cell of origin of this disease in wild type mice, I then investigated what happens when Mll-AF4 hijacks it. In order to investigate the early stages of transformation, I performed an RNA sequencing experiment comparing murine foetal liver Mll-AF4 expressing LMPPs with control LMPPs. Initially, it was observed that the two populations appear very similar and this would explain why the Mll-AF4 mouse model does not develop acute leukaemia. However, *Hoxa9* was upregulated in the Mll-AF4 expressing cells suggesting that in the mouse model some aspects of the disease are recapitulated. Of particular interest was the expression pattern of *Skida1*, which was upregulated in the Mll-AF4 expressing LMPPs. Further

investigation into its expression in a clinical setting revealed that this gene was upregulated in infant patients with MLL-AF4-driven ALL compared to paediatric patients with the same disease and compared to healthy controls. Intriguingly, *DACH1*, another gene of the same family of proteins was downregulated in the infant patients. These findings suggest that this family of proteins could play a role in the initiation and maintenance of the infant disease.

Chapter 4 Defining the transcriptional profile of human foetal and neonatal haematopoietic stem and progenitor cells.

4.1 Defining the transcriptional profile of human foetal liver and cord blood derived HSC/MPPs

4.1.1 Introduction

It has long been speculated that the foetal origin of the leukaemia-initiating cell of infant MLL-AF4-driven ALL plays a critical role in the disease development. In the previous chapter, by defining the transcriptional profile of the cell of origin of the disease in mice, I showed that its over-proliferative and oncogenic nature could contribute to the disease initiation and exert an additive effect to the aggressiveness of this disease. Therefore, we now have a potential explanation of why murine foetal cells are more prone to transformation by Mll-AF4 compared to their adult counterparts.

Due to the fundamental differences that exist between humans and mice, great caution should be taken when projecting conclusions that are true in one species to the other. Following from this, it is important to further confirm and validate that the above findings hold true for human foetal liver-derived cells. Towards this end, an RNA sequencing experiment was performed comparing human foetal liver and cord blood-derived haematopoietic stem and progenitor cells (HSC/MPPs). Additionally, in order to identify the cell of origin of the disease, the transcriptional profile of foetal liver-derived HSC/MPPs was compared to that of LMPPs and the genes differentially expressed were further compared to the targets identified from an MLL-AF4 chromatin

immunoprecipitation sequencing (ChIP-seq) experiment recently published (Kerry et al., 2017)

4.1.2 Experimental design

In order to define the transcriptional profile of foetal liver and cord blood-derived HSC/MPPs (CD34+CD38-CD45RA-), an RNA sequencing experiment was performed (Fig. 4.1).

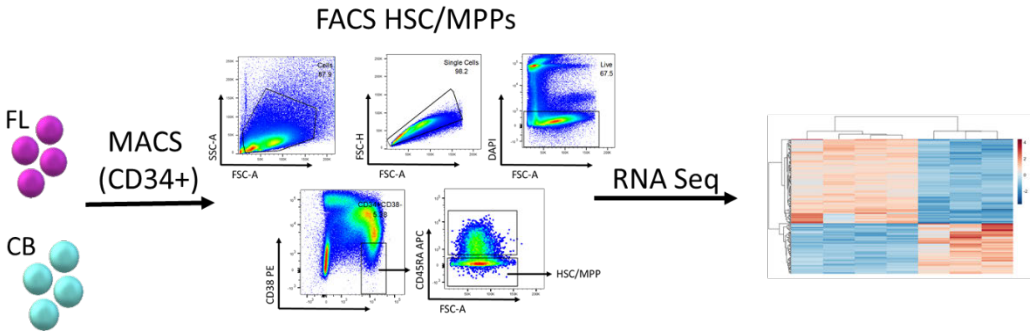

Figure 4.1| Experimental design used to define the transcriptional profile of foetal liver (FL) and cord blood (CB) derived HSC/MPPs (Simplified version)

The steps for this experiment were as follows: 1) dissection of second trimester foetal liver, 2) CD34+ enrichment using magnetic-activated cell sorting (MACS), 3) sorting of HSC/MPPs , 4) RNA extraction, 5) validation of RNA quality and quantity (only samples with RIN≥8 were used), 6) library preparation for RNA sequencing, 7) libraries/samples were sequenced with the HiSeq 4000 platform, 8) sequencing data quality control and analysis.

For the purposes of this experiment, second trimester foetal liver and cord blood-derived samples were used. The samples were initially enriched for CD34 using magnetic-activated cell sorting (MACS). Following from this, the samples were further sorted, using flow cytometry, for HSC/MPPs (CD34+CD38-CD45RA-) and LMPPs (CD34+CD38-CD45RA+). There was a consistency in the percentage of the two populations between foetal liver and cord blood-derived samples (Fig. 4.2).

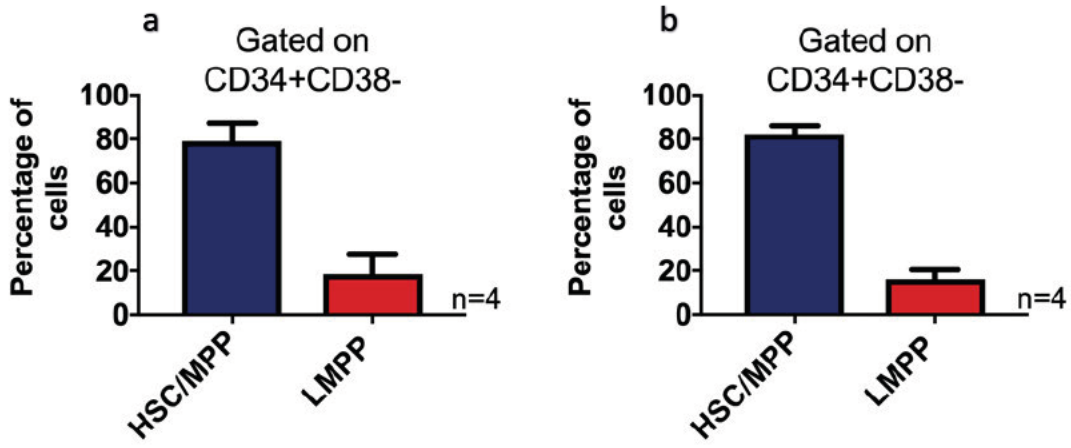

Figure 4.2| Percentage of HSC/MPPs and LMPPs in foetal liver and cord blood samples.

a) Percentage of HSC/MPPs (CD34+CD38-CD45RA-) and LMPPs (CD34+CD38-CD45RA+) in foetal liver samples; gated on cells→ singlets →live→CD34+CD38-. Data are shown as mean +SD. b) Percentage of HSC/MPPs and LMPPs in cord blood samples, gated on cells→ singlets →live→CD34+CD38-. Data are shown as mean +SD.

4.1.3 Quality control of RNA sequencing data

RNA sequencing libraries were prepared as described in the previous chapter. Seven libraries were prepared in total, 4 from the foetal liver and 3 from cord blood-derived HSC/MPPs. The libraries were pooled together and sequenced on the Illumina HiSeq4000 platform. It should be noted that 100bp-paired end sequencing was performed.

In accordance with the previous RNA sequencing experiment, the first step was to perform FASTQC in order to ensure that the raw reads were of good quality. Following success of the first step, the second step was to perform quality control of the libraries. Quality control ensured that there were no outliers amongst the libraries and that there was consistency between them (Fig. 4.3). PCA revealed that there was a clear clustering between the libraries of the same population while there was a nice separation between the two

groups (Fig. 4.3d). Post sort purity check was performed where the high purity of the two populations was ensured (Fig. 4.3e). It should be noted that due to the low number of cells and scarcity of samples, post sort purity check was performed twice, and I assumed that the high purity was maintained in the remaining of the sorted samples. I also ensured expression of cell surface markers used to sort the population where I observed high expression of CD34 and low expression of CD38 (Fig. 4.3f). It should be noted that CD45RA expression could not be checked as due to the presence of multiple transcripts I could not specifically distinguish CD45RA from CD45. Additionally, the expression of CD31 was checked in this experiment where I observed that it was highly expressed in both FL and CB derived samples (Fig. 4.3f). CD31 expression could be indicative of endothelial contaminations in the sorted samples, however, as its expression was high in both foetal liver and cord blood it could be indicative of a different role in the HSPCs compartment. Further experimentation is required to confirm whether CD31 expression is due to contaminants or it is naturally expressed in these populations.

Differential expression analysis revealed 2866 genes differentially expressed (DE) between the two populations, with 1418 upregulated in the foetal liver and 1448 in the cord blood derived cells (Appendix 3). In accordance with the previous RNA sequencing experiments, genes were considered DE if $padj \leq 0.05$.

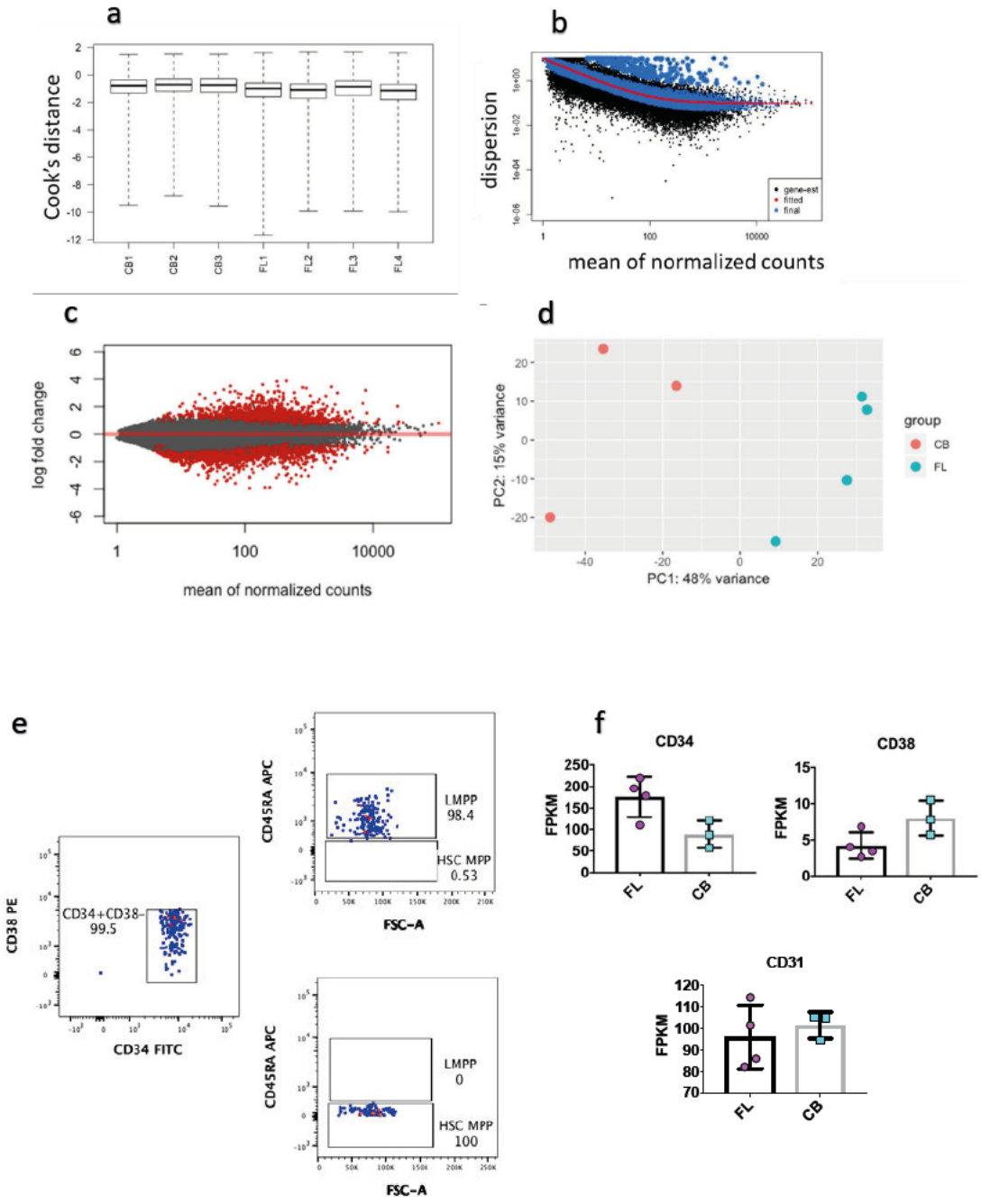

Figure 4.3| Quality control of RNA sequencing libraries.

a) Boxplot of outliers, b) dispersion plot, c) plot MA, d) PCA plot, e) post-sort purity check FACS plot, f) post-sort purity check expression of CD34, cD38 and cD31. RNA sequencing data are shown as mean ± SD, each dot represents a sample.

4.1.4 Genes differentially expressed between foetal liver and cord blood-derived HSC/MPPs

The top 30 DE genes between the two populations are shown in Fig. 4.4. As expected, developmental gene *LIN28B* was amongst those genes, providing validation for this experiment.

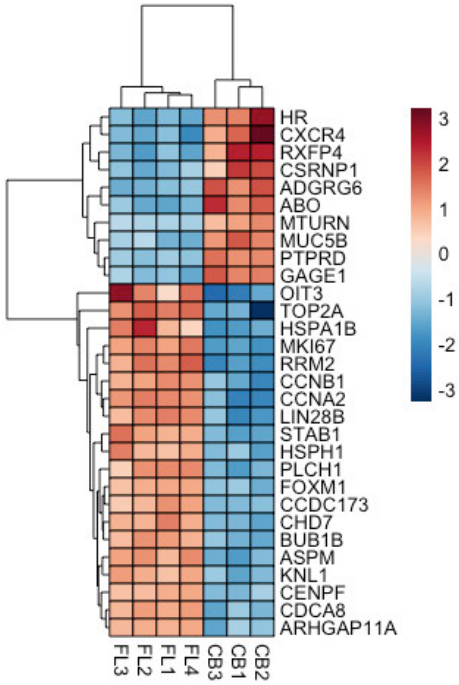

Figure 4.4| Heatmap of the top 30 differentially expressed genes between foetal liver (FL) and cord blood (CB)-derived HSC/MPPs.

Interestingly, the top upregulated gene in the foetal liver-derived cells was *MKI67*, which is a known marker of proliferation. To further investigate the proliferative nature of these cells, I examined the expression of genes that are known to be involved in cell cycle regulation and progression.

Key cell cycle regulators, cyclins (CCN) and cyclin-dependent kinases (CDK) were amongst the DE genes (Fig. 4.5a). The majority of CCNs and CDKs were upregulated in the foetal-derived cells.

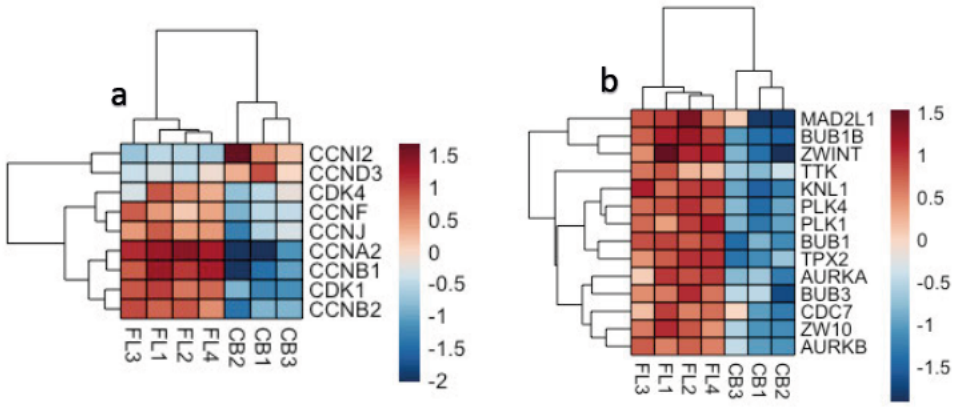

Figure 4.5| Cell proliferation is a predominant feature of the foetal liver-derived cells.

a) Heatmap of cyclins (CCN) and cyclin-dependent kinases (CDK). b) Heatmap of other genes critical for cell cycle/division.

Of critical importance is the *Cyclin B – CDK1* complex as its activation marks initiation of mitosis (Solomon et al., 1990, Atherton-Fessler et al., 1994). Cyclin A2 (*CCNA2*) has been shown to activate two different CDKs, *CDK2* during S phase and *CDK1* during G2 to M (Pagano et al., 1992). Another Cyclin that plays a role in cell cycle transition is Cyclin F (*CCNF*) as its overexpression leads to an increase in the number of cells in the G2 phase of the cell cycle (Bai et al., 1994). Cyclin-dependent kinase 4 *(CDK4*), has been shown to be important for the G1 phase of the cell cycle (Sherr, 1996). Cyclin I-like 2 (*CCNI2*) was upregulated in the cord blood-derived cells, and knockdown of this gene has been shown to decrease cell proliferation (Liu et al., 2017). Cyclin D3 (*CCND3*) also plays a critical role in cell proliferation, as it is required for the G1/S transition (Bartkova et al., 1998). However, not all cyclins play the same role. Cyclin J (*CCNJ*), which was upregulated in the foetal liver-derived cells, has been shown to be essential for *Drosophila* embryogenesis (Kolonin and Finley, 2000). In particular, Kolonin *et al.* established the importance of

this cyclin for the early developmental stages where rapid cell division is a key feature (Kolonin and Finley, 2000).

During M phase, the replicated chromosomes segregate into daughter cells. This is a highly orchestrated process safeguarded by multiple mechanisms. A number of genes involved in this aspect of cell cycle/division were also upregulated in the foetal liver-derived cells (Fig. 4.5b), including, the *ZW10* and *ZWINT* genes, which are critical for the fidelity of chromosome segregation (Williams et al., 1992, Wang et al., 2004), and Aurora kinases A and B (*AURKA* and *AURKB*) that regulate chromosomal alignment and segregation (Chan and Botstein, 1993, Yang et al., 2000, Schumacher et al., 1998). Downstream targets of AURKA, including *PLK1* and *TPX2* (Fig. 4.5b and 4.6a), members of the spindle assembly checkpoint (SAC), including *BUB1*, *BUB1B*, *BUB3* and *MAD2L1* (Fig. 4.5b), as well as cohesins and condensins were also upregulated in the foetal liver-derived cells (Fig.4.6b).

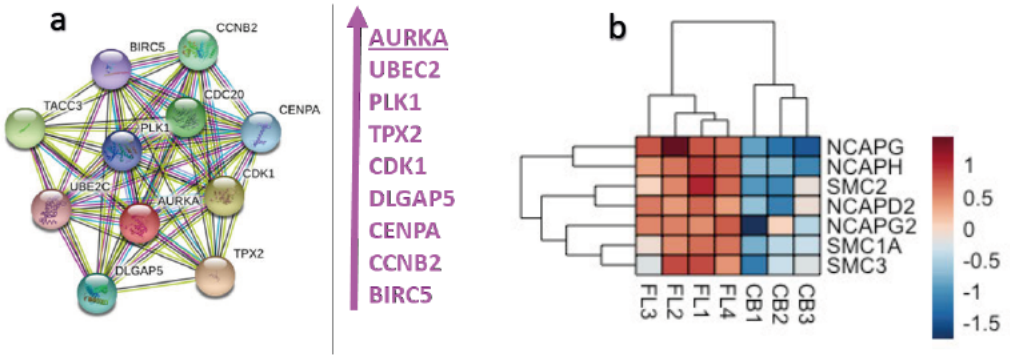

Figure 4.6| Genes involved in cell division upregulated in the foetal liver-derived cells.

a) AURKA and its protein interactome, list of genes that were upregulated in the foetal liver derived HSC/MPPs (Graph obtained from string-db.org). b) Heatmap of cohesins and condensins.

The over-proliferative nature of the foetal cells was further validated with functional assays. CD34+ cells derived from foetal liver and cord blood were placed in methylcellulose assays and liquid cultures. In both, there was a greater number of colonies/cells obtained from the foetal liver-derived samples (Fig 4.7).

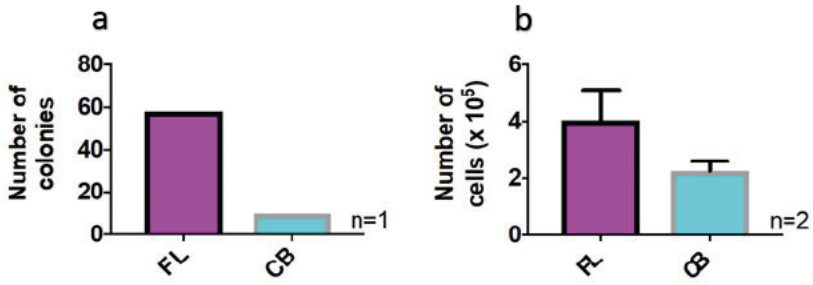

Figure 4.7|Clonogenic and proliferation assays comparing foetal liver and cord blood-derived CD34+ cells.

a) Methylcellulose assay, number of colonies obtained from 2000 CD34+ foetal liver (FL) and cord blood (CB)-derived cells after 14 days in culture. b) Proliferation assay, number of cells obtained from 1000 CD34+ foetal liver (FL) and cord blood (CB)-derived CD34+ cells after 21 days in culture. Data are shown as mean +SD.

Amongst the genes upregulated in the foetal liver-derived cells were Topoisomerase II A (*TOP2A*) and Poly (ADP-Ribose) Polymerase 1 (*PARP1*) (Fig. 4.8). These genes code for enzymes that appear to play a central role in chromosomal translocations. Use of Topoisomerase II poisons, which are potent anticancer drugs, has been shown to induce therapy-related MLL-R acute leukaemias (DeVore et al., 1989, Cowell and Austin, 2012), whereas, *PARP1* has been shown to be a critical mediator of chromosomal translocation as inhibition of PARP1 protein repressed chromosomal translocations (Wray et al., 2013).

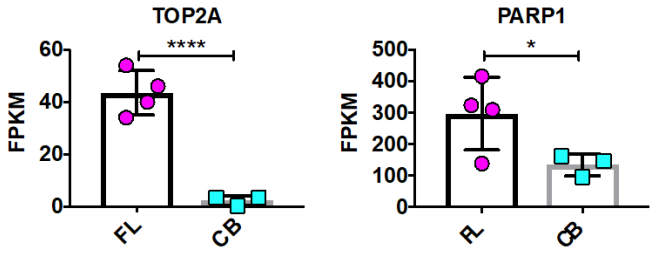

Figure 4.8| Expression of *TOP2A* and *PARP1* in foetal liver (FL) and cord blood (CB)-derived HSC/MPPs. RNA sequencing data are shown as mean ± SD, each dot represents a sample.

In the previous chapter it was shown that murine foetal liver LMPPs upregulate a large number of genes that have previously been linked with cancer or leukaemia. Interestingly, the same is true for the human foetal liver-derived HSC/MPPs; however, the presence of such genes is more prominent in this experiment. In particular, amongst the top 25 DE genes, 12 genes have previously been associated with cancer or leukaemia (Fig. 4.9).

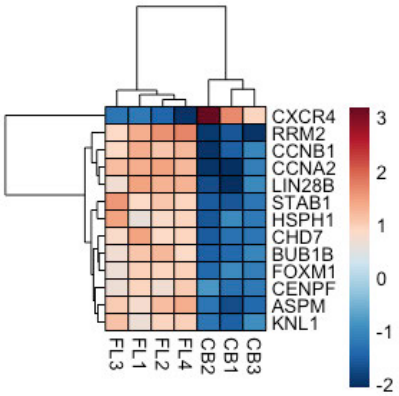

Figure 4.9| Heatmap of genes that have been previously linked with cancer or leukaemia.

Genes upregulated in the foetal liver-derived cells included *LIN28B* which, as mentioned, was overexpressed in JMML and AML (Helsmoortel et al., 2016, Zhou et al., 2017). *RRM2* has been shown to be frequently overexpressed in colorectal and prostate cancer and to confer drug resistance to cancer cells

(Grade et al., 2011, Mazzu et al., 2019). *FOXM1* was upregulated in a number of cancers including liver, lung and paediatric pre-B ALL (Gusarova et al., 2007, Kim et al., 2006, Buchner et al., 2015). Downstream targets of *FOXM1*, *CCNB1* and *CCNA2* were also upregulated in the foetal liver-derived cells and have been shown to be important for AML (Nakamura et al., 2010). *STAB1* plays a critical role in breast cancer, glioblastoma and AML (Riabov et al., 2016, David et al., 2012, Chuang et al., 2015). *HSPH1* expression was positively correlated with B cell non-Hodgkin lymphoma where it was shown to promote stabilization of *Bcl-6* and *c-Myc* (Zappasodi et al., 2015). *CHD7* overexpression promoted glioblastoma, while *CENP-F* has been associated with poor prognosis in breast cancer (Machado et al., 2019, O'Brien et al., 2007). *ASPM* and *BUB1B* were shown to be upregulated in gliomas and relapsed paediatric B ALL (Bikeye et al., 2010, Xu et al., 2019, Chow et al., 2017, Ma et al., 2017). *KLN1* was upregulated in colorectal cancer (Bai et al., 2019). *CXCR4*, a gene that has been shown to play a critical role in a number of cancers including head and neck, glioblastoma and AML, was upregulated in the cord blood- derived cells (De-Colle et al., 2018, Richardson, 2016, Zhang et al., 2017). CXCR4 expression in CD34+ cells derived umbilical cord blood has been well documented and it has been shown to be important for homing and engraftment of these cells (Ramirez et al., 2013).

In addition to these genes, proto-oncogenes *MYC* and *MYNC* were also upregulated in the foetal liver-derived cells (Fig. 4.10a). Interestingly, GSEA revealed that there was an enrichment of *MYC* targets in the foetal liver-derived cells (4.10b). It is well established that mis-regulation of proto-oncogenes is a prominent feature of aggressive types of cancers and leukaemias including MLL-AF4-driven infant ALL (Stumpel et al., 2012).

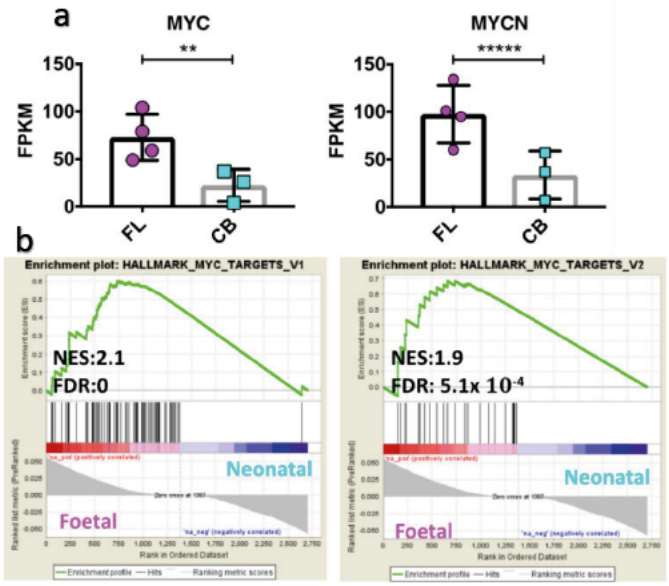

Figure 4.10| MYC and its targets were upregulated in the foetal liver-derived HSC/MPPs.

a) Expression of MYC and MYCN in foetal liver (FL) and cord blood (CB)-derived HSC/MPPs. RNA sequencing data are shown as mean ±SD, each dot represents a sample. b) GSEA plot for MYC targets 1 and 2.

Contrary to the transcriptional profile of the foetal cells, the neonatal cells upregulated a number of tumour suppressor genes (Fig. 4.11). Interestingly, *DACH1* was one of these genes. *Dach1* was also upregulated in the murine bone marrow-derived LMPPs compared to the foetal liver-derived ones. Other tumour suppressor genes included *IGFBP5*, *PTPRD* and *CSRNP1* (Rho et al., 2008, Veeriah et al., 2009, Wang et al., 2013)

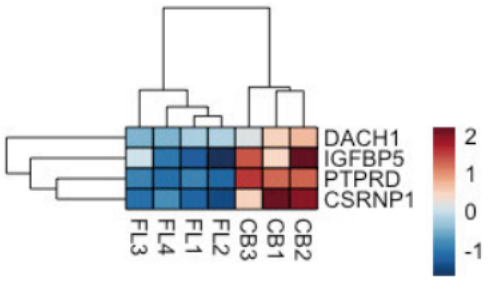

Figure 4.11|Heatmap of tumour suppressor genes upregulated in the cord blood derived samples.

4.1.5 The transcriptional profile of foetal liver and cord blood-derived HSC/MPPs

To obtain a general idea about the transcriptional profile of the foetal liver and cord blood-derived cells, GO and GSEA was performed. Both GO and GSEA group functionally related genes, and this approach allows identification of biological pathways and processes that differ between two populations.

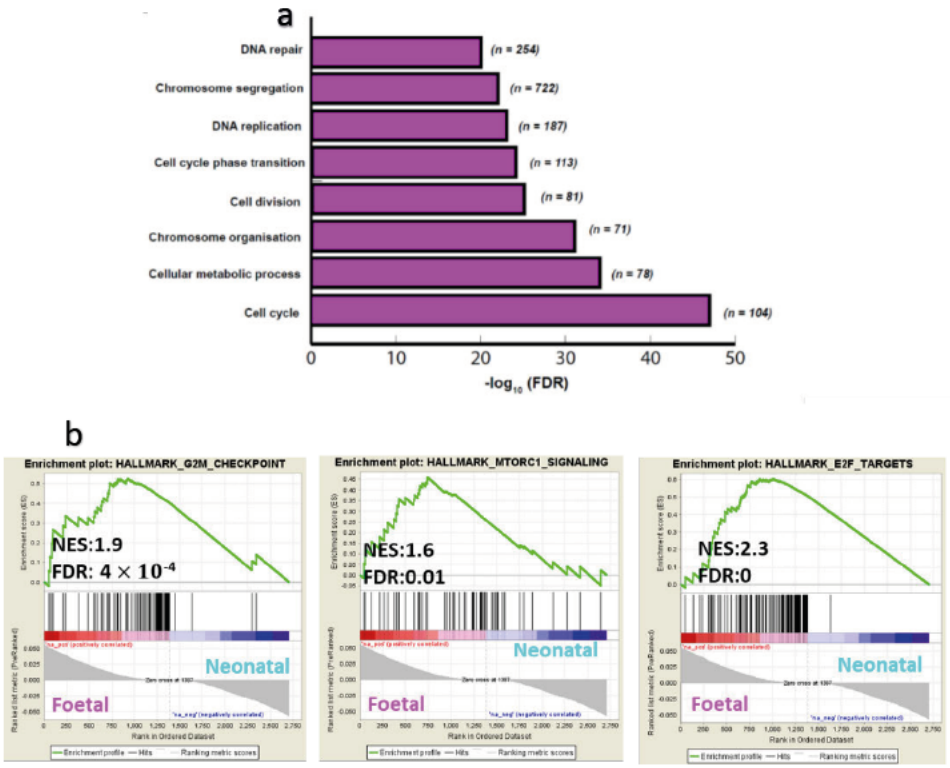

Figure 4.12|GO and GSEA of genes upregulated in the foetal liver-derived HSC/MPPs.

a) GO of processes upregulated in the foetal liver-derived HSC/MPPs. n= number of genes upregulated for a specific process. b) GSEA of pathways upregulated in the foetal liver-derived HSC/MPPs.

Similar to the murine data, GO and GSEA revealed an enrichment of pathways and processes involved in cell proliferation and growth in the foetal liver-derived cells such as G2M, E2F for cell proliferation and MTORC1 for growth (Fig. 4.12). Interestingly, there was a higher number of genes involved in these processes compared to the murine data. It can be observed that there was an

upregulation of processes involved in chromosome segregation and chromosome organisation, which also relate to the proliferative nature of the cells. Additionally, a number of processes involved in cellular metabolism and DNA repair were also enriched in this population.

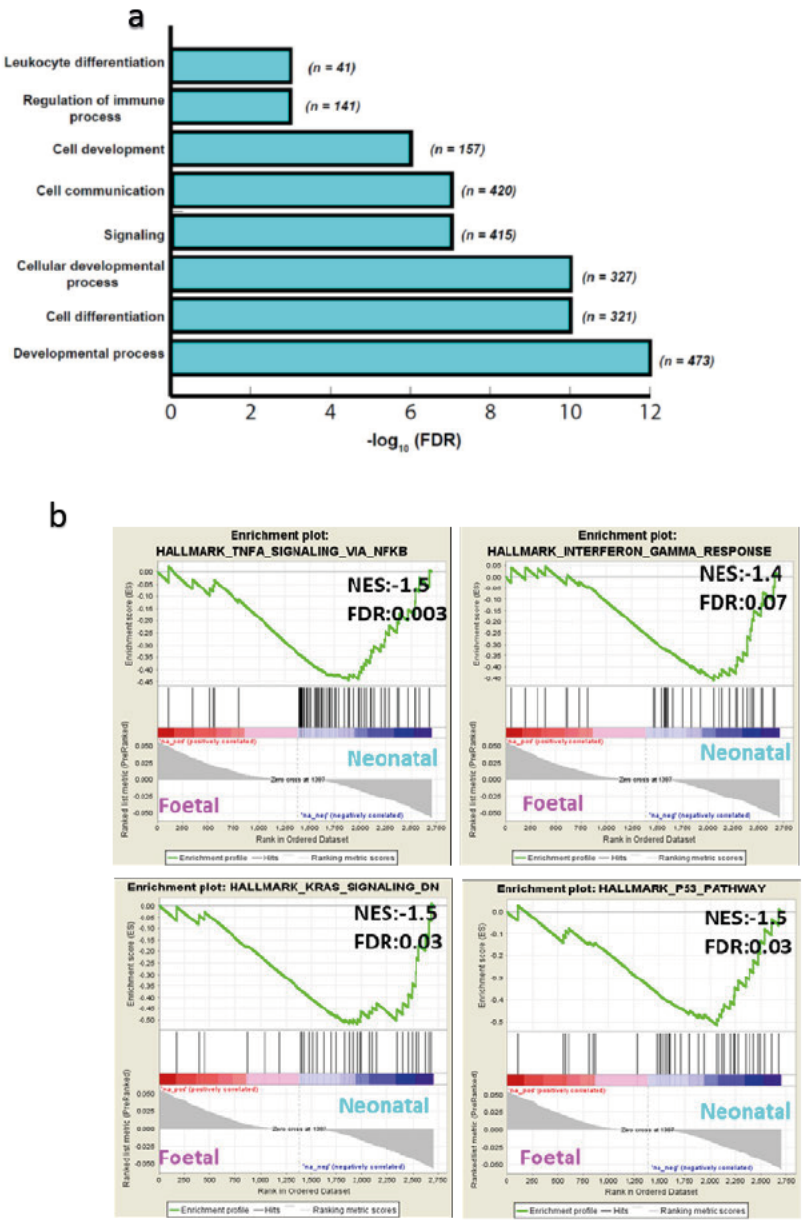

Figure 4.13| GO and GSEA of genes upregulated in the cord blood-derived HSC/MPPs

a) GO of processes upregulated in the cord blood-derived HSC/MPPs. n= number of genes upregulated for a specific process. b) GSEA of pathways upregulated in the cord blood-derived HSC/MPPs.

GO and GSEA of the genes upregulated in the cord blood-derived cells were in line with the murine experiment (Fig. 4.13). In particular, GO and GSEA revealed an upregulation in processes and pathways related to the immune system including TNFA signalling via NFKB and interferon gamma response. In accordance with the murine data, there were also some developmental processes upregulated. Interestingly, GSEA revealed enrichment in KRAS signalling downregulation and p53 pathway upregulation. These two genes are frequently mutated in a number of cancers, and mis-regulation of their pathways are landmarks of cancer, with KRAS being a proto-oncogene and p53 a tumour suppressor (Shimizu et al., 1983, Tsuchida et al., 2016, Baker et al., 1989, Nigro et al., 1989).

4.2 Investigation into the cell of origin of infant MLL-AF4-driven ALL

4.2.1 Introduction

In a recent study, Agraz-Doblas *et al.* showed that blasts derived from infant patients share a similar transcriptional profile with HSPCs (Lin-CD34+CD38-) which include HSC/MPPs and LMPPs (Agraz-Doblas et al., 2019). To identify the cell of origin of the disease, the transcriptional profile of human foetal liver-derived HSC/MPPs and LMPPs were defined and the genes differentially expressed were compared with MLL-AF4 targets, obtained from a previously published ChIP sequencing experiment from (Kerry et al., 2017),

4.2.2 Experimental design

In order to define the transcriptional profile of foetal liver HSC/MPPs and LMPPs, an RNA sequencing experiment was performed (Fig. 4.14). The sequencing experiment had the same design as the previous experiments. 8 RNA sequencing libraries were prepared, 4 from each population. The libraries were pooled together and sequenced on the Illumina HiSeq4000 platform. It should be noted that 100bp-paired end sequencing was performed.

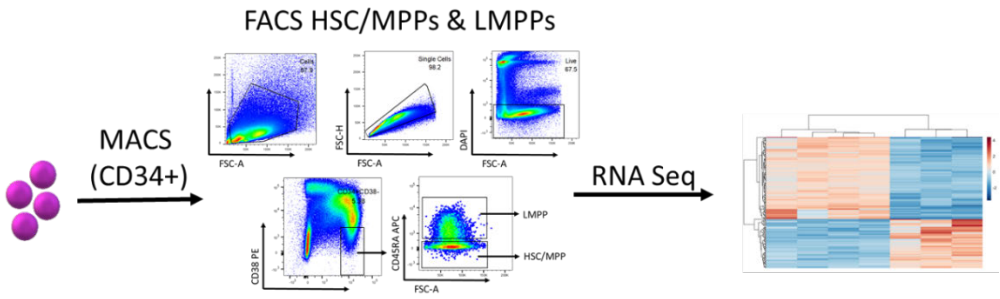

Figure 4.14| Experimental design used to define the transcriptional profile of foetal liver (FL) HSC/MPPs and LMPPs (Simplified version)

The steps for this experiment were as follows: 1) dissection of second trimester foetal liver, 2) CD34+ enrichment using magnetic-activated cell sorting (MACS), 3) sorting of HSC/MPPs and LMPPs, 4) RNA extraction, 5) validation of RNA quality and quantity (only samples with RIN≥8 were used), 6) library preparation for RNA sequencing, 7) libraries/samples were sequenced with the HiSeq 4000 platform, 8) sequencing data quality control and analysis.

As with the previous RNA sequencing experiment, I initially ensured the good quality of the reads and libraries. Interestingly, PCA revealed that the two populations separated in PC2, whereas we can see that in PC1 the populations sorted from the same sample were clustering together (Fig. 4.15). This shows the importance of biological variation that exists between different human foetal liver-derived samples. Differential expression analysis revealed 738 genes differentially expressed (DE) between the two populations, with 499 upregulated in HSC/MPPs and 239 in LMPPs (Appendix 4). As before, genes were considered DE if $padj \leq 0.05$.

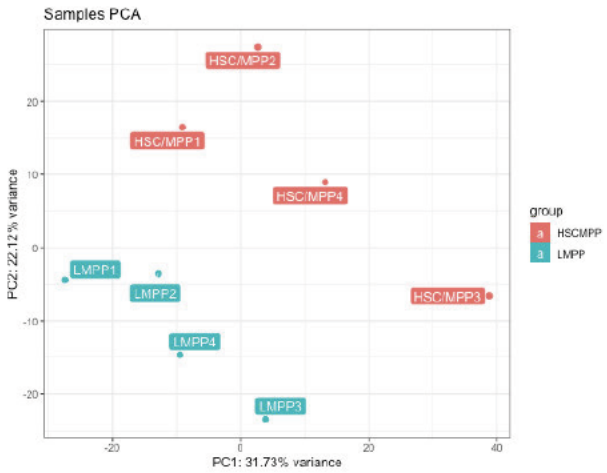

Figure 4.15| PCA of foetal liver-derived HSC/MPPs and LMPPs.

4.2.3 Transcriptional profile of foetal liver-derived HSC/MPPs and LMPPs

In order to validate this experiment, I Investigated the expression of genes important for lymphoid commitment (Fig. 4.16a). As expected, LMPPs upregulated a number of such genes including AFF1 (AF4). Interestingly, AF9, which is another common fusion partner of MLL, was upregulated in the HSC/MPPs (Fig. 4.16b).

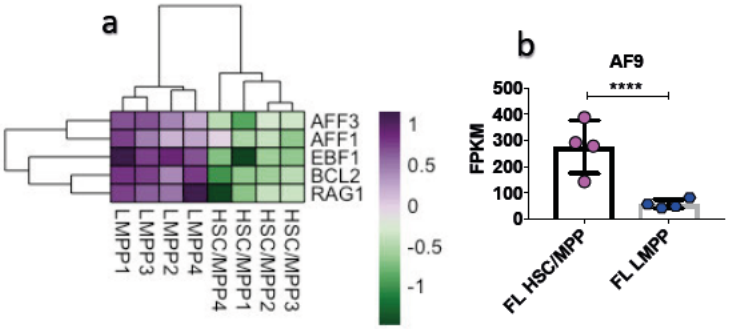

Figure 4.16| Genes differentially expressed between foetal liver HSC/MPPs and LMPPs.

a) Heatmap of genes required for lymphoid commitment upregulated in the foetal liver-derived LMPPs. b) AF9 is upregulated in the HSC/MPPs compared to LMPP. RNA sequencing data are shown as mean ±SD, each dot represents a sample.

GO revealed the more immature transcriptional profile of HSC/MPPs compared to that of LMPPs (Fig. 4.17). As expected, the former upregulated a number of more broad processes, whereas the processes upregulated in the latter were that of committed lymphoid cells including lymphocyte activation and leukocyte differentiation.

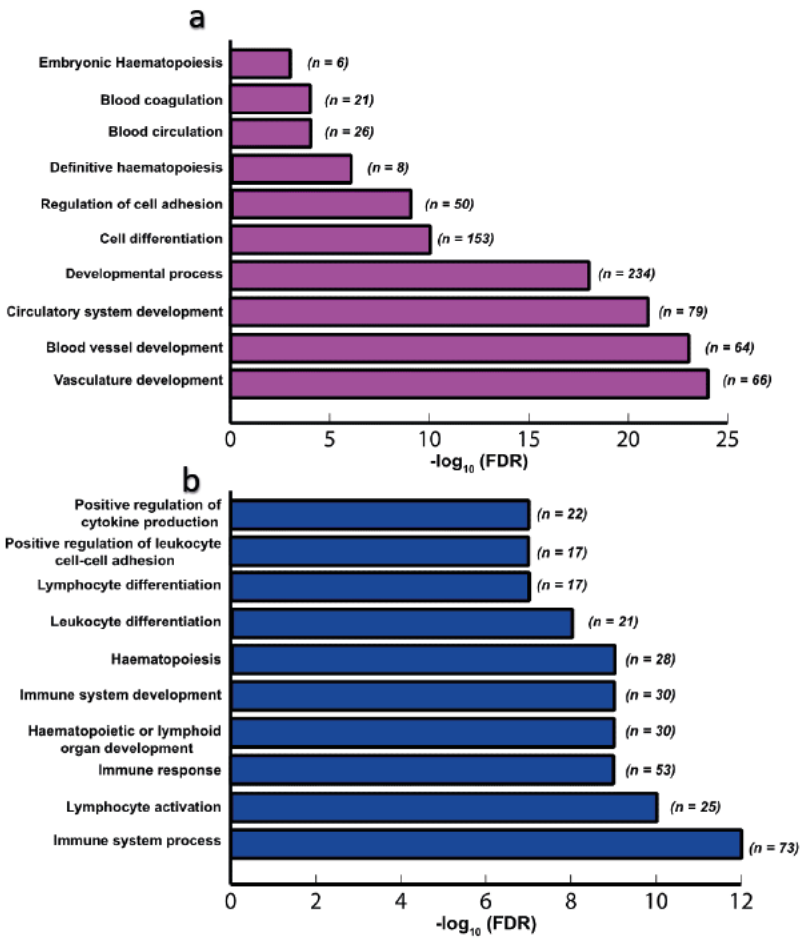

Figure 4.17| Gene ontology of foetal liver-derived HSC/MPPs and LMPPs.

a) Gene ontology of genes upregulated in HSC/MPPs. n= number of genes upregulated for a specific process. b) Gene ontology of genes upregulated in LMPPs. n= number of genes upregulated for a specific process.

4.2.4 Identification of the cell of origin of infant MLL-AF4-driven ALL

For the identification of the cell of origin of the disease, the DE genes between foetal liver-derived HSC/MPPs and LMPPs were compared with the targets identified in a previously published MLL-AF4 ChIP sequencing experiment (Kerry et al., 2017). It should be noted that I did not analyse the ChIP sequence experiment and the data used in this section were obtained by an MLL-FP gene target list that was available with the manuscript.

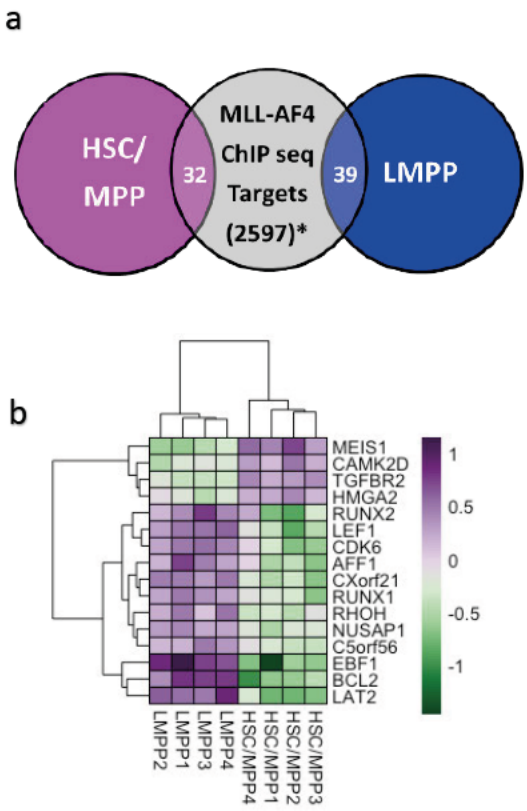

Figure 4.18| Comparison of DE genes between foetal liver-derived HSC/MPPs and LMPPs with MLL-AF4 ChIP-seq targets.

a) Venn diagram of genes differentially expression between HSC/MPPs and LMPPs which are common with SEM MLL-AF4 targets identified in Kerry et al., 2017 b) Heatmap of genes differentially expressed between HSC/MPPs and LMPPs, which are common with SEM MLL-AF4 spreading targets identified in Kerry et al., 2017. It should be noted that I did not analyse the ChIP sequencing experiment and the data shown here were obtained by an MLL-FP gene target list that was available in the manuscript.

Initially I observed that a similar number of genes was common between those identified as SEM MLL-AF4 targets from the ChIP sequencing experiment and those upregulated in HSC/MPPs or LMPPs, with a slightly higher number of genes common with the LMPPs. (Fig 4.18a). Interestingly, in this paper, they describe a binding pattern unique to MLL-AF4, where binding of MLL-AF4 spreads into the gene body, and they suggested that this leads to increased transcription (n=149). I compared the DE genes with the spreading targets of SEM MLL-AF4 and observed that there was a greater overlap of spreading targets and genes upregulated in the LMPP population (Fig.4.18b). From this data, it can be concluded that LMPPs appear to be a closer transcriptional match to infant blasts compared to the HSC/MPPs, suggesting that they could be the cell of origin of the disease.

4.3 Use of *in vitro* assays to establish early disease stages using foetal liver-derived cells

4.3.1 Experimental design

Being able to capture a pre-leukaemic stage is important for better understanding the disease initiation and progression. Having identified a similar stage in the Mll-AF4 mouse model, it would be interesting to investigate whether we can replicate this using human foetal liver-derived cells. To investigate the effect of MLL-AF4 expression in foetal liver cells, a B cell differentiation assay was performed (Fig. 4.19). In particular, foetal liver CD34+ cells were transduced with MLL-AF4 or empty vector lentiviral particles. It should be noted that due to the large size of the MLL-AF4 construct, there was a great difference in the number of transduced cells between the MLL-AF4 and EV transduced cells.

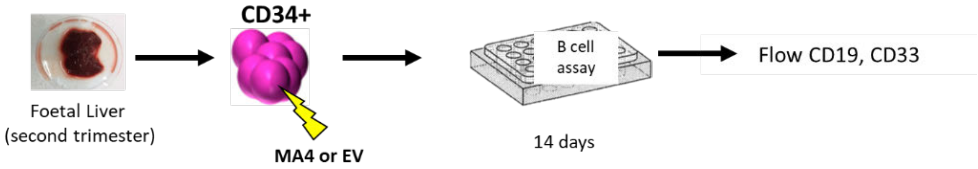

Figure 4.19| Experimental design of in vitro assays used to establish an early disease stage. (Simplified version)

The steps for this experiment were as follows: 1) dissection of second trimester foetal livers, 2) enrichment for CD34 using MACS, 3) transduction of CD34+ cells with MLL-AF4-GFP expressing plasmid or empty vector (EV)-GFP, 4) sorting of GFP+ cells (48 hours post transduction), 5) CD34+ MLL-AF4 expressing and EV expressing cells were placed in a B cell assay and cultured for 14 days, 6) flow cytometric analysis for CD19 and CD33.

4.3.2 *In vitro* B cell differentiation assay

Following transduction and B cell differentiation of the CD34+ cells, flow cytometric analysis was performed in order to identify lymphoid (CD19) and myeloid (CD33) cells. It can be observed in Fig. 4.20 there were no CD19+ cells in the MLL-AF4 (MA4)-expressing cells, whereas there was a clear CD19+ population in the empty vector transduced cells. As mentioned earlier there was a great difference in the percentage of transduced cells when MLL-AF4 or EV lentiviral particles were used. In my opinion, the lack of CD19+ cells is an indication that the correct progenitor was not transduced. The correct progenitor would be in the CD34+CD38- compartment which comprises less than 1% of the CD34+ cells. Given the rarity of these cells and the low viral titers of MLL-AF4, it is unlikely that the correct progenitor was transduced. These findings are particularly interesting, as this would explain why it has been difficult to model this disease and it was only when constructs with better titers were used a disease model was established (Lin et al., 2016).

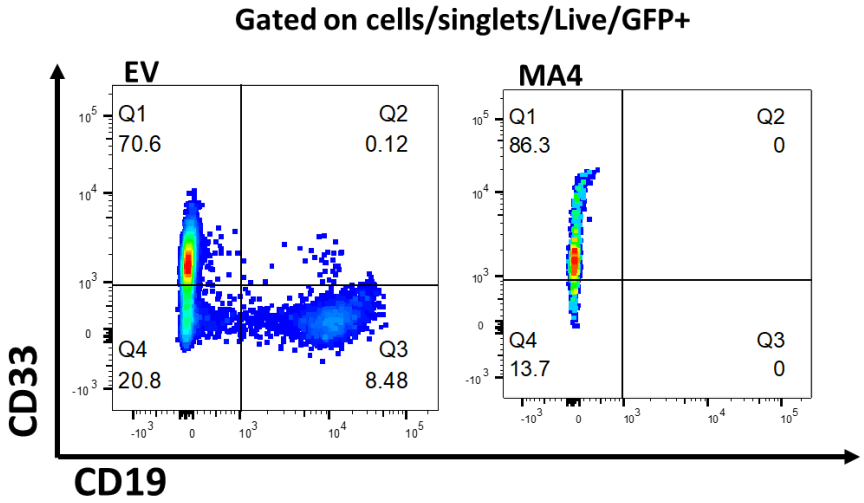

Figure 4.20| Flow cytometric analysis of B cell differentiation assay using MLL-AF4-expressing and control CD34+ foetal liver-derived cells.

Flow cytometric analysis was performed 14 days after transduction of CD34+ cells with either empty vector (EV) or MLL-AF4 (MA4) (n=2; one representative shown).

4.4 Discussion

The latest Interfant study revealed that the prognosis of infant patients with MLL-AF4-driven ALL has not improved in the last decade (Pieters et al., 2019). Pieters *et al.* suggested that there is an urgent need for innovative therapeutic strategies for these patients. However, in order to identify novel therapeutic targets, it is essential to better understand the unique biology of this disease. What makes this disease a unique entity amongst paediatric leukaemias is its *in utero* origin. Therefore, it would be insightful to investigate the foetal cell of origin of the disease.

In order to investigate the *in utero* origin of the disease, I performed an RNA sequencing experiment comparing foetal liver with cord blood-derived HSC/MPPs. From the results it was observed that the human foetal liver-derived cells were characterised by an over-proliferating and oncogenic nature. In contrast to the foetal liver-derived cells, cord blood cells exerted a more mature and immune-cell like transcriptional profile, with a number of tumour suppressor genes upregulated. In addition to this, I further compared the transcriptional profile of foetal liver-derived HSC/MPPs and LMPPs with SEM MLL-AF4 targets obtained from a previously published ChIP-seq experiment, where it was shown that LMPPs are a closer transcriptional match to the infant blasts as represented by the SEM cell line (Kerry et al., 2017).

Transcriptional profiling of human and murine foetal cells revealed a common over-proliferating and oncogenic signature. Following from this, it is safe to assume that the unique nature of the leukaemia-initiating cell could be a key contributor to the disease initiation, maintenance and its aggressiveness.

Having identified the unique features of the cell of origin of the disease, it would now be possible to investigate whether they are maintained in the blasts of infants with MLL-AF4-driven ALL. With this approach, it would be possible to identify genes in the blasts expression of which is a residue of the cell of origin. It is reasonable to speculate that these genes could be of great importance to

the pathogenesis of the disease and could therefore serve as novel therapeutic targets, which is the subject of the next chapter.

Chapter 5 Exploiting the foetal origin of MLL-AF4-driven infant ALL

5.1 Introduction

Infant MLL-AF4-driven ALL is a devastating disease that renders the patients with an extremely poor prognosis. To better understand the unique biology of this disease, I investigated its foetal origin. In particular, I examined the transcriptional profile of foetal and neonatal/adult haematopoietic stem and progenitor cells in humans and mice (chapters 4 and 3, respectively). In both species, the foetal-derived cells were characterised by a proliferative and oncogenic nature, which could serve as the perfect “partner in crime” for the initiation of an aggressive disease. In contrast, neonatal and adult cells were characterised by a more “mature” and protective transcriptional profile. Based on this data, I believe that it is safe to speculate that the foetal origin of the disease could be a critical contributor for the initiation of this aggressive infant disease.

The latest Interfant study revealed that there is an urgent need for innovative therapeutic strategies for the infant patients (Pieters et al., 2019). Following from this, it would be interesting to investigate whether we could therapeutically target aspects of the foetal origin of the disease that are maintained in the blasts of patients. In order to do this, I compared my data with a previously published dataset where they performed RNA sequencing of blasts of 17 infant patients with MLL-AF4-driven ALL (Andersson et al., 2015). With this approach, I identified genes the expression of which was at similar levels between the foetal cells and the blasts. I speculated that expression of these genes could be either a residue of the foetal origin of the disease or aberrantly activated by the fusion protein and therefore of great importance for its maintenance. To validate this, I performed functional assays and with this approach, a number of novel therapeutic targets were identified.

5.2 Investigation of the transcriptional profile of blasts derived from patients with MLL-AF4-driven ALL

Andersson *et al.* recently published a fascinating study where they defined the mutational landscape of infant MLL-R ALL (Andersson et al., 2015). In this study, amongst other sequencing experiments, they performed RNA sequencing experiments comparing different MLL-R ALLs. For the purposes of my project, I focused my attention on their MLL-AF4 ALL dataset. In particular, they performed RNA sequencing of the blasts of 17 infant and 5 paediatric patients with MLL-AF4-driven ALL (Fig. 5.1a). Interestingly, PCA revealed that samples derived from the infant patients formed two clusters and that the paediatric samples clustered closely with one of the infant clusters (Fig. 5.1b).

a

Sample Name	Age of diagnosis
SJINF001	2 months
SJINF002	7 months
SJINF003	7 months
SJINF006	2 months
SJINF011	5 months
SJINF013	11 months
SJINF014	3 months
SJINF017	5 months
SJINF020	2 months
SJINF055	4 months
SJINF062	2 months
SJINF063	5 months
SJINF064	7 months
SJINF065	1 month
SJINF068	3 months
SJINF069	4.1 months
SJINF075	5 months
SJMLL003	16 years
SJMLL005	18 years
SJMLL006	11 years
SJMLL009	18 years
SJMLL010	15 years

b

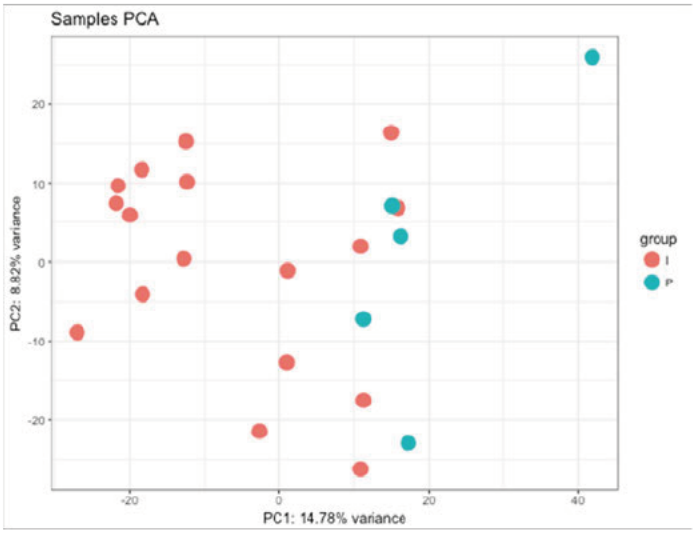

Figure 5.1| RNA sequencing experiment of patients with MLL-AF4-drive ALL. Data obtained from Andersson *et al.* 2015.

a) List of patients' samples used for RNA sequencing. b) PCA of patient samples (I = infant patients - pink, P=paediatric patients - blue.)

To investigate further the clustering pattern of the samples, I identified the top 10 loadings that drive the clustering in PC1 (Fig. 5.2). It was fascinating to see that genes *HOXA9* and *IRX1* were amongst them.

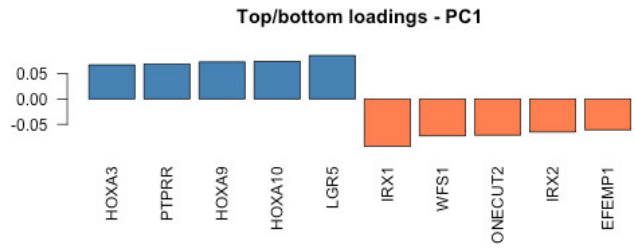

Figure 5.2| Top 10 loadings of PC1 that drive the clustering in Andersson *et al.* dataset.

5.2.1 *HOXA9* and *IRX1* expression defines two subgroups of the disease

It is well known that there are two distinct subgroups of infant MLL-AF4-driven ALL (Trentin et al., 2009, Stam et al., 2010). In most studies, these two groups are defined based on their *HOXA9* expression (as HOXA9 high and low), with patients with high *HOXA9* expression having a better prognosis (Stam et al., 2010, Kang et al., 2012, Agraz-Doblas et al., 2019). Interestingly, Trentin *et al.* and Agraz-Doblas *et al.* identified a positive correlation between *HOXA9* expression and the presence of the reciprocal fusion transcript of MLL-AF4, AF4-MLL (Agraz-Doblas et al., 2019, Trentin et al., 2009). Although in most studies the two subgroups are defined based on their *HOXA9* expression, investigation of the data revealed a clear correlation between *HOXA9* and *IRX1* expression (Kuhn et al., 2016, Stam et al., 2010). In particular, in these studies they observed that one of the top DE genes between *HOXA9*^{h} and *HOXA9*^{ow} was *IRX1*, where *IRX1* was upregulated in the blasts derived from patients with HOXA9^{ow} expression.

To further investigate the correlation between *HOXA9* and *IRX1*, I divided the patient samples based on *HOXA9* and *IRX1* expression and age of diagnosis (Fig. 5.3a).

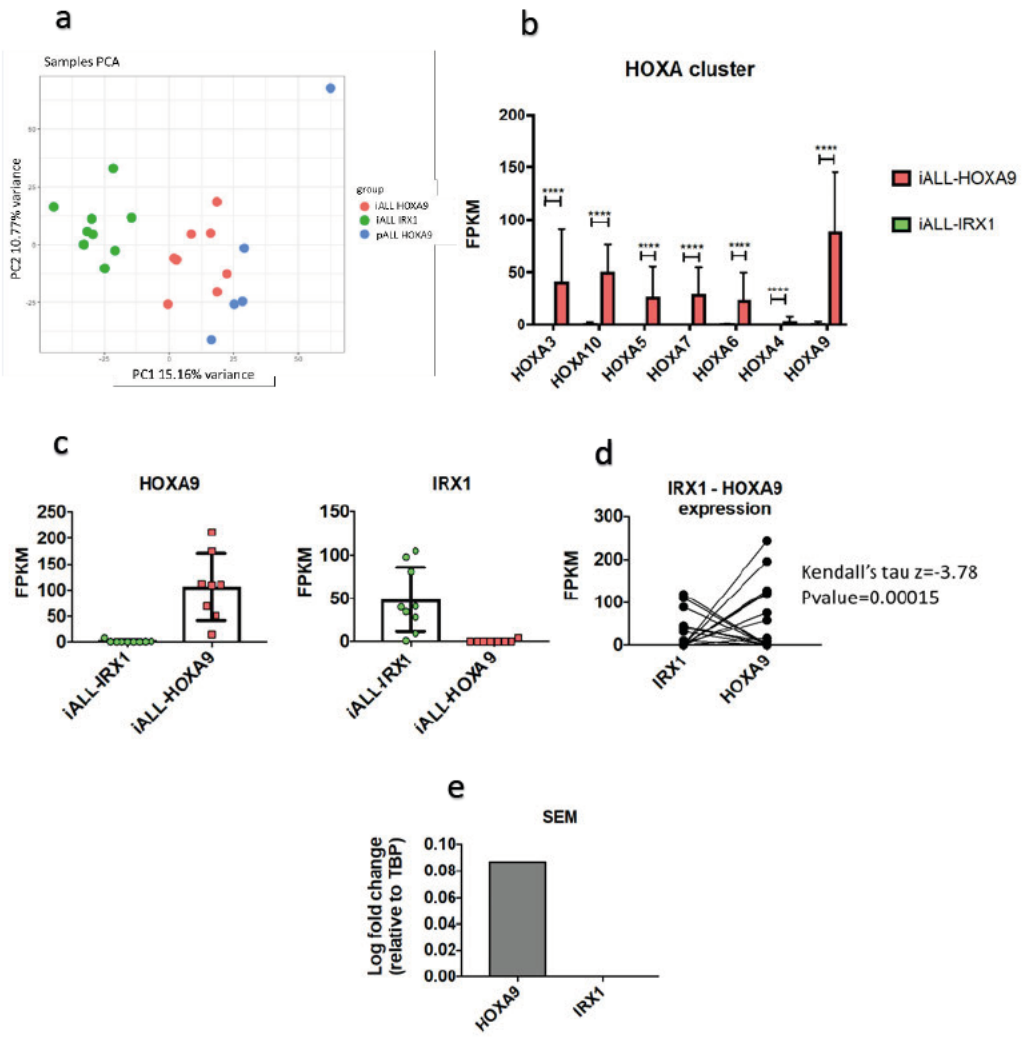

Figure 5.3| *HOXA9* – *IRX1* expression defines two subgroups of infant MLL-AF4-driven ALL.

a) PCA of patients defined by *HOXA9/IRX1* expression and age of diagnosis. Green= infants with *IRX1* expression, pink= infants with *HOXA9* expression, blue= paediatric ALL – all paediatric patients showed *HOXA9* expression. b) Expression of HOXA cluster genes in the 2 subgroups (infant patients only). RNA sequencing data are shown as mean +SD. c) *HOXA9* and *IRX1* expression in the 2 subgroups (infant patients only). RNA sequencing data are shown as mean ±SD, each dot represents a sample. d) Expression of *IRX1* and *HOXA9*, each dot represents a sample and the line connects the same sample (Kendall tau test was performed). e) Expression of *HOXA9* and *IRX1* in SEM cell line (n=1).

It should be noted that all paediatric patient samples expressed *HOXA9*. I then decided to focus only on the infant samples where I observed that samples that express *HOXA9* also upregulate a number of other HOXA cluster genes, which was in accordance with previous publications (Fig. 5.3b) (Stam et al., 2010, Trentin et al., 2009). In contrast, there was very low expression of HOXA cluster genes in the samples that upregulated *IRX1* (Fig. 5.3b). Investigation of *HOXA9* and *IRX1* expression in patient samples revealed a negative correlation between the two (p = 0.00015) (Fig. 5.3c, d).

Kuhn *et al.* ectopically overexpressed *IRX1* in HEK293T and SEM cells. It should be noted that the SEM cell line expressed *HOXA9* and there was very low expression of *IRX1* (Fig. 5.3e). Following from the *IRX1* overexpression Kuhn *et al.* observed that this resulted in a decrease in the transcriptional activity of several HOXA genes including *HOXA9*, *HOXA10* and *HOXA5*. In addition, they observed that *IRX1* binds to *HOXA9* and *HOXA10* promoters only in the presence of MLL-AF4. From this data they concluded that *IRX1* is likely to be responsible for the HOXA expression pattern (Kuhn et al., 2016).

Interestingly, similar to HOXA9, IRX1 is a homeobox protein that is required for embryonic patterning (Cavodeassi et al., 2001, Leyns et al., 1996). Homozygous knockout prevents gastrulation, and it is embryonically lethal at E9.5 (Kuhn et al., 2016).

The negative correlation that exists between *IRX1* and *HOXA9* expression in the blasts of patients with MLL-AF4-driven ALL is of clinical importance, as patients with *HOXA9* expression have a better prognosis. It is interesting how two different homeobox genes seem to be critical for the infant disease. Although these data are of great interest, they should be treated with caution due to the low number of data points. It would be interesting to further investigate how expression of these two genes define the two subgroups of patients; however, more samples would be required to perform this analysis.

5.3 Identification of genes common between humans and mice

Expression of genes that play critical functions is conserved across species. In order to identify genes the expression of which was conserved across humans and mice, I intersected the RNA sequencing datasets of the previous two chapters. With this approach, I identified genes that were commonly upregulated in the foetal liver derived populations (humans and mice) and neonatal and adult populations (humans and mice). Overall, I identified 70 genes that were commonly upregulated in the foetal liver derived population and 55 that were upregulated in the neonatal and adult derived populations (Appendix 5). As expected, investigation of the genes upregulated in the foetal liver-derived populations revealed a number of genes involved in cell proliferation and development. Interestingly, amongst the foetal-upregulated genes, there was a number of genes that have been shown to be upregulated in relapse pALL including *AURKA*, *HMAG1*, *PLK1*, *BUB1B*, *CENPF*, *CCNF* and *ASPM* (Chow et al., 2017, Bhojwani et al., 2006).

From the genes that were common between the human and murine data, I investigated their expression in the blasts of infants with MLL-AF4-driven ALL (Andersson et al., 2015). For the purpose of this comparison, I performed differential expression analysis of the two datasets. In particular, the dataset described in chapter 4, comparing human foetal liver and cord blood-derived HSC/MPPs and the dataset obtained from Andersson *et al.* (infants only) (Fig. 5.4). As expected, the data were clustering based on experiment and there was a great technical error in this comparison. This was taken under consideration and genes of interest were independently validated with qPCR.

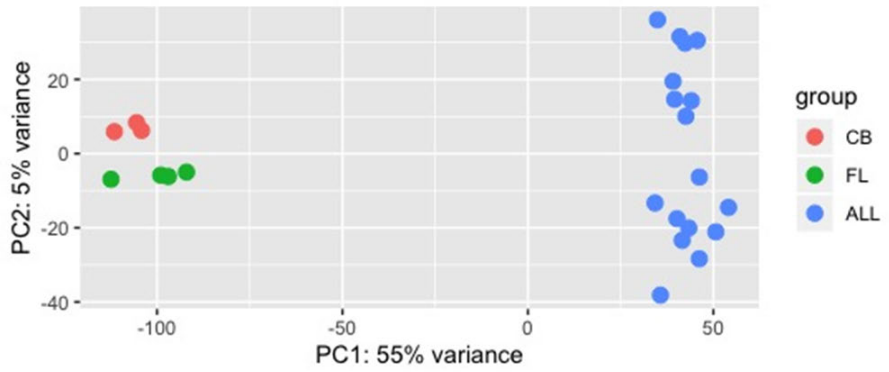

Figure 5.4|PCA of foetal liver HSC/MPPs, cord blood HSC/MPPs and infant ALL samples.

PCA of samples derived from the RNA sequencing experiment described in Chapter 4, foetal liver (FL) and cord blood (CB) derived HSC/MPPs compared with RNA sequencing data obtained from Andersson *et al.* where they sequenced the blasts of 17 infant patients with MLL-AF4-driven ALL (ALL).

With this approach, I selected 21 genes the expression of which was at similar levels between the foetal-derived cells and the blasts (Fig. 5.5). I selected 20 genes that were upregulated in the foetal liver-derived samples and 1 gene (*DACH1*) that was upregulated in the neonatal/adult-derived populations. It should be noted that *DACH1* was not included in the heatmap in Fig. 5.5c, this was due to the fact that its very low expression in the blasts was very prominent and masked the expression levels of the remaining 20 genes.

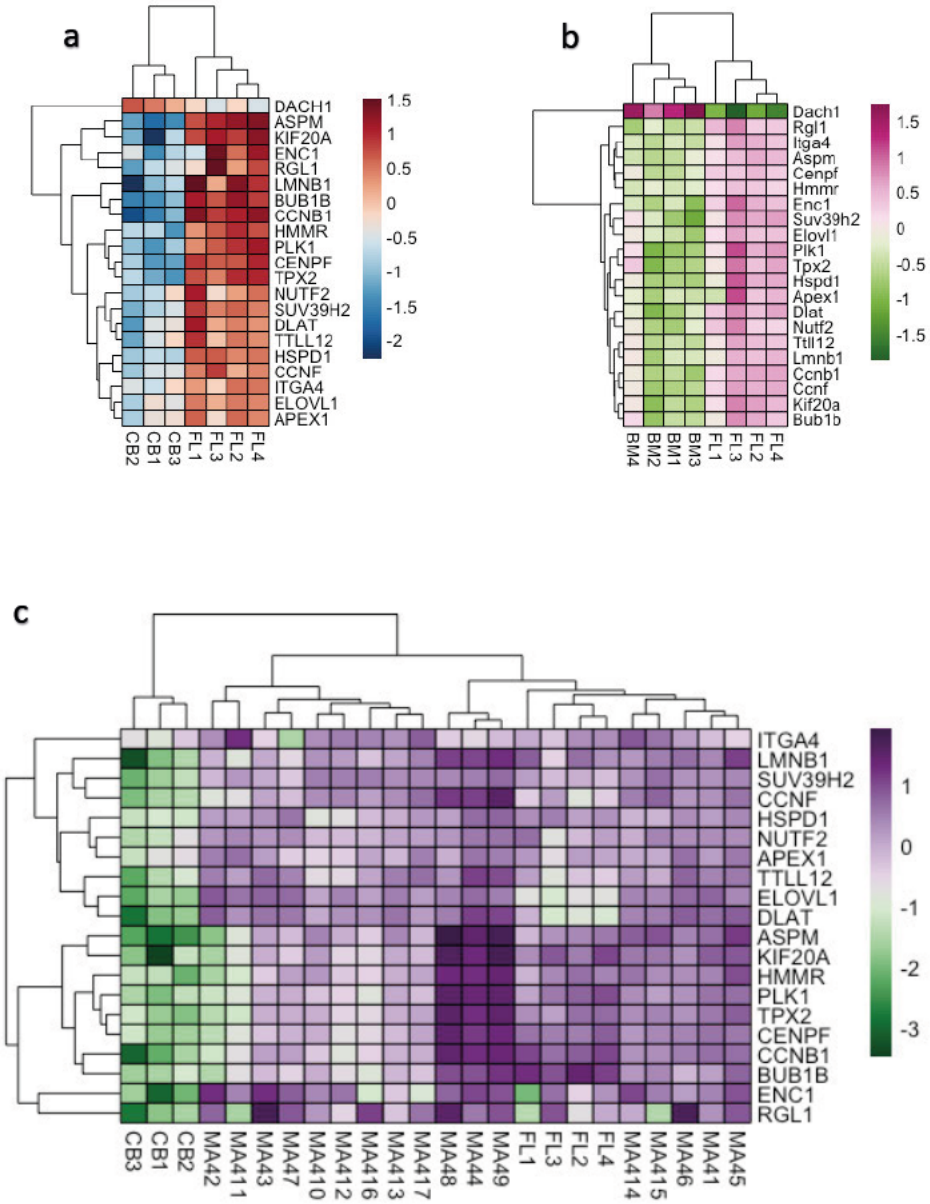

Figure 5.5| Heatmaps of genes the expression of which was at similar levels between the foetal liver-derived populations and infant blasts obtained from patients with MLL-AF4-driven ALL (Andersson *et al.*) a) Heatmap of genes differentially expressed between human foetal liver (FL) and cord blood (CB) derived HSC/MPPs. b) Heatmap of genes differentially expressed between murine foetal liver (FL) and adult bone marrow (BM) derived LMPPs. c) Heatmap of genes the expression of which was at similar levels between human foetal liver (FL) derived HSC/MPPs and infant MLL-AF4-driven blasts (MA4).

5.4 PLK1

Investigation into the genes that were upregulated in the foetal liver-derived cells (both human and murine) identified *PLK1* (Fig. 5.6 a-b). Interestingly, *PLK1* expression was at similar levels between the foetal liver-derived HSC/MPPs and the infant blasts (Fig. 5.6 c-d).

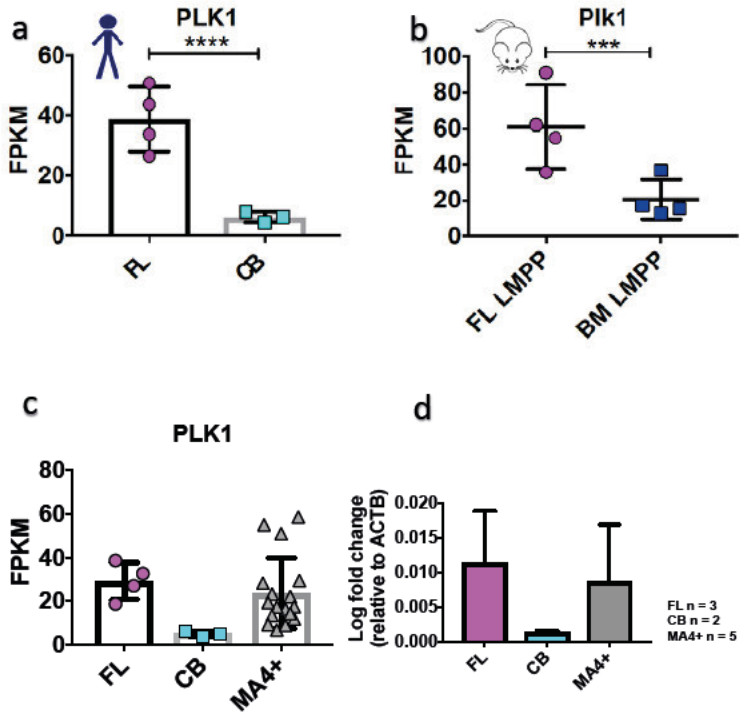

Figure 5.6| *PLK1* expression.

a) *PLK1* expression in human foetal liver (FL) and cord blood (CB) derived HSC/MPPs. RNA sequencing data are shown as mean ±SD, each dot represents a sample. b) *Plk1* expression in murine foetal liver (FL) and adult bone marrow (BM) derived LMPPs. RNA sequencing data are shown as mean ±SD, each dot represents a sample. c) *PLK1* expression in human foetal liver (FL) and cord blood (CB) derived HSC/MPPs and blasts from infants with MLL-AF4-driven ALL (MA4+) from Andersson *et al.* RNA sequencing data are shown as mean ±SD, each dot represents a sample. d) qPCR of *PLK1* expression in human foetal liver (FL) and cord blood (CB) derived HSC/MPPs and blasts from infants with MLL-AF4-driven ALL (MA4+). Data are shown as mean +SD.

PLK1 (Polo-like kinase 1) is a member of the serine/threonine (Ser/Thr) protein kinases that has been shown to play a critical role in cell cycle progression. The importance of this kinase was initially identified in *Drosophila melanogaster* and was later confirmed in higher organisms including humans (Sunkel and Glover, 1988, Descombes and Nigg, 1998, Simizu and Osada, 2000, Knecht et al., 1999, Golsteyn et al., 1994). *PLK1* has been shown to control multiple steps during M-phase progression including mitotic entry, entry to prometaphase, centrosome maturation and separation, chromosome arm resolution, cytokinesis and establishment of the spindle assembly checkpoint (SAC) (Schmucker and Sumara, 2014, Sumara et al., 2004, Lenart et al., 2007, Hanisch et al., 2006, Gimenez-Abian et al., 2004, Petronczki et al., 2008, von Schubert et al., 2015). In addition to its multiple roles in mitosis, *Plk1* has been shown to be an important target of the DNA damage checkpoint (Smits et al., 2000). In particular, Smits *et al.* showed that *Plk1* was inhibited by DNA damage in G2 and mitosis, leading to a DNA-damage induced arrest. The same group later showed that, following recovery from such arrest, *Plk1* re-expression was essential for the cells to enter mitosis (van Vugt et al., 2004).

In homeostasis, *PLK1* has been shown to be expressed during embryonic development and in the adult in proliferative tissues (Schmucker and Sumara, 2014). However, *PLK1* has also been implicated in a number of cancers including non-small-cell lung cancer, breast cancer, oropharyngeal carcinoma, head and neck cancer, melanomas and gliomas (Wolf et al., 1997, Wolf et al., 2000, Knecht et al., 2000, Knecht et al., 1999, Strebhardt et al., 2000, Dietzmann et al., 2001). In addition to solid tumours, *PLK1* has been shown to be overexpressed in AML and relapse p-ALL (Renner et al., 2009, Chow et al., 2017, Bhojwani et al., 2006).

Given the dominant presence of *PLK1* in a number of cancers, it was not surprising that a number of inhibitors have been developed. One of the earliest PLK1 inhibitors developed was BI2536, which was shown to inhibit tumour growth both *in vitro* and *in vivo* (Steegmaier *et al.*, 2007). BI2536 was replaced by BI6727 (Volasertib), which was developed by Boehringer Ingelheim, which

is the newest addition to this family of PLK1 inhibitors. BI6727, similar to BI2536, is an ATP-competitive kinase inhibitor of the dihydropterinone class of compounds, which inhibits proliferation by competitive binding to the ATP-binding pocket of PLK1 (Rudolph et al., 2009). Volasertib was the first PLK1 inhibitor to enter clinical trials and its efficiency has been demonstrated in AML (Brandwein, 2015). Phase I/II clinical trials showed that Volasertib exerted an anti-leukaemic activity and was clinically manageable as monotherapy and in combination with low-dose-cytarabine (LDAC) (Kobayashi et al., 2015, Dohner et al., 2014). Given the promising results, the drug entered phase III clinical trial for AML where it was used in combination with LDAC. However, in 2016 Boehringer Ingelheim announced that the phase III results did not meet the primary endpoint of objective response; however, it should be noted that the trial is ongoing.

As mentioned earlier, *PLK1* was upregulated in the foetal liver-derived cells (human and murine), and it was also expressed at the same levels between foetal liver-derived HSC/MPPs and infant blasts (Fig. 5.5). Given the availability of a potent inhibitor, I decided to investigate whether PLK1 could be used as a therapeutic target for infant MLL-AF4-driven ALL. This was achieved by treating the SEM cell line with 50nM of BI6727. The concentration was selected based on a previous publication where it was shown that treatment of NK cells derived from healthy donors with 50nM of BI6727 did not exert any cytotoxic effects (Gopalakrishnan et al., 2018). In SEM cells, however, the use of 50nM of BI6727 resulted in dramatic changes of their cell cycle profile and viability (Fig. 5.7a-c). In particular, 24 hours after treatment there was a dramatic decrease in the number of cells present in the G0/1 and S phases of the cell cycle, whereas there was a dramatic increase in the number of cells present in G2/M (Fig. 5.7a-b). 48 hours after treatment, almost 50% of the SEM cells were apoptotic and therefore it was difficult to capture an accurate cell cycle profile of these cells (Fig. 5.7a & c). 78 hours after treatment, less than 5% of the cells were viable (Fig. 5.7 c). The cell cycle profile of the cells treated with BI6727 was in accordance with a previous publication, where they observed that treatment of MV4;11 and Kasumi-1 cells

with the inhibitor resulted in mitotic arrest, inhibition of proliferation and induction of apoptosis (Rudolph et al., 2015). Interestingly, in another recent study, they observed that *PLK1* expression was higher in paediatric patients with ALL compared to normal bone marrow mononuclear cells and knock-down of *PLK1* using shRNA dramatically decreased survival of leukaemia cell lines (including SEM cell line) (Hartsink-Segers et al., 2013). This data are very encouraging. Following from this it would be interesting to investigate whether PLK1 inhibitors could be used in a clinical setting to treat infants with MLL-AF4-driven ALL.

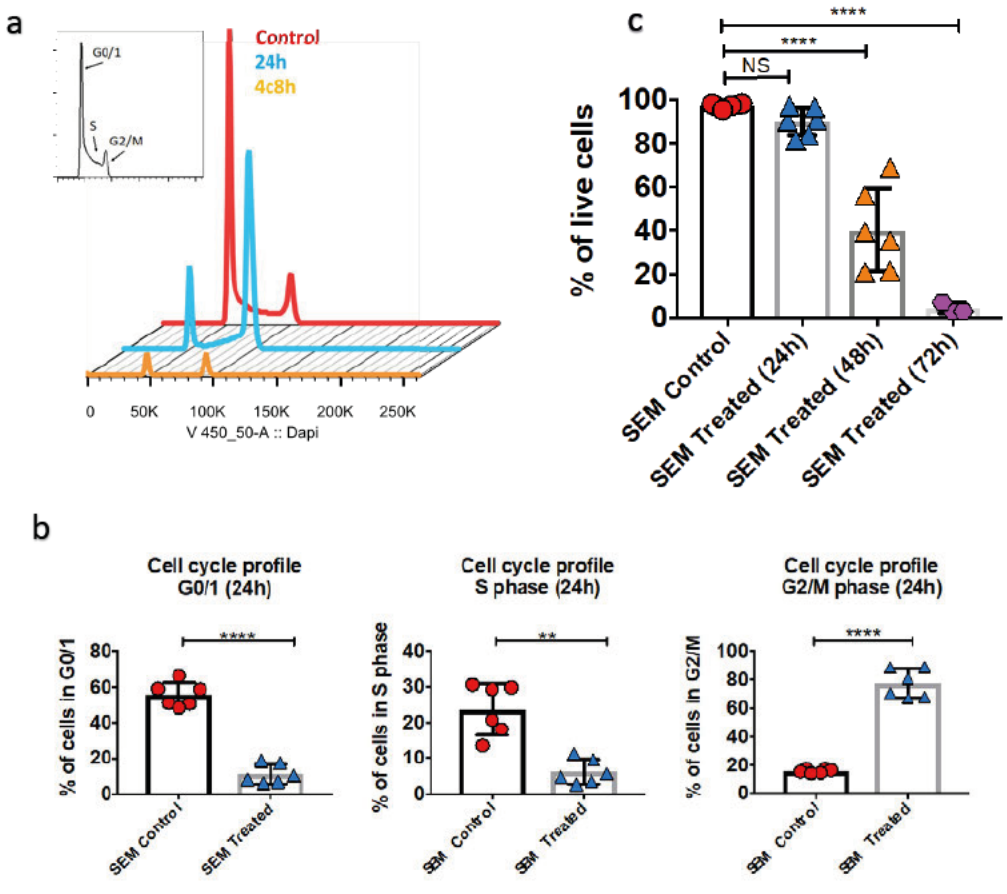

Figure 5.7| Treatment of SEM cells with BI6727 (Volasertib).

a) Cell cycle profile of SEM cells treated with 50nM BI6727, red = SEM control, blue= SEM treated with 50nM BI6727 24 hours, orange=SEM treated with 50nM BI6727 48 hours. b) Cell cycle profile of cells treated with 50nM of BI6727 after 24 hours. Data are shown as mean ±SD. Student's t test was performed. c) Cell viability of cells treated with 50nM of BI6727. Data are shown as mean ±SD. Anova test was performed.

PLK1 is in close connection with Aurora kinase A (AURKA). In particular, AURKA is essential for the activation of PLK1 (Macurek et al., 2008). This is particularly interested as a number of AURKA inhibitors including Alisertib are also available. Alisertib has shown promising results in AML (Fathi et al., 2017, Park et al., 2018). As expected, *AURKA* expression was higher in the foetal liver-derived tissues (both humans and mice) and its expression was at similar levels between the foetal-derived HSC/MPPs and the infant blasts (Fig. 5.8). The expression pattern of *AURKA* suggests that, similar to *PLK1*, it would be interesting to inhibit expression of this gene in a clinical setting.

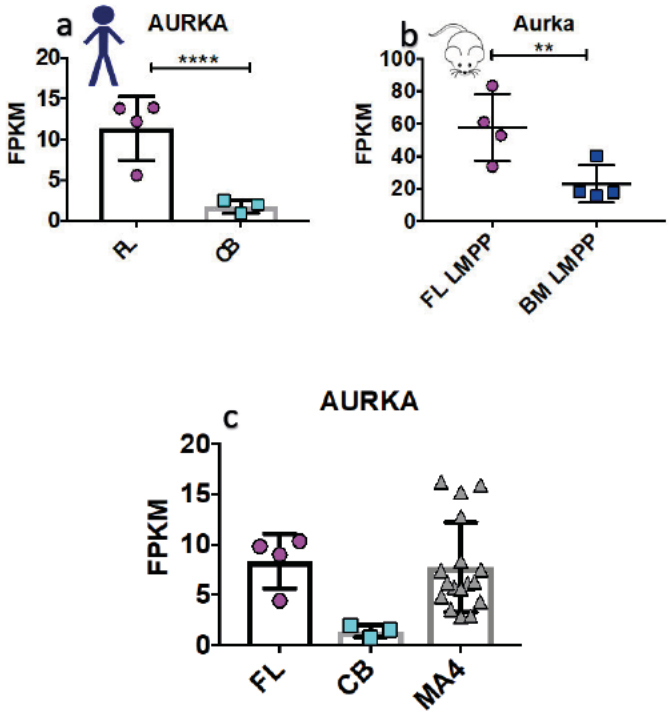

Figure 5.8|Expression of *AURKA*.

a) Expression of *AURKA* in human foetal liver (FL) and cord blood (CB) derived HSC/MPPs. RNA sequencing data are shown as mean ±SD, each dot represents a sample. b) Expression of *Aurka* in the murine foetal liver (FL) and adult bone marrow (BM) derived LMPPs. RNA sequencing data are shown as mean ±SD, each dot represents a sample. c) Expression of *AURKA* in the human foetal liver (FL) and cord blood (CB) derived HSC/MPPs and blasts derived from infants with MLL-AF4-driven ALL (MA4) (Andersson *et al.*2015). RNA sequencing data are shown as mean ±SD, each dot represents a sample.

5.5 Use of CRISPR-Cas9 to identify novel therapeutic targets for MLL-AF4-driven ALL

To investigate whether the foetal origin of the disease is critical for the disease maintenance, I used a CRISPR-Cas9 approach. In particular, I identified 19 genes that were upregulated in the foetal liver-derived populations (human and murine) and expression of which was at similar levels between the foetal liver-derived HSC/MPPs and the infant blasts (Fig. 5.5 a-c). I ensured that these genes were expressed in the SEM cell line; the data for this were obtained from Kerry *et al*. where they performed nascent RNA sequencing of the SEM (Fig. 5.9) (Kerry et al., 2017). It should be noted that I did not analyse the nascent RNA seq experiment, the values of reads per Kilobase of transcript (RPKM) I used were obtained from a table that the authors provided/submitted in Gene Expression Omnibus (GEO). Following from this I generated a SEM-Cas9-GFP cell line and, using sgRNAs knockout studies, I investigated the importance of these genes in the disease maintenance.

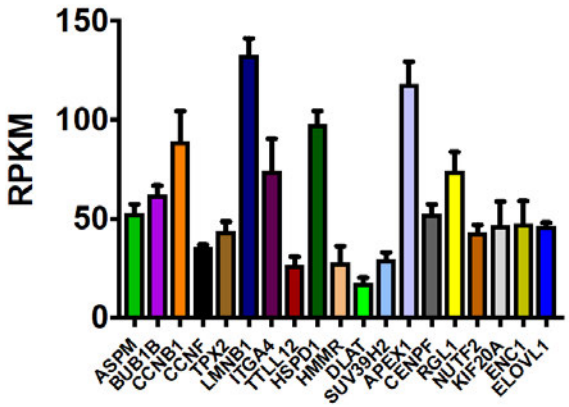

Figure 5.9| Expression of genes of interest in SEM cell line. Data obtained from (Kerry et al., 2017) where they performed nascent RNA sequencing of SEM cell line. It should be noted that I did not analyse the nascent RNA seq experiment, the values (Reads Per Kilobase of transcript = RPKM) I used were obtained from a table that the authors provided/submitted in Gene Expression Omnibus (GEO).

Having generated a SEM-Cas9 system, the next step was to establish an assay where the effect of the knockout could be tested. A competition assay was established where the SEM-Cas9-expressing cells were mixed with SEM wild-type cells (in 1:1 ratio) and the mixture was transduced with the sgRNAs. Following from this, the cells were cultured and the percentage of GFP+ cells was measured using flow cytometry at different time points (Fig. 5.10a,b).

The competition assay allowed for the identification of sgRNAs that exerted a negative effect on the viability of the SEM-Cas9 cells. An example of the competition assay can be seen in Fig. 5.10b. We can observe that for the negative sgRNA (Neg sgRNA) the percentage of GFP+ cells remained consistent between days 2, 6 and 12, suggesting that the sgRNA did not affect survival of the SEM-Cas9 cells. In contrast, the positive sgRNA (Pos sgRNA) had a tremendous impact on the SEM-Cas9 cells, with the percentage of GFP+ (and therefore Cas9 expressing cells) dramatically decreasing starting at day 6 and very few viable SEM-Cas9+ cells remaining by day 12. We can also observe that there were no significant changes in the SEM wild type cells, which suggested that the decrease in the SEM-Cas9 cells was due to the knockout effect.

This suggests that when the percentage of GFP+ cells (and therefore Cas9 expressing cells) decreased, the sgRNA used affected the survival of SEM cells; however, the contrary is true for sgRNAs that did not exert an effect. The SEM wild type cells should not be affected by the sgRNAs used.

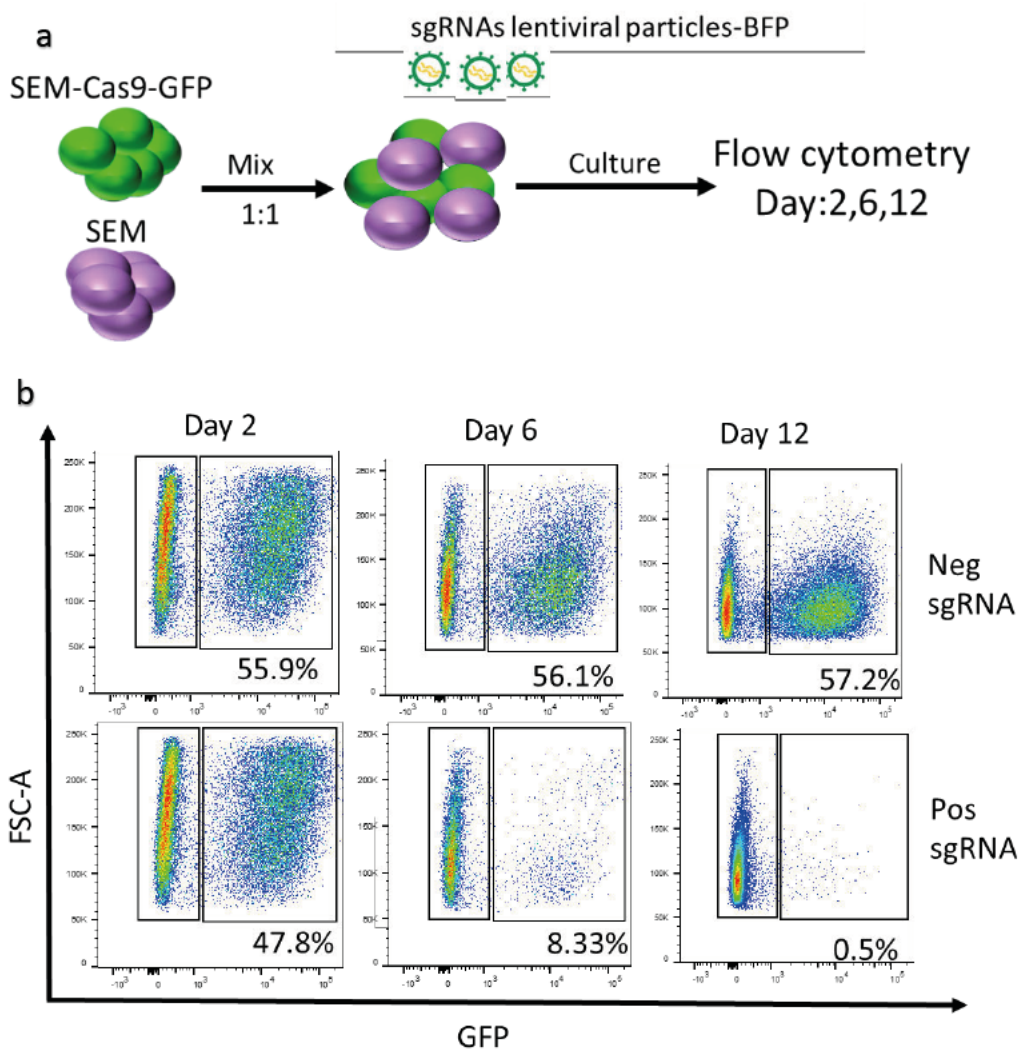

Figure 5.10| Use of CRISPR-Cas9 approach to identify novel therapeutic targets.

a) Experimental design used to identify novel therapeutic targets. b) Flow cytometric analysis of competition assay.

Having established the competition assay, I then investigated how knockout of the different genes affected the SEM-Cas9 cells (2 sgRNAs per gene were used). With this approach, I identified 6 genes the knockout of which had a dramatic effect on the survival of SEM-Cas9 cells (Fig. 5.11). In particular, knockout of *ELOVL1*, *TPX2*, *NUTF2*, *HSPD1*, *CCNB1* and *BUB1B* resulted in apoptosis of SEM-Cas9 cells. We can observe that there was no effect on the

SEM-Cas9-GFP+ cells in the Neg control, whereas there were few viable cells in the positive control (RSP19).

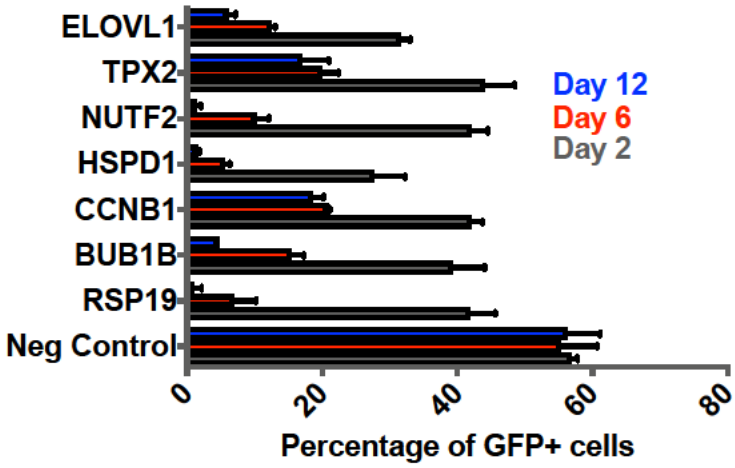

Figure 5.11| CRISPR-Cas9 approach identified novel disease targets.

a) Competition assay identifies 6 genes that affect the SEM-Cas9 viability. Data are shown as mean +SD, n=2.

To identify genes that were specific to the infant disease, I investigated the knockout effect of the genes of interest in other CRISPR screens. Erb *et al.* performed a whole genome CRISPR-Cas9 knockout screen using MV4;11, which is a cell line derived from a patient with MLL-AF4 rearranged AML (Erb et al., 2017). Comparison of this screen with my screen identified two genes, *TPX2* and *NUTF2,* which seem to have an effect in both cell lines. *TPX2* is critical for microtubule assembly and thus cell proliferation, whereas *NUTF2* facilitates protein transport into the nucleus (Heidebrecht et al., 1997, Gruss et al., 2002, Paschal and Gerace, 1995).

In a recent publication, Hart *et al.* also performed a genome-scale CRISPR-Cas9 screen in a number of different cell lines including glioblastoma cell line (GBM), retinal epithelial cell line (RPE1), melanoma cell line (A375), cervical carcinoma (HeLa) and colorectal carcinoma cell lines (HCT116 and DLD1)

(Hart et al., 2015). With this approach, they identified a number of core fitness genes, including *CCNB1*, *BUB1B and TPX2* (*BUB1B* expression can be observed in Fig. 5.12). This suggested that these genes are critical for survival in a number of different cancer cell lines. This is not surprising as all genes play a role in cell proliferation which we know is the hallmark of cancer cells, in particular, their ability to over proliferate. *BUB1B* is a mitotic checkpoint serine/threonine kinase, which has been shown to be involved in spindle checkpoint function, while *CCNB1* is involved in mitosis and *TPX2*, as mentioned earlier, is critical for microtubule assembly (Davenport et al., 1999, Guo et al., 2012, Sartor et al., 1992, Nakamura et al., 2010). These genes seem to be critical for the survival in a number of different cancers and therefore it would be interesting to investigate whether they could be used in a clinical setting.

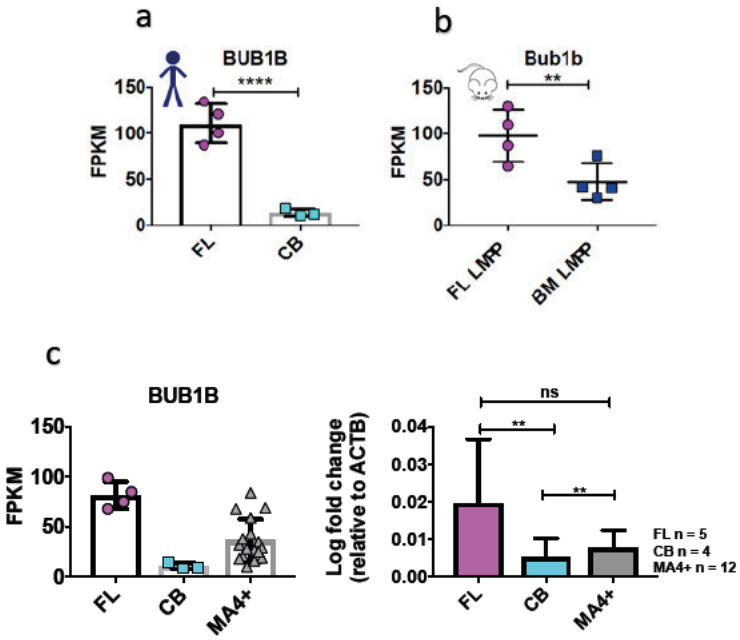

Figure 5.12| *BUB1B* expression.

a) Expression of *BUB1B* in human foetal liver (FL) and cord blood (CB) derived HSC/MPPs. RNA sequencing data are shown as mean ±SD, each dot represents a sample. b) Expression of *Bub1b* in the murine foetal liver (FL) and adult bone marrow (BM) derived LMPPs. RNA sequencing data are shown as mean ±SD, each dot represents a sample. c) Expression of *BUB1B* in the human foetal liver (FL) and cord blood (CB) derived HSC/MPPs and blasts derived from infants with MLL-AF4-driven ALL (MA4) (Andersson *et al.*2015). RNA sequencing data are shown as mean ±SD, each dot represents a sample. d) qPCR of *BUB1B* expression in human foetal liver (FL) and cord blood (CB) derived HSC/MPPs and blasts from infants with MLL-AF4-driven ALL (MA4+). Data are shown as mean +SD, Anova test was performed.

5.5.1 HSPD1

Two genes were uniquely identified in my screen, *HSPD1* (also known as *HSP60*) and *ELOVL1*. *HSPD1* was upregulated in the foetal liver-derived tissues compared to their adult counterparts (in both humans and mice) (Fig. 5.13 a,b). Additionally, expression of this gene was at similar levels between the foetal liver derived HSC/MPPs and the infant blasts in the RNA sequencing data; however, this could not be validated using qPCR (Fig. 5.13 c,d). HSPD1 is a member of the Heat Shock family of proteins.

HSPD1 together with HSP10 forms a chaperonin complex, which has been shown to be important for mitochondrial protein import and the correct folding of the imported proteins (Richardson et al., 2001, Bross and Fernandez-Guerra, 2016). Knockout of *HSPD1* in the SEM-Cas9 expressing cells induced cell death, and we can see that only a small number of cells were viable by day 12 (Fig. 11 and 13e). It should be noted that two sgRNAs were used and exerted the same effect in the SEM-Cas9 cell line, suggesting that the effect was due to the knockout of the gene as opposed to an off-target effect or other technical artefacts (Fig. 5.13e).

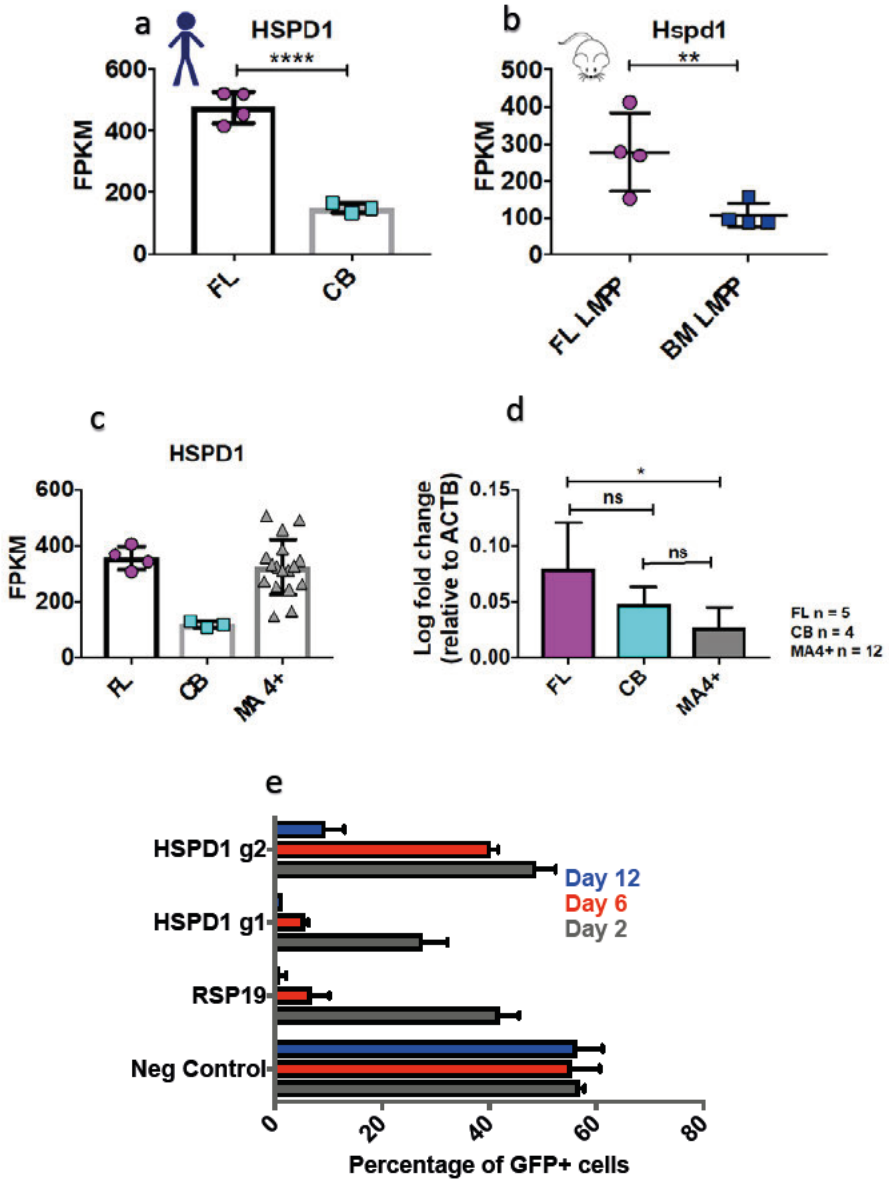

Figure 5.13| *HSPD1* expression and validation.

a) *HSPD1* expression in human foetal liver (FL) and cord blood (CB) derived HSC/MPPs. RNA sequencing data are shown as mean ±SD, each dot represents a sample. b) *Hspd1* expression in murine foetal liver (FL) and adult bone marrow (BM) derived LMPPs. RNA sequencing data are shown as mean ±SD, each dot represents a sample. c) *HSPD1* expression in human foetal liver (FL) and cord blood (CB) derived HSC/MPPs and infant blasts (MA4+) (Infant blasts data were obtained from Andersson *et al.*). RNA sequencing data are shown as mean ±SD, each dot represents a sample. d) qPCR validation of expression of *HSPD1* in human foetal liver (FL) and cord blood (CB) derived HSC/MPPs and infant blasts (MA4+). Data are shown as mean +SD, Anova test was performed. e) Validation of *HSPD1* knockout using two different sgRNAs.

5.5.2 ELOVL1

The second gene identified with this approach was *ELOVL1*. Knockout of *ELOVL1* in SEM-Cas9 cells resulted in a dramatic decrease in the viability of the cells (Fig. 5.11). The decrease was present at day 6 and continued to day 12, where less than 7 per cent of the cells were viable. Interestingly, knockout of *ELOVL1* in AML and other cancer cell lines did not have any effect on the viability of the cells, suggesting this effect could be unique to the infant MLL-AF4-driven ALL (Erb et al., 2017, Hart et al., 2015).

ELOVL1, which is a member of the elongation of very long chain fatty acids (ELOVL) family of proteins, was upregulated in the foetal liver-derived tissues (both human and murine) (Fig. 5.14a,b). Additionally, *ELOVL1* expression was at similar levels between human foetal liver-derived HSC/MPPs and infant blasts (Fig. 5.14c,d). To validate the *ELOVL1* knockout, TIDE assay was performed where the high efficiency of the sgRNA was confirmed (Fig. 5.14e).

To further investigate the mechanisms of action of *ELOVL1*, a lipidomics experiment was performed. The aim of this experiment was to obtain a global profile of the lipids that were affected by knockout of this gene. For this experiment, SEM-Cas9 cells were transduced with sgRNA for *ELOVL1* and compared to SEM-Cas9 cells transduced with sgRNA for neg control. The comparison was performed at two time points – day 2 (D2) and day 4 (D4). After this point, there was a large number of apoptotic cells, and it would be difficult to obtain an accurate representation of the lipids. The SEM cells used for the lipidomics study were sorted using flow cytometry for live, GFP (Cas9), BFP (sgRNA) prior to the lipidomics experiment. It should be noted that the lipidomics experiment and the analysis of the accompanied data was performed by Dr. Andrew Finch at the Cancer Research UK Edinburgh Centre.

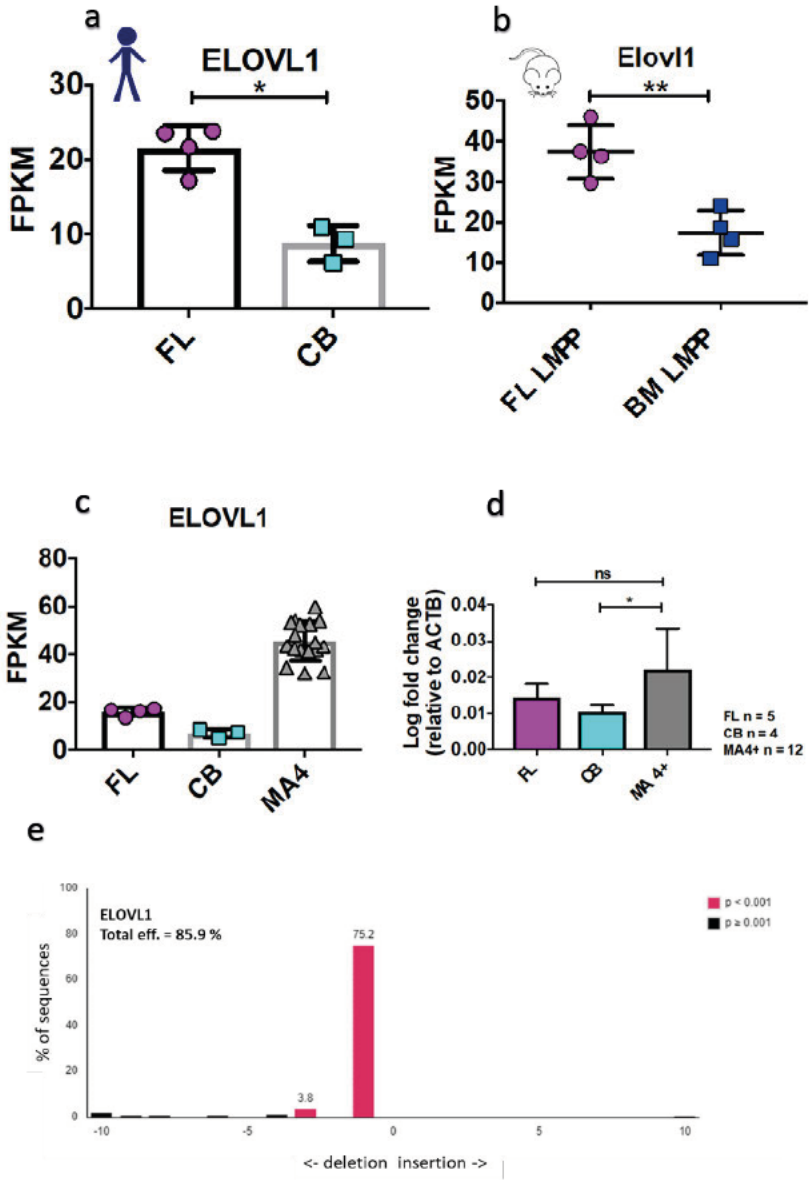

Figure 5.14| *ELOVL1* expression and knockout validation.

a) *ELOVL1* expression in human foetal liver (FL) and cord blood (CB) derived HSC/MPPs. RNA sequencing data are shown as mean ±SD, each dot represents a sample. b) *Elovl1* expression in murine foetal liver (FL) and adult bone marrow (BM) derived LMPPs. RNA sequencing data are shown as mean ±SD, each dot represents a sample. c) *ELOVL1* expression in human foetal liver (FL) and cord blood (CB) derived HSC/MPPs and infant blasts (MA4+) (Infant blasts data were obtained from Andersson *et al.*). RNA sequencing data are shown as mean ±SD, each dot represents a sample. d) qPCR validation of expression of *ELOVL1* in human foetal liver (FL) and cord blood (CB) derived HSC/MPPs and infant blasts (MA4+). Data are shown as mean +SD, Anova test was performed. e) Validation of *ELOVL1* sgRNA using TIDE assay.

PCA analysis of the 4 populations revealed that there was a clear separation in PC1 (Fig. 5.15a). It should be noted that one of the D2 *ELOVL1* knockouts clusters more closely with the D2 neg knockout. The results from the comparison of D4 *ELOVL1* and D4 neg control knockout are shown in Fig. 5.15b where we can observe that a small number of lipids were downregulated (highlighted in green) and a larger number of lipids were upregulated (highlighted in red).

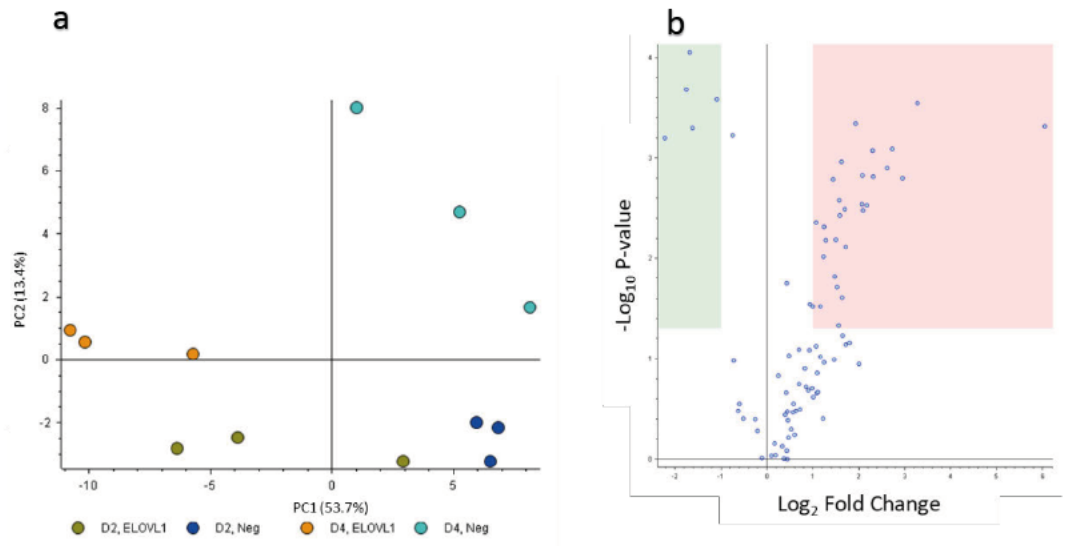

Figure 5.15| Lipidome analysis of ELOVL1 knockout.

a) PCA of lipidomics results. (D2= day2, D4=day 4, ELOVL1 = ELOVL1 knockout, Neg= knockout with negative sgRNA). b) Volcano plot of D4 ELOVL1 knockout compared to D4 neg knockout. Lipids are shown as dots, lipids highlighted in red were upregulated and in green were downregulated.

Further analysis of the results of the lipidome experiment revealed that the top downregulated lipids contained very long saturated and monounsaturated fatty acid chains (Table: 5.1 – highlighted in green). Interestingly, there was an up regulation of lipids with long non-saturated fatty acids; however, this could just be a compensation mechanism (highlighted in blue). There were no statistically significant changes in the lipidome when D2 *ELOVL1* knockout was compared with D2 neg control knockout.

Name	Ratio: (D4, ELOVL1) / (D4, Neg)	Adj. P-value: (D4, ELOVL1) / (D4, Neg)
TG (O-60:0)	0.314	0.008102373
TG (O-64:0)	0.299	0.012014936
TG (O-64:1) or (P-64:0)	0.472	0.01270702
SM (d36:1)	9.714	0.012831068
TG (O-63:0)	0.325	0.013092158
TG (58:8)	3.831	0.013092158
HexCer (d18:1/18:0)	66.473	0.013092158
TG (48:0)	0.597	0.014692934
PC (40:1)	0.216	0.015073834
TG (56:8)	6.619	0.01773447
TG (52:4)	4.935	0.017892373
TG (51:3)	3.078	0.020087593
TG (52:5)	6.172	0.021904798
TG (18:1/16:1/16:1)	4.218	0.024702387
TG (54:7)	4.998	0.024816753
TG (58:9)	7.732	0.02553353
TG (52:3)	2.731	0.026020225
PC (34:2)	2.983	0.035246907
TG (51:2)	4.2	0.035623364
PC (40:4)	4.524	0.035623364
PC (32:2)	3.243	0.036351345
TG (49:2)	4.248	0.036925748
TG (56:7)	3.011	0.040786231
TG (18:1/16:1/16:0)	2.095	0.045406123
TG (46:1)	2.384	0.048614284

Table 5.1| List of lipids identified from the study of the lipidome of SEM-Cas9 ELOVL1 knockout cells. Comparison of day 4 ELOVL1 knockout with day 4 negative control knockout. (triglyceride (TG), sphingomyelin (SM), phosphatidylcholines (PC), hexosyl ceramides (HexCer).

The results obtained from the lipidomics experiments were in accordance with previous publications where it was shown that ELOVL1 is critical for the elongation of very long chain fatty acids (VLCFAs) (Tvrdik et al., 2000), in particular, the elongation of saturated and monounsaturated VLCFAs which are critical for cellular membranes as they contribute to the fluidity and physico-chemical properties of the membranes (Kraft, 2016, Ohno et al., 2010, Asadi et al., 2002).

Interestingly, elongation of very long chain fatty acids has been implicated in breast cancer and lung cancer (Marien et al., 2016, Feng et al., 2016,

Yamashita et al., 2017). In particular, it was shown that high levels of *ELOVL1* in breast cancer and *ELOVL6* in lung cancer lead to aberrant increase of phospholipids with longer fatty acid chains (Yamashita et al., 2017, Marien et al., 2016). In both studies, they suggest that targeting of appropriate ELOVLs could serve as a novel therapeutic approach. Following from this I believe it would be interesting to investigate knockout of *ELOVL1* in a clinical setting using patient-derived samples and examine the membrane lipid composition of blasts derived from infant patients.

5.5.3 Migration assay

In the previous section, using a CRISPR–Cas9 approach I investigated the knockout effect of 19 genes where I identified 6 genes that induced apoptosis of SEM-Cas9 cells. The remaining genes did not have any effect on the survival of the SEM-Cas9 expressing cells.

It is well known that there is a high incidence of central nervous system (CNS) infiltration in infants with MLL-AF4-driven ALL (Silverman, 2007). Following from this it would be interesting to investigate whether any of the genes upregulated in the foetal liver-derived cells (and expressed at similar levels in the infant blasts) had an effect on the migration potential of the SEM-Cas9 cells. In a fascinating study, Yao *et al.* identified the interaction between α6 integrin and laminin to be critical for migration of ALL cells. Additionally, they showed that ALL cells hijack neural migratory pathways in order to invade the CNS in mice (Yao et al., 2018).

Amongst the genes upregulated in the foetal liver-derived tissues (human and murine) I identified a number of genes that have previously been shown to affect cell migration (Fig. 5.5). Amongst those genes were Integrin-α4 (*ITGA4*), Laminin-β1 (*LMNB1*), Ectoderm-neural cortex protein-1 (*ENC1*) and

Hyaluronan Mediated Motility Receptor (*HMMR*) (Yao et al., 2018, Fan et al., 2019, Wang and Zhang, 2016).

In order to investigate whether these genes play a role in the migration potential of the SEM cells, a migration assay was performed using the SEM-Cas9 cell line, transduced with sgRNAs for each of these genes. Following transduction with sgRNA lentiviral particles, a cell line was derived for each of the knockouts. SEM-Cas9-sgRNA cells were placed on top of a transwell, and the number of cells migrated to the bottom of the well was counted following 5 hours incubation (Fig. 5.16a). The cells were counted using a NovoCyte flow cytometer where it was shown that none of the sgRNAs affected the migration potential of the SEM-Cas9 cells (Fig. 5.16b). However, it should be noted that the sgRNAs were not validated for their efficiency.

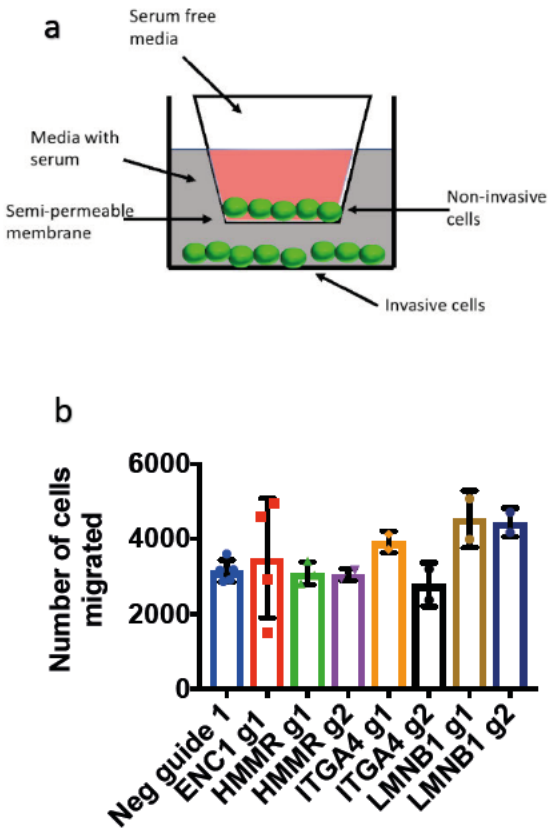

Figure 5.16| Migration assay using SEM-Cas9.

a) Experimental design used for the migration assay. b) Number of cells migrated. Data are shown as mean ±SD, each dot represents a sample.

5.6 DACH1

dach1 (Dachshund Family Transcription Factor 1) was initially identified in mutant fruit flies as it exerted a very interesting phenotype where the flies had characteristically short legs and no eyes (Mardon et al., 1994). More recently, *DACH1* has been shown to be a tumour suppressor gene in a number of cancers (Bu et al., 2016, Cao et al., 2017, Chen et al., 2013, Chu et al., 2014, Liu et al., 2015, Watanabe et al., 2011, Xu et al., 2017, Zhang et al., 2018).

DACH1 was a gene upregulated in the neonatal and adult population (human and murine, respectively), and there was no *DACH1* expression in the blasts derived from infants with MLL-AF4-driven ALL (Fig. 5.17).

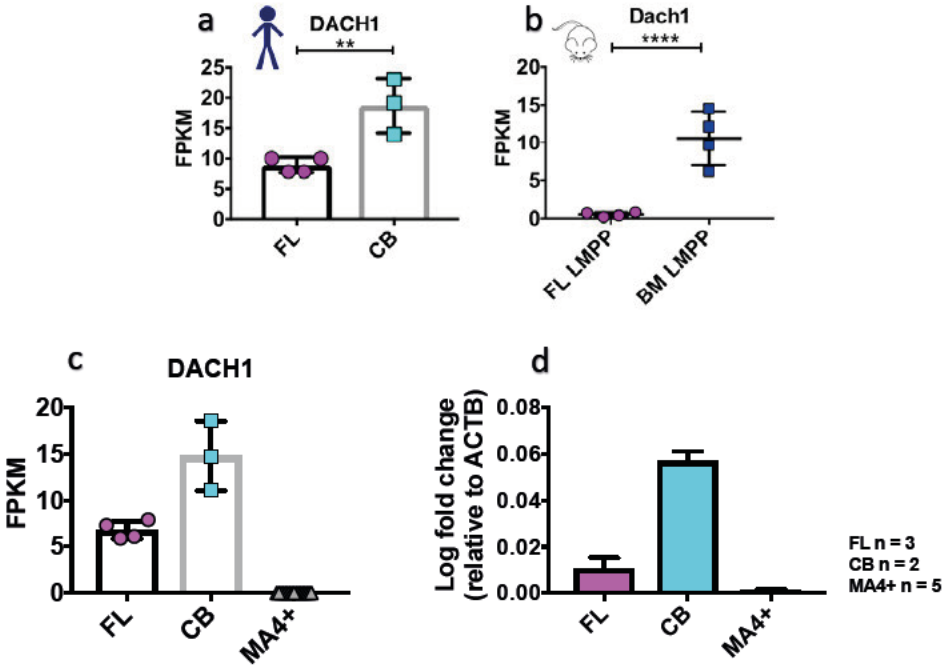

Figure 5.17| *DACH1* expression.

a) *DACH1* expression in human foetal liver (FL) and cord blood (CB) derived HSC/MPPs. RNA sequencing data are shown as mean ±SD, each dot represents a sample. b) *Dach1* expression in murine foetal liver (FL) and adult bone marrow (BM) derived LMPPs. RNA sequencing data are shown as mean ±SD, each dot represents a sample. c) *DACH1* expression in human foetal liver (FL) and cord blood (CB) derived HSC/MPPs and infant blasts (MA4+) (Infant blasts data were obtained from Andersson *et al.*). RNA sequencing data are shown as mean ±SD, each dot represents a sample. d) qPCR validation of expression of *DACH1* in human foetal liver (FL) and cord blood (CB) derived HSC/MPPs and infant blasts (MA4+). Data are shown as mean +SD.

Given its extremely low expression in the blasts derived from infants with MLL-AF4-driven ALL and its known role as a tumour suppressor, I hypothesised that overexpression of this gene might exert a negative effect on the survival of the SEM cells. For this purpose, I generated a SEM-DACH1-GFP overexpressing cell line (Fig. 5.18a). It should be noted that a non-canonical open reading frame was used (transcript variant X5).

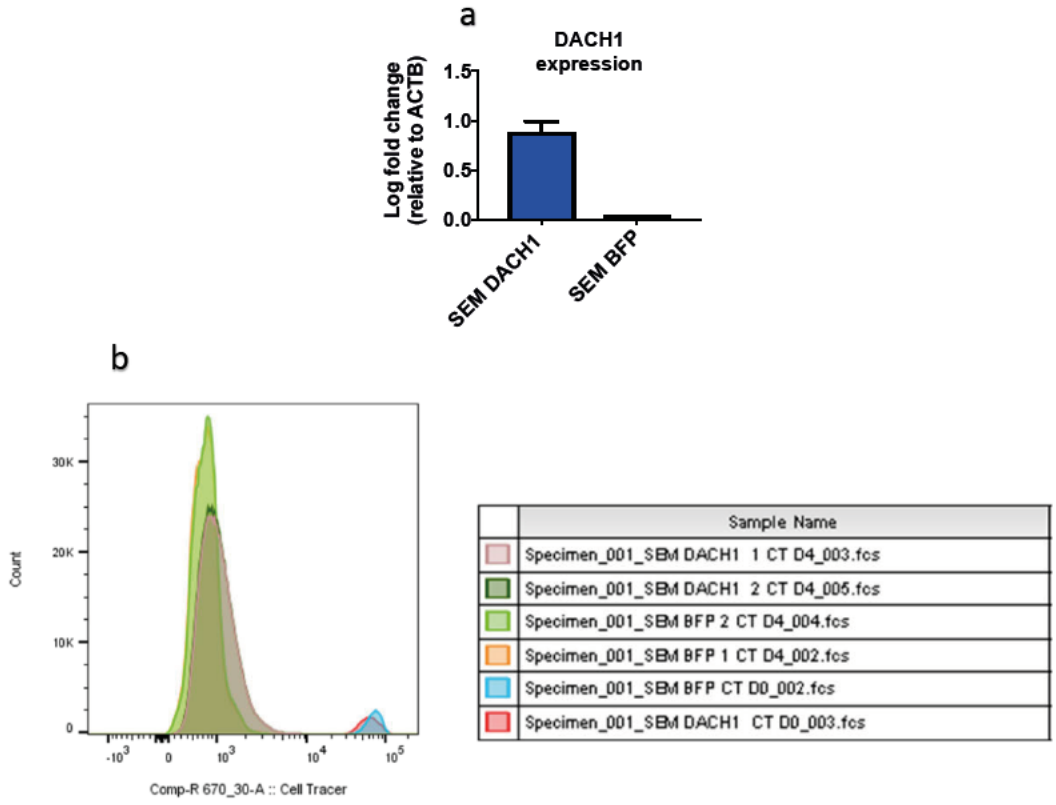

Figure 5.18| DACH1 overexpression in SEM cells.

a) qPCR of SEM-DACH1 and SEM-BFP (control) cells, n=2. b) Cell Tracer experiment of SEM-DACH1 and SEM-BFP (control cells), n=2. Day 0 = D0 and Day 4 =D4.

Overexpression of *DACH1* had no effect on the survival of the SEM cells. Following from this, I decided to investigate whether *DACH1* expression affected the proliferation potential of the cells. A Cell Tracer assay was performed where the SEM-DACH1-GFP and SEM-BFP (control) cells were labelled with a cell tracer dye with which the proliferation of the cells could be

monitored. Flow cytometric analysis revealed that overexpression of *DACH1* in the SEM cells decreased the ability of the cells to proliferate (Fig. 518b). In particular, we can observe that at day 0 (D0) the fluorescent intensity of the cell tracer dye is at similar levels between the *DACH1* expressing cells and the controls (Fig. 5.18b). However, at day 4 (D4) the peaks representing the *DACH1* expressing cells were brighter than the control cells, suggesting that the *DACH1*-expressing cells divided less than the controls. From this, it can be concluded that *DACH1* expression does not affect the survival of the cells; however, it does appear to have an effect of the proliferation potential of the SEM cells.

5.7 Discussion

It has long been speculated that the foetal origin of infant MLL-AF4-driven ALL is responsible for the unique biology of this disease. In the previous two chapters, I investigated the foetal origin of the disease by understanding the transcriptional landscape of foetal-derived cells in humans and mice. It was clear that in both species foetal-derived cells were characterised by a proliferative and oncogenic nature.

Genes that are essential are usually conserved across species, therefore it was safe to speculate that this would hold true for genes that are critical for the foetal and neonatal/adult transcriptional signatures. Comparison of the human and murine datasets identified a number of genes that were common between the two species. As expected, the genes common in the foetal transcriptomes were predominantly developmental genes and genes involved in cell proliferation.

To investigate whether the foetal origin of the disease is critical for the disease maintenance, I selected 20 genes that were upregulated in the foetal liver-derived cells (both human and murine). Those genes were expressed at similar levels between the foetal liver-derived tissues and the blasts. From those genes, I identified seven genes including *PLK1*, *ELOVL1*, *HSPD1*, *TPX2*, *NUTF2*, *BUB1B* and *CCNB1* that were acutely required for the viability of SEM cells. Although the majority of the genes were not unique to the infant disease, I think it would be interesting to further investigate whether they could be used to treat the infant disease. Of particular interest was PLK1 and its close “friend” AURKA as there are inhibitors available. One of the genes that seems to be unique to the infant leukaemia was *ELOVL1*. This gene, that has been shown to be important for the elongation of very long fatty acid chains, is very interesting as it is involved in the maintenance of cell membranes. Given the poor response of infants to chemotherapy for example prednisone, it will

not be surprising if the cell membrane of the blasts has a different composition which renders them more resistant to standard chemotherapy.

A gene that was upregulated in the human neonatal and murine adult cells with very low expression in the blasts was *DACH1*. This gene was interesting, as it has been shown to be a tumour suppressor gene in a number of cancers. Overexpression of this gene in SEM did not exert a negative effect in the survival of the cells; however, it did decrease the proliferation potential of the cells.

Infant MLL-AF4-driven ALL is a devastating disease and the patients have a very poor prognosis. This is mainly due to the fact that we do not completely understand the unique biology of the disease. By understanding which aspects of the disease could be a residue of its foetal origin, we could develop novel therapeutic targets. Using this approach, a number of such targets have been identified in this study, suggesting that the foetal origin of the disease could be its Achilles' heel.

Chapter 6 Discussion

Infant MLL-AF4-driven ALL is a rare but devastating disease with dismal prognosis. MLL-AF4 fusion occurs when the N terminal portion of MLL fuses with AF4 which results in the production of an aberrant fusion protein. Interestingly, the infant patients have a silent mutational landscape suggesting that the fusion is the main disease driver. It is well established that the disease arises *in utero* and that the foetal origin of the disease could be a critical contributor to the unique disease phenotype. It has been shown in many studies that foetal and adult blood cells possess a multitude of different characteristics. In fact, in one of the studies Barrett *et al*. using an Mll-AF4-expressing mouse model showed that foetal liver-derived cells were more prone to transformation by Mll-AF4 compared to their adult counterparts (Barrett et al., 2016).

Following from Barrett *et al.* it would be interesting to investigate how the foetal origin of the disease affects the disease phenotype. Towards this end, I initially defined the transcriptional profile of murine E14.5 foetal liver and adult bone marrow-derived LMPPs. From the data, it was clear that the two populations possessed distinct characteristics, which was a reflection of their different roles in haematopoiesis. Foetal liver-derived cells were characterised by a proliferative nature and upregulated a large number of genes that have previously been linked with cancer or leukaemia. These characteristics are a reflection of cells that are required to support the needs of a growing organism. On the contrary, the adult bone marrow-derived cells were defined by a mature and protective transcriptional profile as there was an upregulation in a number of tumour suppressor genes. To further validate this data and ensure that they hold true for humans, I defined the transcriptional profile of human foetal liver and cord blood-derived HSC/MPPs. A similar picture emerged as that of the murine data; however, it appeared that the proliferative and oncogenic nature of the human foetal liver-derived population was more prominent. One key point is that it is difficult to ensure whether this was a true biological difference

or a technical artefact. I think the main limitation of this study was that different populations were sequenced for humans and mice and therefore the direct comparison came with this drawback. However, the RNA quality of human cord blood-derived LMPPs was consistently poor and inadequate for preparation of RNA sequencing libraries. It should also be mentioned that due to the rarity of human bone marrow samples no effort was made to obtain such samples.

Regardless of the limitations, it was clear, from both the human and murine data, that the foetal-derived cells had a proliferative and oncogenic nature. Following from this, I believe that it is safe to speculate that the unique nature of the foetal cells could be a key contributor to the initiation of the aggressive infant disease.

The next step was to corroborate these findings in the infant disease setting. To do this, I initially identified genes, which were common between the human and murine dataset. In my opinion, the presence of genes in both datasets showed their critical role, as they were conserved across species. Additionally, I used this approach to validate my RNA sequencing data, by validating one experiment with the other. Following from this, I identified genes the expression of which was at similar levels between the foetal liver-derived cells and the infant blasts. With this approach, I speculated that expression of those genes was a residue of the foetal origin of the leukaemia initiating cells. Expression of these genes could also be an aberration caused by the fusion protein; however, it should be mentioned that there were no activating/de-activating mutations in the infant blasts. This point is critical, as in adult leukaemias or cancers the abnormal over-expression of genes is usually linked to a mutation(s); however, as mentioned earlier, infants are characterised by a silent mutational landscape. Therefore, I believe it is safe to assume that expression of the genes was due to its foetal origin and that their sustained expression indicates that they may be important for the disease phenotype.

From the genes the expression of which was common between the foetal liver-derived cells and the blasts, I selected 21 genes. The selection was based on

the role of the gene but also the expression levels of the gene in the SEM cell line. The selected genes were *RGL1, HMMR, ITGA4, ASPM, ENC1, SUV39H2*, *ELOVL1, PLK1, TPX2, HSPD1, APEX1, DLAT, NUTF2, TTLL12, LMNB1, CCNB1, CCNF, KIF20A, BUB1B* and *DACH1*. The majority of the genes selected were involved in different aspects of the cell cycle/proliferation. Amongst those genes were *ASPM, PLK1, TPX2, APEX1, CCNB1, CCNF*, *KIF20A* and *BUB1B*. Other genes have been shown to be important for cell migration including *HMMR, ITGA4, ENC1* and *LMNB1*. The remaining genes have a number of different roles including chromatin binding for *SUV39H2*, pyruvate metabolism for *DLAT* and less defined roles for *RGL1* and *TTLL12*. I have already discussed the roles of *ELOVL1*, *NUTF2* and *HSPD1*.

The first gene I investigated in this study was *PLK1*, as there was an inhibitor readily available (Volasertib). It was fascinating to see the tremendous effect that the inhibitor exerted in the SEM cell line. A key limitation here was that the SEM cells are not an accurate representation of clinical samples derived from infants with MLL-AF4-driven ALL. However, I believe the data obtained from this experiment were promising and it would be interesting to investigate the effect of Volasertib in a clinical setting. Similar to Volasertib, another inhibitor that in my opinion would be worth trying with infant blasts is Alisertib which inhibits AURKA, which was also highly expressed in the blasts.

In order to investigate the role of *RGL1, HMMR, ITGA4, ASPM, ENC1, SUV39H2, ELOVL1, TPX2, HSPD1, APEX1, DLAT, NUTF2, TTLL12, LMNB1, CCNB1, CCNF, KIF20A* and *BUB1B,* I used a CRISPR-Cas9 approach. I generated a SEM-Cas9-expressing cell line and tested two sgRNAs for each gene and performed a knockout screen. The small number of sgRNAs used here is the major drawback, as we cannot be certain that for those genes that did not exerted an effect whether this was due to an inefficient knockout or because the genes are not important for the survival of the SEM cells.

With the CRISPR-Cas9 approach, I identified *ELOVL1, TPX2, HSPD1, NUTF2, CCNB1* and *BUB1B* that affected the viability of the SEM cells. Investigation into other, published CRISPR-Cas9 screens revealed that some

of the genes were not unique to the infant disease, but played similar roles in other leukaemia and cancer cell lines. Amongst those genes were *TPX2, NUTF2, CCNB1* and *BUB1B*. Although they are not unique, I think it is still interesting to investigate the role of those genes and their potential use to treat the infant disease.

HSPD1, was one of the genes that was unique to this screen; however, I was not able to validate the RNA sequencing data with qPCR. Additionally, I investigated expression of *HSPD1* is normal bone marrow cells (using http://www.altanalyze.org/ICGS/HCA/splash.php) where I observed that this gene was highly expressed in the majority of the haematopoietic cells and therefore not the perfect target to inhibit.

Of particular interest was *ELOVL1* as it appears to be unique to the infant leukaemia and its expression in normal bone marrow blood cells is low (as shown in http://www.altanalyze.org/ICGS/HCA/splash.php). *ELOVL1* knockout had a dramatic impact on the SEM cell line and investigation into the mechanisms of action revealed that it only affects lipids with very long fatty acid chains, which are known to be important for cell membranes.

From this data, I believe that it safe to say that the foetal origin of the leukaemia initiating cells is critical not only for the disease initiation but also for its maintenance. Identifying genes, the expression of which could be due to the foetal origin of the disease has proved to be a novel approach for identifying disease targets.

Another aim of the study was to understand the molecular events that take place during the early stages of transformation by MLL-AF4. It is well established that MLL-AF4-driven infant ALL arises *in utero*, and multiple efforts have been made to capture the early disease stages. Towards this end, I investigated how MLL-AF4 co-operates with its environment in order to initiate and drive this aggressive infant leukaemia. For this, I used a mouse model where Mll-AF4 was expressed at the stage of the first definitive haematopoietic cells and defined the transcriptional profile of Mll-AF4-expressing LMPPs. With

this approach, I identified a number of genes that were aberrantly expressed due to the fusion protein. Of particular interest was *Skida1* as it was upregulated in the murine Mll-AF4-expressing LMPPs but also in the blasts of infants with MLL-AF4-driven ALL compared to paediatric patients with the same disease and healthy controls. Interestingly, another gene of the same family came up in the previous screens as it was upregulated in human cord blood and murine adult bone marrow-derived cells. This gene was *DACH1*, which was shown to be a tumour suppressor gene in a number of solid cancers. Investigation of those two genes using the SEM cell line revealed that neither of the genes influenced the survival of the SEM cells; however, DACH1 did decrease the proliferation potential of the cells. Although the data are not very encouraging, I think it is important to consider that the SEM cell line is a reflection of the paediatric disease as opposed to an infant one. Following from this, I believe that it would be interesting to investigate the effect of these genes in samples derived from infant patients.

Given the fundamental differences between humans and mice, I tried to investigate the early disease stages in humans. In particular, I transduced human foetal liver-derived HSPCs with MLL-AF4 lentiviral particles and performed B cell differentiation. However, I was unable to obtain a positive result with this approach.

I believe this has been a proof of concept study where by defining the cell of origin of the disease I was able to identify novel therapeutic targets for infant MLL-AF4-driven ALL. In this study, the cell of origin was identified to be the human foetal liver-derived LMPP; however, this was when compared to the SEM cell line. Given the recent advancement in single RNA sequencing it has been clear that there is tremendous heterogeneity in what was previously thought to be one population. Following from this, I believe that it could be possible that different patients have different cells of origin. Different cells of origin may even explain inter-patient differences in response to treatment and risk of relapse or lineage switching. However, one thing is certain that the disease arises *in utero* and that the foetal origin of the disease is critical. It was

also interesting to see that the infant blasts formed two different clusters and that these clusters could be defined by their *HOXA9/IRX1* expression. There was a clear negative correlation between expression of these two genes and this was of clinical relevance as patients with *IRX1* expression do not have the AF4-MLL reciprocal fusion and also suffer from a worse prognosis than the infants that express *HOXA9*. Although there were very few patients to perform further analysis, I think it is important to investigate these two clusters for further clues as to how to treat these patients.

From this study it is clear that the foetal origin of the disease is critical for the disease initiation, maintenance and unique disease phenotype and, as a consequence, appears to be a promising therapeutic target. Another aspect of the foetal origin of the disease that is likely to further support the initiation of this aggressive disease, but was not investigated in this study, is the microenvironment. Indeed, Barrett *et al* using the Mll-AF4-Vec-Cre mouse model investigated expression of Mll-AF4 in endothelial cells, mesenchymal stromal cells and osteoblasts. They observed that the highest expression was in endothelial cells whereas there was very low expression in both mesenchymal stromal and osteoblasts. This data suggested the possibility that endothelial cells might be involved in the disease initiation by further supporting the Mll-AF4 expressing haematopoietic cells. This was in line with finding in the same study as comparison of Mll-AF4 activation using the mouse model described above, gave a slightly more severe phenotype when compared to a mouse model where Mll-AF4 expression was initiated at the definitive haematopoietic stage (using Vac-Cre). Although further evidence is required, it is very likely that the leukaemia-initiating cells works in synergy with foetal microenvironment to drive this aggressive infant disease.

Chapter 7 Future work

Following from this study, I think it is important to further investigate genes the expression of which was at similar levels between the foetal liver-derived cells and the blasts, with focus on the human dataset. I believe that with this approach, we could identify more therapeutic targets and the focus should be on genes that are not expressed in healthy tissues. For the targets that were identified in this study in particular *PLK1*, *AURKA* and *ELOVL1*, it would be interesting to test the effect of these genes *in vivo* using blasts derived from infant patients.

In my opinion of particular interest is *ELOVL1*, as it appears to be unique to the infant leukaemia. Given the poor response of patients to chemotherapy, for example prednisone, it would be interesting to investigate whether the cell membrane of the blasts derived from infant patients with MLL-AF4-driven ALL differ from healthy ones. Additionally, it would be interesting to investigate differences in the lipid composition of foetal and adult cells and whether these differences allow the foetal cells to escape the effect of chemotherapy.

It has been well established that infant patients with MLL-AF4-driven ALL could be divided into two subcategories based on their HOXA9 expression. This was further confirmed in this study, and I was able to show that there is an inverse correlation between *HOXA9* and *IRX1*. Of course, given the low number of patients, these finding should be treated with caution. One key point here is that now there is another dataset publicly available from Agraz-Doblas *et al.,* it would be possible to further investigate the two sub-clusters of the infant disease (Agraz-Doblas et al., 2019). It would be interesting to investigate the transcriptome of the two different sub-clusters, in order to find clues that would allow improving the prognosis of the patients that express *IRX1*.

Chapter 8 Concluding remarks

Infant MLL-AF4-driven ALL is a devastating disease with a unique underlying biology, which we do not completely understand. The uniqueness of this disease has been attributed to the foetal origin of the leukaemia-initiating cell. We can speculate that the environment that supports rapid growth of the embryo when hijacked by MLL-AF4 could lead to the aggressive leukaemia that is observed in the infant patients.

This has been a proof of concept study where it was shown that by defining the transcriptome of the cell of origin of the disease it was possible to identify novel disease targets. In my opinion, this approach could be valuable for diseases that are rare or difficult to model such as MLL-AF4-driven infant ALL.

Chapter 9 References

ADOLFSSON, J., MANSSON, R., BUZA-VIDAS, N., HULTQUIST, A., LIUBA, K., JENSEN, C. T., BRYDER, D., YANG, L., BORGE, O. J., THOREN, L. A., ANDERSON, K., SITNICKA, E., SASAKI, Y., SIGVARDSSON, M. & JACOBSEN, S. E. 2005. Identification of Flt3+ lympho-myeloid stem cells lacking erythro-megakaryocytic potential a revised road map for adult blood lineage commitment. *Cell,* 121**,** 295-306.

AGRAZ-DOBLAS, A., BUENO, C., BASHFORD-ROGERS, R., ROY, A., SCHNEIDER, P., BARDINI, M., BALLERINI, P., CAZZANIGA, G., MORENO, T., REVILLA, C., GUT, M., VALSECCHI, M. G., ROBERTS, I., PIETERS, R., DE LORENZO, P., VARELA, I., MENENDEZ, P. & STAM, R. W. 2019. Unraveling the cellular origin and clinical prognostic markers of infant B-cell acute lymphoblastic leukemia using genome-wide analysis. *Haematologica,* 104**,** 1176-1188.

AKKAPEDDI, P., FRAGOSO, R., HIXON, J. A., RAMALHO, A. S., OLIVEIRA, M. L., CARVALHO, T., GLOGER, A., MATASCI, M., CORZANA, F., DURUM, S. K., NERI, D., BERNARDES, G. J. L. & BARATA, J. T. 2019. A fully human anti-IL-7Ralpha antibody promotes antitumor activity against T-cell acute lymphoblastic leukemia. *Leukemia,* 33**,** 2155-2168.

ALEXANDER, F. E., PATHEAL, S. L., BIONDI, A., BRANDALISE, S., CABRERA, M. E., CHAN, L. C., CHEN, Z., CIMINO, G., CORDOBA, J. C., GU, L. J., HUSSEIN, H., ISHII, E., KAMEL, A. M., LABRA, S., MAGALHAES, I. Q., MIZUTANI, S., PETRIDOU, E., DE OLIVEIRA, M. P., YUEN, P., WIEMELS, J. L. & GREAVES, M. F. 2001. Transplacental chemical exposure and risk of infant leukemia with MLL gene fusion. *Cancer Res,* 61**,** 2542-6.

ANDERSSON, A. K., MA, J., WANG, J., CHEN, X., GEDMAN, A. L., DANG, J., NAKITANDWE, J., HOLMFELDT, L., PARKER, M., EASTON, J., HUETHER, R., KRIWACKI, R., RUSCH, M., WU, G., LI, Y., MULDER, H., RAIMONDI, S., POUNDS, S., KANG, G., SHI, L., BECKSFORT, J., GUPTA, P., PAYNE-TURNER, D., VADODARIA, B., BOGGS, K., YERGEAU, D., MANNE, J., SONG, G., EDMONSON, M., NAGAHAWATTE, P., WEI, L., CHENG, C., PEI, D., SUTTON, R., VENN, N. C., CHETCUTI, A., RUSH, A., CATCHPOOLE, D., HELDRUP, J., FIORETOS, T., LU, C., DING, L., PUI, C. H., SHURTLEFF, S., MULLIGHAN, C. G., MARDIS, E. R., WILSON, R. K., GRUBER, T. A., ZHANG, J. & DOWNING, J. R. 2015. The landscape of somatic mutations in infant MLL-rearranged acute lymphoblastic leukemias. *Nat Genet,* 47**,** 330-7.

APLAN, P. D., CHERVINSKY, D. S., STANULLA, M. & BURHANS, W. C. 1996. Site-specific DNA cleavage within the MLL breakpoint cluster region induced by topoisomerase II inhibitors. *Blood,* 87**,** 2649-58.
ARMSTRONG, S. A., STAUNTON, J. E., SILVERMAN, L. B., PIETERS, R., DEN BOER, M. L., MINDEN, M. D., SALLAN, S. E., LANDER, E. S., GOLUB, T. R. & KORSMEYER, S. J. 2002. MLL translocations specify a distinct gene expression profile that distinguishes a unique leukemia. *Nat Genet,* 30**,** 41-7.
ASADI, A., JORGENSEN, J. & JACOBSSON, A. 2002. Elovl1 and p55Cdc genes are localized in a tail-to-tail array and are co-expressed in proliferating cells. *J Biol Chem,* 277**,** 18494-500.
ATHERTON-FESSLER, S., LIU, F., GABRIELLI, B., LEE, M. S., PENG, C. Y. & PIWNICA-WORMS, H. 1994. Cell cycle regulation of the p34cdc2 inhibitory kinases. *Mol Biol Cell,* 5**,** 989-1001.
BABOVIC, S. & EAVES, C. J. 2014. Hierarchical organization of fetal and adult hematopoietic stem cells. *Exp Cell Res,* 329**,** 185-91.
BAI, C., RICHMAN, R. & ELLEDGE, S. J. 1994. Human cyclin F. *Embo j,* 13**,** 6087-98.
BAI, T., ZHAO, Y., LIU, Y., CAI, B., DONG, N. & LI, B. 2019. Effect of KNL1 on the proliferation and apoptosis of colorectal cancer cells. *Technol Cancer Res Treat,* 18**,** 1533033819858668.
BAKER, S. J., FEARON, E. R., NIGRO, J. M., HAMILTON, S. R., PREISINGER, A. C., JESSUP, J. M., VANTUINEN, P., LEDBETTER, D. H., BARKER, D. F., NAKAMURA, Y., WHITE, R. & VOGELSTEIN, B. 1989. Chromosome 17 deletions and p53 gene mutations in colorectal carcinomas. *Science,* 244**,** 217-21.
BALLABIO, E. & MILNE, T. A. 2012. Molecular and Epigenetic Mechanisms of MLL in Human Leukemogenesis. *Cancers (Basel),* 4**,** 904-44.
BARDINI, M., WOLL, P. S., CORRAL, L., LUC, S., WITTMANN, L., MA, Z., LO NIGRO, L., BASSO, G., BIONDI, A., CAZZANIGA, G. & JACOBSEN, S. E. 2015. Clonal variegation and dynamic competition of leukemia-initiating cells in infant acute lymphoblastic leukemia with MLL rearrangement. *Leukemia,* 29**,** 38-50.
BARRETT, N. A., MALOUF, C., KAPENI, C., BACON, W. A., GIOTOPOULOS, G., JACOBSEN, S. E. W., HUNTLY, B. J. & OTTERSBACH, K. 2016. Mll-AF4 Confers Enhanced Self-Renewal and Lymphoid Potential during a Restricted Window in Development. *Cell Rep,* 16**,** 1039-1054.
BARSKI, A., CUDDAPAH, S., CUI, K., ROH, T. Y., SCHONES, D. E., WANG, Z., WEI, G., CHEPELEV, I. & ZHAO, K. 2007. High-resolution profiling of histone methylations in the human genome. *Cell,* 129**,** 823-37.
BASSO, G., RONDELLI, R., COVEZZOLI, A. & PUTTI, M. 1994. The role of immunophenotype in acute lymphoblastic leukemia of infant age. *Leuk Lymphoma,* 15**,** 51-60.
BECKER, A. J., MC, C. E. & TILL, J. E. 1963. Cytological demonstration of the clonal nature of spleen colonies derived from transplanted mouse marrow cells. *Nature,* 197**,** 452-4.

BHATLA, T., WANG, J., MORRISON, D. J., RAETZ, E. A., BURKE, M. J., BROWN, P. & CARROLL, W. L. 2012. Epigenetic reprogramming reverses the relapse-specific gene expression signature and restores chemosensitivity in childhood B-lymphoblastic leukemia. *Blood,* 119**,** 5201-10.

BHOJWANI, D., KANG, H., MOSKOWITZ, N. P., MIN, D. J., LEE, H., POTTER, J. W., DAVIDSON, G., WILLMAN, C. L., BOROWITZ, M. J., BELITSKAYA-LEVY, I., HUNGER, S. P., RAETZ, E. A. & CARROLL, W. L. 2006. Biologic pathways associated with relapse in childhood acute lymphoblastic leukemia: a Children's Oncology Group study. *Blood,* 108**,** 711-7.

BIANCHI-SMIRAGLIA, A., PAESANTE, S. & BAKIN, A. V. 2013. Integrin beta5 contributes to the tumorigenic potential of breast cancer cells through the Src-FAK and MEK-ERK signaling pathways. *Oncogene,* 32**,** 3049-58.

BIKEYE, S. N., COLIN, C., MARIE, Y., VAMPOUILLE, R., RAVASSARD, P., ROUSSEAU, A., BOISSELIER, B., IDBAIH, A., CALVO, C. F., LEURAUD, P., LASSALLE, M., EL HALLANI, S., DELATTRE, J. Y. & SANSON, M. 2010. ASPM-associated stem cell proliferation is involved in malignant progression of gliomas and constitutes an attractive therapeutic target. *Cancer Cell Int,* 10**,** 1.

BIRKE, M., SCHREINER, S., GARCIA-CUELLAR, M. P., MAHR, K., TITGEMEYER, F. & SLANY, R. K. 2002. The MT domain of the proto-oncoprotein MLL binds to CpG-containing DNA and discriminates against methylation. *Nucleic Acids Res,* 30**,** 958-65.

BITOUN, E., OLIVER, P. L. & DAVIES, K. E. 2007. The mixed-lineage leukemia fusion partner AF4 stimulates RNA polymerase II transcriptional elongation and mediates coordinated chromatin remodeling. *Hum Mol Genet,* 16**,** 92-106.

BOIERS, C., CARRELHA, J., LUTTEROPP, M., LUC, S., GREEN, J. C., AZZONI, E., WOLL, P. S., MEAD, A. J., HULTQUIST, A., SWIERS, G., PERDIGUERO, E. G., MACAULAY, I. C., MELCHIORI, L., LUIS, T. C., KHARAZI, S., BOURIEZ-JONES, T., DENG, Q., PONTEN, A., ATKINSON, D., JENSEN, C. T., SITNICKA, E., GEISSMANN, F., GODIN, I., SANDBERG, R., DE BRUIJN, M. F. & JACOBSEN, S. E. 2013. Lymphomyeloid contribution of an immune-restricted progenitor emerging prior to definitive hematopoietic stem cells. *Cell Stem Cell,* 13**,** 535-48.

BOIERS, C., RICHARDSON, S. E., LAYCOCK, E., ZRIWIL, A., TURATI, V. A., BROWN, J., WRAY, J. P., WANG, D., JAMES, C., HERRERO, J., SITNICKA, E., KARLSSON, S., SMITH, A. J. H., JACOBSEN, S. E. W. & ENVER, T. 2018. A Human IPS Model Implicates Embryonic B-Myeloid Fate Restriction as Developmental Susceptibility to B Acute Lymphoblastic Leukemia-Associated ETV6-RUNX1. *Dev Cell,* 44**,** 362-377.e7.

BONAVENTURE, A., HAREWOOD, R., STILLER, C. A., GATTA, G., CLAVEL, J., STEFAN, D. C., CARREIRA, H., SPIKA, D., MARCOS-GRAGERA, R., PERIS-BONET, R., PINEROS, M., SANT, M.,

KUEHNI, C. E., MURPHY, M. F. G., COLEMAN, M. P. & ALLEMANI, C. 2017. Worldwide comparison of survival from childhood leukaemia for 1995-2009, by subtype, age, and sex (CONCORD-2): a population-based study of individual data for 89 828 children from 198 registries in 53 countries. *Lancet Haematol,* 4**,** e202-e217.

BORKIN, D., HE, S., MIAO, H., KEMPINSKA, K., POLLOCK, J., CHASE, J., PUROHIT, T., MALIK, B., ZHAO, T., WANG, J., WEN, B., ZONG, H., JONES, M., DANET-DESNOYERS, G., GUZMAN, M. L., TALPAZ, M., BIXBY, D. L., SUN, D., HESS, J. L., MUNTEAN, A. G., MAILLARD, I., CIERPICKI, T. & GREMBECKA, J. 2015. Pharmacologic inhibition of the Menin-MLL interaction blocks progression of MLL leukemia in vivo. *Cancer Cell,* 27**,** 589-602.

BOSCH, F., CAMPO, E., JARES, P., PITTALUGA, S., MUNOZ, J., NAYACH, I., PIRIS, M. A., DEWOLF-PEETERS, C., JAFFE, E. S., ROZMAN, C. & ET AL. 1995. Increased expression of the PRAD-1/CCND1 gene in hairy cell leukaemia. *Br J Haematol,* 91**,** 1025-30.

BOWIE, M. B., KENT, D. G., COPLEY, M. R. & EAVES, C. J. 2007. Steel factor responsiveness regulates the high self-renewal phenotype of fetal hematopoietic stem cells. *Blood,* 109**,** 5043-8.

BOWIE, M. B., MCKNIGHT, K. D., KENT, D. G., MCCAFFREY, L., HOODLESS, P. A. & EAVES, C. J. 2006. Hematopoietic stem cells proliferate until after birth and show a reversible phase-specific engraftment defect. *J Clin Invest,* 116**,** 2808-16.

BRACKEN, A. P., CIRO, M., COCITO, A. & HELIN, K. 2004. E2F target genes: unraveling the biology. *Trends Biochem Sci,* 29**,** 409-17.

BRANDWEIN, J. M. 2015. Targeting polo-like kinase 1 in acute myeloid leukemia. *Ther Adv Hematol,* 6**,** 80-7.

BRAY, N. L., PIMENTEL, H., MELSTED, P. & PACHTER, L. 2016. Near-optimal probabilistic RNA-seq quantification. *Nat Biotechnol,* 34**,** 525-7.

BRINKMAN, E. K., CHEN, T., AMENDOLA, M. & VAN STEENSEL, B. 2014. Easy quantitative assessment of genome editing by sequence trace decomposition. *Nucleic Acids Res,* 42**,** e168.

BROSS, P. & FERNANDEZ-GUERRA, P. 2016. Disease-Associated Mutations in the HSPD1 Gene Encoding the Large Subunit of the Mitochondrial HSP60/HSP10 Chaperonin Complex. *Front Mol Biosci,* 3**,** 49.

BROWN, A. R., SIMMEN, R. C., RAJ, V. R., VAN, T. T., MACLEOD, S. L. & SIMMEN, F. A. 2015. Kruppel-like factor 9 (KLF9) prevents colorectal cancer through inhibition of interferon-related signaling. *Carcinogenesis,* 36**,** 946-55.

BROWN, P. 2013. Treatment of infant leukemias: challenge and promise. *Hematology Am Soc Hematol Educ Program,* 2013**,** 596-600.

BU, X. N., QIU, C., WANG, C. & JIANG, Z. 2016. Inhibition of DACH1 activity by short hairpin RNA represses cell proliferation and tumor invasion in pancreatic cancer. *Oncol Rep,* 36**,** 745-54.

BUCHNER, M., PARK, E., GENG, H., KLEMM, L., FLACH, J., PASSEGUE, E., SCHJERVEN, H., MELNICK, A., PAIETTA, E., KOPANJA, D.,

RAYCHAUDHURI, P. & MUSCHEN, M. 2015. Identification of FOXM1 as a therapeutic target in B-cell lineage acute lymphoblastic leukaemia. *Nat Commun,* 6**,** 6471.

BUENO, C., MONTES, R., MELEN, G. J., RAMOS-MEJIA, V., REAL, P. J., AYLLON, V., SANCHEZ, L., LIGERO, G., GUTIERREZ-ARANDA, I., FERNANDEZ, A. F., FRAGA, M. F., MORENO-GIMENO, I., BURKS, D., PLAZA-CALONGE MDEL, C., RODRIGUEZ-MANZANEQUE, J. C. & MENENDEZ, P. 2012. A human ESC model for MLL-AF4 leukemic fusion gene reveals an impaired early hematopoietic-endothelial specification. *Cell Res,* 22**,** 986-1002.

BUENO, C., VAN ROON, E. H., MUNOZ-LOPEZ, A., SANJUAN-PLA, A., JUAN, M., NAVARRO, A., STAM, R. W. & MENENDEZ, P. 2016. Immunophenotypic analysis and quantification of B-1 and B-2 B cells during human fetal hematopoietic development. *Leukemia.* England.

BUSCH, B., BLEY, N., MULLER, S., GLASS, M., MISIAK, D., LEDERER, M., VETTER, M., STRAUSS, H. G., THOMSSEN, C. & HUTTELMAIER, S. 2016. The oncogenic triangle of HMGA2, LIN28B and IGF2BP1 antagonizes tumor-suppressive actions of the let-7 family. *Nucleic Acids Res,* 44**,** 3845-64.

CAO, J., YAN, X. R., LIU, T., HAN, X. B., YU, J. J., LIU, S. H. & WANG, L. B. 2017. MicroRNA-552 promotes tumor cell proliferation and migration by directly targeting DACH1 via the Wnt/beta-catenin signaling pathway in colorectal cancer. *Oncol Lett,* 14**,** 3795-3802.

CATLIN, S. N., BUSQUE, L., GALE, R. E., GUTTORP, P. & ABKOWITZ, J. L. 2011. The replication rate of human hematopoietic stem cells in vivo. *Blood,* 117**,** 4460-6.

CHAN, C. S. & BOTSTEIN, D. 1993. Isolation and characterization of chromosome-gain and increase-in-ploidy mutants in yeast. *Genetics,* 135**,** 677-91.

CHANG, P. Y., HOM, R. A., MUSSELMAN, C. A., ZHU, L., KUO, A., GOZANI, O., KUTATELADZE, T. G. & CLEARY, M. L. 2010. Binding of the MLL PHD3 finger to histone H3K4me3 is required for MLL-dependent gene transcription. *J Mol Biol,* 400**,** 137-44.

CHARBORD, P., TAVIAN, M., HUMEAU, L. & PEAULT, B. 1996. Early ontogeny of the human marrow from long bones: an immunohistochemical study of hematopoiesis and its microenvironment. *Blood,* 87**,** 4109-19.

CHEN, K., WU, K., CAI, S., ZHANG, W., ZHOU, J., WANG, J., ERTEL, A., LI, Z., RUI, H., QUONG, A., LISANTI, M. P., TOZEREN, A., TANES, C., ADDYA, S., GORMLEY, M., WANG, C., MCMAHON, S. B. & PESTELL, R. G. 2013. Dachshund binds p53 to block the growth of lung adenocarcinoma cells. *Cancer Res,* 73**,** 3262-74.

CHEN, M. J., YOKOMIZO, T., ZEIGLER, B. M., DZIERZAK, E. & SPECK, N. A. 2009. Runx1 is required for the endothelial to haematopoietic cell transition but not thereafter. *Nature,* 457**,** 887-91.

CHEN, S. L., QIN, Z. Y., HU, F., WANG, Y., DAI, Y. J. & LIANG, Y. 2019. The Role of the HOXA Gene Family in Acute Myeloid Leukemia. *Genes (Basel),* 10.

CHEN, W., LI, Q., HUDSON, W. A., KUMAR, A., KIRCHHOF, N. & KERSEY, J. H. 2006. A murine Mll-AF4 knock-in model results in lymphoid and myeloid deregulation and hematologic malignancy. *Blood,* 108**,** 669-77.

CHESHIER, S. H., MORRISON, S. J., LIAO, X. & WEISSMAN, I. L. 1999. In vivo proliferation and cell cycle kinetics of long-term self-renewing hematopoietic stem cells. *Proc Natl Acad Sci U S A,* 96**,** 3120-5.

CHO, S. & SPANGRUDE, G. J. 2011. Enrichment of functionally distinct mouse hematopoietic progenitor cell populations using CD62L. *J Immunol,* 187**,** 5203-10.

CHOW, Y. P., ALIAS, H. & JAMAL, R. 2017. Meta-analysis of gene expression in relapsed childhood B-acute lymphoblastic leukemia. *BMC Cancer,* 17**,** 120.

CHU, Q., HAN, N., YUAN, X., NIE, X., WU, H., CHEN, Y., GUO, M., YU, S. & WU, K. 2014. DACH1 inhibits cyclin D1 expression, cellular proliferation and tumor growth of renal cancer cells. *J Hematol Oncol,* 7**,** 73.

CHUANG, M. K., CHIU, Y. C., CHOU, W. C., HOU, H. A., TSENG, M. H., KUO, Y. Y., CHEN, Y., CHUANG, E. Y. & TIEN, H. F. 2015. An mRNA expression signature for prognostication in de novo acute myeloid leukemia patients with normal karyotype. *Oncotarget,* 6**,** 39098-110.

COPLEY, M. R., BABOVIC, S., BENZ, C., KNAPP, D. J., BEER, P. A., KENT, D. G., WOHRER, S., TRELOAR, D. Q., DAY, C., ROWE, K., MADER, H., KUCHENBAUER, F., HUMPHRIES, R. K. & EAVES, C. J. 2013. The Lin28b-let-7-Hmga2 axis determines the higher self-renewal potential of fetal haematopoietic stem cells. *Nat Cell Biol,* 15**,** 916-25.

COPLEY, M. R. & EAVES, C. J. 2013. Developmental changes in hematopoietic stem cell properties. *Exp Mol Med,* 45**,** e55.

CORTES-CIRIANO, I., LEE, S., PARK, W. Y., KIM, T. M. & PARK, P. J. 2017. A molecular portrait of microsatellite instability across multiple cancers. *Nat Commun,* 8**,** 15180.

COWELL, I. G. & AUSTIN, C. A. 2012. Mechanism of generation of therapy related leukemia in response to anti-topoisomerase II agents. *Int J Environ Res Public Health,* 9**,** 2075-91.

CRUICKSHANK, M. N., FORD, J., CHEUNG, L. C., HENG, J., SINGH, S., WELLS, J., FAILES, T. W., ARNDT, G. M., SMITHERS, N., PRINJHA, R. K., ANDERSON, D., CARTER, K. W., GOUT, A. M., LASSMANN, T., O'REILLY, J., COLE, C. H., KOTECHA, R. S. & KEES, U. R. 2017. Systematic chemical and molecular profiling of MLL-rearranged infant acute lymphoblastic leukemia reveals efficacy of romidepsin. *Leukemia,* 31**,** 40-50.

DAIGLE, S. R., OLHAVA, E. J., THERKELSEN, C. A., BASAVAPATHRUNI, A., JIN, L., BORIACK-SJODIN, P. A., ALLAIN, C. J., KLAUS, C. R., RAIMONDI, A., SCOTT, M. P., WATERS, N. J., CHESWORTH, R., MOYER, M. P., COPELAND, R. A., RICHON, V. M. & POLLOCK, R. M. 2013. Potent inhibition of DOT1L as treatment of MLL-fusion leukemia. *Blood,* 122**,** 1017-25.

DAIGLE, S. R., OLHAVA, E. J., THERKELSEN, C. A., MAJER, C. R., SNEERINGER, C. J., SONG, J., JOHNSTON, L. D., SCOTT, M. P., SMITH, J. J., XIAO, Y., JIN, L., KUNTZ, K. W., CHESWORTH, R., MOYER, M. P., BERNT, K. M., TSENG, J. C., KUNG, A. L., ARMSTRONG, S. A., COPELAND, R. A., RICHON, V. M. & POLLOCK, R. M. 2011. Selective killing of mixed lineage leukemia cells by a potent small-molecule DOT1L inhibitor. *Cancer Cell,* 20**,** 53-65.

DAVENPORT, J. W., FERNANDES, E. R., HARRIS, L. D., NEALE, G. A. & GOORHA, R. 1999. The mouse mitotic checkpoint gene bub1b, a novel bub1 family member, is expressed in a cell cycle-dependent manner. *Genomics,* 55**,** 113-7.

DAVID, C., NANCE, J. P., HUBBARD, J., HSU, M., BINDER, D. & WILSON, E. H. 2012. Stabilin-1 expression in tumor associated macrophages. *Brain Res,* 1481**,** 71-8.

DE BRUIJN, M. F., SPECK, N. A., PEETERS, M. C. & DZIERZAK, E. 2000. Definitive hematopoietic stem cells first develop within the major arterial regions of the mouse embryo. *Embo j,* 19**,** 2465-74.

DE-COLLE, C., MENEGAKIS, A., MONNICH, D., WELZ, S., BOEKE, S., SIPOS, B., FEND, F., MAUZ, P. S., TINHOFER, I., BUDACH, V., ABU JAWAD, J., STUSCHKE, M., BALERMPAS, P., RODEL, C., GROSU, A. L., ABDOLLAHI, A., DEBUS, J., BELKA, C., GANSWINDT, U., PIGORSCH, S., COMBS, S. E., LOHAUS, F., LINGE, A., KRAUSE, M., BAUMANN, M. & ZIPS, D. 2018. SDF-1/CXCR4 expression is an independent negative prognostic biomarker in patients with head and neck cancer after primary radiochemotherapy. *Radiother Oncol,* 126**,** 125-131.

DELMORE, J. E., ISSA, G. C., LEMIEUX, M. E., RAHL, P. B., SHI, J., JACOBS, H. M., KASTRITIS, E., GILPATRICK, T., PARANAL, R. M., QI, J., CHESI, M., SCHINZEL, A. C., MCKEOWN, M. R., HEFFERNAN, T. P., VAKOC, C. R., BERGSAGEL, P. L., GHOBRIAL, I. M., RICHARDSON, P. G., YOUNG, R. A., HAHN, W. C., ANDERSON, K. C., KUNG, A. L., BRADNER, J. E. & MITSIADES, C. S. 2011. BET bromodomain inhibition as a therapeutic strategy to target c-Myc. *Cell,* 146**,** 904-17.

DERYUGINA, E. I., ZAJAC, E., ZILBERBERG, L., MURAMATSU, T., JOSHI, G., DABOVIC, B., RIFKIN, D. & QUIGLEY, J. P. 2018. LTBP3 promotes early metastatic events during cancer cell dissemination. *Oncogene,* 37**,** 1815-1829.

DESCOMBES, P. & NIGG, E. A. 1998. The polo-like kinase Plx1 is required for M phase exit and destruction of mitotic regulators in Xenopus egg extracts. *Embo j,* 17**,** 1328-35.

DEVORE, R., WHITLOCK, J., HAINSWORTH, J. D. & JOHNSON, D. H. 1989. Therapy-related acute nonlymphocytic leukemia with monocytic features and rearrangement of chromosome 11q. *Ann Intern Med,* 110**,** 740-2.

DIETZMANN, K., KIRCHES, E., VON, B., JACHAU, K. & MAWRIN, C. 2001. Increased human polo-like kinase-1 expression in gliomas. *J Neurooncol,* 53**,** 1-11.

DOBSON, C. L., WARREN, A. J., PANNELL, R., FORSTER, A. & RABBITTS, T. H. 2000. Tumorigenesis in mice with a fusion of the leukaemia oncogene Mll and the bacterial lacZ gene. *Embo j,* 19**,** 843-51.

DOHNER, H., LUBBERT, M., FIEDLER, W., FOUILLARD, L., HAALAND, A., BRANDWEIN, J. M., LEPRETRE, S., REMAN, O., TURLURE, P., OTTMANN, O. G., MULLER-TIDOW, C., KRAMER, A., RAFFOUX, E., DOHNER, K., SCHLENK, R. F., VOSS, F., TAUBE, T., FRITSCH, H. & MAERTENS, J. 2014. Randomized, phase 2 trial of low-dose cytarabine with or without volasertib in AML patients not suitable for induction therapy. *Blood,* 124**,** 1426-33.

DOU, Y., MILNE, T. A., RUTHENBURG, A. J., LEE, S., LEE, J. W., VERDINE, G. L., ALLIS, C. D. & ROEDER, R. G. 2006. Regulation of MLL1 H3K4 methyltransferase activity by its core components. *Nat Struct Mol Biol,* 13**,** 713-9.

DOU, Y., MILNE, T. A., TACKETT, A. J., SMITH, E. R., FUKUDA, A., WYSOCKA, J., ALLIS, C. D., CHAIT, B. T., HESS, J. L. & ROEDER, R. G. 2005. Physical association and coordinate function of the H3 K4 methyltransferase MLL1 and the H4 K16 acetyltransferase MOF. *Cell,* 121**,** 873-85.

DOULATOV, S., NOTTA, F., LAURENTI, E. & DICK, J. E. 2012. Hematopoiesis: a human perspective. *Cell Stem Cell,* 10**,** 120-36.

DOWLING, R. J., TOPISIROVIC, I., FONSECA, B. D. & SONENBERG, N. 2010. Dissecting the role of mTOR: lessons from mTOR inhibitors. *Biochim Biophys Acta,* 1804**,** 433-9.

DRIESSEN, E. M. C., DE LORENZO, P., CAMPBELL, M., FELICE, M., FERSTER, A., HANN, I., VORA, A., HOVI, L., ESCHERICH, G., LI, C. K., MANN, G., LEBLANC, T., LOCATELLI, F., BIONDI, A., RUBNITZ, J., SCHRAPPE, M., SILVERMAN, L., STARY, J., SUPPIAH, R., SZCZEPANSKI, T., VALSECCHI, M. & PIETERS, R. 2017. Outcome of relapsed infant acute lymphoblastic leukemia treated on the interfant-99 protocol. *Leukemia,* 31**,** 2854.

DYKSTRA, B., KENT, D., BOWIE, M., MCCAFFREY, L., HAMILTON, M., LYONS, K., LEE, S. J., BRINKMAN, R. & EAVES, C. 2007. Long-term propagation of distinct hematopoietic differentiation programs in vivo. *Cell Stem Cell,* 1**,** 218-29.

EIDAHL, J. O., CROWE, B. L., NORTH, J. A., MCKEE, C. J., SHKRIABAI, N., FENG, L., PLUMB, M., GRAHAM, R. L., GORELICK, R. J., HESS, S., POIRIER, M. G., FOSTER, M. P. & KVARATSKHELIA, M. 2013. Structural basis for high-affinity binding of LEDGF PWWP to mononucleosomes. *Nucleic Acids Res,* 41**,** 3924-36.

ERB, M. A., SCOTT, T. G., LI, B. E., XIE, H., PAULK, J., SEO, H. S., SOUZA, A., ROBERTS, J. M., DASTJERDI, S., BUCKLEY, D. L., SANJANA, N. E., SHALEM, O., NABET, B., ZEID, R., OFFEI-ADDO, N. K., DHE-PAGANON, S., ZHANG, F., ORKIN, S. H., WINTER, G. E.

& BRADNER, J. E. 2017. Transcription control by the ENL YEATS domain in acute leukaemia. *Nature,* 543**,** 270-274.
ERNST, P., FISHER, J. K., AVERY, W., WADE, S., FOY, D. & KORSMEYER, S. J. 2004. Definitive hematopoiesis requires the mixed-lineage leukemia gene. *Dev Cell,* 6**,** 437-43.
ERNST, P., WANG, J., HUANG, M., GOODMAN, R. H. & KORSMEYER, S. J. 2001. MLL and CREB bind cooperatively to the nuclear coactivator CREB-binding protein. *Mol Cell Biol,* 21**,** 2249-58.
FAIR, K., ANDERSON, M., BULANOVA, E., MI, H., TROPSCHUG, M. & DIAZ, M. O. 2001. Protein interactions of the MLL PHD fingers modulate MLL target gene regulation in human cells. *Mol Cell Biol,* 21**,** 3589-97.
FAN, S., WANG, Y., SHENG, N., XIE, Y., LU, J., ZHANG, Z., SHAN, Q., WU, D., SUN, C., LI, M., HU, B. & ZHENG, Y. 2019. Low expression of ENC1 predicts a favorable prognosis in patients with ovarian cancer. *J Cell Biochem,* 120**,** 861-871.
FATHI, A. T., WANDER, S. A., BLONQUIST, T. M., BRUNNER, A. M., AMREIN, P. C., SUPKO, J., HERMANCE, N. M., MANNING, A. L., SADRZADEH, H., BALLEN, K. K., ATTAR, E. C., GRAUBERT, T. A., HOBBS, G., JOSEPH, C., PERRY, A. M., BURKE, M., SILVER, R., FOSTER, J., BERGERON, M., RAMOS, A. Y., SOM, T. T., FISHMAN, K. M., MCGREGOR, K. L., CONNOLLY, C., NEUBERG, D. S. & CHEN, Y. B. 2017. Phase I study of the aurora A kinase inhibitor alisertib with induction chemotherapy in patients with acute myeloid leukemia. *Haematologica,* 102**,** 719-727.
FENG, Y. H., CHEN, W. Y., KUO, Y. H., TUNG, C. L., TSAO, C. J., SHIAU, A. L. & WU, C. L. 2016. Elovl6 is a poor prognostic predictor in breast cancer. *Oncol Lett,* 12**,** 207-212.
FLEISCHMAN, R. A., CUSTER, R. P. & MINTZ, B. 1982. Totipotent hematopoietic stem cells: normal self-renewal and differentiation after transplantation between mouse fetuses. *Cell,* 30**,** 351-9.
FORD, A. M., RIDGE, S. A., CABRERA, M. E., MAHMOUD, H., STEEL, C. M., CHAN, L. C. & GREAVES, M. 1993. In utero rearrangements in the trithorax-related oncogene in infant leukaemias. *Nature,* 363**,** 358-60.
FU, S., FU, Y., CHEN, F., HU, Y., QUAN, B. & ZHANG, J. 2018. Overexpression of MYCT1 Inhibits Proliferation and Induces Apoptosis in Human Acute Myeloid Leukemia HL-60 and KG-1a Cells in vitro and in vivo. *Front Pharmacol,* 9**,** 1045.
FUKUDA, T. 1973. Fetal hemopoiesis. I. Electron microscopic studies on human yolk sac hemopoiesis. *Virchows Arch B Cell Pathol,* 14**,** 197-213.
GALE, K. B., FORD, A. M., REPP, R., BORKHARDT, A., KELLER, C., EDEN, O. B. & GREAVES, M. F. 1997. Backtracking leukemia to birth: identification of clonotypic gene fusion sequences in neonatal blood spots. *Proc Natl Acad Sci U S A,* 94**,** 13950-4.
GARDNER, R., WU, D., CHERIAN, S., FANG, M., HANAFI, L. A., FINNEY, O., SMITHERS, H., JENSEN, M. C., RIDDELL, S. R., MALONEY, D.

G. & TURTLE, C. J. 2016. Acquisition of a CD19-negative myeloid phenotype allows immune escape of MLL-rearranged B-ALL from CD19 CAR-T-cell therapy. *Blood,* 127**,** 2406-10.
GARRIDO CASTRO, P., VAN ROON, E. H. J., PINHANCOS, S. S., TRENTIN, L., SCHNEIDER, P., KERSTJENS, M., TE KRONNIE, G., HEIDENREICH, O., PIETERS, R. & STAM, R. W. 2018. The HDAC inhibitor panobinostat (LBH589) exerts in vivo anti-leukaemic activity against MLL-rearranged acute lymphoblastic leukaemia and involves the RNF20/RNF40/WAC-H2B ubiquitination axis. *Leukemia,* 32**,** 323-331.
GEKAS, C., DIETERLEN-LIEVRE, F., ORKIN, S. H. & MIKKOLA, H. K. 2005. The placenta is a niche for hematopoietic stem cells. *Dev Cell,* 8**,** 365-75.
GIMENEZ-ABIAN, J. F., SUMARA, I., HIROTA, T., HAUF, S., GERLICH, D., DE LA TORRE, C., ELLENBERG, J. & PETERS, J. M. 2004. Regulation of sister chromatid cohesion between chromosome arms. *Curr Biol,* 14**,** 1187-93.
GOLSTEYN, R. M., SCHULTZ, S. J., BARTEK, J., ZIEMIECKI, A., RIED, T. & NIGG, E. A. 1994. Cell cycle analysis and chromosomal localization of human Plk1, a putative homologue of the mitotic kinases Drosophila polo and Saccharomyces cerevisiae Cdc5. *J Cell Sci,* 107 (Pt 6)**,** 1509-17.
GOOD, Z., SARNO, J., JAGER, A., SAMUSIK, N., AGHAEEPOUR, N., SIMONDS, E. F., WHITE, L., LACAYO, N. J., FANTL, W. J., FAZIO, G., GAIPA, G., BIONDI, A., TIBSHIRANI, R., BENDALL, S. C., NOLAN, G. P. & DAVIS, K. L. 2018. Single-cell developmental classification of B cell precursor acute lymphoblastic leukemia at diagnosis reveals predictors of relapse. *Nat Med,* 24**,** 474-483.
GOPALAKRISHNAN, B., CHENEY, C., MANI, R., MO, X., BUCCI, D., WALKER, A., KLISOVIC, R., BHATNAGAR, B., WALSH, K., RUETER, B., WAIZENEGGER, I. C., HEIDER, K. H., BLUM, W., VASU, S. & MUTHUSAMY, N. 2018. Polo-like kinase inhibitor volasertib marginally enhances the efficacy of the novel Fc-engineered anti-CD33 antibody BI 836858 in acute myeloid leukemia. *Oncotarget,* 9**,** 9706-9713.
GOTHERT, J. R., GUSTIN, S. E., HALL, M. A., GREEN, A. R., GOTTGENS, B., IZON, D. J. & BEGLEY, C. G. 2005. In vivo fate-tracing studies using the Scl stem cell enhancer: embryonic hematopoietic stem cells significantly contribute to adult hematopoiesis. *Blood,* 105**,** 2724-32.
GRADE, M., HUMMON, A. B., CAMPS, J., EMONS, G., SPITZNER, M., GAEDCKE, J., HOERMANN, P., EBNER, R., BECKER, H., DIFILIPPANTONIO, M. J., GHADIMI, B. M., BEISSBARTH, T., CAPLEN, N. J. & RIED, T. 2011. A genomic strategy for the functional validation of colorectal cancer genes identifies potential therapeutic targets. *Int J Cancer,* 128**,** 1069-79.
GREAVES, M. 2018. A causal mechanism for childhood acute lymphoblastic leukaemia. *Nat Rev Cancer,* 18**,** 471-484.

GREMBECKA, J., HE, S., SHI, A., PUROHIT, T., MUNTEAN, A. G., SORENSON, R. J., SHOWALTER, H. D., MURAI, M. J., BELCHER, A. M., HARTLEY, T., HESS, J. L. & CIERPICKI, T. 2012. Menin-MLL inhibitors reverse oncogenic activity of MLL fusion proteins in leukemia. *Nat Chem Biol,* 8**,** 277-84.

GRIFFIN, D. O., HOLODICK, N. E. & ROTHSTEIN, T. L. 2011. Human B1 cells in umbilical cord and adult peripheral blood express the novel phenotype CD20+ CD27+ CD43+ CD70. *J Exp Med,* 208**,** 67-80.

GRUSS, O. J., WITTMANN, M., YOKOYAMA, H., PEPPERKOK, R., KUFER, T., SILLJE, H., KARSENTI, E., MATTAJ, I. W. & VERNOS, I. 2002. Chromosome-induced microtubule assembly mediated by TPX2 is required for spindle formation in HeLa cells. *Nat Cell Biol,* 4**,** 871-9.

GU, Y., NAKAMURA, T., ALDER, H., PRASAD, R., CANAANI, O., CIMINO, G., CROCE, C. M. & CANAANI, E. 1992. The t(4;11) chromosome translocation of human acute leukemias fuses the ALL-1 gene, related to Drosophila trithorax, to the AF-4 gene. *Cell,* 71**,** 701-8.

GUENECHEA, G., GAN, O. I., DORRELL, C. & DICK, J. E. 2001. Distinct classes of human stem cells that differ in proliferative and self-renewal potential. *Nat Immunol,* 2**,** 75-82.

GUENTHER, M. G., LAWTON, L. N., ROZOVSKAIA, T., FRAMPTON, G. M., LEVINE, S. S., VOLKERT, T. L., CROCE, C. M., NAKAMURA, T., CANAANI, E. & YOUNG, R. A. 2008. Aberrant chromatin at genes encoding stem cell regulators in human mixed-lineage leukemia. *Genes Dev,* 22**,** 3403-8.

GUO, Y., KIM, C., AHMAD, S., ZHANG, J. & MAO, Y. 2012. CENP-E--dependent BubR1 autophosphorylation enhances chromosome alignment and the mitotic checkpoint. *J Cell Biol,* 198**,** 205-17.

GUSAROVA, G. A., WANG, I. C., MAJOR, M. L., KALINICHENKO, V. V., ACKERSON, T., PETROVIC, V. & COSTA, R. H. 2007. A cell-penetrating ARF peptide inhibitor of FoxM1 in mouse hepatocellular carcinoma treatment. *J Clin Invest,* 117**,** 99-111.

HAAG, T., HERKT, C. E., WALESCH, S. K., RICHTER, A. M. & DAMMANN, R. H. 2014. The apoptosis associated tyrosine kinase gene is frequently hypermethylated in human cancer and is regulated by epigenetic mechanisms. *Genes Cancer,* 5**,** 365-74.

HANISCH, A., WEHNER, A., NIGG, E. A. & SILLJE, H. H. 2006. Different Plk1 functions show distinct dependencies on Polo-Box domain-mediated targeting. *Mol Biol Cell,* 17**,** 448-59.

HART, T., CHANDRASHEKHAR, M., AREGGER, M., STEINHART, Z., BROWN, K. R., MACLEOD, G., MIS, M., ZIMMERMANN, M., FRADET-TURCOTTE, A., SUN, S., MERO, P., DIRKS, P., SIDHU, S., ROTH, F. P., RISSLAND, O. S., DUROCHER, D., ANGERS, S. & MOFFAT, J. 2015. High-Resolution CRISPR Screens Reveal Fitness Genes and Genotype-Specific Cancer Liabilities. *Cell,* 163**,** 1515-26.

HARTSINK-SEGERS, S. A., EXALTO, C., ALLEN, M., WILLIAMSON, D., CLIFFORD, S. C., HORSTMANN, M., CARON, H. N., PIETERS, R. & DEN BOER, M. L. 2013. Inhibiting Polo-like kinase 1 causes growth

reduction and apoptosis in pediatric acute lymphoblastic leukemia cells. *Haematologica,* 98**,** 1539-46.
HAYAKAWA, K., HARDY, R. R. & HERZENBERG, L. A. 1985. Progenitors for Ly-1 B cells are distinct from progenitors for other B cells. *J Exp Med,* 161**,** 1554-68.
HE, S., KIM, I., LIM, M. S. & MORRISON, S. J. 2011. Sox17 expression confers self-renewal potential and fetal stem cell characteristics upon adult hematopoietic progenitors. *Genes Dev,* 25**,** 1613-27.
HE, X., LI, W., LIANG, X., ZHU, X., ZHANG, L., HUANG, Y., YU, T., LI, S. & CHEN, Z. 2018. IGF2BP2 Overexpression Indicates Poor Survival in Patients with Acute Myelocytic Leukemia. *Cell Physiol Biochem,* 51**,** 1945-1956.
HEIDEBRECHT, H. J., BUCK, F., STEINMANN, J., SPRENGER, R., WACKER, H. H. & PARWARESCH, R. 1997. p100: a novel proliferation-associated nuclear protein specifically restricted to cell cycle phases S, G2, and M. *Blood,* 90**,** 226-33.
HELSMOORTEL, H. H., BRESOLIN, S., LAMMENS, T., CAVE, H., NOELLKE, P., CAYE, A., GHAZAVI, F., DE VRIES, A., HASLE, H., LABARQUE, V., MASETTI, R., STARY, J., VAN DEN HEUVEL-EIBRINK, M. M., PHILIPPE, J., VAN ROY, N., BENOIT, Y., SPELEMAN, F., NIEMEYER, C., FLOTHO, C., BASSO, G., TE KRONNIE, G., VAN VLIERBERGHE, P. & DE MOERLOOSE, B. 2016. LIN28B overexpression defines a novel fetal-like subgroup of juvenile myelomonocytic leukemia. *Blood,* 127**,** 1163-72.
HESS, J. L., YU, B. D., LI, B., HANSON, R. & KORSMEYER, S. J. 1997. Defects in yolk sac hematopoiesis in Mll-null embryos. *Blood,* 90**,** 1799-806.
HIDALGO, I., HERRERA-MERCHAN, A., LIGOS, J. M., CARRAMOLINO, L., NUNEZ, J., MARTINEZ, F., DOMINGUEZ, O., TORRES, M. & GONZALEZ, S. 2012. Ezh1 is required for hematopoietic stem cell maintenance and prevents senescence-like cell cycle arrest. *Cell Stem Cell,* 11**,** 649-62.
HILDEN, J. M., DINNDORF, P. A., MEERBAUM, S. O., SATHER, H., VILLALUNA, D., HEEREMA, N. A., MCGLENNEN, R., SMITH, F. O., WOODS, W. G., SALZER, W. L., JOHNSTONE, H. S., DREYER, Z. & REAMAN, G. H. 2006. Analysis of prognostic factors of acute lymphoblastic leukemia in infants: report on CCG 1953 from the Children's Oncology Group. *Blood,* 108**,** 441-51.
HOCK, H., HAMBLEN, M. J., ROOKE, H. M., SCHINDLER, J. W., SALEQUE, S., FUJIWARA, Y. & ORKIN, S. H. 2004a. Gfi-1 restricts proliferation and preserves functional integrity of haematopoietic stem cells. *Nature,* 431**,** 1002-7.
HOCK, H., MEADE, E., MEDEIROS, S., SCHINDLER, J. W., VALK, P. J., FUJIWARA, Y. & ORKIN, S. H. 2004b. Tel/Etv6 is an essential and selective regulator of adult hematopoietic stem cell survival. *Genes Dev,* 18**,** 2336-41.
HOLYOAKE, T. L., NICOLINI, F. E. & EAVES, C. J. 1999. Functional differences between transplantable human hematopoietic stem cells

from fetal liver, cord blood, and adult marrow. *Exp Hematol,* 27**,** 1418-27.
HOM, R. A., CHANG, P. Y., ROY, S., MUSSELMAN, C. A., GLASS, K. C., SELEZNEVA, A. I., GOZANI, O., ISMAGILOV, R. F., CLEARY, M. L. & KUTATELADZE, T. G. 2010. Molecular mechanism of MLL PHD3 and RNA recognition by the Cyp33 RRM domain. *J Mol Biol,* 400**,** 145-54.
HSIEH, J. J., CHENG, E. H. & KORSMEYER, S. J. 2003a. Taspase1: a threonine aspartase required for cleavage of MLL and proper HOX gene expression. *Cell,* 115**,** 293-303.
HSIEH, J. J., ERNST, P., ERDJUMENT-BROMAGE, H., TEMPST, P. & KORSMEYER, S. J. 2003b. Proteolytic cleavage of MLL generates a complex of N- and C-terminal fragments that confers protein stability and subnuclear localization. *Mol Cell Biol,* 23**,** 186-94.
HUGHES, C. M., ROZENBLATT-ROSEN, O., MILNE, T. A., COPELAND, T. D., LEVINE, S. S., LEE, J. C., HAYES, D. N., SHANMUGAM, K. S., BHATTACHARJEE, A., BIONDI, C. A., KAY, G. F., HAYWARD, N. K., HESS, J. L. & MEYERSON, M. 2004. Menin associates with a trithorax family histone methyltransferase complex and with the hoxc8 locus. *Mol Cell,* 13**,** 587-97.
ISNARD, P., CORE, N., NAQUET, P. & DJABALI, M. 2000. Altered lymphoid development in mice deficient for the mAF4 proto-oncogene. *Blood,* 96**,** 705-10.
IVANOVS, A., RYBTSOV, S., NG, E. S., STANLEY, E. G., ELEFANTY, A. G. & MEDVINSKY, A. 2017. Human haematopoietic stem cell development: from the embryo to the dish. *Development,* 144**,** 2323-2337.
IVANOVS, A., RYBTSOV, S., WELCH, L., ANDERSON, R. A., TURNER, M. L. & MEDVINSKY, A. 2011. Highly potent human hematopoietic stem cells first emerge in the intraembryonic aorta-gonad-mesonephros region. *J Exp Med,* 208**,** 2417-27.
JASSINSKAJA, M., JOHANSSON, E., KRISTIANSEN, T. A., AKERSTRAND, H., SJOHOLM, K., HAURI, S., MALMSTROM, J., YUAN, J. & HANSSON, J. 2017. Comprehensive Proteomic Characterization of Ontogenic Changes in Hematopoietic Stem and Progenitor Cells. *Cell Rep,* 21**,** 3285-3297.
JORDAN, C. T. & LEMISCHKA, I. R. 1990. Clonal and systemic analysis of long-term hematopoiesis in the mouse. *Genes Dev,* 4**,** 220-32.
JUDE, C. D., CLIMER, L., XU, D., ARTINGER, E., FISHER, J. K. & ERNST, P. 2007. Unique and independent roles for MLL in adult hematopoietic stem cells and progenitors. *Cell Stem Cell,* 1**,** 324-37.
KANG, H., WILSON, C. S., HARVEY, R. C., CHEN, I. M., MURPHY, M. H., ATLAS, S. R., BEDRICK, E. J., DEVIDAS, M., CARROLL, A. J., ROBINSON, B. W., STAM, R. W., VALSECCHI, M. G., PIETERS, R., HEEREMA, N. A., HILDEN, J. M., FELIX, C. A., REAMAN, G. H., CAMITTA, B., WINICK, N., CARROLL, W. L., DREYER, Z. E., HUNGER, S. P. & WILLMAN, C. L. 2012. Gene expression profiles

predictive of outcome and age in infant acute lymphoblastic leukemia: a Children's Oncology Group study. *Blood,* 119**,** 1872-81.
KANTOR, A. B., STALL, A. M., ADAMS, S. & HERZENBERG, L. A. 1992. Differential development of progenitor activity for three B-cell lineages. *Proc Natl Acad Sci U S A,* 89**,** 3320-4.
KENT, D. G., COPLEY, M. R., BENZ, C., WOHRER, S., DYKSTRA, B. J., MA, E., CHEYNE, J., ZHAO, Y., BOWIE, M. B., GASPARETTO, M., DELANEY, A., SMITH, C., MARRA, M. & EAVES, C. J. 2009. Prospective isolation and molecular characterization of hematopoietic stem cells with durable self-renewal potential. *Blood,* 113**,** 6342-50.
KERRY, J., GODFREY, L., REPAPI, E., TAPIA, M., BLACKLEDGE, N. P., MA, H., BALLABIO, E., O'BYRNE, S., PONTHAN, F., HEIDENREICH, O., ROY, A., ROBERTS, I., KONOPLEVA, M., KLOSE, R. J., GENG, H. & MILNE, T. A. 2017. MLL-AF4 Spreading Identifies Binding Sites that Are Distinct from Super-Enhancers and that Govern Sensitivity to DOT1L Inhibition in Leukemia. *Cell Rep,* 18**,** 482-495.
KIEL, M. J., YILMAZ, O. H., IWASHITA, T., TERHORST, C. & MORRISON, S. J. 2005. SLAM family receptors distinguish hematopoietic stem and progenitor cells and reveal endothelial niches for stem cells. *Cell,* 121**,** 1109-21.
KIKUCHI, K. & KONDO, M. 2006. Developmental switch of mouse hematopoietic stem cells from fetal to adult type occurs in bone marrow after birth. *Proc Natl Acad Sci U S A,* 103**,** 17852-7.
KIM, I., SAUNDERS, T. L. & MORRISON, S. J. 2007. Sox17 dependence distinguishes the transcriptional regulation of fetal from adult hematopoietic stem cells. *Cell,* 130**,** 470-83.
KIM, I. M., ACKERSON, T., RAMAKRISHNA, S., TRETIAKOVA, M., WANG, I. C., KALIN, T. V., MAJOR, M. L., GUSAROVA, G. A., YODER, H. M., COSTA, R. H. & KALINICHENKO, V. V. 2006. The Forkhead Box m1 transcription factor stimulates the proliferation of tumor cells during development of lung cancer. *Cancer Res,* 66**,** 2153-61.
KIM, S. L., LEE, S. T., MIN, I. S., PARK, Y. R., LEE, J. H., KIM, D. G. & KIM, S. W. 2017. Lipocalin 2 negatively regulates cell proliferation and epithelial to mesenchymal transition through changing metabolic gene expression in colorectal cancer. *Cancer Sci,* 108**,** 2176-2186.
KINGSLEY, P. D., MALIK, J., FANTAUZZO, K. A. & PALIS, J. 2004. Yolk sac-derived primitive erythroblasts enucleate during mammalian embryogenesis. *Blood,* 104**,** 19-25.
KLIMCHENKO, O., DI STEFANO, A., GEOERGER, B., HAMIDI, S., OPOLON, P., ROBERT, T., ROUTHIER, M., EL-BENNA, J., DELEZOIDE, A. L., BOUKOUR, S., LESCURE, B., SOLARY, E., VAINCHENKER, W. & NOROL, F. 2011. Monocytic cells derived from human embryonic stem cells and fetal liver share common differentiation pathways and homeostatic functions. *Blood,* 117**,** 3065-75.
KNECHT, R., ELEZ, R., OECHLER, M., SOLBACH, C., VON ILBERG, C. & STREBHARDT, K. 1999. Prognostic significance of polo-like kinase

(PLK) expression in squamous cell carcinomas of the head and neck. *Cancer Res,* 59**,** 2794-7.
KNECHT, R., OBERHAUSER, C. & STREBHARDT, K. 2000. PLK (polo-like kinase), a new prognostic marker for oropharyngeal carcinomas. *Int J Cancer.* United States.
KOBAYASHI, Y., YAMAUCHI, T., KIYOI, H., SAKURA, T., HATA, T., ANDO, K., WATABE, A., HARADA, A., TAUBE, T., MIYAZAKI, Y. & NAOE, T. 2015. Phase I trial of volasertib, a Polo-like kinase inhibitor, in Japanese patients with acute myeloid leukemia. *Cancer Sci,* 106**,** 1590-5.
KOHN, L. A., HAO, Q. L., SASIDHARAN, R., PAREKH, C., GE, S., ZHU, Y., MIKKOLA, H. K. & CROOKS, G. M. 2012. Lymphoid priming in human bone marrow begins before expression of CD10 with upregulation of L-selectin. *Nat Immunol,* 13**,** 963-71.
KOLONIN, M. G. & FINLEY, R. L., JR. 2000. A role for cyclin J in the rapid nuclear division cycles of early Drosophila embryogenesis. *Dev Biol,* 227**,** 661-72.
KRAFT, M. L. 2016. Sphingolipid Organization in the Plasma Membrane and the Mechanisms That Influence It. *Front Cell Dev Biol,* 4**,** 154.
KRIVTSOV, A. V., FENG, Z., LEMIEUX, M. E., FABER, J., VEMPATI, S., SINHA, A. U., XIA, X., JESNECK, J., BRACKEN, A. P., SILVERMAN, L. B., KUTOK, J. L., KUNG, A. L. & ARMSTRONG, S. A. 2008. H3K79 methylation profiles define murine and human MLL-AF4 leukemias. *Cancer Cell,* 14**,** 355-68.
KRIVTSOV, A. V., HOSHII, T. & ARMSTRONG, S. A. 2017. Mixed-Lineage Leukemia Fusions and Chromatin in Leukemia. *Cold Spring Harb Perspect Med,* 7.
KUHN, A., LOSCHER, D. & MARSCHALEK, R. 2016. The IRX1/HOXA connection: insights into a novel t(4;11)- specific cancer mechanism. *Oncotarget,* 7**,** 35341-52.
KUMAR, A. R., YAO, Q., LI, Q., SAM, T. A. & KERSEY, J. H. 2011. t(4;11) leukemias display addiction to MLL-AF4 but not to AF4-MLL. *Leuk Res,* 35**,** 305-9.
LABUN, K., MONTAGUE, T. G., GAGNON, J. A., THYME, S. B. & VALEN, E. 2016. CHOPCHOP v2: a web tool for the next generation of CRISPR genome engineering. *Nucleic Acids Res,* 44**,** W272-6.
LABUN, K., MONTAGUE, T. G., KRAUSE, M., TORRES CLEUREN, Y. N., TJELDNES, H. & VALEN, E. 2019. CHOPCHOP v3: expanding the CRISPR web toolbox beyond genome editing. *Nucleic Acids Res,* 47**,** W171-w174.
LAURENTI, E. & GOTTGENS, B. 2018. From haematopoietic stem cells to complex differentiation landscapes. *Nature,* 553**,** 418-426.
LEE, J., ZHOU, Y. J., MA, W., ZHANG, W., ALJOUFI, A., LUH, T., LUCERO, K., LIANG, D., THOMSEN, M., BHAGAT, G., SHEN, Y. & LIU, K. 2017. Lineage specification of human dendritic cells is marked by IRF8 expression in hematopoietic stem cells and multipotent progenitors. *Nat Immunol,* 18**,** 877-888.

LENART, P., PETRONCZKI, M., STEEGMAIER, M., DI FIORE, B., LIPP, J. J., HOFFMANN, M., RETTIG, W. J., KRAUT, N. & PETERS, J. M. 2007. The small-molecule inhibitor BI 2536 reveals novel insights into mitotic roles of polo-like kinase 1. *Curr Biol,* 17**,** 304-15.

LEY, T. J., DING, L., WALTER, M. J., MCLELLAN, M. D., LAMPRECHT, T., LARSON, D. E., KANDOTH, C., PAYTON, J. E., BATY, J., WELCH, J., HARRIS, C. C., LICHTI, C. F., TOWNSEND, R. R., FULTON, R. S., DOOLING, D. J., KOBOLDT, D. C., SCHMIDT, H., ZHANG, Q., OSBORNE, J. R., LIN, L., O'LAUGHLIN, M., MCMICHAEL, J. F., DELEHAUNTY, K. D., MCGRATH, S. D., FULTON, L. A., MAGRINI, V. J., VICKERY, T. L., HUNDAL, J., COOK, L. L., CONYERS, J. J., SWIFT, G. W., REED, J. P., ALLDREDGE, P. A., WYLIE, T., WALKER, J., KALICKI, J., WATSON, M. A., HEATH, S., SHANNON, W. D., VARGHESE, N., NAGARAJAN, R., WESTERVELT, P., TOMASSON, M. H., LINK, D. C., GRAUBERT, T. A., DIPERSIO, J. F., MARDIS, E. R. & WILSON, R. K. 2010. DNMT3A mutations in acute myeloid leukemia. *N Engl J Med,* 363**,** 2424-33.

LI, L., TAN, J., ZHANG, Y., HAN, N., DI, X., XIAO, T., CHENG, S., GAO, Y. & LIU, Y. 2014. DLK1 promotes lung cancer cell invasion through upregulation of MMP9 expression depending on Notch signaling. *PLoS One,* 9**,** e91509.

LIN, S., LUO, R. T., PTASINSKA, A., KERRY, J., ASSI, S. A., WUNDERLICH, M., IMAMURA, T., KABERLEIN, J. J., RAYES, A., ALTHOFF, M. J., ANASTASI, J., O'BRIEN, M. M., MEETEI, A. R., MILNE, T. A., BONIFER, C., MULLOY, J. C. & THIRMAN, M. J. 2016. Instructive Role of MLL-Fusion Proteins Revealed by a Model of t(4;11) Pro-B Acute Lymphoblastic Leukemia. *Cancer Cell,* 30**,** 737-749.

LIN, S., LUO, R. T., SHRESTHA, M., THIRMAN, M. J. & MULLOY, J. C. 2017. The full transforming capacity of MLL-Af4 is interlinked with lymphoid lineage commitment. *Blood,* 130**,** 903-907.

LING, A., LOFGREN-BURSTROM, A., LARSSON, P., LI, X., WIKBERG, M. L., OBERG, A., STENLING, R., EDIN, S. & PALMQVIST, R. 2017. TAP1 down-regulation elicits immune escape and poor prognosis in colorectal cancer. *Oncoimmunology,* 6**,** e1356143.

LIU, Y., ZHOU, R., YUAN, X., HAN, N., ZHOU, S., XU, H., GUO, M., YU, S., ZHANG, C., YIN, T. & WU, K. 2015. DACH1 is a novel predictive and prognostic biomarker in hepatocellular carcinoma as a negative regulator of Wnt/beta-catenin signaling. *Oncotarget,* 6**,** 8621-34.

LOVE, M. I., HUBER, W. & ANDERS, S. 2014. Moderated estimation of fold change and dispersion for RNA-seq data with DESeq2. *Genome Biol,* 15**,** 550.

LUCKETT, W. P. 1978. Origin and differentiation of the yolk sac and extraembryonic mesoderm in presomite human and rhesus monkey embryos. *Am J Anat,* 152**,** 59-97.

MA, Q., ALDER, H., NELSON, K. K., CHATTERJEE, D., GU, Y., NAKAMURA, T., CANAANI, E., CROCE, C. M., SIRACUSA, L. D. & BUCHBERG, A. M. 1993. Analysis of the murine All-1 gene reveals

conserved domains with human ALL-1 and identifies a motif shared with DNA methyltransferases. *Proc Natl Acad Sci U S A,* 90**,** 6350-4.
MA, Q., LIU, Y., SHANG, L., YU, J. & QU, Q. 2017. The FOXM1/BUB1B signaling pathway is essential for the tumorigenicity and radioresistance of glioblastoma. *Oncol Rep,* 38**,** 3367-3375.
MA, X., GU, L., LI, H., GAO, Y., LI, X., SHEN, D., GONG, H., LI, S., NIU, S., ZHANG, Y., FAN, Y., HUANG, Q., LYU, X. & ZHANG, X. 2015. Hypoxia-induced overexpression of stanniocalcin-1 is associated with the metastasis of early stage clear cell renal cell carcinoma. *J Transl Med,* 13**,** 56.
MACHADO, R. A. C., SCHNEIDER, H., DEOCESANO-PEREIRA, C., LICHTENSTEIN, F., ANDRADE, F., FUJITA, A., TROMBETTA-LIMA, M., WELLER, M., BOWMAN-COLIN, C. & SOGAYAR, M. C. 2019. CHD7 promotes glioblastoma cell motility and invasiveness through transcriptional modulation of an invasion signature. *Sci Rep,* 9**,** 3952.
MACUREK, L., LINDQVIST, A., LIM, D., LAMPSON, M. A., KLOMPMAKER, R., FREIRE, R., CLOUIN, C., TAYLOR, S. S., YAFFE, M. B. & MEDEMA, R. H. 2008. Polo-like kinase-1 is activated by aurora A to promote checkpoint recovery. *Nature,* 455**,** 119-23.
MALOUF, C. & OTTERSBACH, K. 2018. The fetal liver lymphoid-primed multipotent progenitor provides the prerequisites for the initiation of t(4;11) MLL-AF4 infant leukemia. *Haematologica.* Italy.
MAN, N., SUN, X. J., TAN, Y., GARCIA-CAO, M., LIU, F., CHENG, G., HATLEN, M., XU, H., SHAH, R., CHASTAIN, N., LIU, N., HUANG, G., ZHOU, Y., SHENG, M., SONG, J., YANG, F. C., BENEZRA, R., NIMER, S. D. & WANG, L. 2016. Differential role of Id1 in MLL-AF9-driven leukemia based on cell of origin. *Blood,* 127**,** 2322-6.
MARDON, G., SOLOMON, N. M. & RUBIN, G. M. 1994. dachshund encodes a nuclear protein required for normal eye and leg development in Drosophila. *Development,* 120**,** 3473-86.
MARIEN, E., MEISTER, M., MULEY, T., GOMEZ DEL PULGAR, T., DERUA, R., SPRAGGINS, J. M., VAN DE PLAS, R., VANDERHOYDONC, F., MACHIELS, J., BINDA, M. M., DEHAIRS, J., WILLETTE-BROWN, J., HU, Y., DIENEMANN, H., THOMAS, M., SCHNABEL, P. A., CAPRIOLI, R. M., LACAL, J. C., WAELKENS, E. & SWINNEN, J. V. 2016. Phospholipid profiling identifies acyl chain elongation as a ubiquitous trait and potential target for the treatment of lung squamous cell carcinoma. *Oncotarget,* 7**,** 12582-97.
MARQUIS, M., BEAUBOIS, C., LAVALLEE, V. P., ABRAHAMOWICZ, M., DANIELI, C., LEMIEUX, S., AHMAD, I., WEI, A., TING, S. B., FLEMING, S., SCHWARER, A., GRIMWADE, D., GREY, W., HILLS, R. K., VYAS, P., RUSSELL, N., SAUVAGEAU, G. & HEBERT, J. 2018. High expression of HMGA2 independently predicts poor clinical outcomes in acute myeloid leukemia. *Blood Cancer J,* 8**,** 68.
MARSHALL, C. J., MOORE, R. L., THOROGOOD, P., BRICKELL, P. M., KINNON, C. & THRASHER, A. J. 1999. Detailed characterization of the human aorta-gonad-mesonephros region reveals morphological

polarity resembling a hematopoietic stromal layer. *Dev Dyn,* 215**,** 139-47.
MAUDE, S. L., LAETSCH, T. W., BUECHNER, J., RIVES, S., BOYER, M., BITTENCOURT, H., BADER, P., VERNERIS, M. R., STEFANSKI, H. E., MYERS, G. D., QAYED, M., DE MOERLOOSE, B., HIRAMATSU, H., SCHLIS, K., DAVIS, K. L., MARTIN, P. L., NEMECEK, E. R., YANIK, G. A., PETERS, C., BARUCHEL, A., BOISSEL, N., MECHINAUD, F., BALDUZZI, A., KRUEGER, J., JUNE, C. H., LEVINE, B. L., WOOD, P., TARAN, T., LEUNG, M., MUELLER, K. T., ZHANG, Y., SEN, K., LEBWOHL, D., PULSIPHER, M. A. & GRUPP, S. A. 2018. Tisagenlecleucel in Children and Young Adults with B-Cell Lymphoblastic Leukemia. *N Engl J Med,* 378**,** 439-448.
MAZZU, Y. Z., ARMENIA, J., CHAKRABORTY, G., YOSHIKAWA, Y., COGGINS, S. A., NANDAKUMAR, S., GERKE, T. A., POMERANTZ, M. M., QIU, X., ZHAO, H., ATIQ, M., KHAN, N., KOMURA, K., LEE, G. M., FINE, S. W., BELL, C., O'CONNOR, E., LONG, H. W., FREEDMAN, M. L., KIM, B. & KANTOFF, P. W. 2019. A Novel Mechanism Driving Poor-Prognosis Prostate Cancer: Overexpression of the DNA Repair Gene, Ribonucleotide Reductase Small Subunit M2 (RRM2). *Clin Cancer Res,* 25**,** 4480-4492.
MCMAHON, K. A., HIEW, S. Y., HADJUR, S., VEIGA-FERNANDES, H., MENZEL, U., PRICE, A. J., KIOUSSIS, D., WILLIAMS, O. & BRADY, H. J. 2007. Mll has a critical role in fetal and adult hematopoietic stem cell self-renewal. *Cell Stem Cell,* 1**,** 338-45.
MEDVINSKY, A. & DZIERZAK, E. 1996. Definitive hematopoiesis is autonomously initiated by the AGM region. *Cell,* 86**,** 897-906.
MEDVINSKY, A. L., SAMOYLINA, N. L., MULLER, A. M. & DZIERZAK, E. A. 1993. An early pre-liver intraembryonic source of CFU-S in the developing mouse. *Nature,* 364**,** 64-7.
MEJSTRIKOVA, E., HRUSAK, O., BOROWITZ, M. J., WHITLOCK, J. A., BRETHON, B., TRIPPETT, T. M., ZUGMAIER, G., GORE, L., VON STACKELBERG, A. & LOCATELLI, F. 2017. CD19-negative relapse of pediatric B-cell precursor acute lymphoblastic leukemia following blinatumomab treatment. *Blood Cancer J.* United States.
METZLER, M., FORSTER, A., PANNELL, R., ARENDS, M. J., DASER, A., LOBATO, M. N. & RABBITTS, T. H. 2006. A conditional model of MLL-AF4 B-cell tumourigenesis using invertor technology. *Oncogene,* 25**,** 3093-103.
MEYER, C., BURMEISTER, T., GROGER, D., TSAUR, G., FECHINA, L., RENNEVILLE, A., SUTTON, R., VENN, N. C., EMERENCIANO, M., POMBO-DE-OLIVEIRA, M. S., BARBIERI BLUNCK, C., ALMEIDA LOPES, B., ZUNA, J., TRKA, J., BALLERINI, P., LAPILLONNE, H., DE BRAEKELEER, M., CAZZANIGA, G., CORRAL ABASCAL, L., VAN DER VELDEN, V. H. J., DELABESSE, E., PARK, T. S., OH, S. H., SILVA, M. L. M., LUND-AHO, T., JUVONEN, V., MOORE, A. S., HEIDENREICH, O., VORMOOR, J., ZERKALENKOVA, E., OLSHANSKAYA, Y., BUENO, C., MENENDEZ, P., TEIGLER-SCHLEGEL, A., ZUR STADT, U., LENTES, J., GOHRING, G.,

KUSTANOVICH, A., ALEINIKOVA, O., SCHAFER, B. W., KUBETZKO, S., MADSEN, H. O., GRUHN, B., DUARTE, X., GAMEIRO, P., LIPPERT, E., BIDET, A., CAYUELA, J. M., CLAPPIER, E., ALONSO, C. N., ZWAAN, C. M., VAN DEN HEUVEL-EIBRINK, M. M., IZRAELI, S., TRAKHTENBROT, L., ARCHER, P., HANCOCK, J., MORICKE, A., ALTEN, J., SCHRAPPE, M., STANULLA, M., STREHL, S., ATTARBASCHI, A., DWORZAK, M., HAAS, O. A., PANZER-GRUMAYER, R., SEDEK, L., SZCZEPANSKI, T., CAYE, A., SUAREZ, L., CAVE, H. & MARSCHALEK, R. 2018. The MLL recombinome of acute leukemias in 2017. *Leukemia,* 32**,** 273-284.

MI, H., MURUGANUJAN, A., EBERT, D., HUANG, X. & THOMAS, P. D. 2019. PANTHER version 14: more genomes, a new PANTHER GO-slim and improvements in enrichment analysis tools. *Nucleic Acids Res,* 47**,** D419-d426.

MICKLEM, H. S., FORD, C. E., EVANS, E. P., OGDEN, D. A. & PAPWORTH, D. S. 1972. Competitive in vivo proliferation of foetal and adult haematopoietic cells in lethally irradiated mice. *J Cell Physiol,* 79**,** 293-8.

MIGLIACCIO, G., MIGLIACCIO, A. R., PETTI, S., MAVILIO, F., RUSSO, G., LAZZARO, D., TESTA, U., MARINUCCI, M. & PESCHLE, C. 1986. Human embryonic hemopoiesis. Kinetics of progenitors and precursors underlying the yolk sac----liver transition. *J Clin Invest,* 78**,** 51-60.

MILNE, T. A., BRIGGS, S. D., BROCK, H. W., MARTIN, M. E., GIBBS, D., ALLIS, C. D. & HESS, J. L. 2002. MLL targets SET domain methyltransferase activity to Hox gene promoters. *Mol Cell,* 10**,** 1107-17.

MILNE, T. A., HUGHES, C. M., LLOYD, R., YANG, Z., ROZENBLATT-ROSEN, O., DOU, Y., SCHNEPP, R. W., KRANKEL, C., LIVOLSI, V. A., GIBBS, D., HUA, X., ROEDER, R. G., MEYERSON, M. & HESS, J. L. 2005. Menin and MLL cooperatively regulate expression of cyclin-dependent kinase inhibitors. *Proc Natl Acad Sci U S A,* 102**,** 749-54.

MILNE, T. A., KIM, J., WANG, G. G., STADLER, S. C., BASRUR, V., WHITCOMB, S. J., WANG, Z., RUTHENBURG, A. J., ELENITOBA-JOHNSON, K. S., ROEDER, R. G. & ALLIS, C. D. 2010. Multiple interactions recruit MLL1 and MLL1 fusion proteins to the HOXA9 locus in leukemogenesis. *Mol Cell,* 38**,** 853-63.

MOCHIZUKI-KASHIO, M., MISHIMA, Y., MIYAGI, S., NEGISHI, M., SARAYA, A., KONUMA, T., SHINGA, J., KOSEKI, H. & IWAMA, A. 2011. Dependency on the polycomb gene Ezh2 distinguishes fetal from adult hematopoietic stem cells. *Blood,* 118**,** 6553-61.

MONTAGUE, T. G., CRUZ, J. M., GAGNON, J. A., CHURCH, G. M. & VALEN, E. 2014. CHOPCHOP: a CRISPR/Cas9 and TALEN web tool for genome editing. *Nucleic Acids Res,* 42**,** W401-7.

MONTES, R., AYLLON, V., GUTIERREZ-ARANDA, I., PRAT, I., HERNANDEZ-LAMAS, M. C., PONCE, L., BRESOLIN, S., TE KRONNIE, G., GREAVES, M., BUENO, C. & MENENDEZ, P. 2011. Enforced expression of MLL-AF4 fusion in cord blood CD34+ cells

enhances the hematopoietic repopulating cell function and clonogenic potential but is not sufficient to initiate leukemia. *Blood,* 117**,** 4746-58.
MOOTHA, V. K., LINDGREN, C. M., ERIKSSON, K. F., SUBRAMANIAN, A., SIHAG, S., LEHAR, J., PUIGSERVER, P., CARLSSON, E., RIDDERSTRALE, M., LAURILA, E., HOUSTIS, N., DALY, M. J., PATTERSON, N., MESIROV, J. P., GOLUB, T. R., TAMAYO, P., SPIEGELMAN, B., LANDER, E. S., HIRSCHHORN, J. N., ALTSHULER, D. & GROOP, L. C. 2003. PGC-1alpha-responsive genes involved in oxidative phosphorylation are coordinately downregulated in human diabetes. *Nat Genet,* 34**,** 267-73.
MORRISON, S. J., WANDYCZ, A. M., HEMMATI, H. D., WRIGHT, D. E. & WEISSMAN, I. L. 1997. Identification of a lineage of multipotent hematopoietic progenitors. *Development,* 124**,** 1929-39.
MUELLER, D., BACH, C., ZEISIG, D., GARCIA-CUELLAR, M. P., MONROE, S., SREEKUMAR, A., ZHOU, R., NESVIZHSKII, A., CHINNAIYAN, A., HESS, J. L. & SLANY, R. K. 2007. A role for the MLL fusion partner ENL in transcriptional elongation and chromatin modification. *Blood,* 110**,** 4445-54.
MUELLER, D., GARCIA-CUELLAR, M. P., BACH, C., BUHL, S., MAETHNER, E. & SLANY, R. K. 2009. Misguided transcriptional elongation causes mixed lineage leukemia. *PLoS Biol,* 7**,** e1000249.
MUENCH, M. O., KAPIDZIC, M., GORMLEY, M., GUTIERREZ, A. G., PONDER, K. L., FOMIN, M. E., BEYER, A. I., STOLP, H., QI, Z., FISHER, S. J. & BARCENA, A. 2017. The human chorion contains definitive hematopoietic stem cells from the fifteenth week of gestation. *Development,* 144**,** 1399-1411.
MULLER, A. M., MEDVINSKY, A., STROUBOULIS, J., GROSVELD, F. & DZIERZAK, E. 1994. Development of hematopoietic stem cell activity in the mouse embryo. *Immunity,* 1**,** 291-301.
MULLER, S., BLEY, N., GLASS, M., BUSCH, B., ROUSSEAU, V., MISIAK, D., FUCHS, T., LEDERER, M. & HUTTELMAIER, S. 2018. IGF2BP1 enhances an aggressive tumor cell phenotype by impairing miRNA-directed downregulation of oncogenic factors. *Nucleic Acids Res,* 46**,** 6285-6303.
MULLER-SIEBURG, C. E., CHO, R. H., KARLSSON, L., HUANG, J. F. & SIEBURG, H. B. 2004. Myeloid-biased hematopoietic stem cells have extensive self-renewal capacity but generate diminished lymphoid progeny with impaired IL-7 responsiveness. *Blood,* 103**,** 4111-8.
MULLER-SIEBURG, C. E. & SIEBURG, H. B. 2006. The GOD of hematopoietic stem cells: a clonal diversity model of the stem cell compartment. *Cell Cycle,* 5**,** 394-8.
MUNOZ-LOPEZ, A., ROMERO-MOYA, D., PRIETO, C., RAMOS-MEJIA, V., AGRAZ-DOBLAS, A., VARELA, I., BUSCHBECK, M., PALAU, A., CARVAJAL-VERGARA, X., GIORGETTI, A., FORD, A., LAKO, M., GRANADA, I., RUIZ-XIVILLE, N., RODRIGUEZ-PERALES, S., TORRES-RUIZ, R., STAM, R. W., FUSTER, J. L., FRAGA, M. F., NAKANISHI, M., CAZZANIGA, G., BARDINI, M., COBO, I., BAYON, G. F., FERNANDEZ, A. F., BUENO, C. & MENENDEZ, P. 2016.

Development Refractoriness of MLL-Rearranged Human B Cell Acute Leukemias to Reprogramming into Pluripotency. *Stem Cell Reports,* 7**,** 602-618.

MUNTEAN, A. G., TAN, J., SITWALA, K., HUANG, Y., BRONSTEIN, J., CONNELLY, J. A., BASRUR, V., ELENITOBA-JOHNSON, K. S. & HESS, J. L. 2010. The PAF complex synergizes with MLL fusion proteins at HOX loci to promote leukemogenesis. *Cancer Cell,* 17**,** 609-21.

NAKAMURA, S., HIRANO, I., OKINAKA, K., TAKEMURA, T., YOKOTA, D., ONO, T., SHIGENO, K., SHIBATA, K., FUJISAWA, S. & OHNISHI, K. 2010. The FOXM1 transcriptional factor promotes the proliferation of leukemia cells through modulation of cell cycle progression in acute myeloid leukemia. *Carcinogenesis,* 31**,** 2012-21.

NAKAMURA, T., MORI, T., TADA, S., KRAJEWSKI, W., ROZOVSKAIA, T., WASSELL, R., DUBOIS, G., MAZO, A., CROCE, C. M. & CANAANI, E. 2002. ALL-1 is a histone methyltransferase that assembles a supercomplex of proteins involved in transcriptional regulation. *Mol Cell,* 10**,** 1119-28.

NIGRO, J. M., BAKER, S. J., PREISINGER, A. C., JESSUP, J. M., HOSTETTER, R., CLEARY, K., BIGNER, S. H., DAVIDSON, N., BAYLIN, S., DEVILEE, P. & ET AL. 1989. Mutations in the p53 gene occur in diverse human tumour types. *Nature,* 342**,** 705-8.

NOTTA, F., ZANDI, S., TAKAYAMA, N., DOBSON, S., GAN, O. I., WILSON, G., KAUFMANN, K. B., MCLEOD, J., LAURENTI, E., DUNANT, C. F., MCPHERSON, J. D., STEIN, L. D., DROR, Y. & DICK, J. E. 2016. Distinct routes of lineage development reshape the human blood hierarchy across ontogeny. *Science,* 351**,** aab2116.

O'BRIEN, S. L., FAGAN, A., FOX, E. J., MILLIKAN, R. C., CULHANE, A. C., BRENNAN, D. J., MCCANN, A. H., HEGARTY, S., MOYNA, S., DUFFY, M. J., HIGGINS, D. G., JIRSTROM, K., LANDBERG, G. & GALLAGHER, W. M. 2007. CENP-F expression is associated with poor prognosis and chromosomal instability in patients with primary breast cancer. *Int J Cancer,* 120**,** 1434-43.

O'BYRNE, S., ELLIOTT, N., RICE, S., BUCK, G., FORDHAM, N., GARNETT, C., GODFREY, L., CRUMP, N. T., WRIGHT, G., INGLOTT, S., HUA, P., PSAILA, B., POVINELLI, B., KNAPP, D., AGRAZ-DOBLAS, A., BUENO, C., VARELA, I., BENNETT, P., KOOHY, H., WATT, S. M., KARADIMITRIS, A., MEAD, A. J., ANCLIFF, P., VYAS, P., MENENDEZ, P., MILNE, T. A., ROBERTS, I. & ROY, A. 2019. Discovery of a CD10-negative B-progenitor in human fetal life identifies unique ontogeny-related developmental programs. *Blood,* 134**,** 1059-1071.

OBERLIN, E., FLEURY, M., CLAY, D., PETIT-COCAULT, L., CANDELIER, J. J., MENNESSON, B., JAFFREDO, T. & SOUYRI, M. 2010. VE-cadherin expression allows identification of a new class of hematopoietic stem cells within human embryonic liver. *Blood,* 116**,** 4444-55.

OBERLIN, E., TAVIAN, M., BLAZSEK, I. & PEAULT, B. 2002. Blood-forming potential of vascular endothelium in the human embryo. *Development,* 129**,** 4147-57.
OGURO, H., DING, L. & MORRISON, S. J. 2013. SLAM family markers resolve functionally distinct subpopulations of hematopoietic stem cells and multipotent progenitors. *Cell Stem Cell,* 13**,** 102-16.
OHNO, Y., SUTO, S., YAMANAKA, M., MIZUTANI, Y., MITSUTAKE, S., IGARASHI, Y., SASSA, T. & KIHARA, A. 2010. ELOVL1 production of C24 acyl-CoAs is linked to C24 sphingolipid synthesis. *Proc Natl Acad Sci U S A,* 107**,** 18439-44.
OKUDA, H., KANAI, A., ITO, S., MATSUI, H. & YOKOYAMA, A. 2015. AF4 uses the SL1 components of RNAP1 machinery to initiate MLL fusion- and AEP-dependent transcription. *Nat Commun,* 6**,** 8869.
OKUDA, H., KAWAGUCHI, M., KANAI, A., MATSUI, H., KAWAMURA, T., INABA, T., KITABAYASHI, I. & YOKOYAMA, A. 2014. MLL fusion proteins link transcriptional coactivators to previously active CpG-rich promoters. *Nucleic Acids Res,* 42**,** 4241-56.
OTTERSBACH, K. & DZIERZAK, E. 2005. The murine placenta contains hematopoietic stem cells within the vascular labyrinth region. *Dev Cell,* 8**,** 377-87.
PAGANO, M., PEPPERKOK, R., VERDE, F., ANSORGE, W. & DRAETTA, G. 1992. Cyclin A is required at two points in the human cell cycle. *Embo j,* 11**,** 961-71.
PALANICHAMY, J. K., TRAN, T. M., HOWARD, J. M., CONTRERAS, J. R., FERNANDO, T. R., STERNE-WEILER, T., KATZMAN, S., TOLOUE, M., YAN, W., BASSO, G., PIGAZZI, M., SANFORD, J. R. & RAO, D. S. 2016. RNA-binding protein IGF2BP3 targeting of oncogenic transcripts promotes hematopoietic progenitor proliferation. *J Clin Invest,* 126**,** 1495-511.
PARK, J. W., CHO, H., OH, H., KIM, J. Y. & SEO, S. B. 2018. AURKA Suppresses Leukemic THP-1 Cell Differentiation through Inhibition of the KDM6B Pathway. *Mol Cells,* 41**,** 444-453.
PARK, S., OSMERS, U., RAMAN, G., SCHWANTES, R. H., DIAZ, M. O. & BUSHWELLER, J. H. 2010. The PHD3 domain of MLL acts as a CYP33-regulated switch between MLL-mediated activation and repression. *Biochemistry,* 49**,** 6576-86.
PASCHAL, B. M. & GERACE, L. 1995. Identification of NTF2, a cytosolic factor for nuclear import that interacts with nuclear pore complex protein p62. *J Cell Biol,* 129**,** 925-37.
PATEL, A., DHARMARAJAN, V., VOUGHT, V. E. & COSGROVE, M. S. 2009. On the mechanism of multiple lysine methylation by the human mixed lineage leukemia protein-1 (MLL1) core complex. *J Biol Chem,* 284**,** 24242-56.
PEI, W., FEYERABEND, T. B., ROSSLER, J., WANG, X., POSTRACH, D., BUSCH, K., RODE, I., KLAPPROTH, K., DIETLEIN, N., QUEDENAU, C., CHEN, W., SAUER, S., WOLF, S., HOFER, T. & RODEWALD, H. R. 2017. Polylox barcoding reveals haematopoietic stem cell fates realized in vivo. *Nature,* 548**,** 456-460.

PETRONCZKI, M., LENART, P. & PETERS, J. M. 2008. Polo on the Rise-from Mitotic Entry to Cytokinesis with Plk1. *Dev Cell,* 14**,** 646-59.
PHAROAH, P. D., TSAI, Y. Y., RAMUS, S. J., PHELAN, C. M., GOODE, E. L., LAWRENSON, K., BUCKLEY, M., FRIDLEY, B. L., TYRER, J. P., SHEN, H., WEBER, R., KAREVAN, R., LARSON, M. C., SONG, H., TESSIER, D. C., BACOT, F., VINCENT, D., CUNNINGHAM, J. M., DENNIS, J., DICKS, E., ABEN, K. K., ANTON-CULVER, H., ANTONENKOVA, N., ARMASU, S. M., BAGLIETTO, L., BANDERA, E. V., BECKMANN, M. W., BIRRER, M. J., BLOOM, G., BOGDANOVA, N., BRENTON, J. D., BRINTON, L. A., BROOKS-WILSON, A., BROWN, R., BUTZOW, R., CAMPBELL, I., CARNEY, M. E., CARVALHO, R. S., CHANG-CLAUDE, J., CHEN, Y. A., CHEN, Z., CHOW, W. H., CICEK, M. S., COETZEE, G., COOK, L. S., CRAMER, D. W., CYBULSKI, C., DANSONKA-MIESZKOWSKA, A., DESPIERRE, E., DOHERTY, J. A., DORK, T., DU BOIS, A., DURST, M., ECCLES, D., EDWARDS, R., EKICI, A. B., FASCHING, P. A., FENSTERMACHER, D., FLANAGAN, J., GAO, Y. T., GARCIA-CLOSAS, M., GENTRY-MAHARAJ, A., GILES, G., GJYSHI, A., GORE, M., GRONWALD, J., GUO, Q., HALLE, M. K., HARTER, P., HEIN, A., HEITZ, F., HILLEMANNS, P., HOATLIN, M., HOGDALL, E., HOGDALL, C. K., HOSONO, S., JAKUBOWSKA, A., JENSEN, A., KALLI, K. R., KARLAN, B. Y., KELEMEN, L. E., KIEMENEY, L. A., KJAER, S. K., KONECNY, G. E., KRAKSTAD, C., KUPRYJANCZYK, J., LAMBRECHTS, D., LAMBRECHTS, S., LE, N. D., LEE, N., LEE, J., LEMINEN, A., LIM, B. K., LISSOWSKA, J., LUBINSKI, J., LUNDVALL, L., LURIE, G., MASSUGER, L. F., MATSUO, K., MCGUIRE, V., et al. 2013. GWAS meta-analysis and replication identifies three new susceptibility loci for ovarian cancer. *Nat Genet,* 45**,** 362-70, 370e1-2.
PIETERS, R., DE LORENZO, P., ANCLIFFE, P., AVERSA, L. A., BRETHON, B., BIONDI, A., CAMPBELL, M., ESCHERICH, G., FERSTER, A., GARDNER, R. A., KOTECHA, R. S., LAUSEN, B., LI, C. K., LOCATELLI, F., ATTARBASCHI, A., PETERS, C., RUBNITZ, J. E., SILVERMAN, L. B., STARY, J., SZCZEPANSKI, T., VORA, A., SCHRAPPE, M. & VALSECCHI, M. G. 2019. Outcome of Infants Younger Than 1 Year With Acute Lymphoblastic Leukemia Treated With the Interfant-06 Protocol: Results From an International Phase III Randomized Study. *J Clin Oncol,* 37**,** 2246-2256.
POOLE, C. J., ZHENG, W., LODH, A., YEVTODIYENKO, A., LIEFWALKER, D., LI, H., FELSHER, D. W. & VAN RIGGELEN, J. 2017. DNMT3B overexpression contributes to aberrant DNA methylation and MYC-driven tumor maintenance in T-ALL and Burkitt's lymphoma. *Oncotarget,* 8**,** 76898-76920.
PRIETO, C., MARSCHALEK, R., KUHN, A., BURSEN, A., BUENO, C. & MENENDEZ, P. 2017. The AF4-MLL fusion transiently augments multilineage hematopoietic engraftment but is not sufficient to initiate leukemia in cord blood CD34(+) cells. *Oncotarget,* 8**,** 81936-81941.

PUI, C. H., GAYNON, P. S., BOYETT, J. M., CHESSELLS, J. M., BARUCHEL, A., KAMPS, W., SILVERMAN, L. B., BIONDI, A., HARMS, D. O., VILMER, E., SCHRAPPE, M. & CAMITTA, B. 2002. Outcome of treatment in childhood acute lymphoblastic leukaemia with rearrangements of the 11q23 chromosomal region. *Lancet,* 359**,** 1909-15.

RAMIREZ, P., WAGNER, J. E., DEFOR, T. E., EIDE, C. R., MILLER, J. S., WEISDORF, D. J. & BRUNSTEIN, C. G. 2013. CXCR4 expression in CD34+ cells and unit predominance after double umbilical cord blood transplantation. *Leukemia.* England.

RAYES, A., MCMASTERS, R. L. & O'BRIEN, M. M. 2016. Lineage Switch in MLL-Rearranged Infant Leukemia Following CD19-Directed Therapy. *Pediatr Blood Cancer,* 63**,** 1113-5.

REBEL, V. I., MILLER, C. L., EAVES, C. J. & LANSDORP, P. M. 1996. The repopulation potential of fetal liver hematopoietic stem cells in mice exceeds that of their liver adult bone marrow counterparts. *Blood,* 87**,** 3500-7.

RENNER, A. G., DOS SANTOS, C., RECHER, C., BAILLY, C., CREANCIER, L., KRUCZYNSKI, A., PAYRASTRE, B. & MANENTI, S. 2009. Polo-like kinase 1 is overexpressed in acute myeloid leukemia and its inhibition preferentially targets the proliferation of leukemic cells. *Blood,* 114**,** 659-62.

RHO, S. B., DONG, S. M., KANG, S., SEO, S. S., YOO, C. W., LEE, D. O., WOO, J. S. & PARK, S. Y. 2008. Insulin-like growth factor-binding protein-5 (IGFBP-5) acts as a tumor suppressor by inhibiting angiogenesis. *Carcinogenesis,* 29**,** 2106-11.

RIABOV, V., YIN, S., SONG, B., AVDIC, A., SCHLEDZEWSKI, K., OVSIY, I., GRATCHEV, A., LLOPIS VERDIELL, M., STICHT, C., SCHMUTTERMAIER, C., SCHONHABER, H., WEISS, C., FIELDS, A. P., SIMON-KELLER, K., PFISTER, F., BERLIT, S., MARX, A., ARNOLD, B., GOERDT, S. & KZHYSHKOWSKA, J. 2016. Stabilin-1 is expressed in human breast cancer and supports tumor growth in mammary adenocarcinoma mouse model. *Oncotarget,* 7**,** 31097-110.

RICHARDSON, A., SCHWAGER, F., LANDRY, S. J. & GEORGOPOULOS, C. 2001. The importance of a mobile loop in regulating chaperonin/ co-chaperonin interaction: humans versus Escherichia coli. *J Biol Chem,* 276**,** 4981-7.

RICHARDSON, P. J. 2016. CXCR4 and Glioblastoma. *Anticancer Agents Med Chem,* 16**,** 59-74.

ROBIN, C., BOLLEROT, K., MENDES, S., HAAK, E., CRISAN, M., CERISOLI, F., LAUW, I., KAIMAKIS, P., JORNA, R., VERMEULEN, M., KAYSER, M., VAN DER LINDEN, R., IMANIRAD, P., VERSTEGEN, M., NAWAZ-YOUSAF, H., PAPAZIAN, N., STEEGERS, E., CUPEDO, T. & DZIERZAK, E. 2009. Human placenta is a potent hematopoietic niche containing hematopoietic stem and progenitor cells throughout development. *Cell Stem Cell,* 5**,** 385-95.

ROWE, R. G., MANDELBAUM, J., ZON, L. I. & DALEY, G. Q. 2016. Engineering Hematopoietic Stem Cells: Lessons from Development. *Cell Stem Cell,* 18**,** 707-20.
ROY, S., DI CELLO, F., KOWALSKI, J., HRISTOV, A. C., TSAI, H. L., BHOJWANI, D., MEYER, J. A., CARROLL, W. L., BELTON, A. & RESAR, L. M. 2013. HMGA1 overexpression correlates with relapse in childhood B-lineage acute lymphoblastic leukemia. *Leuk Lymphoma,* 54**,** 2565-7.
RUDOLPH, D., IMPAGNATIELLO, M. A., BLAUKOPF, C., SOMMER, C., GERLICH, D. W., ROTH, M., TONTSCH-GRUNT, U., WERNITZNIG, A., SAVARESE, F., HOFMANN, M. H., ALBRECHT, C., GEISELMANN, L., RESCHKE, M., GARIN-CHESA, P., ZUBER, J., MOLL, J., ADOLF, G. R. & KRAUT, N. 2015. Efficacy and mechanism of action of volasertib, a potent and selective inhibitor of Polo-like kinases, in preclinical models of acute myeloid leukemia. *J Pharmacol Exp Ther,* 352**,** 579-89.
RUDOLPH, D., STEEGMAIER, M., HOFFMANN, M., GRAUERT, M., BAUM, A., QUANT, J., HASLINGER, C., GARIN-CHESA, P. & ADOLF, G. R. 2009. BI 6727, a Polo-like kinase inhibitor with improved pharmacokinetic profile and broad antitumor activity. *Clin Cancer Res,* 15**,** 3094-102.
SAMOKHVALOV, I. M., SAMOKHVALOVA, N. I. & NISHIKAWA, S. 2007. Cell tracing shows the contribution of the yolk sac to adult haematopoiesis. *Nature,* 446**,** 1056-61.
SANDOVAL, J. E., HUANG, Y. H., MUISE, A., GOODELL, M. A. & REICH, N. O. 2019. Mutations in the DNMT3A DNA methyltransferase in acute myeloid leukemia patients cause both loss and gain of function and differential regulation by protein partners. *J Biol Chem,* 294**,** 4898-4910.
SANJUAN-PLA, A., MACAULAY, I. C., JENSEN, C. T., WOLL, P. S., LUIS, T. C., MEAD, A., MOORE, S., CARELLA, C., MATSUOKA, S., BOURIEZ JONES, T., CHOWDHURY, O., STENSON, L., LUTTEROPP, M., GREEN, J. C., FACCHINI, R., BOUKARABILA, H., GROVER, A., GAMBARDELLA, A., THONGJUEA, S., CARRELHA, J., TARRANT, P., ATKINSON, D., CLARK, S. A., NERLOV, C. & JACOBSEN, S. E. 2013. Platelet-biased stem cells reside at the apex of the haematopoietic stem-cell hierarchy. *Nature,* 502**,** 232-6.
SARTOR, H., EHLERT, F., GRZESCHIK, K. H., MULLER, R. & ADOLPH, S. 1992. Assignment of two human cell cycle genes, CDC25C and CCNB1, to 5q31 and 5q12, respectively. *Genomics,* 13**,** 911-2.
SCHARF, S., ZECH, J., BURSEN, A., SCHRAETS, D., OLIVER, P. L., KLIEM, S., PFITZNER, E., GILLERT, E., DINGERMANN, T. & MARSCHALEK, R. 2007. Transcription linked to recombination: a gene-internal promoter coincides with the recombination hot spot II of the human MLL gene. *Oncogene,* 26**,** 1361-71.
SCHMUCKER, S. & SUMARA, I. 2014. Molecular dynamics of PLK1 during mitosis. *Mol Cell Oncol,* 1**,** e954507.

SCHUMACHER, J. M., GOLDEN, A. & DONOVAN, P. J. 1998. AIR-2: An Aurora/Ipl1-related protein kinase associated with chromosomes and midbody microtubules is required for polar body extrusion and cytokinesis in Caenorhabditis elegans embryos. *J Cell Biol,* 143**,** 1635-46.

SHENG, Y. H., HE, Y., HASNAIN, S. Z., WANG, R., TONG, H., CLARKE, D. T., LOURIE, R., OANCEA, I., WONG, K. Y., LUMLEY, J. W., FLORIN, T. H., SUTTON, P., HOOPER, J. D., MCMILLAN, N. A. & MCGUCKIN, M. A. 2017. MUC13 protects colorectal cancer cells from death by activating the NF-kappaB pathway and is a potential therapeutic target. *Oncogene,* 36**,** 700-713.

SHERR, C. J. 1996. Cancer cell cycles. *Science,* 274**,** 1672-7.

SHI, Y., ZHAO, Y., ZHANG, Y., AIERKEN, N., SHAO, N., YE, R., LIN, Y. & WANG, S. 2018. AFF3 upregulation mediates tamoxifen resistance in breast cancers. *J Exp Clin Cancer Res,* 37**,** 254.

SHIMIZU, K., GOLDFARB, M., SUARD, Y., PERUCHO, M., LI, Y., KAMATA, T., FERAMISCO, J., STAVNEZER, E., FOGH, J. & WIGLER, M. H. 1983. Three human transforming genes are related to the viral ras oncogenes. *Proc Natl Acad Sci U S A,* 80**,** 2112-6.

SIEBURG, H. B., CHO, R. H., DYKSTRA, B., UCHIDA, N., EAVES, C. J. & MULLER-SIEBURG, C. E. 2006. The hematopoietic stem compartment consists of a limited number of discrete stem cell subsets. *Blood,* 107**,** 2311-6.

SILVER, L. & PALIS, J. 1997. Initiation of murine embryonic erythropoiesis: a spatial analysis. *Blood,* 89**,** 1154-64.

SILVERMAN, L. B. 2007. Acute lymphoblastic leukemia in infancy. *Pediatr Blood Cancer,* 49**,** 1070-3.

SIMIZU, S. & OSADA, H. 2000. Mutations in the Plk gene lead to instability of Plk protein in human tumour cell lines. *Nat Cell Biol,* 2**,** 852-4.

SISON, E. A., RAU, R. E., MCINTYRE, E., LI, L., SMALL, D. & BROWN, P. 2013. MLL-rearranged acute lymphoblastic leukaemia stem cell interactions with bone marrow stroma promote survival and therapeutic resistance that can be overcome with CXCR4 antagonism. *Br J Haematol,* 160**,** 785-97.

SMITS, V. A., KLOMPMAKER, R., ARNAUD, L., RIJKSEN, G., NIGG, E. A. & MEDEMA, R. H. 2000. Polo-like kinase-1 is a target of the DNA damage checkpoint. *Nat Cell Biol,* 2**,** 672-6.

SOLOMON, M. J., GLOTZER, M., LEE, T. H., PHILIPPE, M. & KIRSCHNER, M. W. 1990. Cyclin activation of p34cdc2. *Cell,* 63**,** 1013-24.

SONESON, C., LOVE, M. I. & ROBINSON, M. D. 2015. Differential analyses for RNA-seq: transcript-level estimates improve gene-level inferences. *F1000Res,* 4**,** 1521.

SPECTOR, L. G., XIE, Y., ROBISON, L. L., HEEREMA, N. A., HILDEN, J. M., LANGE, B., FELIX, C. A., DAVIES, S. M., SLAVIN, J., POTTER, J. D., BLAIR, C. K., REAMAN, G. H. & ROSS, J. A. 2005. Maternal diet and infant leukemia: the DNA topoisomerase II inhibitor hypothesis: a report from the children's oncology group. *Cancer Epidemiol Biomarkers Prev,* 14**,** 651-5.

STAM, R. W., SCHNEIDER, P., HAGELSTEIN, J. A., VAN DER LINDEN, M. H., STUMPEL, D. J., DE MENEZES, R. X., DE LORENZO, P., VALSECCHI, M. G. & PIETERS, R. 2010. Gene expression profiling-based dissection of MLL translocated and MLL germline acute lymphoblastic leukemia in infants. *Blood,* 115**,** 2835-44.

STANULLA, M., WANG, J., CHERVINSKY, D. S., THANDLA, S. & APLAN, P. D. 1997. DNA cleavage within the MLL breakpoint cluster region is a specific event which occurs as part of higher-order chromatin fragmentation during the initial stages of apoptosis. *Mol Cell Biol,* 17**,** 4070-9.

STEEGMAIER, M., HOFFMANN, M., BAUM, A., LENART, P., PETRONCZKI, M., KRSSAK, M., GURTLER, U., GARIN-CHESA, P., LIEB, S., QUANT, J., GRAUERT, M., ADOLF, G. R., KRAUT, N., PETERS, J. M. & RETTIG, W. J. 2007. BI 2536, a potent and selective inhibitor of polo-like kinase 1, inhibits tumor growth in vivo. *Curr Biol,* 17**,** 316-22.

STOSKUS, M., EIDUKAITE, A. & GRISKEVICIUS, L. 2016. Defining the significance of IGF2BP1 overexpression in t(12;21)(p13;q22)-positive leukemia REH cells. *Leuk Res,* 47**,** 16-21.

STREBHARDT, K., KNEISEL, L., LINHART, C., BERND, A. & KAUFMANN, R. 2000. Prognostic value of pololike kinase expression in melanomas. *Jama.* United States.

STRISSEL, P. L., STRICK, R., ROWLEY, J. D. & ZELEZNIK-LE, N. J. 1998. An in vivo topoisomerase II cleavage site and a DNase I hypersensitive site colocalize near exon 9 in the MLL breakpoint cluster region. *Blood,* 92**,** 3793-803.

STUMPEL, D. J., SCHNEIDER, P., SESLIJA, L., OSAKI, H., WILLIAMS, O., PIETERS, R. & STAM, R. W. 2012. Connectivity mapping identifies HDAC inhibitors for the treatment of t(4;11)-positive infant acute lymphoblastic leukemia. *Leukemia,* 26**,** 682-92.

SUBRAMANIAN, A., TAMAYO, P., MOOTHA, V. K., MUKHERJEE, S., EBERT, B. L., GILLETTE, M. A., PAULOVICH, A., POMEROY, S. L., GOLUB, T. R., LANDER, E. S. & MESIROV, J. P. 2005. Gene set enrichment analysis: a knowledge-based approach for interpreting genome-wide expression profiles. *Proc Natl Acad Sci U S A,* 102**,** 15545-50.

SUMARA, I., GIMENEZ-ABIAN, J. F., GERLICH, D., HIROTA, T., KRAFT, C., DE LA TORRE, C., ELLENBERG, J. & PETERS, J. M. 2004. Roles of polo-like kinase 1 in the assembly of functional mitotic spindles. *Curr Biol,* 14**,** 1712-22.

SUN, J. J., LI, H. L., GUO, S. J., MA, H., LIU, S. J., LIU, D. & XUE, F. X. 2019. The Increased PTK7 Expression Is a Malignant Factor in Cervical Cancer. *Dis Markers,* 2019**,** 5380197.

SUNKEL, C. E. & GLOVER, D. M. 1988. polo, a mitotic mutant of Drosophila displaying abnormal spindle poles. *J Cell Sci,* 89 (Pt 1)**,** 25-38.

TAN, Y. T., YE, L., XIE, F., BEYER, A. I., MUENCH, M. O., WANG, J., CHEN, Z., LIU, H., CHEN, S. J. & KAN, Y. W. 2018. Respecifying human iPSC-derived blood cells into highly engraftable hematopoietic

stem and progenitor cells with a single factor. *Proc Natl Acad Sci U S A,* 115**,** 2180-2185.
TANIKAWA, C., UEDA, K., NAKAGAWA, H., YOSHIDA, N., NAKAMURA, Y. & MATSUDA, K. 2009. Regulation of protein Citrullination through p53/PADI4 network in DNA damage response. *Cancer Res,* 69**,** 8761-9.
TAVIAN, M., COULOMBEL, L., LUTON, D., CLEMENTE, H. S., DIETERLEN-LIEVRE, F. & PEAULT, B. 1996. Aorta-associated CD34+ hematopoietic cells in the early human embryo. *Blood,* 87**,** 67-72.
TAVIAN, M., HALLAIS, M. F. & PEAULT, B. 1999. Emergence of intraembryonic hematopoietic precursors in the pre-liver human embryo. *Development,* 126**,** 793-803.
TILL, J. E. & MC, C. E. 1961. A direct measurement of the radiation sensitivity of normal mouse bone marrow cells. *Radiat Res,* 14**,** 213-22.
TKACHUK, D. C., KOHLER, S. & CLEARY, M. L. 1992. Involvement of a homolog of Drosophila trithorax by 11q23 chromosomal translocations in acute leukemias. *Cell,* 71**,** 691-700.
TRENTIN, L., GIORDAN, M., DINGERMANN, T., BASSO, G., TE KRONNIE, G. & MARSCHALEK, R. 2009. Two independent gene signatures in pediatric t(4;11) acute lymphoblastic leukemia patients. *Eur J Haematol,* 83**,** 406-19.
TRUETT, G. E., HEEGER, P., MYNATT, R. L., TRUETT, A. A., WALKER, J. A. & WARMAN, M. L. 2000. Preparation of PCR-quality mouse genomic DNA with hot sodium hydroxide and tris (HotSHOT). *Biotechniques,* 29**,** 52, 54.
TSUCHIDA, N., MURUGAN, A. K. & GRIECO, M. 2016. Kirsten Ras* oncogene: significance of its discovery in human cancer research. *Oncotarget,* 7**,** 46717-46733.
TVRDIK, P., WESTERBERG, R., SILVE, S., ASADI, A., JAKOBSSON, A., CANNON, B., LOISON, G. & JACOBSSON, A. 2000. Role of a new mammalian gene family in the biosynthesis of very long chain fatty acids and sphingolipids. *J Cell Biol,* 149**,** 707-18.
VALLA, M., ENGSTROM, M. J., YTTERHUS, B., HANSEN, A. K., AKSLEN, L. A., VATTEN, L. J., OPDAHL, S. & BOFIN, A. M. 2017. FGD5 amplification in breast cancer patients is associated with tumour proliferation and a poorer prognosis. *Breast Cancer Res Treat,* 162**,** 243-253.
VAN GALEN, P., KRESO, A., WIENHOLDS, E., LAURENTI, E., EPPERT, K., LECHMAN, E. R., MBONG, N., HERMANS, K., DOBSON, S., APRIL, C., FAN, J. B. & DICK, J. E. 2014. Reduced lymphoid lineage priming promotes human hematopoietic stem cell expansion. *Cell Stem Cell,* 14**,** 94-106.
VAN VUGT, M. A., BRAS, A. & MEDEMA, R. H. 2004. Polo-like kinase-1 controls recovery from a G2 DNA damage-induced arrest in mammalian cells. *Mol Cell,* 15**,** 799-811.

VEERIAH, S., BRENNAN, C., MENG, S., SINGH, B., FAGIN, J. A., SOLIT, D. B., PATY, P. B., ROHLE, D., VIVANCO, I., CHMIELECKI, J., PAO, W., LADANYI, M., GERALD, W. L., LIAU, L., CLOUGHESY, T. C., MISCHEL, P. S., SANDER, C., TAYLOR, B., SCHULTZ, N., MAJOR, J., HEGUY, A., FANG, F., MELLINGHOFF, I. K. & CHAN, T. A. 2009. The tyrosine phosphatase PTPRD is a tumor suppressor that is frequently inactivated and mutated in glioblastoma and other human cancers. *Proc Natl Acad Sci U S A,* 106**,** 9435-40.

VON SCHUBERT, C., CUBIZOLLES, F., BRACHER, J. M., SLIEDRECHT, T., KOPS, G. & NIGG, E. A. 2015. Plk1 and Mps1 Cooperatively Regulate the Spindle Assembly Checkpoint in Human Cells. *Cell Rep,* 12**,** 66-78.

VON STACKELBERG, A., LOCATELLI, F., ZUGMAIER, G., HANDGRETINGER, R., TRIPPETT, T. M., RIZZARI, C., BADER, P., O'BRIEN, M. M., BRETHON, B., BHOJWANI, D., SCHLEGEL, P. G., BORKHARDT, A., RHEINGOLD, S. R., COOPER, T. M., ZWAAN, C. M., BARNETTE, P., MESSINA, C., MICHEL, G., DUBOIS, S. G., HU, K., ZHU, M., WHITLOCK, J. A. & GORE, L. 2016. Phase I/Phase II Study of Blinatumomab in Pediatric Patients With Relapsed/Refractory Acute Lymphoblastic Leukemia. *J Clin Oncol,* 34**,** 4381-4389.

WANG, H., HU, X., DING, X., DOU, Z., YANG, Z., SHAW, A. W., TENG, M., CLEVELAND, D. W., GOLDBERG, M. L., NIU, L. & YAO, X. 2004. Human Zwint-1 specifies localization of Zeste White 10 to kinetochores and is essential for mitotic checkpoint signaling. *J Biol Chem,* 279**,** 54590-8.

WANG, K., LING, T., WU, H. & ZHANG, J. 2013. Screening of candidate tumor-suppressor genes in 3p21.3 and investigation of the methylation of gene promoters in oral squamous cell carcinoma. *Oncol Rep,* 29**,** 1175-82.

WANG, K. & ZHANG, T. 2016. Prognostic significance of CD168 overexpression in colorectal cancer. *Oncol Lett,* 12**,** 2555-2559.

WATANABE, A., OGIWARA, H., EHATA, S., MUKASA, A., ISHIKAWA, S., MAEDA, D., UEKI, K., INO, Y., TODO, T., YAMADA, Y., FUKAYAMA, M., SAITO, N., MIYAZONO, K. & ABURATANI, H. 2011. Homozygously deleted gene DACH1 regulates tumor-initiating activity of glioma cells. *Proc Natl Acad Sci U S A,* 108**,** 12384-9.

WATCHAM, S., KUCINSKI, I. & GOTTGENS, B. 2019. New insights into hematopoietic differentiation landscapes from single-cell RNA sequencing. *Blood,* 133**,** 1415-1426.

WILKINSON, A. C., BALLABIO, E., GENG, H., NORTH, P., TAPIA, M., KERRY, J., BISWAS, D., ROEDER, R. G., ALLIS, C. D., MELNICK, A., DE BRUIJN, M. F. & MILNE, T. A. 2013. RUNX1 is a key target in t(4;11) leukemias that contributes to gene activation through an AF4-MLL complex interaction. *Cell Rep,* 3**,** 116-27.

WILLIAMS, B. C., KARR, T. L., MONTGOMERY, J. M. & GOLDBERG, M. L. 1992. The Drosophila l(1)zw10 gene product, required for accurate mitotic chromosome segregation, is redistributed at anaphase onset. *J Cell Biol,* 118**,** 759-73.

WINTERS, A. C. & BERNT, K. M. 2017. MLL-Rearranged Leukemias-An Update on Science and Clinical Approaches. *Front Pediatr,* 5**,** 4.
WOLF, G., ELEZ, R., DOERMER, A., HOLTRICH, U., ACKERMANN, H., STUTTE, H. J., ALTMANNSBERGER, H. M., RUBSAMEN-WAIGMANN, H. & STREBHARDT, K. 1997. Prognostic significance of polo-like kinase (PLK) expression in non-small cell lung cancer. *Oncogene,* 14**,** 543-9.
WOLF, G., HILDENBRAND, R., SCHWAR, C., GROBHOLZ, R., KAUFMANN, M., STUTTE, H. J., STREBHARDT, K. & BLEYL, U. 2000. Polo-like kinase: a novel marker of proliferation: correlation with estrogen-receptor expression in human breast cancer. *Pathol Res Pract,* 196**,** 753-9.
WRAY, J., WILLIAMSON, E. A., SINGH, S. B., WU, Y., COGLE, C. R., WEINSTOCK, D. M., ZHANG, Y., LEE, S. H., ZHOU, D., SHAO, L., HAUER-JENSEN, M., PATHAK, R., KLIMEK, V., NICKOLOFF, J. A. & HROMAS, R. 2013. PARP1 is required for chromosomal translocations. *Blood,* 121**,** 4359-65.
XU, H., YU, S., YUAN, X., XIONG, J., KUANG, D., PESTELL, R. G. & WU, K. 2017. DACH1 suppresses breast cancer as a negative regulator of CD44. *Sci Rep,* 7**,** 4361.
XU, Z., ZHANG, Q., LUH, F., JIN, B. & LIU, X. 2019. Overexpression of the ASPM gene is associated with aggressiveness and poor outcome in bladder cancer. *Oncol Lett,* 17**,** 1865-1876.
YAGI, H., DEGUCHI, K., AONO, A., TANI, Y., KISHIMOTO, T. & KOMORI, T. 1998. Growth disturbance in fetal liver hematopoiesis of Mll-mutant mice. *Blood,* 92**,** 108-17.
YAMAMOTO, R., MORITA, Y., OOEHARA, J., HAMANAKA, S., ONODERA, M., RUDOLPH, K. L., EMA, H. & NAKAUCHI, H. 2013. Clonal analysis unveils self-renewing lineage-restricted progenitors generated directly from hematopoietic stem cells. *Cell,* 154**,** 1112-1126.
YAMASHITA, Y., NISHIUMI, S., KONO, S., TAKAO, S., AZUMA, T. & YOSHIDA, M. 2017. Differences in elongation of very long chain fatty acids and fatty acid metabolism between triple-negative and hormone receptor-positive breast cancer. *BMC Cancer,* 17**,** 589.
YANG, S. C., HUANG, C. H., CHEN, N. J., CHOU, C. K. & LIN, C. H. 2000. Functional implication of human serine/threonine kinase, hAIK, in cell cycle progression. *J Biomed Sci,* 7**,** 484-93.
YANG, X., WOOD, P. A., ANSELL, C. M., QUITON, D. F., OH, E. Y., DU-QUITON, J. & HRUSHESKY, W. J. 2009. The circadian clock gene Per1 suppresses cancer cell proliferation and tumor growth at specific times of day. *Chronobiol Int,* 26**,** 1323-39.
YANO, T., NAKAMURA, T., BLECHMAN, J., SORIO, C., DANG, C. V., GEIGER, B. & CANAANI, E. 1997. Nuclear punctate distribution of ALL-1 is conferred by distinct elements at the N terminus of the protein. *Proc Natl Acad Sci U S A,* 94**,** 7286-91.
YAO, H., PRICE, T. T., CANTELLI, G., NGO, B., WARNER, M. J., OLIVERE, L., RIDGE, S. M., JABLONSKI, E. M., THERRIEN, J., TANNHEIMER, S., MCCALL, C. M., CHENN, A. & SIPKINS, D. A. 2018. Leukaemia

hijacks a neural mechanism to invade the central nervous system. *Nature,* 560**,** 55-60.
YE, M., ZHANG, H., AMABILE, G., YANG, H., STABER, P. B., ZHANG, P., LEVANTINI, E., ALBERICH-JORDA, M., ZHANG, J., KAWASAKI, A. & TENEN, D. G. 2013. C/EBPa controls acquisition and maintenance of adult haematopoietic stem cell quiescence. *Nat Cell Biol,* 15**,** 385-94.
YE, S., SONG, W., XU, X., ZHAO, X. & YANG, L. 2016. IGF2BP2 promotes colorectal cancer cell proliferation and survival through interfering with RAF-1 degradation by miR-195. *FEBS Lett,* 590**,** 1641-50.
YODER, M. C. 2004. Generation of HSCs in the embryo and assays to detect them. *Oncogene,* 23**,** 7161-3.
YOKOYAMA, A. & CLEARY, M. L. 2008. Menin critically links MLL proteins with LEDGF on cancer-associated target genes. *Cancer Cell,* 14**,** 36-46.
YOKOYAMA, A., SOMERVAILLE, T. C., SMITH, K. S., ROZENBLATT-ROSEN, O., MEYERSON, M. & CLEARY, M. L. 2005. The menin tumor suppressor protein is an essential oncogenic cofactor for MLL-associated leukemogenesis. *Cell,* 123**,** 207-18.
YOSHIMOTO, M., MONTECINO-RODRIGUEZ, E., FERKOWICZ, M. J., PORAYETTE, P., SHELLEY, W. C., CONWAY, S. J., DORSHKIND, K. & YODER, M. C. 2011. Embryonic day 9 yolk sac and intra-embryonic hemogenic endothelium independently generate a B-1 and marginal zone progenitor lacking B-2 potential. *Proc Natl Acad Sci U S A,* 108**,** 1468-73.
YU, B. D., HANSON, R. D., HESS, J. L., HORNING, S. E. & KORSMEYER, S. J. 1998. MLL, a mammalian trithorax-group gene, functions as a transcriptional maintenance factor in morphogenesis. *Proc Natl Acad Sci U S A,* 95**,** 10632-6.
YU, B. D., HESS, J. L., HORNING, S. E., BROWN, G. A. & KORSMEYER, S. J. 1995. Altered Hox expression and segmental identity in Mll-mutant mice. *Nature,* 378**,** 505-8.
YUAN, J., NGUYEN, C. K., LIU, X., KANELLOPOULOU, C. & MULJO, S. A. 2012. Lin28b reprograms adult bone marrow hematopoietic progenitors to mediate fetal-like lymphopoiesis. *Science,* 335**,** 1195-200.
ZAPPASODI, R., RUGGIERO, G., GUARNOTTA, C., TORTORETO, M., TRINGALI, C., CAVANE, A., CABRAS, A. D., CASTAGNOLI, L., VENERANDO, B., ZAFFARONI, N., GIANNI, A. M., DE BRAUD, F., TRIPODO, C., PUPA, S. M. & DI NICOLA, M. 2015. HSPH1 inhibition downregulates Bcl-6 and c-Myc and hampers the growth of human aggressive B-cell non-Hodgkin lymphoma. *Blood,* 125**,** 1768-71.
ZELEZNIK-LE, N. J., HARDEN, A. M. & ROWLEY, J. D. 1994. 11q23 translocations split the "AT-hook" cruciform DNA-binding region and the transcriptional repression domain from the activation domain of the mixed-lineage leukemia (MLL) gene. *Proc Natl Acad Sci U S A,* 91**,** 10610-4.
ZENATTI, P. P., RIBEIRO, D., LI, W., ZUURBIER, L., SILVA, M. C., PAGANIN, M., TRITAPOE, J., HIXON, J. A., SILVEIRA, A. B.,

CARDOSO, B. A., SARMENTO, L. M., CORREIA, N., TORIBIO, M. L., KOBARG, J., HORSTMANN, M., PIETERS, R., BRANDALISE, S. R., FERRANDO, A. A., MEIJERINK, J. P., DURUM, S. K., YUNES, J. A. & BARATA, J. T. 2011. Oncogenic IL7R gain-of-function mutations in childhood T-cell acute lymphoblastic leukemia. *Nat Genet,* 43**,** 932-9.

ZHANG, J., REN, X., WANG, B., CAO, J., TIAN, L. & LIU, M. 2018. Effect of DACH1 on proliferation and invasion of laryngeal squamous cell carcinoma. *Head Face Med,* 14**,** 20.

ZHANG, Y., SAAVEDRA, E., TANG, R., GU, Y., LAPPIN, P., TRAJKOVIC, D., LIU, S. H., SMEAL, T., FANTIN, V., DE BOTTON, S., LEGRAND, O., DELHOMMEAU, F., PERNASETTI, F. & LOUACHE, F. 2017. Targeting primary acute myeloid leukemia with a new CXCR4 antagonist IgG1 antibody (PF-06747143). *Sci Rep,* 7**,** 7305.

ZHAO, W., LU, D., LIU, L., CAI, J., ZHOU, Y., YANG, Y., ZHANG, Y. & ZHANG, J. 2017. Insulin-like growth factor 2 mRNA binding protein 3 (IGF2BP3) promotes lung tumorigenesis via attenuating p53 stability. *Oncotarget,* 8**,** 93672-93687.

ZHOU, J., BI, C., CHING, Y. Q., CHOOI, J. Y., LU, X., QUAH, J. Y., TOH, S. H., CHAN, Z. L., TAN, T. Z., CHONG, P. S. & CHNG, W. J. 2017. Inhibition of LIN28B impairs leukemia cell growth and metabolism in acute myeloid leukemia. *J Hematol Oncol,* 10**,** 138.

Chapter 10 Appendices

10.1 Appendix 1

List of genes differentially expressed between murine foetal liver and bone marrow derived LMPPs (positive log fold represents genes upregulated in the foetal liver derived LMPPs), described in chapter 3.

Ensemb ID	og2 Fo d Change	padj	Gene Name
ENSMUSG00000029814	5.092845825	1.16E 47	Igf2bp3
ENSMUSG00000022824	5.336799901	4.08E 40	Muc13
ENSMUSG00000055413	6.634453962	2.88E 38	H2 Q5
ENSMUSG00000061232	3.12051343	2.22E 35	H2 K1
ENSMUSG00000025330	4.430730244	1.41E 27	Pad 4
ENSMUSG00000024940	4.60709422	2.93E 25	Ltbp3
ENSMUSG00000013415	3.542743884	6.36E 23	Igf2bp1
ENSMUSG00000056758	3.487073113	4.84E 21	Hmga2
ENSMUSG00000064147	3.608096007	6.41E 19	Rab44
ENSMUSG00000055639	4.262475575	9.87E 19	Dach1
ENSMUSG00000074151	3.638787671	1.33E 18	N rc5
ENSMUSG00000073411	2.727067828	2.97E 18	H2 D1
ENSMUSG00000027073	5.952321216	8.92E 18	Prg2
ENSMUSG00000004952	3.201717229	1.46E 16	Rasa4
ENSMUSG00000021262	2.789650262	5.69E 16	Ev
ENSMUSG00000024924	3.003836961	6.11E 16	V d r
ENSMUSG00000032265	4.189100534	1.46E 15	Fam46a
ENSMUSG00000037280	2.956430692	2.09E 15	Ga nt6
ENSMUSG00000025877	4.492537264	1.04E 14	Hk3
ENSMUSG00000029581	3.813553495	1.61E 14	Fscn1
ENSMUSG00000078922	4.597168139	3.64E 14	Tgtp1
ENSMUSG00000070348	2.846442494	4.83E 14	Ccnd1
ENSMUSG00000061311	3.219218547	4.83E 14	Rag1
ENSMUSG00000070348	2.172355157	2.02E 13	Dnmt3b
ENSMUSG00000063804	3.182723333	2.62E 13	L n28b
ENSMUSG00000024900	2.21786076	3.34E 13	Cpt1a
ENSMUSG00000073409	3.209016995	9.06E 13	H2 Q8
ENSMUSG00000034361	3.889494414	3.18E 12	Cpne2
ENSMUSG00000039315	3.198390493	4.15E 12	C nk
ENSMUSG00000070643	2.435760317	7.78E 12	Sox13
ENSMUSG00000026581	2.67251405	8.63E 12	Se
ENSMUSG00000004891	3.646496156	4.06E 11	Nes
ENSMUSG00000038370	4.946659004	4.41E 11	Pcp4 1
ENSMUSG00000022636	3.212690119	5.17E 11	A cam
ENSMUSG00000007682	4.333140837	5.64E 11	D o2
ENSMUSG00000034485	2.307494917	1.63E 10	Uaca
ENSMUSG00000078921	3.507238528	2.44E 10	Tgtp2
ENSMUSG00000033863	3.98339275	2.45E 10	K f9
ENSMUSG00000025014	7.697730133	2.51E 10	Dntt
ENSMUSG00000020893	2.599305767	3.31E 10	Per1
ENSMUSG00000053931	2.350802597	4.57E 10	Cnn3
ENSMUSG00000003882	3.222059829	6.73E 10	I 7r
ENSMUSG00000015970	3.475637556	7.39E 10	Chdh
ENSMUSG00000029716	3.340231599	9.10E 10	Tfr2
ENSMUSG00000023972	2.218672622	1.56E 09	Ptk7
ENSMUSG00000037169	2.192825496	2.20E 09	Mycn
ENSMUSG00000026822	5.122360547	2.67E 09	Lcn2
ENSMUSG00000037138	2.401265593	2.82E 09	Aff3
ENSMUSG00000035929	2.671368888	3.43E 09	H2 Q4
ENSMUSG00000034930	2.74218158	3.71E 09	Rtkn
ENSMUSG00000025529	4.279764418	3.87E 09	Zfp711

ENSMUSG00000022534	4.774416057	4.12E 09	Mefv
ENSMUSG00000054435	2.97057295	4.96E 09	G map4
ENSMUSG00000071226	2.066225734	5.81E 09	Cecr2
ENSMUSG00000005474	4.742905876	5.90E 09	My 10
ENSMUSG00000022817	3.433792523	6.42E 09	Itgb5
ENSMUSG00000024164	3.566174301	8.31E 09	C3
ENSMUSG00000022755	2.966345358	9.08E 09	Adgrg7
ENSMUSG00000026921	2.55650818	1.20E 08	Egf 7
ENSMUSG00000022686	2.674718341	1.39E 08	B3gnt5
ENSMUSG00000060550	2.994227037	1.42E 08	H2 Q7
ENSMUSG00000029561	2.059571822	1.83E 08	Oas 2
ENSMUSG00000048612	2.794064176	2.40E 08	Myof
ENSMUSG00000037922	3.371133442	2.68E 08	Bank1
ENSMUSG00000028528	3.899223799	3.40E 08	Dnajc6
ENSMUSG00000026222	1.622990809	3.53E 08	Sp100
ENSMUSG00000015053	1.926578339	4.97E 08	Gata2
ENSMUSG00000000782	3.457572647	5.02E 08	Tcf7
ENSMUSG00000051397	4.37224512	7.02E 08	Tacstd2
ENSMUSG00000020715	2.267850687	7.68E 08	Ern1
ENSMUSG00000036594	3.166403746	7.79E 08	H2 Aa
ENSMUSG00000054072	3.931977848	8.10E 08	I gp1
ENSMUSG00000039234	2.57344171	8.21E 08	Sec24d
ENSMUSG00000040856	3.410733195	9.11E 08	D k1
ENSMUSG00000098411	3.410733195	9.11E 08	D k1
ENSMUSG00000048148	2.841850077	9.14E 08	Nwd1
ENSMUSG00000034037	1.92280688	1.25E 07	Fgd5
ENSMUSG00000043557	3.192754951	1.25E 07	Mdga1
ENSMUSG00000033826	2.009191428	1.72E 07	Dnah8
ENSMUSG00000014813	2.958982354	2.07E 07	Stc1
ENSMUSG00000050105	3.424603487	2.54E 07	Grrp1
ENSMUSG00000039497	2.830522244	2.77E 07	Dse
ENSMUSG00000045679	2.159394815	2.77E 07	Pq c3
ENSMUSG00000073599	2.873221168	3.04E 07	Ecscr
ENSMUSG00000060802	1.714171003	3.61E 07	B2m
ENSMUSG00000052234	2.741831376	4.14E 07	Epx
ENSMUSG00000022240	2.736699814	5.67E 07	Ctnnd2
ENSMUSG00000040957	2.500027634	6.53E 07	Cab es1
ENSMUSG00000037321	1.576347758	6.53E 07	Tap1
ENSMUSG00000030559	2.564362217	7.78E 07	Rab38
ENSMUSG00000025375	2.775890341	9.05E 07	Aatk
ENSMUSG00000056071	7.748328823	9.05E 07	S100a9
ENSMUSG00000020644	3.063200317	9.41E 07	Id2
ENSMUSG00000056749	2.375293813	1.12E 06	Nf 3
ENSMUSG00000078606	1.485922908	1.17E 06	Gm4070
ENSMUSG00000046916	2.433548116	1.23E 06	Myct1
ENSMUSG00000042700	1.667431327	1.23E 06	S pa1 1
ENSMUSG00000036155	1.904065229	1.25E 06	Mgat5
ENSMUSG00000029530	2.41230358	1.73E 06	Ccr9
ENSMUSG00000018819	1.819448753	2.59E 06	Lsp1
ENSMUSG00000043336	1.958384845	2.59E 06	F p1
ENSMUSG00000019564	2.186565146	2.61E 06	Ar d3a
ENSMUSG00000072601	7.273712872	2.61E 06	Ear1
ENSMUSG00000020077	1.817698451	2.68E 06	Srgn
ENSMUSG00000038648	1.844706942	2.73E 06	Creb3 2
ENSMUSG00000044220	2.279468529	3.09E 06	Nkx2 3
ENSMUSG00000001173	1.565088511	3.66E 06	Ocr
ENSMUSG00000032698	1.598124622	3.81E 06	Lmo2
ENSMUSG00000027199	2.980045	4.98E 06	Gatm
ENSMUSG00000031097	2.791267937	5.16E 06	Tnn 2
ENSMUSG00000051934	3.223498416	5.96E 06	Spats2
ENSMUSG00000046711	1.997024362	6.34E 06	Hmga1
ENSMUSG00000019768	2.56656866	6.46E 06	Esr1
ENSMUSG00000038357	5.245884741	7.02E 06	Camp
ENSMUSG00000025094	2.079997232	7.02E 06	S c18a2
ENSMUSG00000025887	4.002566039	7.03E 06	Casp12
ENSMUSG00000024339	2.021948881	7.99E 06	Tap2
ENSMUSG00000031822	1.328329844	8.98E 06	Gse1

ENSMUSG00000027201	1.475151392	9.57E 06	Myef2
ENSMUSG00000038894	3.026949792	9.64E 06	Irs2
ENSMUSG00000018008	1.400120057	9.71E 06	Cyth4
ENSMUSG00000047945	1.72610153	1.07E 05	Marcks 1
ENSMUSG00000045868	1.872412311	1.24E 05	Gv n1
ENSMUSG00000004612	2.753099919	1.41E 05	Nkg7
ENSMUSG00000024533	2.072174348	1.41E 05	Sp re1
ENSMUSG00000028859	1.471385955	1.53E 05	Csf3r
ENSMUSG00000005125	1.841358782	1.59E 05	Ndrg1
ENSMUSG00000023034	5.093595666	1.74E 05	Nr4a1
ENSMUSG00000017144	2.382775945	1.76E 05	Rnd3
ENSMUSG00000007872	3.212318054	1.99E 05	Id3
ENSMUSG00000070576	2.313349444	2.06E 05	Mn1
ENSMUSG00000023951	2.494488958	2.32E 05	Vegfa
ENSMUSG00000030657	1.818612803	2.51E 05	Xy t1
ENSMUSG00000026893	2.939122225	2.56E 05	Gca
ENSMUSG00000061665	1.35814136	2.86E 05	Cd2ap
ENSMUSG00000056116	2.115679771	2.96E 05	H2 T22
ENSMUSG00000033581	2.160631467	3.44E 05	Igf2bp2
ENSMUSG00000030847	2.449026596	3.88E 05	Bag3
ENSMUSG00000016239	2.289542238	4.42E 05	Lonrf3
ENSMUSG00000018474	1.407389794	4.44E 05	Chd3
ENSMUSG00000034612	1.670983001	4.89E 05	Chst11
ENSMUSG00000059336	1.939827424	4.96E 05	S c14a1
ENSMUSG00000042042	1.820551116	4.97E 05	Csga nact2
ENSMUSG00000044037	2.235068031	5.20E 05	A s2c
ENSMUSG00000003206	1.872213701	5.38E 05	Eb 3
ENSMUSG00000051124	1.536865753	5.38E 05	G map9
ENSMUSG00000069662	1.720710547	5.38E 05	Marcks
ENSMUSG00000047821	2.296187898	5.38E 05	Tr m16
ENSMUSG00000038712	1.652169083	6.16E 05	M ndy1
ENSMUSG00000031266	1.9870316	6.26E 05	G a
ENSMUSG00000037966	1.792526287	6.36E 05	N nj1
ENSMUSG00000042289	1.837147271	6.97E 05	Hsd3b7
ENSMUSG00000049804	1.432957895	7.12E 05	Armcx4
ENSMUSG00000059994	2.866055184	7.12E 05	Fcr 1
ENSMUSG00000035356	2.012077491	7.13E 05	Nfkb z
ENSMUSG00000020227	2.364271066	7.17E 05	Irak3
ENSMUSG00000069045	3.89504276	7.72E 05	Ddx3y
ENSMUSG00000028341	3.303781803	7.72E 05	Nr4a3
ENSMUSG00000042745	2.941862538	8.06E 05	Id1
ENSMUSG00000040809	3.810750221	8.55E 05	Ch 3
ENSMUSG00000024610	2.35167414	9.41E 05	Cd74
ENSMUSG00000063171	2.347573775	9.42E 05	Rps4
ENSMUSG00000027381	2.209889372	0.00010504	Bc 2 11
ENSMUSG00000019889	1.797665248	0.00010852	Ptprk
ENSMUSG00000055053	1.513076017	0.00011104	Nf c
ENSMUSG00000021215	1.335736882	0.00011618	Net1
ENSMUSG00000050953	2.017475978	0.00014499	G a1
ENSMUSG00000021846	1.669962373	0.00015755	Pe 2
ENSMUSG00000024968	1.718146791	0.00015803	Rcor2
ENSMUSG00000016024	1.479398732	0.00015989	Lbp
ENSMUSG00000029093	2.419512751	0.00016478	Sorcs2
ENSMUSG00000062148	4.771065821	0.00017261	Ear7
ENSMUSG00000073421	2.362826313	0.00019112	H2 Ab1
ENSMUSG00000043263	1.877871671	0.00019638	If 209
ENSMUSG00000027514	2.792858839	0.00019937	Zbp1
ENSMUSG00000025880	1.744811022	0.00020222	Smad7
ENSMUSG00000030157	1.357537428	0.00020259	C ec2d
ENSMUSG00000015312	3.985792296	0.00021487	Gadd45b
ENSMUSG00000031431	1.499305735	0.00022366	Tsc22d3
ENSMUSG00000052776	1.720932973	0.0002315	Oas1a
ENSMUSG00000058624	2.863422725	0.00023592	Gda
ENSMUSG00000033355	1.793835532	0.00023592	Rtp4
ENSMUSG00000052914	3.298658863	0.00026463	Cyp2j6
ENSMUSG00000003452	2.420498229	0.00027838	B cd1
ENSMUSG00000026580	2.497795436	0.00029317	Se p

ENSMUSG00000028037	2.582591691	0.00030663	If 44
ENSMUSG00000032231	2.557025791	0.00031042	Anxa2
ENSMUSG00000032496	2.904645894	0.00031042	Ltf
ENSMUSG00000020120	1.831216732	0.00032099	P ek
ENSMUSG00000047394	3.04279858	0.00032481	Odf3b
ENSMUSG00000028551	2.55187503	0.00033567	Cdkn2c
ENSMUSG00000029596	3.897307392	0.00037681	Sds
ENSMUSG00000067235	2.106766129	0.00038858	H2 Q10
ENSMUSG00000064023	1.486759906	0.00038858	K k8
ENSMUSG00000020323	3.473731633	0.00038858	Prss57
ENSMUSG00000061186	1.879355515	0.00038858	Sfmbt2
ENSMUSG00000025203	1.458351689	0.00043303	Scd2
ENSMUSG00000040681	1.887340657	0.00043712	Hmgn1
ENSMUSG00000029798	1.38570757	0.00044766	Herc6
ENSMUSG00000015224	2.245695997	0.00048279	Cyp2j9
ENSMUSG00000036478	1.721740478	0.00049149	Btg1
ENSMUSG00000036944	2.581288899	0.00052033	Tmem71
ENSMUSG00000031239	2.535703023	0.00052663	Itm2a
ENSMUSG00000032484	6.034200756	0.00053158	Ngp
ENSMUSG00000047844	2.860251497	0.00053774	Bex4
ENSMUSG00000041773	1.68307215	0.00054711	Enc1
ENSMUSG00000028464	1.992282504	0.00058104	Tpm2
ENSMUSG00000026482	1.327618682	0.00060803	Rg 1
ENSMUSG00000053113	2.011089511	0.00067809	Socs3
ENSMUSG00000024665	1.546483494	0.00070416	Fads2
ENSMUSG00000020272	1.290851049	0.00070416	Stk10
ENSMUSG00000087141	2.165361929	0.00071489	P cxd2
ENSMUSG00000054404	1.689697874	0.00071612	S fn5
ENSMUSG00000047959	1.36782188	0.00072342	Kcna3
ENSMUSG00000055541	2.338926875	0.00073215	La r1
ENSMUSG00000057596	1.733715738	0.00073872	Tr m30d
ENSMUSG00000032803	1.486770658	0.00080726	Cdv3
ENSMUSG00000041431	1.307993713	0.00081422	Ccnb1
ENSMUSG00000063605	1.618691346	0.00081908	Ccdc102a
ENSMUSG00000040548	1.149594722	0.00082801	Tex2
ENSMUSG00000024424	2.571540832	0.00082801	Ttc39c
ENSMUSG00000037012	1.029953161	0.00086417	Hk1
ENSMUSG00000039055	1.553720702	0.00087604	Eme1
ENSMUSG00000054641	1.654255904	0.00090291	Mmrn1
ENSMUSG00000018362	1.560884989	0.00097839	Kpna2
ENSMUSG00000069633	1.359775897	0.00098613	Pex11g
ENSMUSG00000023495	1.798995297	0.00101928	Pcbp4
ENSMUSG00000039304	1.739185444	0.0010207	Tnfsf10
ENSMUSG00000005774	1.455721392	0.00102912	Rfx5
ENSMUSG00000026737	1.405902554	0.0010355	P p4k2a
ENSMUSG00000032690	2.022594445	0.00105944	Oas2
ENSMUSG00000038058	2.63534993	0.0010802	Nod1
ENSMUSG00000004328	2.031861134	0.00111998	H f3a
ENSMUSG00000072082	1.319472747	0.00112655	Ccnf
ENSMUSG00000005580	1.65494841	0.00113708	Adcy9
ENSMUSG00000024867	2.072013751	0.001141	P p5k1b
ENSMUSG00000002957	1.159950245	0.00120063	Ap2a2
ENSMUSG00000030921	1.24974147	0.00121505	Tr m30a
ENSMUSG00000032965	1.208382318	0.00122184	Ift57
ENSMUSG00000006398	1.261086801	0.00122874	Cdc20
ENSMUSG00000030671	1.382371318	0.00122874	Pde3b
ENSMUSG00000020732	1.467874465	0.00123261	Rab37
ENSMUSG00000030287	1.671301267	0.00123599	Itpr2
ENSMUSG00000027082	1.471908495	0.00127653	Tfp
ENSMUSG00000064215	1.696945669	0.00128317	If 27
ENSMUSG00000025498	1.656013382	0.00129177	Irf7
ENSMUSG00000040997	1.520972967	0.00132553	Abhd4
ENSMUSG00000056888	1.277234623	0.00136385	G pr1
ENSMUSG00000027009	1.079145777	0.00136822	Itga4
ENSMUSG00000062991	4.399543565	0.00137929	Nrg1
ENSMUSG00000031799	1.629387822	0.00140776	Tpm4
ENSMUSG00000029705	1.292721634	0.00145818	Cux1

ENSMUSG00000064262	1.646798566	0.00146213	G map8
ENSMUSG00000000168	1.436401665	0.00151917	D at
ENSMUSG00000032936	2.650856557	0.00154477	Camkv
ENSMUSG00000074682	1.944235654	0.00155312	Zcchc3
ENSMUSG00000036611	2.172770333	0.00157212	Eepd1
ENSMUSG00000028159	1.248612147	0.00157407	Dapp1
ENSMUSG00000021281	2.631741843	0.00158103	Tnfa p2
ENSMUSG00000046223	1.805757507	0.00165697	P aur
ENSMUSG00000037731	1.631539132	0.00165697	Them s2
ENSMUSG00000004044	2.589659191	0.0016745	Cav n1
ENSMUSG00000033107	2.084451312	0.0016745	Rnf125
ENSMUSG00000025980	1.382242215	0.00168091	Hspd1
ENSMUSG00000022607	1.685938129	0.00172893	Ptk2
ENSMUSG00000026980	1.926400413	0.00176547	Ly75
ENSMUSG00000034462	1.538551168	0.00176547	Pkd2
ENSMUSG00000019699	1.077227189	0.00182159	Akt3
ENSMUSG00000000290	1.27655598	0.00182159	Itgb2
ENSMUSG00000071203	1.226582445	0.00188423	Na p5
ENSMUSG00000034614	1.609031272	0.00193918	P k3 p1
ENSMUSG00000026458	1.466091602	0.0020789	Ppf a4
ENSMUSG00000028970	1.166738406	0.00209796	Abcb1b
ENSMUSG00000008845	2.53305754	0.00222291	Cd163
ENSMUSG00000060131	1.875027968	0.00222528	Atp8b4
ENSMUSG00000079523	1.263132263	0.00229854	Tmsb10
ENSMUSG00000036863	1.592884074	0.00233941	Syde2
ENSMUSG00000021065	1.137577143	0.00234129	Fut8
ENSMUSG00000000078	2.041534808	0.00235094	K f6
ENSMUSG00000028035	1.707668637	0.00239201	Dna b4
ENSMUSG00000003779	1.331379511	0.00239201	K f20a
ENSMUSG00000046658	1.510146602	0.00246227	Zfp316
ENSMUSG00000030867	1.564143959	0.00251245	P k1
ENSMUSG00000042726	1.252268697	0.00252728	Trafd1
ENSMUSG00000029925	1.698782393	0.00253568	Tbxas1
ENSMUSG00000033952	1.06173199	0.00261634	Aspm
ENSMUSG00000022309	1.476302248	0.00270613	Angpt1
ENSMUSG00000024353	2.693615156	0.00271592	Mzb1
ENSMUSG00000075010	3.095214585	0.00284507	AW112010
ENSMUSG00000043991	1.113204784	0.00287692	Pura
ENSMUSG00000026034	1.155800489	0.00288522	C k1
ENSMUSG00000001270	2.063352142	0.00291514	Ckb
ENSMUSG00000063564	3.336013879	0.00292947	Co 23a1
ENSMUSG00000030045	1.658194325	0.00299051	Mrp 19
ENSMUSG00000025195	1.329514541	0.00307466	Dnmbp
ENSMUSG00000036526	1.6111188	0.00322416	Card11
ENSMUSG00000039976	1.339793827	0.00330971	Tbc1d16
ENSMUSG00000035513	1.92324159	0.00331278	Ntng2
ENSMUSG00000038545	1.080728153	0.00337081	Cu 7
ENSMUSG00000052534	1.395572391	0.00337081	Pbx1
ENSMUSG00000038349	3.003205543	0.00339975	P c 1
ENSMUSG00000042097	1.99345701	0.00349012	Zfp239
ENSMUSG00000005609	1.086642439	0.00353328	Ctr9
ENSMUSG00000056515	1.437187812	0.00353328	Rab31
ENSMUSG00000036553	1.707425976	0.00353328	Sh3tc1
ENSMUSG00000036402	1.673231659	0.00357528	Gng12
ENSMUSG00000005057	1.457580041	0.00358563	Sh2b2
ENSMUSG00000015702	2.061509049	0.00362056	Anxa9
ENSMUSG00000040152	5.182027138	0.00362056	Thbs1
ENSMUSG00000025932	1.538655191	0.00363528	Eya1
ENSMUSG00000026104	1.14663502	0.00363528	Stat1
ENSMUSG00000074480	1.11774641	0.00378819	Mex3a
ENSMUSG00000037902	1.050182458	0.0038396	S rpa
ENSMUSG00000029185	2.130264766	0.00386804	Fam114a1
ENSMUSG00000070327	0.958498547	0.0038817	Rnf213
ENSMUSG00000049916	1.472028969	0.00390185	2610318N02R k
ENSMUSG00000060913	2.48777942	0.00404212	Tr m55
ENSMUSG00000040907	1.53391124	0.00422983	Atp1a3
ENSMUSG00000036334	1.749551922	0.00423112	Igsf10

ENSMUSG00000030142	1.743583244	0.0042502	C ec4e
ENSMUSG00000063458	2.416891778	0.00433606	Lrmda
ENSMUSG00000014905	1.65315032	0.00436892	Dnajb9
ENSMUSG00000001403	1.346657118	0.0044257	Ube2c
ENSMUSG00000000915	1.170625905	0.00460623	H p1r
ENSMUSG00000073079	1.802079557	0.00474661	Srp54a
ENSMUSG00000003746	1.197888916	0.0049024	Man1a
ENSMUSG00000028268	1.544487065	0.00492866	Gbp3
ENSMUSG00000022564	1.544733229	0.00493549	Gr na
ENSMUSG00000030283	1.231239852	0.00497335	St8s a1
ENSMUSG00000022108	1.086359916	0.00506464	Itm2b
ENSMUSG00000032577	1.3295776	0.00512772	Mapkapk3
ENSMUSG00000022091	1.531620402	0.00523053	Sorbs3
ENSMUSG00000023805	1.486707479	0.00523053	Synj2
ENSMUSG00000024921	1.070597112	0.00534626	Smarca2
ENSMUSG00000039286	1.487707013	0.0053991	Fndc3b
ENSMUSG00000029298	2.320999129	0.0054004	Gbp9
ENSMUSG00000034674	1.193329741	0.0054004	Tdg
ENSMUSG00000079547	1.92547091	0.00544708	H2 DMb1
ENSMUSG00000059921	1.528474639	0.00579907	Unc5c
ENSMUSG00000044068	1.373285905	0.00579907	Zrsr1
ENSMUSG00000051727	1.807595726	0.00582491	Kctd14
ENSMUSG00000033880	1.381493747	0.00582988	Lga s3bp
ENSMUSG00000027750	2.344942935	0.00582988	Postn
ENSMUSG00000027219	1.479202488	0.00582988	S c28a2
ENSMUSG00000017132	1.528127753	0.00590323	Cyth1
ENSMUSG00000020798	1.120114829	0.00591006	Spns3
ENSMUSG00000031997	2.661897677	0.00591006	Trpc6
ENSMUSG00000041488	1.605341088	0.00595096	Stx3
ENSMUSG00000045328	1.14436025	0.0061536	Cenpe
ENSMUSG00000026833	2.275499952	0.0061536	O fm1
ENSMUSG00000024975	1.527811878	0.0061536	Pdcd4
ENSMUSG00000038375	1.956628213	0.0061536	Trp53 np2
ENSMUSG00000020661	0.875587893	0.00626945	Dnmt3a
ENSMUSG00000040128	1.171043295	0.0065542	Pnrc1
ENSMUSG00000033470	3.638802475	0.00679252	Cys tr2
ENSMUSG00000059708	1.526481125	0.0069338	Akap17b
ENSMUSG00000031562	0.980929656	0.00696356	Dctd
ENSMUSG00000040264	1.463707294	0.00713731	Gbp2b
ENSMUSG00000040537	2.420962568	0.00715489	Adam22
ENSMUSG00000090113	3.155299123	0.00727767	Nh rc4
ENSMUSG00000035329	1.545436048	0.00743546	Fbxo33
ENSMUSG00000038677	1.711542321	0.00745869	Scube3
ENSMUSG00000020777	1.201985948	0.00746486	Acox1
ENSMUSG00000028034	0.918910813	0.00746486	Fubp1
ENSMUSG00000031613	2.428631463	0.00746486	Hpgd
ENSMUSG00000062098	1.286256892	0.007479	Btbd3
ENSMUSG00000022175	1.107121523	0.007479	Lrp10
ENSMUSG00000051910	2.197065786	0.00757411	Sox6
ENSMUSG00000028270	1.441280198	0.00764164	Gbp2
ENSMUSG00000003541	1.800089821	0.00792235	Ier3
ENSMUSG00000038507	1.607500512	0.00797413	Parp12
ENSMUSG00000090015	2.925260707	0.00797847	Gm15446
ENSMUSG00000075602	2.068741423	0.00798587	Ly6a
ENSMUSG00000032661	1.588669023	0.00798587	Oas3
ENSMUSG00000026509	1.221500247	0.00803936	Capn2
ENSMUSG00000001156	1.35261648	0.00828686	Mxd1
ENSMUSG00000019790	1.215683638	0.00835783	Stxbp5
ENSMUSG00000024659	1.342438464	0.0083772	Anxa1
ENSMUSG00000022102	1.293818211	0.00870416	Dok2
ENSMUSG00000026478	1.304302932	0.00874835	Lamc1
ENSMUSG00000022883	1.956113467	0.00875164	Robo1
ENSMUSG00000026360	1.488846797	0.00875905	Rgs2
ENSMUSG00000059326	1.239555685	0.00884117	Csf2ra
ENSMUSG00000041912	1.517334402	0.00884117	Tdrkh
ENSMUSG00000020592	1.438507652	0.00888881	Sdc1
ENSMUSG00000040549	1.068942953	0.00899791	Ckap5

ENSMUSG00000020492	1.417525862	0.00930732	Ska2
ENSMUSG00000060586	2.4555391	0.00950215	H2 Eb1
ENSMUSG00000024007	1.112019861	0.00950215	Pp 1
ENSMUSG00000046402	1.513921999	0.00950215	Rbp1
ENSMUSG00000019856	1.430218325	0.0095076	Fam184a
ENSMUSG00000041632	1.280321301	0.00953506	Mrps27
ENSMUSG00000036330	1.814401064	0.00955818	S c18a1
ENSMUSG00000024462	1.872219433	0.00958243	Gabbr1
ENSMUSG00000051457	1.119538257	0.00958243	Spn
ENSMUSG00000038070	1.106510518	0.00963191	Cnt n
ENSMUSG00000084883	2.484052865	0.00966062	Ccdc85c
ENSMUSG00000029387	1.19465835	0.00966062	Gtf2h3
ENSMUSG00000021360	1.39320221	0.00989824	Gcnt2
ENSMUSG00000022748	1.605988563	0.00996208	Cmss1
ENSMUSG00000034926	1.322115433	0.00996208	Dhcr24
ENSMUSG00000041538	1.725969461	0.01022165	H2 Ob
ENSMUSG00000020189	1.071094072	0.01022165	Osbp 8
ENSMUSG00000054619	1.239612712	0.01037428	Mett 7a1
ENSMUSG00000032177	1.202014204	0.01039076	Pde4a
ENSMUSG00000032733	1.458179754	0.01045154	Snx33
ENSMUSG00000018427	2.184139353	0.01051476	Ype 2
ENSMUSG00000035365	1.158525125	0.01070883	Parpbp
ENSMUSG00000044456	1.182422057	0.01070883	R n3
ENSMUSG00000036622	0.982206871	0.01075287	Atp13a2
ENSMUSG00000028525	1.207710226	0.01095425	Pde4b
ENSMUSG00000005417	0.841316353	0.01099048	Mpr p
ENSMUSG00000027405	1.034401549	0.01112348	Nop56
ENSMUSG00000027298	2.29307377	0.01112348	Tyro3
ENSMUSG00000025876	1.919731511	0.01112348	Unc5a
ENSMUSG00000048497	1.274804164	0.01125544	Mmgt2
ENSMUSG00000026605	0.882782563	0.01150905	Cenpf
ENSMUSG00000029708	1.293028931	0.01163928	Gcc1
ENSMUSG00000026473	1.327549025	0.01163928	G u
ENSMUSG00000030677	1.064256081	0.01163928	K f22
ENSMUSG00000021823	1.020434589	0.01163928	Vc
ENSMUSG00000028040	2.527177607	0.01165177	Efna4
ENSMUSG00000034171	1.299862935	0.01165177	Faah
ENSMUSG00000040945	1.136706007	0.01165177	Rcc2
ENSMUSG00000063884	1.093258365	0.01186433	Ptcd3
ENSMUSG00000053007	2.27702297	0.0122337	Creb5
ENSMUSG00000067206	3.594635401	0.0122337	Lrrc66
ENSMUSG00000066258	1.138535511	0.0122337	Tr m12a
ENSMUSG00000030707	1.014769939	0.01246385	Coro1a
ENSMUSG00000041268	1.213916943	0.01273294	Dmx 2
ENSMUSG00000026014	1.435389864	0.01273294	Raph1
ENSMUSG00000026986	2.366784193	0.01274676	Hnmt
ENSMUSG00000026003	1.138909407	0.01290196	Acad
ENSMUSG00000031441	1.659272099	0.01292951	Atp11a
ENSMUSG00000005667	1.465342883	0.01292951	Mthfd2
ENSMUSG00000005803	1.838299715	0.01292951	Sqor
ENSMUSG00000001482	0.994008405	0.01311631	Def8
ENSMUSG00000016552	1.10088401	0.01316463	Foxred2
ENSMUSG00000020737	1.161287825	0.01316463	Jpt1
ENSMUSG00000066456	1.541263828	0.0133492	Hmgn3
ENSMUSG00000040183	1.229739727	0.01339881	Ankrd6
ENSMUSG00000020454	0.976896303	0.01340277	E f4en f1
ENSMUSG00000044162	2.550371419	0.01351643	Tn p3
ENSMUSG00000031984	1.057963089	0.01356482	2810004N23R k
ENSMUSG00000020647	1.13322137	0.01357768	Ncoa1
ENSMUSG00000024109	1.51724315	0.01374528	Nrxn1
ENSMUSG00000036067	2.057915505	0.01399404	S c2a6
ENSMUSG00000020935	1.12428131	0.0140674	Dcakd
ENSMUSG00000014980	1.213833902	0.01429499	Tsen15
ENSMUSG00000038587	1.808367821	0.01457385	Akap12
ENSMUSG00000021213	2.02983537	0.01461761	Akr1c13
ENSMUSG00000044258	1.275180645	0.01461761	Ct a2a
ENSMUSG00000056091	1.347417043	0.01461761	St3ga 5

ENSMUSG00000011148	1.492266566	0.01463547	Adss 1
ENSMUSG00000023927	1.011806248	0.0148257	Satb1
ENSMUSG00000007659	1.252433103	0.01495668	Bc 2 1
ENSMUSG00000022265	1.321521527	0.01526976	Ank
ENSMUSG00000026582	2.871825761	0.01539362	Se e
ENSMUSG00000022237	2.938153396	0.01551794	Ankrd33b
ENSMUSG00000036356	1.974731751	0.01551794	Csga nact1
ENSMUSG00000052040	1.112918361	0.01551794	K f13
ENSMUSG00000036432	1.519467573	0.01551794	S ah2
ENSMUSG00000037921	1.562650514	0.01552688	Ddx60
ENSMUSG00000020921	1.467422852	0.01556506	Tmem101
ENSMUSG00000027496	1.322492527	0.0155742	Aurka
ENSMUSG00000069516	1.507005659	0.01570657	Lyz2
ENSMUSG00000052160	1.844456605	0.01581657	P d4
ENSMUSG00000028678	0.947333956	0.0162211	K f2c
ENSMUSG00000042249	1.054014256	0.01626963	Grk3
ENSMUSG00000033900	1.810021453	0.01626963	Map9
ENSMUSG00000057113	1.180717897	0.01626963	Npm1
ENSMUSG00000052212	2.64255297	0.0165181	Cd177
ENSMUSG00000024664	1.462131224	0.0166298	Fads3
ENSMUSG00000030612	1.408006028	0.0166298	Mrp 46
ENSMUSG00000063229	1.278607353	0.01667308	Ldha
ENSMUSG00000090394	1.473242267	0.01680359	4930523C07R k
ENSMUSG00000035208	1.055015211	0.01680949	S fn8
ENSMUSG00000051329	1.313725948	0.01681259	Nup160
ENSMUSG00000056666	1.396246762	0.01681259	Retsat
ENSMUSG00000018654	0.967714378	0.01698564	Ikzf1
ENSMUSG00000012519	1.191187403	0.01712543	M k
ENSMUSG00000038510	1.340849845	0.01712543	Rpf2
ENSMUSG00000076441	1.264290371	0.01727991	Ass1
ENSMUSG00000014226	1.291021298	0.01734601	Cacybp
ENSMUSG00000026826	2.127380299	0.01742873	Nr4a2
ENSMUSG00000028173	1.247397118	0.01742873	W s
ENSMUSG00000055782	1.865726661	0.01764328	Abcd2
ENSMUSG00000021318	2.106084699	0.01778896	G 3
ENSMUSG00000022899	2.029223777	0.01778896	S c15a2
ENSMUSG00000058755	2.25466646	0.01800401	Osm
ENSMUSG00000059900	1.654510704	0.01801158	Tmem40
ENSMUSG00000053080	1.475763823	0.01813196	2700081O15R k
ENSMUSG00000034903	1.161680468	0.01813196	Cob 1
ENSMUSG00000026923	1.264333493	0.01813196	Notch1
ENSMUSG00000017639	1.335867135	0.01821369	Rab11f p4
ENSMUSG00000051223	1.075400631	0.01824251	Bzw1
ENSMUSG00000022575	0.964972726	0.01827143	Gsdmd
ENSMUSG00000076437	1.393146387	0.01827143	Se enoh
ENSMUSG00000029014	1.154978873	0.01837463	Dnajc2
ENSMUSG00000020307	1.385822906	0.01844855	Cdc34
ENSMUSG00000003031	1.219817689	0.01877851	Cdkn1b
ENSMUSG00000023456	1.118546651	0.01877851	Tp 1
ENSMUSG00000023032	1.83356162	0.01896685	S c4a8
ENSMUSG00000032549	2.145034035	0.01927961	Rab6b
ENSMUSG00000041707	2.108715779	0.01930413	1810011H11R k
ENSMUSG00000029859	1.820663277	0.01941162	Epha1
ENSMUSG00000038612	1.133923219	0.01941162	Mc 1
ENSMUSG00000025986	1.049282319	0.01941162	S c39a10
ENSMUSG00000042524	0.940098221	0.01941162	Sun2
ENSMUSG00000024359	1.036117551	0.01948531	Hspa9
ENSMUSG00000032254	0.886126151	0.01948531	K f23
ENSMUSG00000067212	1.046833577	0.0195938	H2 T23
ENSMUSG00000040274	1.008690896	0.02017328	Cdk6
ENSMUSG00000079057	1.68508627	0.02017328	Cyp4v3
ENSMUSG00000026127	1.308835031	0.02017328	Imp4
ENSMUSG00000027227	1.00536357	0.02045816	Sord
ENSMUSG00000042351	1.509269979	0.02118792	Grap2
ENSMUSG00000037111	0.844233021	0.02129605	Setd7
ENSMUSG00000056054	5.400902529	0.02137179	S100a8
ENSMUSG00000030930	0.872067885	0.02176343	Chst15

ENSMUSG00000026672	1.668171075	0.02176343	Optn
ENSMUSG00000060860	1.166329665	0.02176343	Ube2s
ENSMUSG00000002984	1.036540404	0.02240772	Tomm40
ENSMUSG00000056018	1.031329556	0.02257923	Ccdc7b
ENSMUSG00000031129	1.196750127	0.02268272	S c9a9
ENSMUSG00000030400	0.897455043	0.02269993	Ercc2
ENSMUSG00000026121	1.531866313	0.02271419	Sema4c
ENSMUSG00000038331	1.593128462	0.02323979	Satb2
ENSMUSG00000009378	3.041443691	0.02327297	S c16a12
ENSMUSG00000042675	1.2006022	0.02327297	Ype 3
ENSMUSG00000023259	1.795023045	0.02329699	S c26a6
ENSMUSG00000051343	1.624334132	0.02360375	Rab11f p5
ENSMUSG00000034330	0.887350068	0.02360831	P cg2
ENSMUSG00000001435	1.391333925	0.02400427	Co 18a1
ENSMUSG00000004263	1.187289364	0.02420181	Atn1
ENSMUSG00000031502	1.349269083	0.0242738	Co 4a1
ENSMUSG00000062209	2.989215667	0.0242738	Erbb4
ENSMUSG00000052749	1.487435628	0.0242738	Tr m30b
ENSMUSG00000034427	1.433854501	0.02446798	Myo15b
ENSMUSG00000024208	1.086140722	0.0244719	Uqcc2
ENSMUSG00000028803	1.015640493	0.02510263	N pa 3
ENSMUSG00000060477	1.538044551	0.02522905	Irak2
ENSMUSG00000008450	1.23280065	0.02522905	Nutf2
ENSMUSG00000041390	1.860917002	0.02523114	Mdf c
ENSMUSG00000059248	0.923569507	0.02554656	Sept9
ENSMUSG00000025920	1.408737515	0.02554656	Stau2
ENSMUSG00000026832	1.258864728	0.02581408	Cyt p
ENSMUSG00000024308	1.048267299	0.02592775	Tapbp
ENSMUSG00000003134	1.139028218	0.02597101	Tbc1d8
ENSMUSG00000042082	1.129974817	0.02608116	Arsb
ENSMUSG00000060962	2.896188416	0.02618869	Dmkn
ENSMUSG00000037822	1.20858869	0.02622511	Sm m14
ENSMUSG00000068184	1.293588843	0.0266613	Ndufaf2
ENSMUSG00000030413	3.206970455	0.0266613	Pg yrp1
ENSMUSG00000048285	1.191684057	0.02667108	Frmd6
ENSMUSG00000020894	1.115550621	0.02684065	Vamp2
ENSMUSG00000040938	1.672971566	0.02703375	S c16a11
ENSMUSG00000060227	1.091732884	0.02713017	Casc4
ENSMUSG00000004609	1.309246725	0.02713017	Cd33
ENSMUSG00000026646	1.51897804	0.02713017	Suv39h2
ENSMUSG00000036533	1.330063573	0.02730923	Cdc42ep3
ENSMUSG00000068587	2.278256337	0.02730923	Mgam
ENSMUSG00000055717	1.337008383	0.02744897	S a n1
ENSMUSG00000016206	2.12836278	0.02748361	H2 M3
ENSMUSG00000020361	1.054593837	0.02748361	Hspa4
ENSMUSG00000011257	1.017751438	0.02748361	Pabpc4
ENSMUSG00000029623	1.197728841	0.02748361	Pdap1
ENSMUSG00000022391	1.036340948	0.02748361	Rangap1
ENSMUSG00000042677	1.594825247	0.02748361	Zc3h12a
ENSMUSG00000018666	0.967486864	0.02769886	Cbx1
ENSMUSG00000067586	1.8028337	0.02769886	S1pr3
ENSMUSG00000019850	1.901691271	0.02827087	Tnfa p3
ENSMUSG00000032849	1.251481485	0.02827934	Abcc4
ENSMUSG00000036504	1.187547006	0.02835075	Phpt1
ENSMUSG00000032624	0.994746349	0.02867123	Em 4
ENSMUSG00000009863	1.10778962	0.02887984	Sdhb
ENSMUSG00000038059	1.406193849	0.02887984	Sm m3
ENSMUSG00000035203	0.96564928	0.02927828	Epn1
ENSMUSG00000090019	1.084038187	0.02932674	G map1
ENSMUSG00000049047	1.031378088	0.02950346	Armcx3
ENSMUSG00000028292	1.260205311	0.02950346	Rars2
ENSMUSG00000020638	1.520775922	0.02966763	Cmpk2
ENSMUSG00000025665	2.129483969	0.02966763	Rps6ka6
ENSMUSG00000031827	1.034276887	0.02998579	Cot 1
ENSMUSG00000006390	1.103810968	0.02998579	E ov 1
ENSMUSG00000004698	1.362110109	0.02998579	Hdac9
ENSMUSG00000001240	1.909749503	0.02998579	Ramp2

ENSMUSG00000035960	1.216175915	0.03001012	Apex1
ENSMUSG00000057329	0.817710221	0.03006094	Bc 2
ENSMUSG00000063953	1.510985221	0.03032116	Amd2
ENSMUSG00000034957	1.468708565	0.03046894	Cebpa
ENSMUSG00000002265	1.52765487	0.03093598	Peg3
ENSMUSG00000013629	0.974580506	0.03132463	Cad
ENSMUSG00000025869	1.269546713	0.03140311	Nop16
ENSMUSG00000014932	2.164084537	0.03169311	Yes1
ENSMUSG00000072663	1.86674038	0.03188727	Spef2
ENSMUSG00000039167	0.877084697	0.03216441	Adgr 4
ENSMUSG00000029822	1.088978223	0.03222658	Osbp 3
ENSMUSG00000031821	1.187846685	0.03227299	G ns2
ENSMUSG00000020330	0.75347698	0.03243509	Hmmr
ENSMUSG00000042331	0.877861209	0.03247862	Specc1
ENSMUSG00000031337	1.185638312	0.03253296	Mtm1
ENSMUSG00000024588	1.09210122	0.03271192	Fech
ENSMUSG00000019194	3.03831198	0.03271192	Scn1b
ENSMUSG00000071653	1.221571502	0.03311998	1810009A15R k
ENSMUSG00000022508	1.607071545	0.03311998	Bc 6
ENSMUSG00000009575	1.032823074	0.03311998	Cbx5
ENSMUSG00000003545	4.179192216	0.03311998	Fosb
ENSMUSG00000029777	1.057247513	0.03311998	Gars
ENSMUSG00000006014	2.531320305	0.03311998	Prg4
ENSMUSG00000035000	1.569532593	0.03323275	Dpp4
ENSMUSG00000009013	1.226049376	0.03323275	Dyn 1
ENSMUSG00000053398	1.0273859	0.03323275	Phgdh
ENSMUSG00000071076	1.40984111	0.03325422	Jund
ENSMUSG00000034055	1.873380348	0.03325422	Phka1
ENSMUSG00000052751	0.944226244	0.03325422	Rep n1
ENSMUSG00000025962	1.374882856	0.03363945	Fastkd2
ENSMUSG00000074896	2.674327264	0.03363945	If t3
ENSMUSG00000039410	1.335093609	0.03363945	Prdm16
ENSMUSG00000052926	0.959073221	0.03381724	Rnaseh2a
ENSMUSG00000039081	2.174630267	0.03384209	Zfp503
ENSMUSG00000079363	2.15489895	0.03386271	Gbp4
ENSMUSG00000025776	3.732056727	0.03406521	Cr sp d1
ENSMUSG00000056612	1.131789915	0.03432166	Ppp1r14b
ENSMUSG00000031954	0.920295485	0.03458616	Cfdp1
ENSMUSG00000094626	2.015147798	0.03458616	Tmem121b
ENSMUSG00000031870	4.384534897	0.03476133	Pgr
ENSMUSG00000068742	0.977477666	0.03479395	Cry2
ENSMUSG00000057193	0.865983926	0.03479395	S c44a2
ENSMUSG00000052539	0.960851381	0.03493629	Mag 3
ENSMUSG00000061086	1.536228939	0.03502296	My 4
ENSMUSG00000006931	3.016245758	0.03502296	P3h4
ENSMUSG00000021217	1.897685769	0.03502296	Tshz3
ENSMUSG00000033585	2.84256567	0.0351192	Ndn
ENSMUSG00000034664	1.847824942	0.03518945	Itga2b
ENSMUSG00000009418	1.283942431	0.03528285	Nav1
ENSMUSG00000033257	0.868277471	0.03533169	Tt 4
ENSMUSG00000028849	1.086289105	0.03550935	Map7d1
ENSMUSG00000034438	2.047483228	0.03573667	Gbp8
ENSMUSG00000072596	2.446097822	0.03600904	Ear2
ENSMUSG00000000204	2.466961302	0.03623511	S fn4
ENSMUSG00000079017	1.939328187	0.03646321	If 27 2a
ENSMUSG00000025888	1.573258547	0.03653549	Casp1
ENSMUSG00000013089	1.481387853	0.03653549	Etv5
ENSMUSG00000040010	1.165256461	0.03653549	S c7a5
ENSMUSG00000046572	1.208077042	0.03653549	Zfp518b
ENSMUSG00000023089	1.198194305	0.03660884	Ndufa5
ENSMUSG00000018381	1.289084641	0.03666364	Ab 3
ENSMUSG00000003812	0.999082217	0.03684301	Dnase2a
ENSMUSG00000021009	1.188697685	0.03695233	Ptpn21
ENSMUSG00000056592	1.553482547	0.03695233	Zfp658
ENSMUSG00000016757	1.031606226	0.03723725	Tt 12
ENSMUSG00000028651	1.10552606	0.03758815	Pp e
ENSMUSG00000040463	1.00585743	0.03765097	Mybbp1a

ENSMUSG00000005583	0.971246795	0.0377308	Mef2c
ENSMUSG00000032216	0.757059093	0.0377308	Nedd4
ENSMUSG00000024480	1.747579447	0.0379734	Ap3s1
ENSMUSG00000028664	1.121870583	0.03830312	Ephb2
ENSMUSG00000027589	1.107335663	0.03830312	Pcmtd2
ENSMUSG00000048764	3.461885316	0.03830312	Tmprss11f
ENSMUSG00000011263	1.655138609	0.03859247	Exoc3 2
ENSMUSG00000021069	1.321024975	0.03859247	Pyg
ENSMUSG00000021256	1.491492195	0.03859247	Vash1
ENSMUSG00000029570	1.138213567	0.03908024	Lfng
ENSMUSG00000090100	1.488371877	0.03976087	Ttbk2
ENSMUSG00000009687	0.857965319	0.03982134	Fxyd5
ENSMUSG00000007617	1.106704863	0.03982134	Homer1
ENSMUSG00000060601	0.921859985	0.03982134	Nr1h2
ENSMUSG00000048546	1.01002164	0.03982134	Tob2
ENSMUSG00000027469	1.173116165	0.03982134	Tpx2
ENSMUSG00000040592	1.281237309	0.03984786	Cd79b
ENSMUSG00000035711	2.044344875	0.04001088	Dok3
ENSMUSG00000063904	0.989754065	0.04001088	Dpp3
ENSMUSG00000027364	1.580295362	0.04001088	Usp50
ENSMUSG00000033287	1.492444352	0.04007924	Kctd17
ENSMUSG00000028459	1.431511411	0.04010577	Cd72
ENSMUSG00000030830	0.84203817	0.04019769	Itga
ENSMUSG00000028455	1.096594653	0.04020303	Stom 2
ENSMUSG00000030319	0.931515148	0.04025189	Cand2
ENSMUSG00000015966	2.397286752	0.04025189	I 17rb
ENSMUSG00000021356	1.964610618	0.04025189	Irf4
ENSMUSG00000036768	0.886634595	0.04048463	K f15
ENSMUSG00000022436	0.894146409	0.04048463	Sh3bp1
ENSMUSG00000020167	0.74349892	0.04048463	Tcf3
ENSMUSG00000022015	2.169054846	0.04048463	Tnfsf11
ENSMUSG00000036902	1.229559736	0.04066079	Neto2
ENSMUSG00000032556	1.64859875	0.04085837	Bfsp2
ENSMUSG00000020261	1.210947169	0.04085837	S c36a1
ENSMUSG00000043279	0.818133485	0.04085837	Tr m56
ENSMUSG00000040084	1.038957697	0.04095059	Bub1b
ENSMUSG00000064037	0.908667376	0.0409813	Gpn1
ENSMUSG00000006378	1.489217605	0.04158195	Gcat
ENSMUSG00000038943	0.749630835	0.04158195	Prc1
ENSMUSG00000024235	1.604370441	0.04167402	Map3k8
ENSMUSG00000037795	0.828149086	0.04167402	N4bp2
ENSMUSG00000037490	3.12655474	0.04181952	S c2a12
ENSMUSG00000004661	1.119788497	0.04216028	Ar d3b
ENSMUSG00000028518	2.909333601	0.0423783	Prkaa2
ENSMUSG00000041115	1.280450108	0.04261412	Iqsec2
ENSMUSG00000029594	1.028847797	0.04262387	Rbm19
ENSMUSG00000026979	0.918055964	0.04271092	Psd4
ENSMUSG00000000184	0.959235352	0.04294505	Ccnd2
ENSMUSG00000061479	1.031511249	0.04298061	Snrpa
ENSMUSG00000024590	0.88598343	0.04300089	Lmnb1
ENSMUSG00000024217	1.004165892	0.04309871	Snrpc
ENSMUSG00000049191	1.480912268	0.04322465	Rt 5
ENSMUSG00000027843	1.002328205	0.04346908	Ptpn22
ENSMUSG00000063787	1.313015856	0.04354111	Chchd1
ENSMUSG00000006392	1.098663326	0.04356063	Med8
ENSMUSG00000070871	1.334048312	0.0447849	Ccny 1
ENSMUSG00000034413	1.421221557	0.04492309	Neur 1b
ENSMUSG00000000552	1.139020342	0.04511928	Zfp385a
ENSMUSG00000038085	0.857850007	0.04531323	Cnbd2
ENSMUSG00000079173	1.476471067	0.0453782	Zan
ENSMUSG00000024887	1.062188916	0.04586163	Asah2
ENSMUSG00000062007	1.656342796	0.04586163	Hsh2d
ENSMUSG00000017713	1.665629288	0.04586163	Tha1
ENSMUSG00000023832	1.311128544	0.04590485	Acat2
ENSMUSG00000037432	1.164373824	0.0459699	Fer1 5
ENSMUSG00000027712	1.080427125	0.04603132	Anxa5
ENSMUSG00000029790	1.455535861	0.04603132	Cep41

ENSMUSG00000031633	1.132611599	0.04618589	S c25a4
ENSMUSG00000040061	0.9188053	0.04629189	P cb2
ENSMUSG00000050914	2.483438947	0.04645238	Ankrd37
ENSMUSG00000024063	1.150705654	0.04645238	Lbh
ENSMUSG00000060427	1.255446493	0.04645238	Zfp868
ENSMUSG00000020290	1.031812055	0.04656379	Xpo1
ENSMUSG00000039217	2.172467654	0.04658134	I 18
ENSMUSG00000028124	1.175877543	0.0466752	Gc m
ENSMUSG00000023960	2.260639734	0.04706203	Enpp5
ENSMUSG00000030031	1.558519378	0.04711052	Kbtbd8
ENSMUSG00000028693	0.999665315	0.04733094	Nasp
ENSMUSG00000089669	2.915653023	0.04747579	Tnfsf13
ENSMUSG00000037940	1.451809538	0.04782985	Inpp4b
ENSMUSG00000047592	1.692740753	0.04789106	Nxpe5
ENSMUSG00000019139	1.034246269	0.04823667	Isyna1
ENSMUSG00000020160	0.969009473	0.04830186	Me s1
ENSMUSG00000022270	0.975199613	0.04830241	Retreg1
ENSMUSG00000067071	1.102346786	0.0485858	Hes6
ENSMUSG00000028882	0.922408637	0.04860666	Ppp1r8
ENSMUSG00000036106	0.995056666	0.04886507	Prr5
ENSMUSG00000038535	1.177216906	0.04895286	Zfp280d
ENSMUSG00000046598	1.256594041	0.04940525	Bdh1
ENSMUSG00000040236	0.853920286	0.04940525	Trappc5
ENSMUSG00000039693	1.563411116	0.04981489	Msantd3
ENSMUSG00000021990	0.861202059	0.04993034	Spata13

10.2 Appendix 2

List of genes differentially expressed between murine foetal liver Mll-AF4 expressing and control LMPPs (positive log fold represents genes upregulated in control LMPPs), described in chapter 3.

Ensemb ID	og2 Fo d Change	padj	Gene Name
ENSMUSG00000026185	3.738711553	3.39E 05	Igfbp5
ENSMUSG00000028842	2.454889876	8.27E 05	Ago3
ENSMUSG00000029108	1.778396401	0.00053864	Pcdh7
ENSMUSG00000054074	2.929767218	0.00075377	Sk da1
ENSMUSG00000040434	4.718079818	0.00099866	Large2
ENSMUSG00000029640	1.610432546	0.00099866	Usp12
ENSMUSG00000042129	1.746862471	0.00099866	Rassf4
ENSMUSG00000026826	4.287646289	0.00099866	Nr4a2
ENSMUSG00000026009	4.830723256	0.00175573	Icos
ENSMUSG00000044768	2.056149289	0.00177908	D1Ertd622e
ENSMUSG00000071516	1.404147396	0.00203439	H st1h2a
ENSMUSG00000020303	4.641900197	0.0023237	Stc2
ENSMUSG00000044645	8.647851666	0.00396915	Gm7334
ENSMUSG00000026921	1.293103057	0.00415524	Egf 7
ENSMUSG00000049539	1.317109491	0.00432333	H st1h1a
ENSMUSG00000026792	2.414244101	0.00525646	Lrsam1
ENSMUSG00000068855	1.444836166	0.00525646	H st2h2ac
ENSMUSG00000078249	8.249162763	0.005775	Hmga1b
ENSMUSG00000021911	1.28203562	0.00638099	Parg
ENSMUSG00000004837	2.763341622	0.00845366	Grap
ENSMUSG00000017950	1.885020047	0.00845366	Hnf4a
ENSMUSG00000024501	7.541278071	0.01134386	Dpys 3
ENSMUSG00000028339	5.733546995	0.01333867	Co 15a1
ENSMUSG00000008682	1.115329378	0.01333867	Rp 10
ENSMUSG00000049624	2.567986944	0.01614021	S c17a5
ENSMUSG00000043986	7.346866141	0.01710793	Spata31d1d
ENSMUSG00000020053	2.347073059	0.0204358	Igf1
ENSMUSG00000042770	3.338144188	0.02118367	Hebp1
ENSMUSG00000036040	4.430949292	0.02168957	Adamts 2
ENSMUSG00000079157	4.66347091	0.02481842	Fam155a
ENSMUSG00000032702	7.382998029	0.02702348	Kank1
ENSMUSG00000027750	2.104274853	0.02702348	Postn
ENSMUSG00000022623	1.375368005	0.02702348	Shank3
ENSMUSG00000005611	1.652032709	0.02905611	Mrv 1
ENSMUSG00000045636	2.283523963	0.02905611	Mtus1
ENSMUSG00000027447	1.244535804	0.03214762	Cst3
ENSMUSG00000023341	3.029450771	0.03817316	Mx2
ENSMUSG00000068263	1.89122449	0.03817316	Efcc1
ENSMUSG00000031871	3.168228447	0.04641966	Cdh5

10.3 Appendix 3

List of genes differentially expressed between human foetal liver and cord blood derived HSC/MPPs (positive log fold represents genes upregulated in the foetal liver derived HSC/MPPs), described in chapter 4.

Ensemb ID	og2 Fo d Change	padj	Gene Name
ENSG00000148773	3.678028191	1.74E 34	MKI67
ENSG00000171848	4.311828438	9.16E 30	RRM2
ENSG00000112414	3.790156785	1.00E 25	ADGRG6
ENSG00000175164	4.033047393	2.43E 24	ABO
ENSG00000153707	3.107578312	1.78E 23	PTPRD
ENSG00000010327	3.248204484	6.17E 22	STAB1
ENSG00000066279	3.284183021	3.09E 21	ASPM
ENSG00000171316	3.03584906	6.80E 19	CHD7
ENSG00000173080	4.780011177	8.44E 17	RXFP4
ENSG00000145386	4.314420415	2.64E 16	CCNA2
ENSG00000156970	3.001664859	4.16E 16	BUB1B
ENSG00000168453	5.007578435	7.24E 16	HR
ENSG00000114805	3.40910624	2.30E 15	PLCH1
ENSG00000111206	2.66323754	2.33E 15	FOXM1
ENSG00000205777	4.39169507	7.05E 15	GAGE1
ENSG00000137812	2.824350342	1.22E 14	KNL1
ENSG00000117724	2.439880328	1.24E 14	CENPF
ENSG00000121966	5.109975459	3.28E 14	CXCR4
ENSG00000134690	3.215432043	3.81E 14	CDCA8
ENSG00000187772	3.672812154	3.81E 14	LIN28B
ENSG00000138315	5.507958886	1.53E 13	OIT3
ENSG00000120694	2.795970354	2.33E 13	HSPH1
ENSG00000212866	3.820837936	3.15E 13	HSPA1B
ENSG00000134057	3.592345623	3.36E 13	CCNB1
ENSG00000144655	3.577252444	4.62E 13	CSRNP1
ENSG00000154479	3.230283937	7.36E 13	CCDC173
ENSG00000198826	2.695242437	1.16E 12	ARHGAP11A
ENSG00000131747	4.236273811	1.33E 12	TOP2A
ENSG00000180354	2.275924052	1.38E 12	MTURN
ENSG00000117983	3.709117685	1.62E 12	MUC5B
ENSG00000169679	2.709893887	3.14E 12	BUB1
ENSG00000260314	4.67428378	3.14E 12	MRC1
ENSG00000171522	3.829893469	3.14E 12	PTGER4
ENSG00000115541	2.591148192	3.49E 12	HSPE1
ENSG00000137804	2.197596996	6.94E 12	NUSAP1
ENSG00000131016	4.50566973	9.97E 12	AKAP12
ENSG00000277059	3.504811127	1.47E 11	FAM30A
ENSG00000080824	2.176348567	2.02E 11	HSP90AA1
ENSG00000164045	3.061976513	2.08E 11	CDC25A
ENSG00000204197	2.760025652	4.56E 11	KIFC1
ENSG00000092853	2.618356649	4.93E 11	CLSPN
ENSG00000109805	2.875769913	4.93E 11	NCAPG
ENSG00000170312	3.032725202	5.50E 11	CDK1
ENSG00000186185	2.437599602	9.77E 11	KIF18B
ENSG00000124610	4.733351533	1.13E 10	HIST1H1A
ENSG00000169607	2.950568764	1.23E 10	CKAP2L
ENSG00000162645	3.767641418	1.24E 10	GBP2
ENSG00000037280	3.02117776	1.71E 10	FLT4
ENSG00000126787	3.453630116	1.81E 10	DLGAP5
ENSG00000088325	2.397139965	2.51E 10	TPX2
ENSG00000122952	3.215215433	2.92E 10	ZWINT
ENSG00000142731	2.493708873	4.03E 10	PLK4
ENSG00000116962	3.985069982	5.37E 10	NID1
ENSG00000159217	2.191312834	1.59E 09	IGF2BP1
ENSG00000188305	4.317215152	1.90E 09	PEAK3
ENSG00000066056	1.770635797	2.20E 09	TIE1

ENSG00000163687	4.149292392	2.32E 09	DNASE1L3
ENSG00000138160	2.260134921	2.63E 09	KIF11
ENSG00000100100	2.778957864	2.78E 09	PIK3IP1
ENSG00000115194	2.828211607	2.88E 09	SLC30A3
ENSG00000132313	2.619268264	3.72E 09	MRPL35
ENSG00000122966	1.768491682	4.81E 09	CIT
ENSG00000144381	1.666396606	5.11E 09	HSPD1
ENSG00000133800	4.194376982	6.09E 09	LYVE1
ENSG00000157456	2.720254709	6.12E 09	CCNB2
ENSG00000213085	4.322328223	6.25E 09	CFAP45
ENSG00000101057	2.833733994	7.53E 09	MYBL2
ENSG00000121211	3.771077326	9.39E 09	MND1
ENSG00000136011	6.411810943	9.39E 09	STAB2
ENSG00000126583	4.21121871	1.06E 08	PRKCG
ENSG00000159674	3.021304691	1.20E 08	SPON2
ENSG00000139318	2.501196493	1.25E 08	DUSP6
ENSG00000177084	1.722874804	1.25E 08	POLE
ENSG00000173276	2.470638086	1.25E 08	ZBTB21
ENSG00000186777	4.510613658	1.31E 08	ZNF732
ENSG00000111602	2.208751665	1.81E 08	TIMELESS
ENSG00000166851	2.637904852	1.91E 08	PLK1
ENSG00000164087	3.890120907	2.19E 08	POC1A
ENSG00000079819	1.882262294	2.23E 08	EPB41L2
ENSG00000196565	4.142130553	2.81E 08	HBG2
ENSG00000244242	3.444307647	2.81E 08	IFITM10
ENSG00000213799	2.718843121	2.81E 08	ZNF845
ENSG00000175514	3.691465979	2.82E 08	GPR152
ENSG00000179094	2.954637638	3.41E 08	PER1
ENSG00000104738	2.462050529	3.43E 08	MCM4
ENSG00000164104	2.245148964	3.61E 08	HMGB2
ENSG00000180044	5.768476395	3.81E 08	C3orf80
ENSG00000118193	2.046801648	3.89E 08	KIF14
ENSG00000188389	6.01885514	4.12E 08	PDCD1
ENSG00000163808	3.063521641	4.60E 08	KIF15
ENSG00000011426	2.927133328	5.31E 08	ANLN
ENSG00000155090	2.912969385	5.37E 08	KLF10
ENSG00000119408	2.052363233	6.82E 08	NEK6
ENSG00000179399	6.198741435	9.39E 08	GPC5
ENSG00000112312	2.615080444	1.02E 07	GMNN
ENSG00000101200	4.190595714	1.11E 07	AVP
ENSG00000130787	2.48086093	1.29E 07	HIP1R
ENSG00000228716	2.559623836	1.56E 07	DHFR
ENSG00000126259	5.278848763	1.83E 07	KIRREL2
ENSG00000140534	2.202033106	1.83E 07	TICRR
ENSG00000163874	4.111434916	1.93E 07	ZC3H12A
ENSG00000276043	2.663658876	2.19E 07	UHRF1
ENSG00000184661	2.747448349	2.27E 07	CDCA2
ENSG00000004139	2.095171115	2.27E 07	SARM1
ENSG00000185022	2.85141979	2.62E 07	MAFF
ENSG00000100968	2.619095494	2.80E 07	NFATC4
ENSG00000176890	2.163518393	3.19E 07	TYMS
ENSG00000013573	1.631455223	3.30E 07	DDX11
ENSG00000112984	3.170611109	4.04E 07	KIF20A
ENSG00000160339	6.040827751	4.19E 07	FCN2
ENSG00000175063	2.495566021	4.31E 07	UBE2C
ENSG00000206560	1.668917604	4.53E 07	ANKRD28
ENSG00000165682	3.829901803	4.92E 07	CLEC1B
ENSG00000136982	2.728153057	5.60E 07	DSCC1
ENSG00000173218	2.120180651	5.74E 07	VANGL1
ENSG00000105711	3.858145578	6.20E 07	SCN1B
ENSG00000107968	2.290786425	6.23E 07	MAP3K8
ENSG00000086827	2.297253251	7.52E 07	ZW10
ENSG00000119969	1.975153105	7.53E 07	HELLS
ENSG00000108669	1.823083917	7.75E 07	CYTH1
ENSG00000139364	3.306860202	7.75E 07	TMEM132B
ENSG00000127564	2.621064416	7.85E 07	PKMYT1
ENSG00000146278	1.574981566	7.86E 07	PNRC1

ENSG00000093217	2.018971742	7.88E 07	XYLB
ENSG00000152760	1.939184398	9.95E 07	TCTEX1D1
ENSG00000119138	4.57386661	1.00E 06	KLF9
ENSG00000100767	2.03815236	1.06E 06	PAPLN
ENSG00000093009	2.734699435	1.17E 06	CDC45
ENSG00000113368	2.821541111	1.18E 06	LMNB1
ENSG00000105383	2.533462049	1.25E 06	CD33
ENSG00000138778	2.638944578	1.40E 06	CENPE
ENSG00000014138	2.066412036	1.51E 06	POLA2
ENSG00000140525	1.73173758	1.58E 06	FANCI
ENSG00000103187	1.730949493	1.68E 06	COTL1
ENSG00000185559	2.94248447	1.68E 06	DLK1
ENSG00000121152	2.088734773	1.68E 06	NCAPH
ENSG00000143369	3.592890419	1.74E 06	ECM1
ENSG00000156427	4.772482475	1.83E 06	FGF18
ENSG00000277236	8.258214562	1.86E 06	CCL14
ENSG00000130518	3.485805792	2.36E 06	IQCN
ENSG00000059915	3.216530248	2.48E 06	PSD
ENSG00000161103	2.300908602	2.57E 06	LOC102725072
ENSG00000072571	2.299525922	2.81E 06	HMMR
ENSG00000132646	2.729766002	3.19E 06	PCNA
ENSG00000129173	2.288253434	3.33E 06	E2F8
ENSG00000161270	4.202159113	3.70E 06	NPHS1
ENSG00000119508	3.348680834	3.88E 06	NR4A3
ENSG00000138829	2.478685509	3.89E 06	FBN2
ENSG00000139722	1.983818943	4.15E 06	VPS37B
ENSG00000138080	2.082114019	4.35E 06	EMILIN1
ENSG00000146670	2.067184803	4.57E 06	CDCA5
ENSG00000188549	2.383260509	4.77E 06	CCDC9B
ENSG00000105486	1.508038317	4.85E 06	LIG1
ENSG00000132002	2.571714695	4.99E 06	DNAJB1
ENSG00000213672	2.366009657	4.99E 06	NCKIPSD
ENSG00000121753	3.521627688	5.02E 06	ADGRB2
ENSG00000220008	2.740457986	5.02E 06	LINGO3
ENSG00000182759	3.912320295	5.48E 06	MAFA
ENSG00000116161	1.813984258	5.78E 06	CACYBP
ENSG00000112182	1.790255643	5.90E 06	BACH2
ENSG00000076003	2.074445456	5.99E 06	MCM6
ENSG00000118898	3.212720421	6.53E 06	PPL
ENSG00000104369	2.188378567	6.75E 06	JPH1
ENSG00000058804	2.052486031	6.75E 06	NDC1
ENSG00000121104	1.434645523	7.00E 06	FAM117A
ENSG00000143228	2.468071564	7.44E 06	NUF2
ENSG00000175745	4.336779873	7.47E 06	NR2F1
ENSG00000128655	2.425425972	8.37E 06	PDE11A
ENSG00000135047	3.739579731	8.64E 06	CTSL
ENSG00000120885	2.950305584	9.43E 06	CLU
ENSG00000197536	2.595954778	9.97E 06	C5orf56
ENSG00000153291	2.601709841	1.03E 05	SLC25A27
ENSG00000117748	2.36337171	1.11E 05	RPA2
ENSG00000179869	2.617569116	1.15E 05	ABCA13
ENSG00000161011	2.262170573	1.15E 05	SQSTM1
ENSG00000167604	2.411176201	1.21E 05	NFKBID
ENSG00000091483	1.932255447	1.22E 05	FH
ENSG00000112029	2.148166228	1.26E 05	FBXO5
ENSG00000161981	2.04057804	1.27E 05	SNRNP25
ENSG00000151136	1.794433591	1.28E 05	BTBD11
ENSG00000178999	2.035272688	1.29E 05	AURKB
ENSG00000069399	2.430700182	1.29E 05	BCL3
ENSG00000260220	3.226960523	1.29E 05	CCDC187
ENSG00000117650	2.457967759	1.34E 05	NEK2
ENSG00000109321	6.934445028	1.36E 05	AREG
ENSG00000118298	2.935447407	1.46E 05	CA14
ENSG00000138669	2.54697573	1.46E 05	PRKG2
ENSG00000101407	2.06925318	1.46E 05	TTI1
ENSG00000075426	2.450056522	1.54E 05	FOSL2
ENSG00000169302	4.100633897	1.54E 05	STK32A

ENSG00000089692	3.891795749	1.62E 05	LAG3
ENSG00000156103	2.592761015	1.62E 05	MMP16
ENSG00000274750	3.21998286	1.68E 05	HIST1H3E
ENSG00000175768	2.072372663	1.68E 05	TOMM5
ENSG00000158987	1.671432328	1.72E 05	RAPGEF6
ENSG00000040275	2.441387165	1.77E 05	SPDL1
ENSG00000185112	1.980122042	1.84E 05	FAM43A
ENSG00000058335	3.136432227	1.84E 05	RASGRF1
ENSG00000126803	2.052889106	1.85E 05	HSPA2
ENSG00000109971	1.674372144	2.25E 05	HSPA8
ENSG00000141753	2.640279128	2.27E 05	IGFBP4
ENSG00000177103	3.282742997	2.43E 05	DSCAML1
ENSG00000149927	2.435130834	2.46E 05	DOC2A
ENSG00000122490	2.304415029	2.46E 05	PQLC1
ENSG00000111247	2.708271058	2.46E 05	RAD51AP1
ENSG00000081320	1.574260999	2.46E 05	STK17B
ENSG00000147852	2.101017992	2.46E 05	VLDLR
ENSG00000164362	2.98380964	2.49E 05	TERT
ENSG00000065328	2.766426879	2.52E 05	MCM10
ENSG00000124942	2.357102761	2.58E 05	AHNAK
ENSG00000077782	1.904425624	2.58E 05	FGFR1
ENSG00000132819	3.235608326	2.62E 05	RBM38
ENSG00000149554	1.674995917	2.77E 05	CHEK1
ENSG00000152455	1.938390917	2.79E 05	SUV39H2
ENSG00000178809	2.428601791	2.85E 05	TRIM73
ENSG00000125810	1.483619853	2.86E 05	CD93
ENSG00000172889	1.362755016	2.86E 05	EGFL7
ENSG00000076248	2.697677529	3.21E 05	UNG
ENSG00000160949	1.788186352	3.22E 05	TONSL
ENSG00000051180	2.055187534	3.42E 05	RAD51
ENSG00000258947	3.435218523	3.42E 05	TUBB3
ENSG00000013364	1.539236617	3.51E 05	MVP
ENSG00000109674	2.8346941	3.70E 05	NEIL3
ENSG00000120802	1.889420419	3.81E 05	TMPO
ENSG00000088305	1.611251825	3.85E 05	DNMT3B
ENSG00000116830	1.593376261	4.00E 05	TTF2
ENSG00000196227	2.258781419	4.19E 05	FAM217B
ENSG00000087586	2.639376551	4.25E 05	AURKA
ENSG00000143751	2.416857195	4.27E 05	SDE2
ENSG00000134291	1.894671786	4.39E 05	TMEM106C
ENSG00000138180	2.539437038	4.59E 05	CEP55
ENSG00000227231	4.701372186	4.59E 05	IER3
ENSG00000181991	1.63514659	4.59E 05	MRPS11
ENSG00000023041	1.914202988	4.60E 05	ZDHHC6
ENSG00000165655	2.26974934	4.60E 05	ZNF503
ENSG00000232804	5.040571546	4.74E 05	HSPA1B
ENSG00000091127	2.163220019	4.76E 05	PUS7
ENSG00000275019	4.88825365	4.77E 05	LILRB3
ENSG00000022267	1.848065292	4.79E 05	FHL1
ENSG00000073111	2.101371896	4.91E 05	MCM2
ENSG00000092020	1.622211788	4.91E 05	PPP2R3C
ENSG00000081059	2.638280991	4.91E 05	TCF7
ENSG00000128513	1.962444985	5.05E 05	POT1
ENSG00000204420	4.11429157	5.21E 05	MPIG6B
ENSG00000144354	1.854901469	5.36E 05	CDCA7
ENSG00000176208	1.773125177	5.39E 05	ATAD5
ENSG00000198056	1.911672139	5.49E 05	PRIM1
ENSG00000149257	1.481285	5.56E 05	SERPINH1
ENSG00000156876	1.817906012	6.04E 05	SASS6
ENSG00000151090	2.971466713	6.17E 05	THRB
ENSG00000078804	2.388841949	6.25E 05	TP53INP2
ENSG00000114796	1.721001831	6.31E 05	KLHL24
ENSG00000138346	1.574465111	6.84E 05	DNA2
ENSG00000130164	2.158985597	7.10E 05	LDLR
ENSG00000115758	1.993852055	7.11E 05	ODC1
ENSG00000117632	1.809488234	7.11E 05	STMN1
ENSG00000156049	4.223622216	7.19E 05	GNA14

ENSG00000138658	1.748384259	7.37E 05	ZGRF1
ENSG00000215045	2.994763684	7.41E 05	GRID2IP
ENSG00000090273	1.62566833	7.43E 05	NUDC
ENSG00000159335	1.76350335	7.56E 05	PTMS
ENSG00000154188	2.048257385	8.03E 05	ANGPT1
ENSG00000166856	3.226403066	8.21E 05	GPR182
ENSG00000107819	1.917157504	8.60E 05	SFXN3
ENSG00000105808	1.614928166	8.91E 05	RASA4
ENSG00000118257	2.235127898	8.94E 05	NRP2
ENSG00000004478	1.525680211	9.02E 05	FKBP4
ENSG00000163602	2.088644956	9.11E 05	RYBP
ENSG00000115648	2.617451389	9.13E 05	MLPH
ENSG00000223609	5.370505173	9.44E 05	HBD
ENSG00000128944	1.824501254	9.51E 05	KNSTRN
ENSG00000214688	2.951162435	9.53E 05	C10orf105
ENSG00000149577	2.044734266	9.73E 05	SIDT2
ENSG00000099797	1.963907688	9.96E 05	TECR
ENSG00000123240	1.929978325	0.000102472	OPTN
ENSG00000085840	1.795406109	0.000105489	ORC1
ENSG00000178342	3.199112227	0.00011082	KCNG2
ENSG00000011485	1.651852861	0.000111131	PPP5C
ENSG00000118785	3.273537046	0.000111131	SPP1
ENSG00000100234	1.690453118	0.000111131	TIMP3
ENSG00000070985	3.496975337	0.000111131	TRPM5
ENSG00000139734	1.937897092	0.000111772	DIAPH3
ENSG00000171206	1.436443375	0.000116065	TRIM8
ENSG00000067533	2.088348299	0.000118607	RRP15
ENSG00000145604	1.915258186	0.000120183	SKP2
ENSG00000124164	1.551401806	0.000120183	VAPB
ENSG00000132780	1.637915812	0.000120454	NASP
ENSG00000123416	1.892334681	0.000127723	TUBA1B
ENSG00000131002	7.737254381	0.000130066	TXLNGY
ENSG00000204165	2.854254492	0.000130326	CXorf65
ENSG00000027644	4.100428913	0.000131645	INSRR
ENSG00000155657	1.680842957	0.000131645	TTN
ENSG00000184227	4.5875217	0.000132262	ACOT1
ENSG00000178966	2.215332241	0.000132262	RMI1
ENSG00000156675	1.676048866	0.000132498	RAB11FIP1
ENSG00000005381	2.423678224	0.000141651	MPO
ENSG00000143622	2.029895164	0.000151471	RIT1
ENSG00000175592	3.029215068	0.000152276	FOSL1
ENSG00000099860	2.351929949	0.000156183	GADD45B
ENSG00000174099	1.413119458	0.000156636	MSRB3
ENSG00000224393	3.261761482	0.000163048	MPIG6B
ENSG00000230060	3.261761482	0.000163048	MPIG6B
ENSG00000231003	3.261761482	0.000163048	MPIG6B
ENSG00000237459	3.261761482	0.000163048	MPIG6B
ENSG00000246922	1.979899029	0.000172216	UBAP1L
ENSG00000145075	2.446017675	0.000172265	CCDC39
ENSG00000101003	1.886836032	0.000173432	GINS1
ENSG00000175197	2.764007142	0.000179134	DDIT3
ENSG00000130222	4.323665978	0.000179134	GADD45G
ENSG00000169914	1.855338437	0.000179414	OTUD3
ENSG00000186868	3.248100381	0.000180663	MAPT
ENSG00000133063	2.815578407	0.000182659	CHIT1
ENSG00000198355	2.255727794	0.000183992	PIM3
ENSG00000198825	1.269229563	0.000192267	INPP5F
ENSG00000112246	3.764862903	0.000194219	SIM1
ENSG00000128595	1.647227998	0.000195461	CALU
ENSG00000117054	1.661669643	0.000195883	ACADM
ENSG00000167900	1.845937796	0.000200618	TK1
ENSG00000166004	1.229528906	0.000203085	CEP295
ENSG00000166086	1.744816684	0.000203085	JAM3
ENSG00000205089	3.898036606	0.000203157	CCNI2
ENSG00000176624	1.576211687	0.000203157	MEX3C
ENSG00000088986	1.818002162	0.000203686	DYNLL1
ENSG00000108840	1.430539301	0.000203699	HDAC5

ENSG00000159388	2.310875908	0.000204045	BTG2
ENSG00000101213	2.065557183	0.000204306	PTK6
ENSG00000170558	2.122630718	0.000206475	CDH2
ENSG00000105650	3.441268519	0.000206475	PDE4C
ENSG00000143870	1.614907108	0.000206475	PDIA6
ENSG00000008513	1.698014684	0.000206475	ST3GAL1
ENSG00000115750	1.74450864	0.000209133	TAF1B
ENSG00000169926	2.172746073	0.000211825	KLF13
ENSG00000198155	1.956258295	0.000212204	ZNF876P
ENSG00000151849	1.852663019	0.000214387	CENPJ
ENSG00000103067	2.550608085	0.000216772	ESRP2
ENSG00000162913	2.712968629	0.000216772	OBSCN AS1
ENSG00000172840	1.992452098	0.000217131	PDP2
ENSG00000221968	1.718940493	0.000220452	FADS3
ENSG00000197261	2.505350619	0.000220766	C6orf141
ENSG00000114395	2.274517446	0.000220766	CYB561D2
ENSG00000115457	2.057192053	0.000220766	IGFBP2
ENSG00000205978	1.241718272	0.000220766	NYNRIN
ENSG00000113761	1.54535801	0.000220766	ZNF346
ENSG00000132681	2.256103061	0.000234192	ATP1A4
ENSG00000170075	2.213376897	0.000234192	GPR37L1
ENSG00000182628	2.072737238	0.000234192	SKA2
ENSG00000013016	2.090452998	0.000236253	EHD3
ENSG00000128165	3.49544319	0.00023659	ADM2
ENSG00000112118	2.170991148	0.00023659	MCM3
ENSG00000064309	2.573916192	0.00024447	CDON
ENSG00000110172	1.483015279	0.00024447	CHORDC1
ENSG00000159131	1.606511487	0.00024447	GART
ENSG00000175643	2.179289003	0.000250228	RMI2
ENSG00000170482	2.123999508	0.000258795	SLC23A1
ENSG00000066294	1.68213496	0.000266239	CD84
ENSG00000165757	1.424070207	0.000266239	JCAD
ENSG00000148468	3.454158796	0.000267501	FAM171A1
ENSG00000053747	2.662454282	0.000267501	LAMA3
ENSG00000197557	2.374059991	0.000267501	TTC30A
ENSG00000170893	1.858363211	0.000270726	TRH
ENSG00000142748	3.337269913	0.000279025	FCN3
ENSG00000074266	1.591917476	0.000280695	EED
ENSG00000124207	1.54745116	0.000281843	CSE1L
ENSG00000165929	2.529538955	0.000282629	TC2N
ENSG00000262418	1.632212585	0.000282639	PTPRC
ENSG00000152193	2.019519777	0.000283595	RNF219
ENSG00000167088	1.893078215	0.000284059	SNRPD1
ENSG00000115875	1.581999771	0.000291503	SRSF7
ENSG00000129355	3.549483244	0.000291842	CDKN2D
ENSG00000071539	2.116752305	0.000292795	TRIP13
ENSG00000178718	2.432927961	0.000293696	RPP25
ENSG00000119616	1.532241878	0.000297874	FCF1
ENSG00000184205	1.887596779	0.000297874	TSPYL2
ENSG00000225824	3.764754591	0.000300724	HLA DQB1
ENSG00000174197	1.246375707	0.000300724	MGA
ENSG00000083093	1.73703741	0.000300724	PALB2
ENSG00000110328	2.302238528	0.000300922	GALNT18
ENSG00000117480	2.299148659	0.000303834	FAAH
ENSG00000167670	1.507517612	0.0003069	CHAF1A
ENSG00000155561	1.81762521	0.0003069	NUP205
ENSG00000121764	2.966104323	0.000319071	HCRTR1
ENSG00000168264	1.430967788	0.000319071	IRF2BP2
ENSG00000154473	1.925173508	0.000320543	BUB3
ENSG00000094804	1.887636346	0.000332351	CDC6
ENSG00000111906	1.459446871	0.000344585	HDDC2
ENSG00000169744	2.547199752	0.000346553	LDB2
ENSG00000164938	1.769068031	0.000346553	TP53INP1
ENSG00000106328	4.91988237	0.000365254	FSCN3
ENSG00000206557	1.675594948	0.000367505	TRIM71
ENSG00000134571	2.793276523	0.00036783	MYBPC3
ENSG00000132341	1.695826381	0.00036783	RAN

ENSG00000102096	2.185805328	0.000373442	PIM2
ENSG00000240505	2.460674557	0.000373442	TNFRSF13B
ENSG00000182175	1.904806235	0.000373755	RGMA
ENSG00000128050	1.622343783	0.000376891	PAICS
ENSG00000165934	1.662953539	0.000382124	CPSF2
ENSG00000133401	1.201808771	0.000382288	PDZD2
ENSG00000239305	1.593891796	0.000382288	RNF103
ENSG00000205710	3.023959336	0.000387257	C17orf107
ENSG00000165480	2.587072535	0.000388769	SKA3
ENSG00000140564	1.94297013	0.000395862	FURIN
ENSG00000100906	2.548401392	0.00039668	NFKBIA
ENSG00000198785	3.189500992	0.000400452	GRIN3A
ENSG00000065534	2.10271767	0.000411739	MYLK
ENSG00000107807	4.947769063	0.000421514	TLX1
ENSG00000130520	1.889048666	0.000427412	LSM4
ENSG00000145911	2.539655224	0.000443899	N4BP3
ENSG00000105875	1.939177703	0.000445169	WDR91
ENSG00000105856	1.466373386	0.000446942	HBP1
ENSG00000144893	1.67595341	0.000450636	MED12L
ENSG00000122547	1.560490809	0.000452877	EEPD1
ENSG00000115461	3.828162101	0.000459718	IGFBP5
ENSG00000148925	1.479637951	0.000470897	BTBD10
ENSG00000213066	1.438211671	0.000470897	FGFR1OP
ENSG00000070808	3.142482688	0.00047393	CAMK2A
ENSG00000185650	2.008781417	0.00049371	ZFP36L1
ENSG00000177511	3.448482697	0.00051496	ST8SIA3
ENSG00000109586	1.315013619	0.000515553	GALNT7
ENSG00000152256	1.57770903	0.000516579	PDK1
ENSG00000012048	1.573454935	0.00051868	BRCA1
ENSG00000148908	1.594636492	0.00052793	RGS10
ENSG00000100297	1.592786186	0.000530253	MCM5
ENSG00000008441	1.794401525	0.000530253	NFIX
ENSG00000216775	2.677541316	0.000538371	LOC730101
ENSG00000089195	2.077681388	0.000538371	TRMT6
ENSG00000242114	2.357575651	0.00054493	MTFP1
ENSG00000111674	2.28556978	0.000546372	ENO2
ENSG00000188612	1.426905982	0.000550646	SUMO2
ENSG00000106366	2.808441328	0.000561621	SERPINE1
ENSG00000170448	1.558446459	0.000561911	NFXL1
ENSG00000135838	2.479660045	0.000562256	NPL
ENSG00000008226	2.417869264	0.000583854	DLEC1
ENSG00000091262	1.479094729	0.000585952	ABCC6
ENSG00000189067	1.57109079	0.000595504	LITAF
ENSG00000153044	1.878479113	0.000601056	CENPH
ENSG00000183484	2.478495065	0.000607816	GPR132
ENSG00000171223	2.703184765	0.000607816	JUNB
ENSG00000138587	2.120171166	0.000607816	MNS1
ENSG00000079313	1.560996882	0.000607816	REXO1
ENSG00000168907	2.718078646	0.00061354	PLA2G4F
ENSG00000069812	2.587466868	0.000620537	HES2
ENSG00000108561	1.786227026	0.00062831	C1QBP
ENSG00000183853	1.712092726	0.000636148	KIRREL1
ENSG00000278318	1.624470278	0.000659094	ZNF229
ENSG00000141756	1.553117648	0.000659152	FKBP10
ENSG00000169291	1.936246526	0.000666752	SHE
ENSG00000163082	2.057797669	0.000676554	SGPP2
ENSG00000068323	1.784061496	0.000679863	TFE3
ENSG00000067048	11.74398947	0.000689547	DDX3Y
ENSG00000127418	2.219353069	0.000690573	FGFRL1
ENSG00000089723	2.443012546	0.000695427	OTUB2
ENSG00000026751	2.606738348	0.000695427	SLAMF7
ENSG00000140403	1.479265889	0.000696568	DNAJA4
ENSG00000198932	1.37238421	0.000696568	GPRASP1
ENSG00000158042	1.818415628	0.000696568	MRPL17
ENSG00000108679	1.946836308	0.000719971	LGALS3BP
ENSG00000198858	2.170988102	0.000725522	R3HDM4
ENSG00000125414	3.309414334	0.000728304	MYH2

ENSG00000079616	1.254545278	0.000728875	KIF22
ENSG00000141030	1.290551938	0.000735416	COPS3
ENSG00000034152	2.300282843	0.000735422	MAP2K3
ENSG00000064933	1.476887064	0.000735474	PMS1
ENSG00000127423	2.063196421	0.000740507	AUNIP
ENSG00000167325	1.490454962	0.000740507	RRM1
ENSG00000167565	2.078918123	0.00074212	SERTAD3
ENSG00000137494	2.179430295	0.00076431	ANKRD42
ENSG00000123219	1.47106549	0.000765133	CENPK
ENSG00000138735	2.064897192	0.000765133	PDE5A
ENSG00000100399	2.758087904	0.000765925	CHADL
ENSG00000134755	1.81189364	0.000777379	DSC2
ENSG00000050344	2.223731457	0.000780032	NFE2L3
ENSG00000163520	1.786045397	0.000780302	FBLN2
ENSG00000131470	1.646877484	0.000785752	PSMC3IP
ENSG00000155428	2.967508126	0.000786859	TRIM74
ENSG00000151576	1.213338701	0.000806562	QTRT2
ENSG00000177169	2.350050204	0.000840821	ULK1
ENSG00000129007	2.239016657	0.000848243	CALML4
ENSG00000164332	1.579375147	0.0008647	UBLCP1
ENSG00000100030	1.168938967	0.000894836	MAPK1
ENSG00000162073	1.663948086	0.000898434	PAQR4
ENSG00000159618	2.109977675	0.000901248	ADGRG5
ENSG00000173588	1.295837255	0.00093216	CEP83
ENSG00000161800	1.91022084	0.00093216	RACGAP1
ENSG00000203760	2.506895744	0.00093238	CENPW
ENSG00000183196	1.78739151	0.00093238	CHST6
ENSG00000198517	2.111732169	0.00093238	MAFK
ENSG00000188786	2.052906458	0.00093238	MTF1
ENSG00000275430	2.855207742	0.00093238	MUC20
ENSG00000076242	1.451357246	0.000939349	MLH1
ENSG00000125347	2.118108798	0.000945735	IRF1
ENSG00000109756	1.415963768	0.000945735	RAPGEF2
ENSG00000138095	1.506097566	0.000981145	LRPPRC
ENSG00000099901	1.711313947	0.000981145	RANBP1
ENSG00000120833	1.333954606	0.000982167	SOCS2
ENSG00000127329	2.307053199	0.000985956	PTPRB
ENSG00000163154	2.259672989	0.000995777	TNFAIP8L2
ENSG00000108953	1.483312163	0.001000533	YWHAE
ENSG00000213988	1.505997925	0.001038768	ZNF90
ENSG00000273703	2.503743454	0.001041719	HIST1H2BM
ENSG00000137309	1.501081788	0.00104362	HMGA1
ENSG00000276600	2.972331503	0.001054693	RAB7B
ENSG00000135218	2.797934171	0.001073222	CD36
ENSG00000165355	2.133576575	0.001073222	FBXO33
ENSG00000114850	1.569592676	0.001082697	SSR3
ENSG00000125885	1.493517344	0.001100754	MCM8
ENSG00000281500	6.268392199	0.00110489	SLC37A4
ENSG00000146463	1.231572176	0.001107281	ZMYM4
ENSG00000188312	1.808855787	0.001113884	CENPP
ENSG00000186480	2.152686076	0.001120881	INSIG1
ENSG00000185298	1.508369898	0.001130385	CCDC137
ENSG00000136205	1.295908894	0.001135431	TNS3
ENSG00000230989	1.709442387	0.00114843	HSBP1
ENSG00000153140	1.732897764	0.001163673	CETN3
ENSG00000101444	1.468280129	0.001214346	AHCY
ENSG00000092470	1.605229607	0.00122982	WDR76
ENSG00000241697	2.28374043	0.001240649	TMEFF1
ENSG00000150753	1.773194084	0.001249738	CCT5
ENSG00000165476	1.566435563	0.001263717	REEP3
ENSG00000081237	1.464938571	0.001275767	PTPRC
ENSG00000149636	1.758147856	0.001280231	DSN1
ENSG00000088899	2.457052411	0.001280231	LZTS3
ENSG00000187510	5.596679534	0.001294527	PLEKHG7
ENSG00000133636	4.77622093	0.001315527	NTS
ENSG00000143819	1.494421488	0.001326619	EPHX1
ENSG00000110777	1.960192886	0.001326619	POU2AF1

ENSG00000165490	2.569963011	0.001331102	DDIAS
ENSG00000151465	1.44466487	0.001344518	CDC123
ENSG00000179115	1.377519924	0.001348417	FARSA
ENSG00000111665	1.489429911	0.001353352	CDCA3
ENSG00000105722	2.125771651	0.001374811	ERF
ENSG00000169519	1.712127257	0.001376628	METTL15
ENSG00000100241	1.391753937	0.001387257	SBF1
ENSG00000089685	1.983689144	0.001403356	BIRC5
ENSG00000164136	1.925891702	0.001403645	IL15
ENSG00000167378	1.666512153	0.001403645	IRGQ
ENSG00000133119	2.099108891	0.001403645	RFC3
ENSG00000054793	1.19396221	0.001403878	ATP9A
ENSG00000173039	1.708013298	0.001424185	RELA
ENSG00000143498	1.639661074	0.001434566	TAF1A
ENSG00000239672	2.046725809	0.001458804	NME1
ENSG00000113790	1.806026646	0.001460225	EHHADH
ENSG00000164167	1.811780392	0.001460225	LSM6
ENSG00000144043	1.705282089	0.001460225	TEX261
ENSG00000115355	1.000855567	0.001467025	CCDC88A
ENSG00000185338	2.0677506	0.001487631	SOCS1
ENSG00000240370	2.825745384	0.001487833	RPL13P5
ENSG00000051596	2.00648147	0.001487833	THOC3
ENSG00000047617	3.44553311	0.001521622	ANO2
ENSG00000114115	2.553911654	0.001551062	RBP1
ENSG00000014824	1.513118493	0.001551062	SLC30A9
ENSG00000198554	2.555124258	0.001566077	WDHD1
ENSG00000099365	1.999209022	0.001568927	STX1B
ENSG00000167470	2.030319915	0.001573213	MIDN
ENSG00000253882	2.288683764	0.001582022	LOC154761
ENSG00000164403	2.663835877	0.001597469	SHROOM1
ENSG00000145687	1.029843637	0.001618664	SSBP2
ENSG00000137807	1.591927072	0.001618839	KIF23
ENSG00000168676	1.947841141	0.001623574	KCTD19
ENSG00000113916	4.420015498	0.001634234	BCL6
ENSG00000012171	4.555070855	0.001675755	SEMA3B
ENSG00000142230	1.67551427	0.001680942	SAE1
ENSG00000146386	2.159053645	0.001682797	ABRACL
ENSG00000080839	2.129535132	0.001689743	RBL1
ENSG00000100307	1.656026995	0.00169353	CBX7
ENSG00000178904	1.291427029	0.00169353	DPY19L3
ENSG00000178295	1.680905931	0.00169353	GEN1
ENSG00000092054	2.740043229	0.00169353	MYH7
ENSG00000131196	1.728485442	0.00169353	NFATC1
ENSG00000129824	11.2041093	0.001697621	RPS4Y1
ENSG00000115085	1.764483053	0.00170995	ZAP70
ENSG00000109814	1.672409385	0.001751556	UGDH
ENSG00000186193	1.930219292	0.001752767	SAPCD2
ENSG00000124813	1.789218964	0.001762555	RUNX2
ENSG00000256870	6.497336374	0.001772717	SLC5A8
ENSG00000156136	1.710631284	0.001775576	DCK
ENSG00000168309	3.071456634	0.001775649	FAM107A
ENSG00000164855	2.554309277	0.001775649	TMEM184A
ENSG00000121410	1.407216704	0.001788428	A1BG
ENSG00000182050	2.506890721	0.001798198	MGAT4C
ENSG00000163918	2.122219586	0.001819339	RFC4
ENSG00000156299	1.462684946	0.001819339	TIAM1
ENSG00000187595	1.836682552	0.001819339	ZNF385C
ENSG00000008323	2.307250935	0.001824368	PLEKHG6
ENSG00000221886	2.658653521	0.001843875	ZBED8
ENSG00000146232	2.23863827	0.001846249	NFKBIE
ENSG00000127311	1.244965859	0.001851955	HELB
ENSG00000118961	1.585310834	0.001851955	LDAH
ENSG00000006453	2.485770633	0.00185665	BAIAP2L1
ENSG00000180917	1.547422698	0.00186143	CMTR2
ENSG00000276256	1.656980664	0.00186271	LOC389831
ENSG00000130775	2.020437705	0.00186271	THEMIS2
ENSG00000137441	5.761698275	0.001873393	FGFBP2

ENSG00000128408	2.970438622	0.001880961	RIBC2
ENSG00000266028	1.129569573	0.001880961	SRGAP2
ENSG00000073910	1.588829844	0.001886695	FRY
ENSG00000111276	1.751207484	0.001894686	CDKN1B
ENSG00000100196	2.263878341	0.00190231	KDELR3
ENSG00000140307	1.755745702	0.001903414	GTF2A2
ENSG00000125505	1.716820203	0.001903414	MBOAT7
ENSG00000168566	1.238409525	0.001903414	SNRNP48
ENSG00000182885	1.917533148	0.001904529	ADGRG3
ENSG00000100350	1.685549402	0.001936028	FOXRED2
ENSG00000163492	1.664174007	0.001939352	CCDC141
ENSG00000163629	1.564979676	0.001939352	PTPN13
ENSG00000122862	2.036594592	0.001939352	SRGN
ENSG00000165816	3.047043697	0.001939352	VWA2
ENSG00000170891	1.865257412	0.001942307	CYTL1
ENSG00000162063	1.517205524	0.001958153	CCNF
ENSG00000172828	1.645601028	0.001958153	CES3
ENSG00000169813	1.357318762	0.001958153	HNRNPF
ENSG00000160460	2.965599234	0.001958153	SPTBN4
ENSG00000127124	1.097372382	0.001968579	HIVEP3
ENSG00000150977	1.323874801	0.001977941	RILPL2
ENSG00000146731	1.177019632	0.001977967	CCT6A
ENSG00000176845	2.145253577	0.001989723	METRNL
ENSG00000162924	1.439657244	0.001989723	REL
ENSG00000046889	1.117349324	0.002037067	PREX2
ENSG00000277518	2.297240558	0.002043972	MUC6
ENSG00000166473	1.687472867	0.002072237	PKD1L2
ENSG00000186638	1.560569618	0.002093991	KIF24
ENSG00000111581	1.296787483	0.002093991	NUP107
ENSG00000118473	2.481419949	0.00209789	SGIP1
ENSG00000149503	1.755267533	0.002104291	INCENP
ENSG00000104938	2.95563559	0.002160829	CLEC4M
ENSG00000088881	2.521540438	0.002160829	EBF4
ENSG00000145990	1.511137428	0.002160829	GFOD1
ENSG00000073060	1.36415227	0.002160829	SCARB1
ENSG00000167780	4.743256994	0.002160829	SOAT2
ENSG00000171617	2.53639364	0.002173501	ENC1
ENSG00000102172	1.404432353	0.002176083	SMS
ENSG00000276409	3.251555649	0.00217795	CCL14
ENSG00000100442	1.432354778	0.00219076	FKBP3
ENSG00000111639	1.644554028	0.002204002	MRPL51
ENSG00000255346	1.911140198	0.002204002	NOX5
ENSG00000130309	1.469823961	0.00223909	COLGALT1
ENSG00000241394	2.616153272	0.00223909	HLA DMA
ENSG00000163346	1.244990476	0.00223909	PBXIP1
ENSG00000186834	1.599253254	0.002240054	HEXIM1
ENSG00000136628	1.259655535	0.002245147	EPRS
ENSG00000166111	2.576606688	0.00225383	SVOP
ENSG00000100522	2.171475349	0.002303381	GNPNAT1
ENSG00000134575	1.402187785	0.0023267	ACP2
ENSG00000138092	1.393211129	0.0023267	CENPO
ENSG00000136824	1.614508399	0.0023267	SMC2
ENSG00000137720	1.963510077	0.002359469	C11orf1
ENSG00000174177	1.717086735	0.002359469	CTU2
ENSG00000167315	1.51761786	0.002364082	ACAA2
ENSG00000023287	1.901094645	0.002427241	RB1CC1
ENSG00000143862	1.553660669	0.002430814	ARL8A
ENSG00000134438	3.865550539	0.002432443	RAX
ENSG00000175697	3.651588559	0.002440058	GPR156
ENSG00000109861	1.219041702	0.0024477	CTSC
ENSG00000151725	1.692238676	0.002448906	CENPU
ENSG00000077152	2.288642335	0.002448906	UBE2T
ENSG00000163655	1.355706852	0.002469009	GMPS
ENSG00000235162	1.581261378	0.002470767	C12orf75
ENSG00000176532	2.588298098	0.002470767	PRR15
ENSG00000068976	4.474982084	0.002477156	PYGM
ENSG00000124532	1.947714818	0.002478416	MRS2

ENSG00000162510	2.340483513	0.002482985	MATN1
ENSG00000164163	1.234655062	0.002492979	ABCE1
ENSG00000128284	1.336595286	0.002519695	APOL3
ENSG00000006625	1.547956967	0.002556727	GGCT
ENSG00000170255	4.263621738	0.002589007	MRGPRX1
ENSG00000088682	1.57018761	0.002611139	COQ9
ENSG00000196305	1.093053477	0.002637068	IARS
ENSG00000162600	1.594663058	0.002637068	OMA1
ENSG00000163406	1.365835678	0.002637068	SLC15A2
ENSG00000107443	1.744877018	0.002637777	CCNJ
ENSG00000165810	2.315354745	0.002637779	BTNL9
ENSG00000131759	1.650864796	0.002645148	RARA
ENSG00000263528	1.721721152	0.002650426	IKBKE
ENSG00000253729	1.129230541	0.002680183	PRKDC
ENSG00000164109	2.381559832	0.002684315	MAD2L1
ENSG00000154099	1.997252592	0.002687186	DNAAF1
ENSG00000160741	1.632720186	0.00270715	CRTC2
ENSG00000128052	3.70692521	0.00270715	KDR
ENSG00000112640	1.232948353	0.002743403	PPP2R5D
ENSG00000168026	2.528997409	0.002743403	TTC21A
ENSG00000274768	6.894511354	0.002759137	CISD3
ENSG00000145736	2.134282844	0.002767984	GTF2H2
ENSG00000172000	1.846166013	0.002767984	ZNF556
ENSG00000168496	1.543840834	0.002815467	FEN1
ENSG00000148481	1.450757781	0.002815467	MINDY3
ENSG00000048540	3.002076434	0.002816581	LMO3
ENSG00000175262	2.702367823	0.002828835	C1orf127
ENSG00000205403	2.95581385	0.002833726	CFI
ENSG00000197444	2.784694886	0.002869158	OGDHL
ENSG00000134874	1.859929503	0.002875384	DZIP1
ENSG00000135698	1.604526825	0.002883853	MPHOSPH6
ENSG00000235925	8.553770048	0.002896656	LY6G6C
ENSG00000241484	2.4597669	0.002905274	ARHGAP8
ENSG00000146038	2.628393385	0.00293051	DCDC2
ENSG00000205339	1.415001356	0.002957338	IPO7
ENSG00000163938	1.367662296	0.002957804	GNL3
ENSG00000175928	2.063287054	0.002957804	LRRN1
ENSG00000143217	2.298081783	0.002985931	NECTIN4
ENSG00000254996	1.247511131	0.002989619	ANKHD1 EIF4EBP3
ENSG00000109881	1.381397677	0.002989619	CCDC34
ENSG00000011028	1.334323454	0.002989619	MRC2
ENSG00000148459	1.898624134	0.002989619	PDSS1
ENSG00000160584	1.265290951	0.002989619	SIK3
ENSG00000104447	2.085131956	0.002989619	TRPS1
ENSG00000010292	1.358007529	0.003011169	NCAPD2
ENSG00000120318	2.145930429	0.003141328	ARAP3
ENSG00000132510	1.671002426	0.003141328	KDM6B
ENSG00000003509	1.406426915	0.003141328	NDUFAF7
ENSG00000099985	2.59011196	0.003153252	OSM
ENSG00000083535	1.226463796	0.003153252	PIBF1
ENSG00000006071	2.533731035	0.003179744	ABCC8
ENSG00000177602	2.019568075	0.00318472	HASPIN
ENSG00000092621	1.321731124	0.003194296	PHGDH
ENSG00000151135	1.164826378	0.003198216	TMEM263
ENSG00000107485	2.014131897	0.0032009	GATA3
ENSG00000142149	2.040004806	0.003207851	HUNK
ENSG00000146281	1.341258486	0.003233364	PM20D2
ENSG00000156711	1.942874846	0.003248324	MAPK13
ENSG00000165672	1.826047902	0.003274293	PRDX3
ENSG00000166405	1.972683392	0.003329147	RIC3
ENSG00000166147	1.290377957	0.003359498	FBN1
ENSG00000024526	2.269674339	0.003373812	DEPDC1
ENSG00000114988	1.801253482	0.003373812	LMAN2L
ENSG00000145794	3.073882541	0.003394904	MEGF10
ENSG00000261210	4.902288856	0.003413275	CLEC19A
ENSG00000123360	1.467608573	0.003414724	PDE1B
ENSG00000184357	1.771828019	0.00345652	HIST1H1B

ENSG00000172586	1.843377858	0.003474407	CHCHD1
ENSG00000110074	1.12681087	0.003482206	FOXRED1
ENSG00000130816	1.224813336	0.003486002	DNMT1
ENSG00000068724	1.325489487	0.003495659	TTC7A
ENSG00000183304	2.071969388	0.003509398	FAM9A
ENSG00000182255	3.218112369	0.003510872	KCNA4
ENSG00000109046	0.990460791	0.003510872	WSB1
ENSG00000257242	3.945579594	0.00352187	LINC01619
ENSG00000100226	1.289204464	0.003548733	GTPBP1
ENSG00000183856	1.506937319	0.00355678	IQGAP3
ENSG00000214114	2.232500633	0.00355678	MYCBP
ENSG00000163584	1.425338367	0.003557278	RPL22L1
ENSG00000148019	1.313043662	0.003572968	CEP78
ENSG00000153234	2.061821944	0.003604694	NR4A2
ENSG00000101138	1.413698957	0.003624736	CSTF1
ENSG00000068971	1.753207083	0.003630545	PPP2R5B
ENSG00000157303	1.695074243	0.003630545	SUSD3
ENSG00000250722	1.967393421	0.003641028	SELENOP
ENSG00000139133	1.496938192	0.003675594	ALG10
ENSG00000115295	1.623844435	0.003675594	CLIP4
ENSG00000131435	3.713628634	0.003752498	PDLIM4
ENSG00000072501	1.1846659	0.003754716	SMC1A
ENSG00000145391	1.345912373	0.003782505	SETD7
ENSG00000116237	1.711663145	0.003787753	ICMT
ENSG00000060558	1.533737998	0.003802027	GNA15
ENSG00000100441	1.159888498	0.003802027	KHNYN
ENSG00000105617	3.973610164	0.003802027	LENG1
ENSG00000132334	1.625259462	0.003802027	PTPRE
ENSG00000076382	1.370110053	0.003802027	SPAG5
ENSG00000144118	1.150051478	0.003802845	RALB
ENSG00000174038	2.080069816	0.003833525	C9orf131
ENSG00000274542	6.800931876	0.003837902	CHRNA7
ENSG00000171310	1.421342827	0.003837902	CHST11
ENSG00000106078	2.139064976	0.003837902	COBL
ENSG00000173145	1.435015287	0.003837902	NOC3L
ENSG00000274474	1.436086245	0.003838426	YWHAE
ENSG00000137841	1.178515169	0.003884964	PLCB2
ENSG00000172382	1.933973887	0.003914159	PRSS27
ENSG00000170903	1.570783312	0.00392244	MSANTD4
ENSG00000085662	1.403844012	0.003932542	AKR1B1
ENSG00000136731	1.34354136	0.003943477	UGGT1
ENSG00000188818	2.13847284	0.003947757	ZDHHC11
ENSG00000198042	1.590129704	0.003962659	MAK16
ENSG00000165669	1.107449949	0.003991068	FAM204A
ENSG00000166257	1.931245781	0.004006933	SCN3B
ENSG00000276234	1.227723938	0.004006933	TADA2A
ENSG00000156860	1.24042391	0.004033307	FBRS
ENSG00000204301	3.052503472	0.004044145	NOTCH4
ENSG00000186767	1.269002733	0.004044145	SPIN4
ENSG00000109919	1.604201541	0.004122489	MTCH2
ENSG00000111452	1.638124036	0.004135751	ADGRD1
ENSG00000127586	1.598272293	0.004135751	CHTF18
ENSG00000134901	1.724706096	0.004135751	KDELC1
ENSG00000110077	2.76129034	0.004135751	MS4A6A
ENSG00000140538	2.463559703	0.004135751	NTRK3
ENSG00000117450	1.508970946	0.004135751	PRDX1
ENSG00000113369	1.590311241	0.004174305	ARRDC3
ENSG00000185090	2.583957541	0.004174305	MANEAL
ENSG00000101856	1.519610537	0.004174305	PGRMC1
ENSG00000125870	1.377028107	0.004174305	SNRPB2
ENSG00000149591	2.152511028	0.004174305	TAGLN
ENSG00000275246	1.600127648	0.004174305	TLCD2
ENSG00000159958	1.740170721	0.004174305	TNFRSF13C
ENSG00000179041	1.846240062	0.004191504	RRS1
ENSG00000060069	1.850808054	0.004196676	CTDP1
ENSG00000119771	2.29043958	0.004239081	KLHL29
ENSG00000196139	1.985947166	0.004261761	AKR1C3

ENSG00000114904	1.657377468	0.004261761	NEK4
ENSG00000138411	2.437320875	0.004263498	HECW2
ENSG00000115421	1.057749519	0.004267511	PAPOLG
ENSG00000145675	1.205235347	0.004270674	PIK3R1
ENSG00000115364	1.274159208	0.004276279	MRPL19
ENSG00000100028	1.453803867	0.004279312	SNRPD3
ENSG00000077150	1.914359804	0.004289238	NFKB2
ENSG00000198743	1.162303579	0.004307179	SLC5A3
ENSG00000099219	1.482793917	0.004347985	ERMP1
ENSG00000152404	1.230327123	0.004352101	CWF19L2
ENSG00000274290	1.889090382	0.004365438	HIST1H2BE
ENSG00000161013	1.378168787	0.004367279	MGAT4B
ENSG00000164674	2.952855958	0.004383581	SYTL3
ENSG00000187790	1.199594114	0.00441009	FANCM
ENSG00000135604	2.697465366	0.00445858	STX11
ENSG00000105011	1.727248117	0.004507041	ASF1B
ENSG00000166912	1.555462786	0.004535745	MTMR10
ENSG00000041357	1.50139695	0.004535745	PSMA4
ENSG00000089335	1.060531122	0.004561402	ZNF302
ENSG00000164867	2.355829024	0.004604126	NOS3
ENSG00000143344	2.379598616	0.004604265	RGL1
ENSG00000160883	4.344588629	0.00461622	HK3
ENSG00000075643	2.076716934	0.004621867	MOCOS
ENSG00000121101	2.582817522	0.004628825	TEX14
ENSG00000205022	2.96953884	0.004647282	PABPN1L
ENSG00000077800	2.375695571	0.00467593	FKBP6
ENSG00000165304	1.929098084	0.00467593	MELK
ENSG00000006530	1.334709695	0.004677506	AGK
ENSG00000175189	4.423049789	0.004679509	INHBC
ENSG00000118412	1.318299691	0.004680777	CASP8AP2
ENSG00000087263	1.296072664	0.004693757	OGFOD1
ENSG00000203852	1.387033323	0.004705661	HIST2H3A
ENSG00000203811	1.387033323	0.004705661	HIST2H3C
ENSG00000065621	1.291490876	0.004707621	GSTO2
ENSG00000020181	1.016893452	0.004710753	ADGRA2
ENSG00000183530	1.347349392	0.004721805	PRR14L
ENSG00000130300	1.949218013	0.004776598	PLVAP
ENSG00000133477	1.529867972	0.004804233	FAM83F
ENSG00000204138	1.384996934	0.004818751	PHACTR4
ENSG00000157542	1.667602324	0.004833287	KCNJ6
ENSG00000120903	1.967583523	0.004837919	CHRNA2
ENSG00000197943	1.037169367	0.00484358	PLCG2
ENSG00000022567	2.080491716	0.004875528	SLC45A4
ENSG00000275118	1.779644177	0.004876204	MBOAT7
ENSG00000119318	1.243991972	0.004896393	RAD23B
ENSG00000225697	1.226183694	0.004896393	SLC26A6
ENSG00000100242	1.299280659	0.004896393	SUN2
ENSG00000011332	2.216660725	0.004902927	DPF1
ENSG00000020577	1.600484781	0.004907643	SAMD4A
ENSG00000206505	2.354922455	0.004964171	HLA A
ENSG00000254685	2.066381145	0.004964264	FPGT
ENSG00000150768	1.694973305	0.004985465	DLAT
ENSG00000076344	2.35911036	0.004985465	RGS11
ENSG00000123737	1.452612374	0.004991111	EXOSC9
ENSG00000188263	5.613817821	0.004991111	IL17REL
ENSG00000169288	1.568774758	0.004991111	MRPL1
ENSG00000113924	5.2548152	0.005004004	HGD
ENSG00000100312	2.293344022	0.005088777	ACR
ENSG00000277775	2.061454692	0.005118465	HIST1H3F
ENSG00000139269	2.742812148	0.005123189	INHBE
ENSG00000099338	1.630377899	0.005127858	CATSPERG
ENSG00000108590	1.971717677	0.005188715	MED31
ENSG00000164877	1.40769639	0.005189118	MICALL2
ENSG00000158747	2.158942936	0.005205478	NBL1
ENSG00000169255	1.579135546	0.005226335	B3GALNT1
ENSG00000067064	1.45300286	0.005226335	IDI1
ENSG00000179564	3.60842845	0.005226335	LSMEM2

ENSG00000165030	1.531286246	0.005226335	NFIL3
ENSG00000124568	4.538180501	0.005226335	SLC17A1
ENSG00000163898	2.282742557	0.005230764	LIPH
ENSG00000198176	1.34300919	0.005230764	TFDP1
ENSG00000112742	1.772781511	0.005230764	TTK
ENSG00000119403	1.031535959	0.00524087	PHF19
ENSG00000172590	1.31732053	0.005261987	MRPL52
ENSG00000147168	1.60519647	0.005269338	IL2RG
ENSG00000100528	1.444825155	0.005274848	CNIH1
ENSG00000186716	1.244859377	0.005284784	BCR
ENSG00000182004	1.594157384	0.005284784	SNRPE
ENSG00000160908	1.407973683	0.005286631	ZNF394
ENSG00000170779	1.847622865	0.005289418	CDCA4
ENSG00000138442	1.656889778	0.005314091	WDR12
ENSG00000153303	3.087505155	0.005338491	FRMD1
ENSG00000177426	1.443983072	0.005378771	TGIF1
ENSG00000169762	1.302709844	0.005400686	TAPT1
ENSG00000009694	2.958079499	0.00542515	TENM1
ENSG00000075131	1.853002588	0.005435492	TIPIN
ENSG00000172172	1.755101249	0.00544211	MRPL13
ENSG00000196091	2.828647962	0.00544211	MYBPC1
ENSG00000006432	1.683508818	0.005449361	MAP3K9
ENSG00000114204	3.800697535	0.005481399	SERPINI2
ENSG00000116661	4.951713282	0.005482806	FBXO2
ENSG00000129744	4.012694701	0.005510112	ART1
ENSG00000187260	2.463099637	0.005510112	WDR86
ENSG00000177383	1.661099718	0.005548604	MAGEF1
ENSG00000167641	1.798068558	0.005555839	PPP1R14A
ENSG00000099290	1.303843498	0.005568552	WASHC2A
ENSG00000128596	1.163588084	0.005587459	CCDC136
ENSG00000165194	2.638496787	0.005592199	PCDH19
ENSG00000176974	1.255701242	0.005622127	SHMT1
ENSG00000134996	1.473775576	0.005648586	OSTF1
ENSG00000130699	1.231584361	0.005648586	TAF4
ENSG00000132436	1.765347013	0.005651932	FIGNL1
ENSG00000075336	1.832148553	0.005665081	TIMM21
ENSG00000144827	1.605484613	0.005703983	ABHD10
ENSG00000173915	1.430423264	0.005703983	USMG5
ENSG00000100714	1.180745253	0.005731962	MTHFD1
ENSG00000132911	4.57496194	0.005866998	NMUR2
ENSG00000281742	1.584999052	0.005880388	MCCC2
ENSG00000008311	1.3354697	0.005881621	AASS
ENSG00000091428	2.078241136	0.005915837	RAPGEF4
ENSG00000197063	1.734035787	0.005925205	MAFG
ENSG00000197771	1.597031623	0.005925205	MCMBP
ENSG00000166181	1.231174849	0.005930347	API5
ENSG00000155962	1.805298948	0.005931678	CLIC2
ENSG00000120675	1.563360168	0.005931678	DNAJC15
ENSG00000134532	2.154419176	0.005931678	SOX5
ENSG00000184445	0.926616708	0.005957028	KNTC1
ENSG00000116478	0.902874114	0.005971153	HDAC1
ENSG00000145375	1.228331201	0.006093504	SPATA5
ENSG00000124208	6.524228768	0.006093504	TMEM189 UBE2V1
ENSG00000169857	1.490954832	0.006140643	AVEN
ENSG00000121005	1.909255585	0.006163634	CRISPLD1
ENSG00000156858	1.415354545	0.006190284	PRR14
ENSG00000137834	1.839690182	0.006190284	SMAD6
ENSG00000089048	1.419603885	0.006190808	ESF1
ENSG00000233345	2.732230837	0.006190808	MSH5
ENSG00000115687	1.266380202	0.006190808	PASK
ENSG00000112759	1.690828838	0.006190808	SLC29A1
ENSG00000082014	1.825754446	0.006190808	SMARCD3
ENSG00000215397	3.714885026	0.006191009	SCRT2
ENSG00000129757	1.550206615	0.006206668	CDKN1C
ENSG00000133561	1.766030593	0.006206668	GIMAP6
ENSG00000178297	1.659438593	0.006206668	TMPRSS9
ENSG00000105447	1.868560866	0.0062643	GRWD1

ENSG00000166133	1.878750302	0.00627195	RPUSD2
ENSG00000177853	1.220720287	0.006276821	ZNF518A
ENSG00000160957	1.386185603	0.006288879	RECQL4
ENSG00000101000	2.429573899	0.006317571	PROCR
ENSG00000135045	2.324329287	0.006322274	C9orf40
ENSG00000121579	1.269090384	0.006354939	NAA50
ENSG00000085265	1.357709428	0.006405768	FCN1
ENSG00000130589	1.325271939	0.00640994	HELZ2
ENSG00000120696	1.346960046	0.006452496	KBTBD7
ENSG00000013523	1.181751871	0.006459656	ANGEL1
ENSG00000166881	1.180717219	0.006465492	NEMP1
ENSG00000156030	1.820242547	0.006503531	ELMSAN1
ENSG00000185950	1.587171316	0.006540221	IRS2
ENSG00000228836	5.888539538	0.006590705	CT45A5
ENSG00000277161	3.717940659	0.006590705	PIGW
ENSG00000275464	1.449894779	0.006657048	LOC102724159
ENSG00000120526	1.827339505	0.006657048	NUDCD1
ENSG00000206455	2.84509105	0.006657048	TCF19
ENSG00000234674	2.84509105	0.006657048	TCF19
ENSG00000156261	1.039891991	0.006661966	CCT8
ENSG00000115241	1.367275662	0.006665684	PPM1G
ENSG00000081721	1.305823284	0.00669276	DUSP12
ENSG00000162607	1.291842907	0.00669276	USP1
ENSG00000143149	1.392532847	0.00671762	ALDH9A1
ENSG00000183023	2.319306922	0.006736217	SLC8A1
ENSG00000228278	3.337340991	0.00679515	ORM2
ENSG00000142528	1.545355932	0.00679515	ZNF473
ENSG00000139687	1.071994374	0.006900193	RB1
ENSG00000241685	1.411033589	0.006905008	ARPC1A
ENSG00000085117	1.563165126	0.006940712	CD82
ENSG00000088992	1.630874402	0.006989064	TESC
ENSG00000198830	1.326460819	0.007042544	HMGN2
ENSG00000085831	2.131424456	0.007047918	TTC39A
ENSG00000154678	1.484978059	0.007118906	PDE1C
ENSG00000153015	1.248238802	0.007147102	CWC27
ENSG00000127081	1.372631194	0.007159168	ZNF484
ENSG00000157978	1.754164579	0.00717457	LDLRAP1
ENSG00000177108	2.900731981	0.00723997	ZDHHC22
ENSG00000233136	2.207746321	0.007255237	USP17L11
ENSG00000162521	1.094817603	0.007257143	RBBP4
ENSG00000236334	1.663902729	0.007263406	PPIAL4G
ENSG00000179958	1.815652658	0.007269237	DCTPP1
ENSG00000243492	2.5099197	0.007279303	HLA L
ENSG00000165792	1.132580932	0.007282271	METTL17
ENSG00000101773	1.387019061	0.007345156	RBBP8
ENSG00000136518	1.213389347	0.007366268	ACTL6A
ENSG00000015592	2.489606519	0.007378432	STMN4
ENSG00000173110	4.250479301	0.007392048	HSPA6
ENSG00000179387	1.663776696	0.007400901	ELMOD2
ENSG00000156475	1.347643425	0.007400901	PPP2R2B
ENSG00000168209	1.806991353	0.007448699	DDIT4
ENSG00000118702	6.238651866	0.007448699	GHRH
ENSG00000143434	1.228387651	0.007448699	SEMA6C
ENSG00000189091	1.275437036	0.007448699	SF3B3
ENSG00000243667	2.118727654	0.007464273	WDR92
ENSG00000089006	0.94840949	0.007583617	SNX5
ENSG00000109572	1.138647879	0.007620316	CLCN3
ENSG00000184752	1.600470972	0.007620316	NDUFA12
ENSG00000073169	1.746409034	0.007620316	SELENOO
ENSG00000127526	1.251823488	0.007620316	SLC35E1
ENSG00000175216	1.04032636	0.007640703	CKAP5
ENSG00000181722	1.172752927	0.007641009	ZBTB20
ENSG00000260596	1.880290205	0.007652671	DUX4
ENSG00000188428	1.470866395	0.007659064	BLOC1S5
ENSG00000101695	1.241746231	0.007696777	RNF125
ENSG00000092201	1.119348264	0.007699895	SUPT16H
ENSG00000161958	1.72000388	0.007754877	FGF11

ENSG00000146648	2.334651527	0.007759749	EGFR
ENSG00000187902	2.994538833	0.007765083	SHISA7
ENSG00000214787	1.806146147	0.00779157	MS4A4E
ENSG00000149136	1.29340815	0.007836899	SSRP1
ENSG00000136141	1.075636097	0.007912552	LRCH1
ENSG00000197870	3.61919038	0.007912552	PRB3
ENSG00000120156	1.619944292	0.007912552	TEK
ENSG00000111196	1.323275815	0.007913646	MAGOHB
ENSG00000129951	1.686624618	0.007927534	PLPPR3
ENSG00000005379	3.5184503	0.007952909	TSPOAP1
ENSG00000141437	6.164792674	0.007954421	SLC25A52
ENSG00000233622	1.901732506	0.007994476	CYP2T1P
ENSG00000086991	2.148194481	0.007994476	NOX4
ENSG00000171793	1.408450156	0.008011135	CTPS1
ENSG00000107331	0.989842434	0.008031138	ABCA2
ENSG00000090382	1.681499678	0.008031138	LYZ
ENSG00000229859	2.060645068	0.008031138	PGA3
ENSG00000180043	2.852921115	0.008032832	FAM71E2
ENSG00000004779	1.75746862	0.008032832	NDUFAB1
ENSG00000085760	1.502333649	0.008177372	MTIF2
ENSG00000164175	5.675959312	0.008180502	SLC45A2
ENSG00000166183	3.674486409	0.008204043	ASPG
ENSG00000135535	1.280326143	0.008204043	CD164
ENSG00000185182	4.79848925	0.008204043	GOLGA8EP
ENSG00000142945	2.252817217	0.008204043	KIF2C
ENSG00000092345	4.103247154	0.008250239	DAZL
ENSG00000108474	1.038268418	0.008252721	PIGL
ENSG00000124193	1.161612424	0.008266582	SRSF6
ENSG00000023516	1.04579089	0.008298683	AKAP11
ENSG00000166263	1.380061726	0.008303633	STXBP4
ENSG00000125775	2.281638064	0.008304978	SDCBP2
ENSG00000099625	2.280151145	0.008306227	CBARP
ENSG00000206306	9.005249644	0.008307595	HLA DRB1
ENSG00000147166	2.016626965	0.008307595	ITGB1BP2
ENSG00000067842	2.614563081	0.008316296	ATP2B3
ENSG00000162889	1.327362297	0.008316296	MAPKAPK2
ENSG00000223760	2.954296448	0.008316296	MED15P9
ENSG00000277104	6.142769206	0.008316296	TADA2A
ENSG00000184465	1.418328262	0.008316296	WDR27
ENSG00000097046	1.616065701	0.008321598	CDC7
ENSG00000009954	1.04306041	0.008327288	BAZ1B
ENSG00000152518	1.607547713	0.008327288	ZFP36L2
ENSG00000111481	1.175085	0.008338187	COPZ1
ENSG00000157933	4.296215543	0.008338187	SKI
ENSG00000129244	1.934849384	0.008340718	ATP1B2
ENSG00000197299	1.407219434	0.008340718	BLM
ENSG00000140718	1.172420737	0.008340718	FTO
ENSG00000089818	1.493490174	0.008340718	NECAP1
ENSG00000121578	1.077480797	0.008371516	B4GALT4
ENSG00000231021	7.068140137	0.008371516	HLA DRB4
ENSG00000033178	1.089814059	0.008371516	UBA6
ENSG00000111087	2.304997488	0.008389961	GLI1
ENSG00000276286	6.111018953	0.008418003	ADAM2
ENSG00000104312	1.112459019	0.008511427	RIPK2
ENSG00000069188	1.558291816	0.008546881	SDK2
ENSG00000179921	2.634637239	0.008563101	GPBAR1
ENSG00000095319	0.949233194	0.008565592	NUP188
ENSG00000124635	1.636937455	0.008598755	HIST1H2BJ
ENSG00000136826	2.16340185	0.008598755	KLF4
ENSG00000277140	3.382064225	0.008598755	MARF1
ENSG00000154358	0.958131282	0.008598755	OBSCN
ENSG00000100979	1.411308448	0.008598755	PLTP
ENSG00000171928	1.39821857	0.008598755	TVP23B
ENSG00000155367	3.162479927	0.008613634	PPM1J
ENSG00000166839	1.473254047	0.008621777	ANKDD1A
ENSG00000168952	2.131824488	0.008704823	STXBP6
ENSG00000164638	1.67557183	0.008732156	SLC29A4

ENSG00000127184	1.135052963	0.008755544	COX7C
ENSG00000159433	0.940280159	0.008779389	STARD9
ENSG00000100749	1.181378414	0.008779389	VRK1
ENSG00000112110	2.240788245	0.008829296	MRPL18
ENSG00000164056	1.239648555	0.008832215	SPRY1
ENSG00000166477	1.212099389	0.008833082	LEO1
ENSG00000121931	1.333716426	0.008901767	LRIF1
ENSG00000154415	4.811505495	0.008926401	PPP1R3A
ENSG00000055732	1.665678451	0.009097709	MCOLN3
ENSG00000214491	1.52062648	0.009116974	SEC14L6
ENSG00000162069	2.369918846	0.009177889	BICDL2
ENSG00000006210	2.232110207	0.009177889	CX3CL1
ENSG00000175606	1.644037875	0.009177889	TMEM70
ENSG00000178171	2.85928264	0.00918804	AMER3
ENSG00000164303	2.638736299	0.009245414	ENPP6
ENSG00000177697	1.790789641	0.009246775	CD151
ENSG00000143179	1.533978548	0.009246775	UCK2
ENSG00000131732	1.43269714	0.009278577	ZCCHC9
ENSG00000229676	1.629662178	0.009278577	ZNF492
ENSG00000118194	1.911603492	0.009403973	TNNT2
ENSG00000153071	1.867344793	0.009434318	DAB2
ENSG00000204583	4.876567012	0.009450609	LRCOL1
ENSG00000166069	2.743874741	0.009450609	TMCO5A
ENSG00000101493	1.56496551	0.009450609	ZNF516
ENSG00000109452	1.022148862	0.009488976	INPP4B
ENSG00000125462	1.934747739	0.009515069	C1orf61
ENSG00000196937	1.764406914	0.009515069	FAM3C
ENSG00000144136	1.164716661	0.009515069	SLC20A1
ENSG00000106484	1.253075235	0.0095563	MEST
ENSG00000277422	2.004112657	0.009586491	REXO1L2P
ENSG00000198865	1.365008084	0.009597372	CCDC152
ENSG00000116032	2.033630719	0.009597372	GRIN3B
ENSG00000163531	1.733879251	0.009598193	NFASC
ENSG00000115392	1.391499424	0.009632763	FANCL
ENSG00000106591	1.200198651	0.009632763	MRPL32
ENSG00000188536	3.555761554	0.009720975	HBA2
ENSG00000206240	8.040330788	0.009772039	HLA DRB1
ENSG00000119013	2.155060519	0.009772039	NDUFB3
ENSG00000276293	1.094557619	0.009772039	PIP4K2B
ENSG00000234511	1.759265801	0.009788868	C5orf58
ENSG00000126001	1.313174235	0.009794365	CEP250
ENSG00000093134	1.542812507	0.009794365	VNN3
ENSG00000164687	1.449219677	0.009804865	FABP5
ENSG00000167874	2.325152383	0.009804865	TMEM88
ENSG00000125901	1.58448351	0.009927009	MRPS26
ENSG00000196843	1.920663911	0.009945247	ARID5A
ENSG00000129235	2.147786392	0.009989615	TXNDC17
ENSG00000184905	3.25599323	0.010004445	TCEAL2
ENSG00000183508	2.145990332	0.010008926	FAM46C
ENSG00000166948	5.329378002	0.010008926	TGM6
ENSG00000116604	1.301336009	0.010011	MEF2D
ENSG00000183605	1.72059035	0.010011	SFXN4
ENSG00000273983	1.845376818	0.010031635	HIST1H3G
ENSG00000185436	2.956139129	0.010031635	IFNLR1
ENSG00000141622	2.002959736	0.010031635	RNF165
ENSG00000143933	1.145597093	0.010170029	CALM2
ENSG00000144283	1.182783317	0.010184834	PKP4
ENSG00000187268	3.098728128	0.010198731	FAM9C
ENSG00000057608	1.197634546	0.010198731	GDI2
ENSG00000144554	0.999814426	0.010247307	FANCD2
ENSG00000131153	1.673490294	0.010304245	GINS2
ENSG00000186417	2.293787396	0.010355766	GLDN
ENSG00000185262	1.611943878	0.010355766	UBALD2
ENSG00000128951	1.169687264	0.010360011	DUT
ENSG00000174013	1.313735047	0.010416912	FBXO45
ENSG00000110852	1.897735555	0.010425128	CLEC2B
ENSG00000126524	1.278096527	0.010457887	SBDS

ENSG00000009844	1.553822084	0.010468488	VTA1
ENSG00000112149	1.896193317	0.010495225	CD83
ENSG00000159086	1.045269478	0.010496985	PAXBP1
ENSG00000182831	1.050178522	0.010531385	C16orf72
ENSG00000101203	2.511189401	0.010532017	COL20A1
ENSG00000144736	1.316081044	0.010532991	SHQ1
ENSG00000074964	2.811845447	0.010571213	ARHGEF10L
ENSG00000086061	1.181327856	0.010571213	DNAJA1
ENSG00000145934	3.256106878	0.010571213	TENM2
ENSG00000162772	1.779424532	0.010648467	ATF3
ENSG00000140374	1.238907082	0.010648467	ETFA
ENSG00000169403	1.393936814	0.010648467	PTAFR
ENSG00000106069	1.523400438	0.01066329	CHN2
ENSG00000180776	1.299676512	0.01066329	ZDHHC20
ENSG00000163029	1.049899088	0.010664634	SMC6
ENSG00000111049	5.471830714	0.010687324	MYF5
ENSG00000118655	1.708757035	0.010722365	DCLRE1B
ENSG00000181610	1.636752601	0.010858038	MRPS23
ENSG00000141682	1.938384531	0.010858038	PMAIP1
ENSG00000178217	2.697362275	0.010858038	SH2D4B
ENSG00000178996	1.483943644	0.010936765	SNX18
ENSG00000149256	2.274528577	0.010948242	TENM4
ENSG00000203618	2.133539908	0.010951354	GP1BB
ENSG00000065485	1.305825494	0.010951354	PDIA5
ENSG00000134109	1.02446809	0.011084023	EDEM1
ENSG00000171115	1.588688092	0.011084023	GIMAP8
ENSG00000155438	1.67077537	0.011084023	NIFK
ENSG00000274843	3.119499799	0.011108476	MUC20
ENSG00000277753	3.119499799	0.011108476	MUC20
ENSG00000133321	1.82469965	0.011108476	RARRES3
ENSG00000009724	1.429464755	0.011138854	MASP2
ENSG00000198842	1.652548725	0.011164478	DUSP27
ENSG00000177947	2.137643036	0.011183871	ODF3
ENSG00000100678	1.15934889	0.011183871	SLC8A3
ENSG00000172508	1.558906403	0.011184708	CARNS1
ENSG00000163026	2.02373559	0.011198161	WDCP
ENSG00000172340	1.448205074	0.011222767	SUCLG2
ENSG00000100815	1.317265094	0.011225658	TRIP11
ENSG00000162552	2.862005771	0.011225658	WNT4
ENSG00000137747	1.62946044	0.011290852	TMPRSS13
ENSG00000206395	2.011476084	0.011292664	DDAH2
ENSG00000095951	1.198982131	0.011292664	HIVEP1
ENSG00000136750	3.005315959	0.011293579	GAD2
ENSG00000146856	1.738222468	0.011300851	AGBL3
ENSG00000184730	1.589745953	0.01134038	APOBR
ENSG00000142227	1.233949579	0.011374257	EMP3
ENSG00000142207	1.059737953	0.011381315	URB1
ENSG00000105854	1.059633782	0.01140247	PON2
ENSG00000164649	1.165832621	0.01140537	CDCA7L
ENSG00000198015	1.064883349	0.011574024	MRPL42
ENSG00000121067	0.981667468	0.011574024	SPOP
ENSG00000254535	1.499715387	0.011642254	PABPC4L
ENSG00000160360	0.989333903	0.011662143	GPSM1
ENSG00000178053	1.690071606	0.011732342	MLF1
ENSG00000112902	1.888876115	0.011732342	SEMA5A
ENSG00000123243	1.517918185	0.011736647	ITIH5
ENSG00000157570	1.663939203	0.011736647	TSPAN18
ENSG00000103365	1.043673622	0.011737259	GGA2
ENSG00000146233	5.986634337	0.011757842	CYP39A1
ENSG00000064989	1.030033672	0.011761704	CALCRL
ENSG00000166816	1.719532759	0.011798559	LDHD
ENSG00000116299	1.889776276	0.011805565	KIAA1324
ENSG00000171385	2.543004244	0.011860827	KCND3
ENSG00000151304	1.094635656	0.011954344	SRFBP1
ENSG00000196352	1.426195412	0.011956255	CD55
ENSG00000012232	1.14957136	0.011961876	EXTL3
ENSG00000107518	2.725641779	0.012096215	ATRNL1

ENSG00000114767	1.987930354	0.012118463	RRP9
ENSG00000133028	1.151762829	0.012118463	SCO1
ENSG00000214517	1.149143156	0.012145794	PPME1
ENSG00000145362	2.081034668	0.012155257	ANK2
ENSG00000157240	1.999579345	0.012155257	FZD1
ENSG00000109158	2.60899858	0.012155257	GABRA4
ENSG00000166206	1.93493118	0.012155257	GABRB3
ENSG00000133706	1.239637291	0.012155257	LARS
ENSG00000174175	1.782271168	0.012216789	SELP
ENSG00000197312	1.116908113	0.012222464	DDI2
ENSG00000273706	3.356153472	0.012222464	LHX1
ENSG00000135624	1.126328749	0.01224373	CCT7
ENSG00000172339	1.759163982	0.012253807	ALG14
ENSG00000006695	1.652124904	0.012266508	COX10
ENSG00000134222	2.094490247	0.012266508	PSRC1
ENSG00000163104	1.19721371	0.012266508	SMARCAD1
ENSG00000128973	1.162020327	0.012330939	CLN6
ENSG00000166508	1.11643075	0.012330939	MCM7
ENSG00000197483	1.241486075	0.012343905	ZNF628
ENSG00000122483	0.975382912	0.012364151	CCDC18
ENSG00000198756	2.352469638	0.012368271	COLGALT2
ENSG00000135451	1.440361973	0.012368271	TROAP
ENSG00000122783	1.431063704	0.012368551	C7orf49
ENSG00000066322	1.272064854	0.012372745	ELOVL1
ENSG00000164611	1.878578951	0.012405305	PTTG1
ENSG00000100867	1.377440985	0.012414417	DHRS2
ENSG00000156110	1.121818717	0.012416588	ADK
ENSG00000131462	1.280619178	0.012431214	TUBG1
ENSG00000132432	1.418533168	0.012494069	SEC61G
ENSG00000161835	3.90493084	0.012498601	GRASP
ENSG00000184588	1.710277229	0.012498601	PDE4B
ENSG00000068354	1.373835001	0.012498601	TBC1D25
ENSG00000075223	1.71348329	0.012500863	SEMA3C
ENSG00000188760	2.999649409	0.012500863	TMEM198
ENSG00000149243	1.923815701	0.012540745	KLHL35
ENSG00000196793	2.290523958	0.012540745	ZNF239
ENSG00000147174	2.521808672	0.012630388	GCNA
ENSG00000138182	1.509674795	0.012630388	KIF20B
ENSG00000204099	3.890285299	0.012630388	NEU4
ENSG00000277926	3.890285299	0.012630388	NEU4
ENSG00000241119	6.252839957	0.012630388	UGT1A9
ENSG00000163637	2.696779619	0.012646782	PRICKLE2
ENSG00000107736	1.781873681	0.012761981	CDH23
ENSG00000115165	1.234191926	0.012761981	CYTIP
ENSG00000176358	1.305496658	0.012768022	TAC4
ENSG00000239732	2.935065234	0.012804222	TLR9
ENSG00000123933	1.318937612	0.012822953	MXD4
ENSG00000149782	1.307705558	0.01288557	PLCB3
ENSG00000004455	1.113491084	0.012942701	AK2
ENSG00000179833	1.300115316	0.012983005	SERTAD2
ENSG00000163166	1.088948026	0.013031684	IWS1
ENSG00000117174	1.055428083	0.013066264	ZNHIT6
ENSG00000198633	4.241659247	0.013068694	ZNF534
ENSG00000130595	1.489542403	0.013100099	TNNT3
ENSG00000080573	3.018460451	0.013105539	COL5A3
ENSG00000106541	3.759717821	0.013107763	AGR2
ENSG00000152076	3.157434053	0.013107763	CCDC74B
ENSG00000102230	1.434357536	0.013186151	PCYT1B
ENSG00000099994	2.80059349	0.013268624	SUSD2
ENSG00000116721	2.86605118	0.013269015	PRAMEF1
ENSG00000174282	1.413170666	0.013272228	ZBTB4
ENSG00000280688	5.792468997	0.013285548	CEP72
ENSG00000154380	1.559485482	0.013285548	ENAH
ENSG00000080608	1.284449098	0.013285548	PUM3
ENSG00000188089	2.351076928	0.013307938	PLA2G4E
ENSG00000129810	1.699138433	0.013332895	SGO1
ENSG00000256235	1.651894432	0.013372483	SMIM3

ENSG00000206013	3.885157298	0.013391628	IFITM5
ENSG00000126261	1.122453907	0.013391628	UBA2
ENSG00000112033	2.071100079	0.013449503	PPARD
ENSG00000126950	2.411430097	0.013451882	TMEM35A
ENSG00000172543	1.39582987	0.01348848	CTSW
ENSG00000204439	6.469622382	0.013526604	C6orf47
ENSG00000242950	1.253719162	0.013618809	ERVW 1
ENSG00000172602	1.922308194	0.013630928	RND1
ENSG00000171241	1.620274762	0.013630928	SHCBP1
ENSG00000115053	1.207353832	0.013641201	NCL
ENSG00000153406	1.566703016	0.013645345	NMRAL1
ENSG00000134070	1.736604334	0.013725654	IRAK2
ENSG00000090889	2.194244771	0.013725654	KIF4A
ENSG00000072657	1.836118007	0.013725654	TRHDE
ENSG00000181444	1.243474095	0.013725654	ZNF467
ENSG00000183978	1.88961546	0.013729279	COA3
ENSG00000188981	2.014227875	0.013729279	MSANTD1
ENSG00000129317	1.135999514	0.013729279	PUS7L
ENSG00000127129	2.983228638	0.013826931	EDN2
ENSG00000135052	1.127570733	0.013826931	GOLM1
ENSG00000111237	1.300895855	0.013886686	VPS29
ENSG00000143028	2.628809154	0.013923664	SYPL2
ENSG00000022840	1.400894972	0.013972471	RNF10
ENSG00000222009	1.676146338	0.014051646	BTBD19
ENSG00000159079	1.267723297	0.014051646	C21orf59
ENSG00000158669	1.097342155	0.014051646	GPAT4
ENSG00000119285	1.167060106	0.014051646	HEATR1
ENSG00000171246	2.201661441	0.014051646	NPTX1
ENSG00000184226	1.555058494	0.014051646	PCDH9
ENSG00000154146	1.391564686	0.01413147	NRGN
ENSG00000110700	1.026712179	0.01413147	RPS13
ENSG00000176490	2.555033605	0.014176727	DIRAS1
ENSG00000166845	1.356821728	0.014192649	C18orf54
ENSG00000153936	1.797217965	0.014280088	HS2ST1
ENSG00000146722	1.92361612	0.014290809	LOC541473
ENSG00000239900	1.205218784	0.014337904	ADSL
ENSG00000155115	1.8405654	0.014337904	GTF3C6
ENSG00000189410	2.830231747	0.01436801	SH2D5
ENSG00000196922	1.414791855	0.01443529	ZNF252P
ENSG00000144406	1.196705948	0.014461263	UNC80
ENSG00000146555	1.76700559	0.014466061	SDK1
ENSG00000138071	1.234519137	0.014469658	ACTR2
ENSG00000125630	0.991733876	0.014470139	POLR1B
ENSG00000109738	2.448263079	0.014471274	GLRB
ENSG00000280789	1.472714162	0.014484699	PAGR1
ENSG00000113845	1.611753801	0.014484699	TIMMDC1
ENSG00000181126	1.876362339	0.014498009	HLA V
ENSG00000093144	1.301411889	0.014543152	ECHDC1
ENSG00000153395	1.528299018	0.014548585	LPCAT1
ENSG00000127125	1.480874399	0.01456366	PPCS
ENSG00000135749	1.117557762	0.014591581	PCNX2
ENSG00000169169	2.168023155	0.014615372	CPT1C
ENSG00000198734	2.268867393	0.014615372	F5
ENSG00000161888	1.096440735	0.014621706	SPC24
ENSG00000167721	1.141992554	0.014621706	TSR1
ENSG00000105219	2.398129872	0.014635901	CNTD2
ENSG00000162852	1.083358996	0.014715147	CNST
ENSG00000092607	3.136467817	0.014715147	TBX15
ENSG00000162438	2.057019825	0.014719059	CTRC
ENSG00000184305	1.472339357	0.014740538	CCSER1
ENSG00000175538	1.628494801	0.014745777	KCNE3
ENSG00000066557	1.133472585	0.014745777	LRRC40
ENSG00000187144	1.635965599	0.014745777	SPATA21
ENSG00000160803	1.004057296	0.014745777	UBQLN4
ENSG00000167553	1.311099002	0.014787632	TUBA1C
ENSG00000180210	3.488908638	0.014849393	F2
ENSG00000165983	1.407787785	0.014920897	PTER

ENSG00000180900	1.16843965	0.014931209	SCRIB
ENSG00000166428	1.267661237	0.015032209	PLD4
ENSG00000241127	2.053573178	0.015072053	YAE1D1
ENSG00000140057	2.176004239	0.015137955	AK7
ENSG00000157445	3.237332598	0.015137955	CACNA2D3
ENSG00000150776	1.104360987	0.015137955	NKAPD1
ENSG00000197728	1.779039204	0.015139566	RPS26
ENSG00000172650	1.718532286	0.015211979	AGAP5
ENSG00000113552	2.044217127	0.015335664	GNPDA1
ENSG00000124831	1.081079785	0.015358133	LRRFIP1
ENSG00000167106	1.609512089	0.015374997	FAM102A
ENSG00000011143	1.411268037	0.015378644	MKS1
ENSG00000170476	1.296340071	0.015424479	MZB1
ENSG00000038427	2.51731346	0.015482246	VCAN
ENSG00000116133	1.648962572	0.015508016	DHCR24
ENSG00000198952	1.08785005	0.01553584	SMG5
ENSG00000136213	1.403024375	0.015544711	CHST12
ENSG00000166197	1.339684476	0.015548154	NOLC1
ENSG00000184014	1.30046723	0.015561967	DENND5A
ENSG00000131187	2.544255016	0.015573601	F12
ENSG00000081791	1.113960503	0.015573601	KIAA0141
ENSG00000277564	1.835423453	0.015573601	RBFOX2
ENSG00000151500	1.383239645	0.01572288	THYN1
ENSG00000155980	2.486722174	0.015730585	KIF5A
ENSG00000154174	1.065978106	0.015775575	TOMM70
ENSG00000181773	2.477514915	0.015779533	GPR3
ENSG00000179270	2.99174857	0.015819919	C2orf71
ENSG00000164741	1.811355659	0.015819919	DLC1
ENSG00000179097	1.193518127	0.015819919	HTR1F
ENSG00000078668	1.226948904	0.015819919	VDAC3
ENSG00000140030	1.747372178	0.015838901	GPR65
ENSG00000073849	0.965695492	0.01585293	ST6GAL1
ENSG00000102057	1.679168132	0.01585391	KCND1
ENSG00000158864	0.977791619	0.016037364	NDUFS2
ENSG00000196262	1.136698996	0.016066699	PPIA
ENSG00000213390	1.500703997	0.016121185	ARHGAP19
ENSG00000136541	2.040582519	0.016121185	ERMN
ENSG00000196277	1.955008864	0.016121185	GRM7
ENSG00000196878	2.225563362	0.016121185	LAMB3
ENSG00000108055	1.325853316	0.016121185	SMC3
ENSG00000100304	1.360910792	0.016121185	TTLL12
ENSG00000166444	1.344666312	0.016125804	ST5
ENSG00000189350	1.199875549	0.016161292	TOGARAM2
ENSG00000217801	1.285853418	0.01621374	LOC100288175
ENSG00000276644	1.038512791	0.016223299	DACH1
ENSG00000169016	1.340663379	0.016223299	E2F6
ENSG00000188163	2.261529577	0.016223299	FAM166A
ENSG00000174718	1.185788888	0.016223299	KIAA1551
ENSG00000244482	3.231456515	0.016223299	LILRA6
ENSG00000198754	5.385493041	0.016223299	OXCT2
ENSG00000233954	1.505926129	0.016223299	UQCRHL
ENSG00000164902	1.515376828	0.01625069	PHAX
ENSG00000134001	1.154832385	0.016313259	EIF2S1
ENSG00000141551	1.534713898	0.01635364	CSNK1D
ENSG00000172830	1.577960092	0.01635364	SSH3
ENSG00000197279	1.772098199	0.01635364	ZNF165
ENSG00000121486	1.537919016	0.016357621	TRMT1L
ENSG00000139719	1.171489587	0.016357621	VPS33A
ENSG00000080345	0.875105089	0.016380381	RIF1
ENSG00000119185	1.218707589	0.016465709	ITGB1BP1
ENSG00000104549	1.312665473	0.016471705	SQLE
ENSG00000213397	1.327764794	0.016480043	HAUS7
ENSG00000177946	1.416101684	0.016522483	CENPBD1
ENSG00000136108	1.115365341	0.016645876	CKAP2
ENSG00000145833	0.845181311	0.016710916	DDX46
ENSG00000142102	1.481696253	0.016741137	PGGHG
ENSG00000188486	1.085680644	0.016743597	H2AFX

ENSG00000183638	1.424840518	0.016774252	RP1L1
ENSG00000189007	1.041045425	0.016777818	ADAT2
ENSG00000106771	0.967038819	0.016822368	TMEM245
ENSG00000116001	1.27801757	0.016823572	TIA1
ENSG00000155755	1.288040491	0.016827815	TMEM237
ENSG00000122705	1.132405738	0.016837731	CLTA
ENSG00000102100	2.024246054	0.016888132	SLC35A2
ENSG00000177238	1.401791538	0.016989323	TRIM72
ENSG00000173662	2.493804998	0.017002593	TAS1R1
ENSG00000105176	0.971112605	0.017078777	URI1
ENSG00000142864	1.083257067	0.017104096	SERBP1
ENSG00000146674	2.254499508	0.017118343	IGFBP3
ENSG00000115738	1.844476173	0.017127675	ID2
ENSG00000101311	3.15244413	0.017166984	FERMT1
ENSG00000141582	1.324578809	0.017181427	CBX4
ENSG00000127337	1.878839648	0.017181427	YEATS4
ENSG00000116120	1.159540047	0.017185457	FARSB
ENSG00000115484	1.104221732	0.017197404	CCT4
ENSG00000164946	1.452370944	0.017206254	FREM1
ENSG00000109762	2.269643281	0.017226534	SNX25
ENSG00000086730	1.029773816	0.017246808	LAT2
ENSG00000101150	0.971433929	0.017308289	TPD52L2
ENSG00000124562	1.203964478	0.017373651	SNRPC
ENSG00000232423	5.90504843	0.017427805	PRAMEF6
ENSG00000119421	1.658578247	0.017439205	NDUFA8
ENSG00000276910	1.577927179	0.017454915	GTF2H2
ENSG00000055957	2.225861034	0.017478279	ITIH1
ENSG00000105143	1.25271651	0.017494482	SLC1A6
ENSG00000225828	2.311799541	0.017513725	FAM229A
ENSG00000163170	1.506177837	0.01752019	BOLA3
ENSG00000154642	1.188499164	0.01752019	C21orf91
ENSG00000141404	1.9135735	0.01752019	GNAL
ENSG00000150477	1.343043669	0.01752019	KIAA1328
ENSG00000029725	1.10244446	0.01752019	RABEP1
ENSG00000139890	2.254120816	0.01752019	REM2
ENSG00000116171	1.084675777	0.01752019	SCP2
ENSG00000120800	1.051274765	0.01752019	UTP20
ENSG00000100722	1.219599346	0.01752019	ZC3H14
ENSG00000251247	1.238399515	0.017532317	ZNF345
ENSG00000150764	1.744940417	0.017680999	DIXDC1
ENSG00000142347	0.94152046	0.017772488	MYO1F
ENSG00000129675	0.932068435	0.017849755	ARHGEF6
ENSG00000100162	1.188521243	0.017849755	CENPM
ENSG00000164418	2.218504502	0.017849755	GRIK2
ENSG00000136802	0.967380178	0.017849755	LRRC8A
ENSG00000021645	1.976283168	0.017849755	NRXN3
ENSG00000178279	3.610917538	0.017849755	TNP2
ENSG00000118640	1.16610322	0.017849755	VAMP8
ENSG00000165061	2.867580351	0.017849755	ZMAT4
ENSG00000111845	2.083708452	0.017862779	PAK1IP1
ENSG00000270392	1.111157181	0.017867428	PFN1P2
ENSG00000230445	2.817277451	0.017872798	LRRC37A6P
ENSG00000177646	0.980736455	0.017897548	ACAD9
ENSG00000111058	2.373032267	0.017957602	ACSS3
ENSG00000198924	1.48796458	0.017973241	DCLRE1A
ENSG00000116584	0.990329855	0.018003952	ARHGEF2
ENSG00000196834	1.485765999	0.018003952	POTEI
ENSG00000139287	1.149920662	0.018003952	TPH2
ENSG00000170959	1.824781924	0.018016301	DCDC1
ENSG00000248496	5.627704482	0.018016301	ZBED9
ENSG00000128654	1.632966824	0.01812035	MTX2
ENSG00000198805	1.699475424	0.018153574	PNP
ENSG00000136045	1.278162748	0.018153574	PWP1
ENSG00000160796	0.738742254	0.018230581	NBEAL2
ENSG00000143851	0.944457426	0.018274278	PTPN7
ENSG00000277224	1.164695916	0.018287797	HIST1H2BF
ENSG00000167476	2.215353751	0.018287797	JSRP1

ENSG00000156564	3.758748085	0.018287797	LRFN2
ENSG00000116044	0.970136856	0.018287797	NFE2L2
ENSG00000204909	1.114193823	0.018383329	SPINK9
ENSG00000179335	0.940913428	0.018459136	CLK3
ENSG00000118246	1.154744536	0.018499673	FASTKD2
ENSG00000234651	1.035913131	0.018507351	BAG6
ENSG00000165995	1.58648958	0.018507351	CACNB2
ENSG00000175595	1.115478313	0.018507351	ERCC4
ENSG00000151876	1.397522298	0.018516183	FBXO4
ENSG00000168291	1.327142263	0.018516183	PDHB
ENSG00000084733	1.363220851	0.018516183	RAB10
ENSG00000139636	1.202514442	0.01859327	LMBR1L
ENSG00000257501	1.844949832	0.018654444	LOC643711
ENSG00000188368	2.050275234	0.018654466	PRR19
ENSG00000198793	0.925678624	0.018683234	MTOR
ENSG00000123473	1.138003224	0.018693692	STIL
ENSG00000163618	1.735014594	0.01871141	CADPS
ENSG00000180957	0.881263689	0.01871141	PITPNB
ENSG00000205176	1.462798856	0.01871141	REXO1L1P
ENSG00000088448	0.770207679	0.018910453	ANKRD10
ENSG00000116396	1.043174813	0.0189158	KCNC4
ENSG00000206481	2.619011634	0.018961199	MDC1
ENSG00000088876	1.533898746	0.019005755	ZNF343
ENSG00000078018	2.081149326	0.019041501	MAP2
ENSG00000106443	0.897686934	0.019041501	PHF14
ENSG00000137760	1.293178466	0.019062914	ALKBH8
ENSG00000137547	1.563670751	0.019091849	MRPL15
ENSG00000103811	1.857250705	0.019141407	CTSH
ENSG00000050767	2.700345797	0.019171293	COL23A1
ENSG00000274811	1.26840308	0.019176578	CLPTM1L
ENSG00000100591	1.340908777	0.01920611	AHSA1
ENSG00000140986	1.398755687	0.019292303	RPL3L
ENSG00000155052	2.787540822	0.019432339	CNTNAP5
ENSG00000133835	1.114756963	0.019432339	HSD17B4
ENSG00000070444	1.406977731	0.019432339	MNT
ENSG00000120458	1.315470688	0.019432339	MSANTD2
ENSG00000085063	1.017680197	0.019435101	CD59
ENSG00000150457	1.618576886	0.019440022	LATS2
ENSG00000105643	1.516349774	0.019462874	ARRDC2
ENSG00000198000	1.084978302	0.019462874	NOL8
ENSG00000138078	1.173286745	0.019462874	PREPL
ENSG00000167635	1.228341035	0.019462874	ZNF146
ENSG00000157766	2.102824125	0.019518893	ACAN
ENSG00000165233	1.389533082	0.019518893	CARD19
ENSG00000100439	1.726459287	0.019537571	ABHD4
ENSG00000167747	0.948846424	0.019537571	C19orf48
ENSG00000049656	1.293857735	0.019537571	CLPTM1L
ENSG00000100632	1.435052266	0.019537571	ERH
ENSG00000172216	1.46967762	0.019624101	CEBPB
ENSG00000137288	1.217127574	0.019624101	UQCC2
ENSG00000169604	2.57850417	0.019659085	ANTXR1
ENSG00000175581	0.957370932	0.019659085	MRPL48
ENSG00000066248	2.719583474	0.019672471	NGEF
ENSG00000162366	2.361147345	0.019672471	PDZK1IP1
ENSG00000120594	1.036406157	0.019672471	PLXDC2
ENSG00000130844	1.692938372	0.019672471	ZNF331
ENSG00000147614	1.74683545	0.019695966	ATP6V0D2
ENSG00000112406	1.2910073	0.019723073	HECA
ENSG00000272395	2.448637459	0.019723073	IFNL4
ENSG00000163607	1.071123913	0.019746349	GTPBP8
ENSG00000173898	1.665097546	0.019858588	SPTBN2
ENSG00000164404	2.467531279	0.01987584	GDF9
ENSG00000181333	3.10067663	0.01987584	HEPHL1
ENSG00000122566	0.83476133	0.01987584	HNRNPA2B1
ENSG00000089693	0.978783757	0.01987584	MLF2
ENSG00000126822	1.769968977	0.01987584	PLEKHG3
ENSG00000183963	1.450402974	0.01987584	SMTN

ENSG00000107679	0.966965734	0.019921032	PLEKHA1
ENSG00000124659	1.618554026	0.019968727	TBCC
ENSG00000082996	1.369198052	0.020029481	RNF13
ENSG00000112333	2.853592724	0.020058825	NR2E1
ENSG00000277443	0.993011377	0.020180172	MARCKS
ENSG00000050030	2.222621224	0.020180172	NEXMIF
ENSG00000235376	5.33590607	0.020252127	RPEL1
ENSG00000102898	1.397388092	0.020280629	NUTF2
ENSG00000145708	1.750558784	0.02031315	CRHBP
ENSG00000144596	2.108283944	0.020330129	GRIP2
ENSG00000137819	1.755773645	0.020334685	PAQR5
ENSG00000270647	0.99366068	0.020417467	TAF15
ENSG00000131044	2.040369195	0.020427122	TTLL9
ENSG00000065183	1.450680614	0.020427122	WDR3
ENSG00000003147	0.912249827	0.020463334	ICA1
ENSG00000154832	1.01624784	0.020477671	CXXC1
ENSG00000181544	1.713656115	0.020477671	FANCB
ENSG00000181904	0.999536819	0.020552057	C5orf24
ENSG00000110887	3.105438175	0.020552057	DAO
ENSG00000204103	2.646448465	0.02055848	MAFB
ENSG00000065357	0.919870383	0.020566835	DGKA
ENSG00000277157	1.522823531	0.020618346	HIST1H4D
ENSG00000136997	1.684850095	0.020817452	MYC
ENSG00000027075	1.020791178	0.020830444	PRKCH
ENSG00000139117	1.20873035	0.020854061	CPNE8
ENSG00000007866	2.464509828	0.020905315	TEAD3
ENSG00000105290	4.559578393	0.020920707	APLP1
ENSG00000178772	1.219371041	0.020925834	CPN2
ENSG00000206053	1.596925153	0.020931813	JPT2
ENSG00000186871	1.459462777	0.020960221	ERCC6L
ENSG00000133612	1.539332124	0.020981332	AGAP3
ENSG00000111716	1.15305858	0.020981332	LDHB
ENSG00000156925	2.253679615	0.021037251	ZIC3
ENSG00000170802	1.357184569	0.02109636	FOXN2
ENSG00000162971	1.002983068	0.02109636	TYW5
ENSG00000078295	1.350287499	0.021096899	ADCY2
ENSG00000122188	1.225300689	0.021108892	LAX1
ENSG00000135913	1.016988689	0.021108892	USP37
ENSG00000168066	0.928968159	0.021116508	SF1
ENSG00000183629	2.9906715	0.021237525	GOLGA8G
ENSG00000054690	1.990793577	0.021237525	PLEKHH1
ENSG00000134318	1.351487294	0.021268281	ROCK2
ENSG00000178163	1.025482378	0.021285902	ZNF518B
ENSG00000079785	1.09525637	0.021332897	DDX1
ENSG00000092036	1.252319211	0.021357348	HAUS4
ENSG00000168246	1.498187015	0.021357348	UBTD2
ENSG00000257950	1.277834911	0.021412465	P2RX5 TAX1BP3
ENSG00000104856	1.490055575	0.02144633	RELB
ENSG00000175334	1.72656243	0.021520205	BANF1
ENSG00000205363	1.44215108	0.021538031	C15orf59
ENSG00000177000	1.430532271	0.021538031	MTHFR
ENSG00000049245	1.233959582	0.021538031	VAMP3
ENSG00000121335	3.178910972	0.021543501	PRB2
ENSG00000110958	0.906247848	0.021543501	PTGES3
ENSG00000120008	0.977011911	0.021543501	WDR11
ENSG00000164935	3.474485116	0.021544725	DCSTAMP
ENSG00000124882	1.716855743	0.021544725	EREG
ENSG00000109576	1.46823606	0.021563871	AADAT
ENSG00000132591	1.133144488	0.021587346	ERAL1
ENSG00000163833	1.999144401	0.021587346	FBXO40
ENSG00000103056	1.162913747	0.021587346	SMPD3
ENSG00000139343	1.193162616	0.021587346	SNRPF
ENSG00000155660	1.156213691	0.021593401	PDIA4
ENSG00000149100	1.044285226	0.021597719	EIF3M
ENSG00000111254	2.361532477	0.021747643	AKAP3
ENSG00000118503	1.417704625	0.021747643	TNFAIP3
ENSG00000101298	2.961237736	0.021843319	SNPH

ENSG00000163286	4.357038101	0.021907066	ALPPL2
ENSG00000162396	2.033624591	0.021975024	PARS2
ENSG00000160679	1.159239733	0.021988622	CHTOP
ENSG00000101052	1.468706818	0.022009193	IFT52
ENSG00000137860	1.73767077	0.022009193	SLC28A2
ENSG00000100285	1.176771889	0.022012437	NEFH
ENSG00000127074	1.922516172	0.022032084	RGS13
ENSG00000171314	1.307318289	0.022054736	PGAM1
ENSG00000139405	1.852106733	0.022054736	RITA1
ENSG00000143977	1.378151199	0.022054736	SNRPG
ENSG00000275885	1.126010884	0.022096307	PRPF31
ENSG00000159166	3.216219152	0.022267043	LAD1
ENSG00000073969	1.521719159	0.022289405	NSF
ENSG00000163810	2.910962542	0.02229763	TGM4
ENSG00000281886	2.910962542	0.02229763	TGM4
ENSG00000171791	1.103891904	0.022304253	BCL2
ENSG00000156411	1.255991144	0.022304253	C14orf2
ENSG00000262814	1.407352032	0.022304253	MRPL12
ENSG00000138166	2.220753103	0.022323464	DUSP5
ENSG00000242028	1.692117307	0.022378828	HYPK
ENSG00000072163	2.215531749	0.022390125	LIMS2
ENSG00000196547	0.81159322	0.022390125	MAN2A2
ENSG00000198650	2.372317736	0.022390125	TAT
ENSG00000178988	1.261888948	0.022417846	MRFAP1L1
ENSG00000188176	3.074650277	0.022422782	SMTNL2
ENSG00000160014	1.183718676	0.022479625	CALM2
ENSG00000176046	1.468413909	0.022479625	NUPR1
ENSG00000150433	1.568034615	0.022479625	TMEM218
ENSG00000144908	1.62407611	0.022549276	ALDH1L1
ENSG00000198692	2.643066093	0.022561047	EIF1AY
ENSG00000172244	1.676699348	0.022570061	C5orf34
ENSG00000157119	4.000829355	0.022570061	KLHL40
ENSG00000271605	1.785952584	0.022570061	MILR1
ENSG00000187098	1.31774454	0.022570061	MITF
ENSG00000168081	3.370598249	0.022570061	PNOC
ENSG00000100823	1.064780388	0.022586411	APEX1
ENSG00000131188	1.426938251	0.022586411	PRR7
ENSG00000147654	1.211522937	0.022702609	EBAG9
ENSG00000197345	1.169558585	0.022702609	MRPL21
ENSG00000122176	2.29071764	0.022806686	FMOD
ENSG00000109118	1.33081625	0.022820238	PHF12
ENSG00000147408	1.184268427	0.022961331	CSGALNACT1
ENSG00000131148	1.304687649	0.022961331	EMC8
ENSG00000120699	1.063487784	0.022997057	EXOSC8
ENSG00000126218	3.327831654	0.02300058	F10
ENSG00000198856	1.273568194	0.02300058	OSTC
ENSG00000165105	1.096510964	0.02300058	RASEF
ENSG00000118363	1.272976744	0.02300058	SPCS2
ENSG00000165409	2.042208683	0.02300058	TSHR
ENSG00000198873	1.161307292	0.023015664	GRK5
ENSG00000023445	1.33492502	0.023062393	BIRC3
ENSG00000068878	1.22288122	0.023064168	PSME4
ENSG00000197162	1.043762326	0.023080815	ZNF785
ENSG00000181751	1.603462806	0.023163132	C5orf30
ENSG00000198648	1.24188633	0.023169717	STK39
ENSG00000135241	1.387044749	0.023253296	PNPLA8
ENSG00000088826	2.043441565	0.023253296	SMOX
ENSG00000121898	1.903482743	0.023273683	CPXM2
ENSG00000179698	1.400933233	0.023279617	WDR97
ENSG00000173578	3.07135102	0.023279617	XCR1
ENSG00000269343	1.132343108	0.023279617	ZNF587B
ENSG00000151806	1.083704472	0.023293568	GUF1
ENSG00000129682	1.164942514	0.023340347	FGF13
ENSG00000274026	1.709510691	0.023453172	FAM27E3
ENSG00000080031	2.885077336	0.023453172	PTPRH
ENSG00000115112	2.293705961	0.02347112	TFCP2L1
ENSG00000010322	0.792772029	0.023481103	NISCH

ENSG00000186130	1.699881004	0.023522551	ZBTB6
ENSG00000104413	3.561900501	0.02354407	ESRP1
ENSG00000235715	2.235053329	0.02354407	PSMB8
ENSG00000189120	3.317506045	0.02354407	SP6
ENSG00000131467	1.041949083	0.023547701	PSME3
ENSG00000132541	1.66314797	0.023574127	RIDA
ENSG00000079950	1.195812581	0.023605675	STX7
ENSG00000274734	8.611605629	0.023647355	ARHGAP11B
ENSG00000118369	1.817762369	0.023647355	USP35
ENSG00000172939	0.918967403	0.023655208	OXSR1
ENSG00000125844	1.304515129	0.023688576	RRBP1
ENSG00000204653	1.674824528	0.023820573	ASPDH
ENSG00000166801	1.018253307	0.023820573	FAM111A
ENSG00000161031	2.674717661	0.023820573	PGLYRP2
ENSG00000189056	1.81131678	0.023820573	RELN
ENSG00000065057	1.413411651	0.023821883	NTHL1
ENSG00000136371	1.32768135	0.023833192	MTHFS
ENSG00000055483	1.449483932	0.023924016	USP36
ENSG00000123146	1.132395164	0.023970585	ADGRE5
ENSG00000110104	1.464176438	0.023970585	CCDC86
ENSG00000179091	1.167208447	0.023970585	CYC1
ENSG00000178084	3.27688701	0.023970585	HTR3C
ENSG00000155636	1.909850786	0.023970585	RBM45
ENSG00000196600	1.545591397	0.023970585	SLC22A25
ENSG00000018699	1.101401856	0.023979495	TTC27
ENSG00000141446	0.829810222	0.024024219	ESCO1
ENSG00000147894	1.033342387	0.024071663	C9orf72
ENSG00000188107	1.249462332	0.024071663	EYS
ENSG00000110169	2.909278827	0.024071663	HPX
ENSG00000130294	2.443034743	0.024071663	KIF1A
ENSG00000180764	1.73345513	0.024071663	PIPSL
ENSG00000103472	1.118988757	0.024071663	RRN3P2
ENSG00000162923	1.048624824	0.024071663	WDR26
ENSG00000186529	1.836272528	0.024094898	CYP4F3
ENSG00000112039	1.152964293	0.024094898	FANCE
ENSG00000177272	4.124268562	0.024094898	KCNA3
ENSG00000182253	2.064149818	0.024156902	SYNM
ENSG00000143401	1.239938353	0.024248485	ANP32E
ENSG00000151718	1.074221844	0.024248485	WWC2
ENSG00000104081	1.637472513	0.024293189	BMF
ENSG00000164032	1.194820615	0.024293189	H2AFZ
ENSG00000116649	1.330830655	0.024308842	SRM
ENSG00000109079	1.11389564	0.024308842	TNFAIP1
ENSG00000122574	2.021074141	0.024308842	WIPF3
ENSG00000148408	2.507291845	0.024386624	CACNA1B
ENSG00000228284	1.006489292	0.024386624	HLA DQA1
ENSG00000166126	2.473081452	0.024419405	AMN
ENSG00000189233	1.339038514	0.024419405	NUGGC
ENSG00000174990	1.310418807	0.024438043	CA5A
ENSG00000124313	1.768464575	0.024531794	IQSEC2
ENSG00000007062	0.930186718	0.024531794	PROM1
ENSG00000187862	1.662140312	0.024557763	TTC24
ENSG00000100726	1.074281782	0.02460044	TELO2
ENSG00000168275	2.095560601	0.024806299	COA6
ENSG00000135912	1.07148502	0.02482324	TTLL4
ENSG00000108342	3.062754768	0.024873674	CSF3
ENSG00000027869	1.554519753	0.024873674	SH2D2A
ENSG00000065923	1.059951481	0.024873674	SLC9A7
ENSG00000143476	1.328904054	0.024908853	DTL
ENSG00000077684	0.977169057	0.024908853	JADE1
ENSG00000263006	1.563110216	0.024908853	ROCK1P1
ENSG00000129946	2.18078659	0.024908853	SHC2
ENSG00000274803	1.567278084	0.024911913	BDP1
ENSG00000101220	1.588766562	0.024911913	C20orf27
ENSG00000145293	1.287747188	0.024962265	ENOPH1
ENSG00000197406	3.770935802	0.025012946	DIO3
ENSG00000188343	1.186991755	0.025048388	FAM92A

ENSG00000101076	1.70843872	0.025055765	HNF4A
ENSG00000166897	2.299503327	0.025182589	ELFN2
ENSG00000145332	1.103038453	0.02518835	KLHL8
ENSG00000165283	1.255296037	0.025205143	STOML2
ENSG00000105609	2.061606024	0.025208823	LILRB5
ENSG00000056050	1.796865656	0.02524732	HPF1
ENSG00000054967	1.381629968	0.02524732	RELT
ENSG00000139437	0.968900737	0.02524732	TCHP
ENSG00000148154	1.59204825	0.025397838	UGCG
ENSG00000105472	1.499695285	0.025414834	CLEC11A
ENSG00000020129	1.170698108	0.025414834	NCDN
ENSG00000164168	1.187074906	0.025414834	TMEM184C
ENSG00000164393	1.711305021	0.025451128	ADGRF2
ENSG00000125485	1.261206191	0.025451128	DDX31
ENSG00000175054	1.005120508	0.025468043	ATR
ENSG00000105549	2.380771125	0.025469604	THEG
ENSG00000158786	2.553424744	0.025522551	PLA2G2F
ENSG00000122025	1.167689434	0.025572332	FLT3
ENSG00000275342	1.314139166	0.025572332	PRAG1
ENSG00000134987	1.327091017	0.025613988	WDR36
ENSG00000205642	3.112164886	0.025638964	VCX3B
ENSG00000221914	0.920547524	0.025641696	PPP2R2A
ENSG00000105388	2.628653893	0.025660843	CEACAM5
ENSG00000185664	1.944698014	0.025660843	PMEL
ENSG00000163751	2.252078031	0.025661559	CPA3
ENSG00000179348	1.328428811	0.025661559	GATA2
ENSG00000153767	1.454529871	0.025661559	GTF2E1
ENSG00000173113	1.199811361	0.025661559	TRMT112
ENSG00000044459	0.917852979	0.025692037	CNTLN
ENSG00000142459	1.022957289	0.025712456	EVI5L
ENSG00000206579	1.466197301	0.025712456	XKR4
ENSG00000172478	1.85692088	0.025722853	C2orf54
ENSG00000185483	2.288580819	0.025806428	ROR1
ENSG00000124733	1.263259261	0.025913607	MEA1
ENSG00000116353	1.287302551	0.025947583	MECR
ENSG00000100068	1.313639415	0.025966965	LRP5L
ENSG00000168906	1.082211698	0.025966965	MAT2A
ENSG00000152359	1.476531195	0.025966965	POC5
ENSG00000124092	1.151010884	0.026020563	CTCFL
ENSG00000173227	1.999259098	0.026020563	SYT12
ENSG00000181458	1.206852839	0.026021284	TMEM45A
ENSG00000007384	1.309419733	0.026026915	RHBDF1
ENSG00000128342	2.465680912	0.02602734	LIF
ENSG00000148308	0.835229323	0.026034134	GTF3C5
ENSG00000168758	1.099923997	0.026076708	SEMA4C
ENSG00000130305	1.230678661	0.026088324	NSUN5
ENSG00000078237	2.064721432	0.026093995	TIGAR
ENSG00000146926	5.238271556	0.026157091	ASB10
ENSG00000189182	3.342910376	0.026157091	KRT77
ENSG00000095303	1.239641575	0.02618663	PTGS1
ENSG00000151967	1.400418684	0.02618663	SCHIP1
ENSG00000177830	0.883562495	0.026218043	CHID1
ENSG00000139344	1.594513313	0.0263227	AMDHD1
ENSG00000113749	2.061448815	0.0263227	HRH2
ENSG00000129194	2.653494254	0.0263227	SOX15
ENSG00000152936	1.645263045	0.026420686	LMNTD1
ENSG00000123485	1.606679977	0.026450663	HJURP
ENSG00000115232	0.926184096	0.026454423	ITGA4
ENSG00000186564	2.688529135	0.026542862	FOXD2
ENSG00000130762	1.434213695	0.026559069	ARHGEF16
ENSG00000086696	1.110045075	0.026559069	HSD17B2
ENSG00000231824	5.273694306	0.026559608	AKAIN1
ENSG00000186665	1.928610465	0.026559608	C17orf58
ENSG00000065618	1.611810775	0.026583462	COL17A1
ENSG00000158486	1.675789632	0.026583462	DNAH3
ENSG00000137094	2.277445766	0.026583462	DNAJB5
ENSG00000197102	1.0899515	0.026583462	DYNC1H1

ENSG00000152580	1.253321764	0.026584857	IGSF10
ENSG00000162407	2.015840518	0.026584857	PLPP3
ENSG00000185507	1.072000561	0.02664246	IRF7
ENSG00000134830	1.203886068	0.026660206	C5AR2
ENSG00000198286	0.992183399	0.026660206	CARD11
ENSG00000130202	1.135945403	0.026660206	NECTIN2
ENSG00000134815	1.015792175	0.026728612	DHX34
ENSG00000146263	0.927165558	0.0267635	MMS22L
ENSG00000172403	1.505090332	0.026774024	SYNPO2
ENSG00000119547	2.704010016	0.026844462	ONECUT2
ENSG00000184281	1.495421592	0.026844462	TSSC4
ENSG00000076108	1.213921861	0.026951862	BAZ2A
ENSG00000074071	1.518082068	0.026951862	MRPS34
ENSG00000269437	2.232868294	0.026951862	NXF2B
ENSG00000119392	1.210703788	0.027013196	GLE1
ENSG00000151834	1.649567639	0.027038372	GABRA2
ENSG00000176945	3.784364205	0.02705488	MUC20
ENSG00000279761	6.150585875	0.02705488	OR5D13
ENSG00000117868	0.953007988	0.027066969	ESYT2
ENSG00000185958	1.382623215	0.027098399	FAM186A
ENSG00000116062	1.125805983	0.027098399	MSH6
ENSG00000161714	1.442710024	0.027098399	PLCD3
ENSG00000085377	1.161609337	0.027098399	PREP
ENSG00000165186	1.798343609	0.027098399	PTCHD1
ENSG00000100647	1.281690441	0.027098399	SUSD6
ENSG00000187066	1.653201087	0.027098399	TMEM262
ENSG00000149150	1.01497603	0.027099433	SLC43A1
ENSG00000198298	1.581998368	0.027116333	ZNF485
ENSG00000102796	1.000400252	0.02712817	DHRS12
ENSG00000099139	1.634909232	0.02712817	PCSK5
ENSG00000146070	1.693701463	0.02712817	PLA2G7
ENSG00000176170	1.80401585	0.02712817	SPHK1
ENSG00000120438	0.842935501	0.027254654	TCP1
ENSG00000197601	0.826313403	0.027284955	FAR1
ENSG00000148834	0.990504863	0.027300003	GSTO1
ENSG00000226763	1.578647917	0.027300003	SRRM5
ENSG00000148700	0.98568878	0.027316786	ADD3
ENSG00000138759	1.906462218	0.027316786	FRAS1
ENSG00000197713	1.193232949	0.027316786	RPE
ENSG00000185238	1.169447423	0.027363466	PRMT3
ENSG00000155868	1.348022853	0.027403563	MED7
ENSG00000170458	2.361336292	0.027416571	CD14
ENSG00000116127	0.989941141	0.027435093	ALMS1
ENSG00000141526	1.659019875	0.027435093	SLC16A3
ENSG00000163041	1.077542078	0.027473502	H3F3A
ENSG00000143106	1.177817979	0.027662131	PSMA5
ENSG00000251380	6.227523852	0.0276826	DCANP1
ENSG00000189299	5.254445566	0.027758789	FOXR2
ENSG00000147883	3.056916967	0.027817597	CDKN2B
ENSG00000117036	1.290154892	0.027852338	ETV3
ENSG00000184454	1.476440364	0.027929854	NCMAP
ENSG00000040341	1.219508263	0.027954667	STAU2
ENSG00000116785	2.052773748	0.027989949	CFHR3
ENSG00000005175	1.359437191	0.027989949	RPAP3
ENSG00000058085	2.614816603	0.028041892	LAMC2
ENSG00000185164	1.128545699	0.028041892	NOMO2
ENSG00000204444	2.001544577	0.028131753	APOM
ENSG00000167447	1.140008982	0.028194109	SMG8
ENSG00000074201	0.939002232	0.02826198	CLNS1A
ENSG00000009765	1.517879626	0.028297968	IYD
ENSG00000173465	1.926669137	0.028297968	SSSCA1
ENSG00000173334	1.675048445	0.028301992	TRIB1
ENSG00000185055	1.608273509	0.028351642	EFCAB10
ENSG00000170370	1.641400007	0.028351642	EMX2
ENSG00000139974	1.480071353	0.028351642	SLC38A6
ENSG00000094916	1.145484948	0.028357762	CBX5
ENSG00000229185	4.246798974	0.028380617	OR2H2

ENSG00000168118	1.186741108	0.028380617	RAB4A
ENSG00000107295	3.453050435	0.028380617	SH3GL2
ENSG00000156009	4.040645776	0.028408426	MAGEA8
ENSG00000125977	1.128901496	0.028528421	EIF2S2
ENSG00000100629	0.941973285	0.028547189	CEP128
ENSG00000119203	1.106635634	0.02857179	CPSF3
ENSG00000167723	1.863555962	0.028574376	TRPV3
ENSG00000269404	1.311730765	0.028605216	SPIB
ENSG00000143183	1.252791206	0.028692429	TMCO1
ENSG00000121766	1.174913443	0.028721495	ZCCHC17
ENSG00000198700	1.225525398	0.028733588	IPO9
ENSG00000197768	2.6512992	0.028733588	STPG3
ENSG00000178209	1.108860086	0.028743995	PLEC
ENSG00000112667	1.53404538	0.028778199	DNPH1
ENSG00000154813	1.273171941	0.028778199	DPH3
ENSG00000105939	1.042183623	0.028778199	ZC3HAV1
ENSG00000103496	0.972714156	0.028829689	STX4
ENSG00000135046	2.26812839	0.028831931	ANXA1
ENSG00000139684	1.209815586	0.028831931	ESD
ENSG00000174776	1.989412169	0.028831931	WDR49
ENSG00000154359	1.139398464	0.02886942	LONRF1
ENSG00000114270	1.688025924	0.028873827	COL7A1
ENSG00000176124	1.087411146	0.028896525	DLEU1
ENSG00000171657	2.247671656	0.028899232	GPR82
ENSG00000099725	1.744692073	0.028953214	PRKY
ENSG00000152253	1.311869978	0.028953214	SPC25
ENSG00000263247	1.367210427	0.028987456	PRR4
ENSG00000152495	2.153245107	0.029003074	CAMK4
ENSG00000196188	2.327234943	0.029003074	CTSE
ENSG00000114491	1.672265085	0.029003074	UMPS
ENSG00000007516	1.444005893	0.029025967	BAIAP3
ENSG00000132823	1.282268624	0.029082569	OSER1
ENSG00000086189	1.066310381	0.029140593	DIMT1
ENSG00000106348	1.310351525	0.029140593	IMPDH1
ENSG00000146918	1.416918709	0.029140593	NCAPG2
ENSG00000100567	0.984080218	0.029140593	PSMA3
ENSG00000108064	1.321228164	0.029140593	TFAM
ENSG00000147124	1.462307948	0.029159718	ZNF41
ENSG00000197965	1.20695602	0.029179812	MPZL1
ENSG00000230873	1.691472828	0.029179812	STMND1
ENSG00000169627	1.445227317	0.029317761	BOLA2
ENSG00000188483	1.277414011	0.02935328	IER5L
ENSG00000072840	1.197084356	0.029385412	EVC
ENSG00000096006	5.234552448	0.029386611	CRISP3
ENSG00000216490	1.727630602	0.029396596	IFI30
ENSG00000135002	1.09289308	0.029514814	RFK
ENSG00000164430	1.160910554	0.02954794	CGAS
ENSG00000111358	1.284993298	0.02954794	GTF2H3
ENSG00000099284	1.294911247	0.02954794	H2AFY2
ENSG00000206052	2.466484676	0.02955195	DOK6
ENSG00000150637	1.663723115	0.029574914	CD226
ENSG00000205085	1.146024935	0.029647519	FAM71F2
ENSG00000139645	0.975637173	0.029663443	ANKRD52
ENSG00000123191	1.788969816	0.029663443	ATP7B
ENSG00000156162	1.202362533	0.029663443	DPY19L4
ENSG00000011600	1.84667464	0.029663443	TYROBP
ENSG00000144366	2.252391201	0.029675184	GULP1
ENSG00000278637	1.471990755	0.029705834	HIST1H4A
ENSG00000135925	3.802955916	0.029705834	WNT10A
ENSG00000157087	2.083358801	0.029737871	ATP2B2
ENSG00000145451	2.055151962	0.029840791	GLRA3
ENSG00000237071	2.851085605	0.029971447	TRIM27
ENSG00000236279	3.950958091	0.029980333	CLEC2L
ENSG00000148824	0.951447049	0.029980333	MTG1
ENSG00000187583	4.038142523	0.029980333	PLEKHN1
ENSG00000100462	1.023032791	0.030014121	PRMT5
ENSG00000183878	5.721143664	0.030014121	UTY

ENSG00000197405	1.513130498	0.030140185	C5AR1
ENSG00000128510	1.89706843	0.030224692	CPA4
ENSG00000180881	1.136889694	0.030252855	CAPS2
ENSG00000175311	1.398956721	0.030261303	ANKS4B
ENSG00000106211	1.121085773	0.030261303	HSPB1
ENSG00000112096	1.067690741	0.030282527	SOD2
ENSG00000258839	1.260938686	0.030287292	MC1R
ENSG00000188959	1.794620325	0.030288333	C9orf152
ENSG00000008256	1.570193358	0.030312331	CYTH3
ENSG00000161638	1.58937639	0.030312331	ITGA5
ENSG00000188011	5.123188524	0.030312331	RTP5
ENSG00000277949	5.123188524	0.030312331	RTP5
ENSG00000211450	1.202360655	0.030312331	SELENOH
ENSG00000032219	1.082543387	0.030347871	ARID4A
ENSG00000140598	0.856274082	0.030347871	EFL1
ENSG00000133216	1.611105294	0.030347871	EPHB2
ENSG00000198885	1.562581399	0.030347871	ITPRIPL1
ENSG00000182450	4.735617295	0.030347871	KCNK4
ENSG00000163935	1.969584291	0.030347871	SFMBT1
ENSG00000052749	1.098007834	0.030402054	RRP12
ENSG00000251595	2.070904212	0.030402438	ABCA11P
ENSG00000162383	2.860878326	0.030402438	SLC1A7
ENSG00000182583	2.30487779	0.030402438	VCX
ENSG00000173715	1.466614366	0.030419141	C11orf80
ENSG00000240972	1.311223432	0.030419141	MIF
ENSG00000276701	1.311223432	0.030419141	MIF
ENSG00000174607	1.367212173	0.030419141	UGT8
ENSG00000124557	3.042153645	0.030443937	BTN1A1
ENSG00000136274	2.440939911	0.030470938	NACAD
ENSG00000135845	1.702029121	0.030470938	PIGC
ENSG00000156218	1.165842102	0.030495375	ADAMTSL3
ENSG00000272916	1.124468998	0.030553523	NDST2
ENSG00000181788	1.579614078	0.030553523	SIAH2
ENSG00000188710	3.28570236	0.030569325	QRFP
ENSG00000076864	2.257006588	0.030569325	RAP1GAP
ENSG00000126768	1.233847626	0.030569325	TIMM17B
ENSG00000130598	1.930828356	0.030569325	TNNI2
ENSG00000130204	1.356703141	0.030569325	TOMM40
ENSG00000147394	1.606548672	0.030606947	ZNF185
ENSG00000141664	1.229077681	0.030614307	ZCCHC2
ENSG00000105771	0.830207165	0.030677631	SMG9
ENSG00000196391	1.272593313	0.030677631	ZNF774
ENSG00000007174	1.994037955	0.03068621	DNAH9
ENSG00000203734	2.266279744	0.030744049	ECT2L
ENSG00000153391	1.090365772	0.030744049	INO80C
ENSG00000213024	1.112708847	0.030744049	NUP62
ENSG00000197417	1.056226519	0.030744049	SHPK
ENSG00000164543	1.325697954	0.030744049	STK17A
ENSG00000023902	1.288904215	0.030867182	PLEKHO1
ENSG00000145220	1.50319018	0.03092628	LYAR
ENSG00000213619	0.949066505	0.03092628	NDUFS3
ENSG00000198723	1.955853149	0.031050631	TEX45
ENSG00000173214	1.099485977	0.031062662	MFSD4B
ENSG00000125741	1.503252479	0.031062662	OPA3
ENSG00000175785	4.346786898	0.031062662	PRIMA1
ENSG00000274089	4.346786898	0.031062662	PRIMA1
ENSG00000183576	0.861606159	0.031099253	SETD3
ENSG00000077348	1.21308395	0.031115716	EXOSC5
ENSG00000134317	1.796524863	0.031115716	GRHL1
ENSG00000144224	1.257075034	0.031115716	UBXN4
ENSG00000236446	5.841529816	0.031133857	CT47B1
ENSG00000196924	1.464064177	0.031133857	FLNA
ENSG00000163395	2.329340098	0.031133857	IGFN1
ENSG00000170807	2.828494744	0.031133857	LMOD2
ENSG00000111341	1.6193564	0.031133857	MGP
ENSG00000143799	1.139138	0.031133857	PARP1
ENSG00000106344	1.241959976	0.031133857	RBM28

ENSG00000171729	1.48530256	0.031133857	TMEM51
ENSG00000160953	0.752379143	0.031195323	MUM1
ENSG00000100813	1.005315406	0.03128579	ACIN1
ENSG00000115526	1.801153805	0.03128579	CHST10
ENSG00000110492	1.328098203	0.03128579	MDK
ENSG00000189308	0.933254412	0.03131918	LIN54
ENSG00000033867	1.103985946	0.031445805	SLC4A7
ENSG00000048707	0.785396733	0.031456474	VPS13D
ENSG00000186642	1.811347716	0.03147138	PDE2A
ENSG00000198346	1.115232579	0.03147138	ZNF813
ENSG00000146540	1.135976778	0.031510116	C7orf50
ENSG00000183765	1.132744077	0.031510116	CHEK2
ENSG00000111364	1.026522647	0.031510116	DDX55
ENSG00000111834	1.867564564	0.031510116	RSPH4A
ENSG00000106355	1.040615486	0.031566058	LSM5
ENSG00000113905	1.569168332	0.031705751	HRG
ENSG00000170153	0.990654783	0.031717712	RNF150
ENSG00000122367	2.49371028	0.031727977	LDB3
ENSG00000137801	2.037892311	0.031754826	THBS1
ENSG00000104327	1.460878198	0.031755709	CALB1
ENSG00000275045	2.08531608	0.031814977	GTF2H2
ENSG00000162616	1.327258934	0.031830244	DNAJB4
ENSG00000222047	1.952193911	0.031932336	C10orf55
ENSG00000124701	2.912826216	0.031955408	APOBEC2
ENSG00000261236	1.032705006	0.031991099	BOP1
ENSG00000075790	1.417846995	0.031995585	BCAP29
ENSG00000183311	1.638117493	0.032083936	TUBB
ENSG00000164011	1.61051789	0.032117581	ZNF691
ENSG00000169019	2.423009235	0.032126924	COMMD8
ENSG00000140044	1.325672043	0.032126924	JDP2
ENSG00000173212	1.170242036	0.032126924	MAB21L3
ENSG00000111731	0.969867015	0.032195686	C2CD5
ENSG00000119729	1.128035054	0.032202986	RHOQ
ENSG00000126432	1.261939323	0.032250342	PRDX5
ENSG00000166557	1.032997845	0.032250342	TMED3
ENSG00000141655	1.54573351	0.032250342	TNFRSF11A
ENSG00000119801	0.93709271	0.032250342	YPEL5
ENSG00000165891	1.835793901	0.032253537	E2F7
ENSG00000143554	1.122046029	0.032295385	SLC27A3
ENSG00000197540	3.244512731	0.032310962	GZMM
ENSG00000100644	0.880214462	0.032310962	HIF1A
ENSG00000221826	2.437115556	0.032310962	PSG3
ENSG00000157782	1.617545622	0.032326733	CABP1
ENSG00000166265	1.62546006	0.032422142	CYYR1
ENSG00000081277	3.046596095	0.032422142	PKP1
ENSG00000165731	2.580072095	0.03242599	RET
ENSG00000159450	1.707445289	0.032431428	TCHH
ENSG00000112782	2.78455657	0.032484815	CLIC5
ENSG00000065150	0.931625199	0.032484815	IPO5
ENSG00000148362	1.404158744	0.032484815	PAXX
ENSG00000182054	1.046575682	0.032503809	IDH2
ENSG00000213801	1.6180132	0.032544522	ZNF321P
ENSG00000008517	1.406722374	0.032555257	IL32
ENSG00000104320	0.939528921	0.032555257	NBN
ENSG00000112365	1.139803449	0.032555257	ZBTB24
ENSG00000075340	1.932692953	0.032561327	ADD2
ENSG00000162757	1.470234515	0.032561327	C1orf74
ENSG00000188313	0.954555375	0.032575571	PLSCR1
ENSG00000109819	1.40278595	0.032598668	PPARGC1A
ENSG00000168404	0.814784094	0.032631697	MLKL
ENSG00000034677	0.80391202	0.03263874	RNF19A
ENSG00000141543	0.950440581	0.032687527	EIF4A3
ENSG00000162728	3.019248388	0.032687527	KCNJ9
ENSG00000138050	0.884010059	0.032688673	THUMPD2
ENSG00000006747	1.186913668	0.032754919	SCIN
ENSG00000146267	1.998320047	0.032770194	FAXC
ENSG00000162813	1.291619928	0.032772757	BPNT1

ENSG00000275397	5.835359138	0.032772757	DHRS11
ENSG00000186453	3.307000816	0.032772757	FAM228A
ENSG00000123104	0.872499029	0.032772757	ITPR2
ENSG00000147955	1.413700513	0.032772757	SIGMAR1
ENSG00000197106	1.55626937	0.032772757	SLC6A17
ENSG00000213551	1.109566259	0.032795035	DNAJC9
ENSG00000135778	1.135063339	0.03286672	NTPCR
ENSG00000050438	0.975750936	0.03287528	SLC4A8
ENSG00000159055	1.942121407	0.033129422	MIS18A
ENSG00000168658	1.863773274	0.033197519	VWA3B
ENSG00000115590	3.776753652	0.033234249	IL1R2
ENSG00000184270	0.957586285	0.033277715	HIST2H2AB
ENSG00000114378	1.954040193	0.033277715	HYAL1
ENSG00000163161	0.856294013	0.033304751	ERCC3
ENSG00000158691	0.93261064	0.033305368	ZSCAN12
ENSG00000278272	1.604698089	0.03336114	HIST1H3C
ENSG00000170442	3.981545234	0.03336114	KRT86
ENSG00000160193	1.2196639	0.03336114	WDR4
ENSG00000123131	1.314183725	0.033481952	PRDX4
ENSG00000169174	2.840828604	0.033566434	PCSK9
ENSG00000171621	2.723614518	0.033641006	SPSB1
ENSG00000169894	1.415479327	0.033689104	MUC3A
ENSG00000107758	1.175359503	0.033777769	PPP3CB
ENSG00000189292	3.275089937	0.033791917	ALKAL2
ENSG00000278437	3.791087278	0.033791917	LILRB5
ENSG00000137727	1.252068928	0.033841693	ARHGAP20
ENSG00000164776	1.448531668	0.033933351	PHKG1
ENSG00000258130	1.46867673	0.033950161	LOC613038
ENSG00000136143	1.418269219	0.034264154	SUCLA2
ENSG00000188130	0.960879708	0.034288289	MAPK12
ENSG00000206073	5.89385689	0.034317073	SERPINB4
ENSG00000166797	1.33400616	0.034375464	FAM96A
ENSG00000196767	2.924720063	0.034474962	POU3F4
ENSG00000166073	2.583515753	0.034488314	GPR176
ENSG00000132383	0.912406063	0.034488314	RPA1
ENSG00000165724	1.277235613	0.034488314	ZMYND19
ENSG00000177034	1.194660546	0.034491754	MTX3
ENSG00000135540	0.882853704	0.034523873	NHSL1
ENSG00000117592	0.976178336	0.034551702	PRDX6
ENSG00000108370	1.752563567	0.034551702	RGS9
ENSG00000186448	1.25762046	0.034560874	ZNF197
ENSG00000281709	1.25762046	0.034560874	ZNF197
ENSG00000174353	0.956969203	0.034737257	TRIM74
ENSG00000188816	4.135406437	0.03484838	HMX2
ENSG00000173085	1.290157902	0.034888087	COQ2
ENSG00000144488	2.662637804	0.034940398	ESPNL
ENSG00000134533	1.580479892	0.03495407	RERG
ENSG00000175110	1.095574623	0.034969846	MRPS22
ENSG00000218336	2.335206751	0.034982666	TENM3
ENSG00000166167	0.908476706	0.035002744	BTRC
ENSG00000119333	1.235711268	0.03504354	WDR34
ENSG00000274821	3.778331191	0.035092997	SERPINA2
ENSG00000101868	1.034379954	0.03524419	POLA1
ENSG00000134323	1.520752435	0.035284099	MYCN
ENSG00000141574	3.378398466	0.035284099	SECTM1
ENSG00000163159	1.128575177	0.035307456	VPS72
ENSG00000168610	1.137033257	0.035425934	STAT3
ENSG00000125962	1.230638948	0.035475181	ARMCX5
ENSG00000140379	2.203747192	0.035494143	BCL2A1
ENSG00000103550	1.414263603	0.035513094	KNOP1
ENSG00000148400	0.89627652	0.035535377	NOTCH1
ENSG00000149527	1.985652415	0.035537674	PLCH2
ENSG00000176472	1.50014108	0.035537674	ZNF575
ENSG00000170498	5.642600654	0.035554612	KISS1
ENSG00000148143	1.03137453	0.035575426	ZNF462
ENSG00000109787	1.19161398	0.035688369	KLF3
ENSG00000052850	2.162425892	0.035751455	ALX4

ENSG00000216937	1.182621449	0.035751455	CCDC7
ENSG00000082516	1.159223972	0.035751455	GEMIN5
ENSG00000175287	1.497304301	0.035751455	PHYHD1
ENSG00000156171	1.298021138	0.035772867	DRAM2
ENSG00000131142	5.555967141	0.035860421	CCL25
ENSG00000138663	1.219547978	0.035889998	COPS4
ENSG00000038295	2.868196474	0.035889998	TLL1
ENSG00000119777	1.034351957	0.035889998	TMEM214
ENSG00000188290	2.450537313	0.035938488	HES4
ENSG00000135824	2.70369277	0.036019106	RGS8
ENSG00000181789	0.905608042	0.036021614	COPG1
ENSG00000174326	2.265557475	0.036033946	SLC16A11
ENSG00000167612	3.041270699	0.036073385	ANKRD33
ENSG00000123843	1.15201882	0.036078395	C4BPB
ENSG00000183317	1.788024759	0.036133675	EPHA10
ENSG00000276907	2.48293276	0.036177417	ARHGAP27
ENSG00000119977	1.185708741	0.036272277	TCTN3
ENSG00000119714	2.152273152	0.036387843	GPR68
ENSG00000155827	1.045071357	0.036387843	RNF20
ENSG00000149742	1.712627571	0.036387843	SLC22A9
ENSG00000128915	0.907485118	0.036398639	ICE2
ENSG00000179477	2.500397383	0.036554065	ALOX12B
ENSG00000172260	1.087699165	0.036554065	NEGR1
ENSG00000164463	0.958753223	0.036584561	CREBRF
ENSG00000184647	2.606417061	0.036584561	PRSS55
ENSG00000104941	2.035131103	0.036584561	RSPH6A
ENSG00000139921	1.36838089	0.036584561	TMX1
ENSG00000260103	1.024480495	0.036589846	LOC101929333
ENSG00000214290	4.927154162	0.036596373	COLCA2
ENSG00000235942	5.046393035	0.036622766	LCE6A
ENSG00000171530	0.987089687	0.036622766	TBCA
ENSG00000163518	2.530336395	0.03665078	FCRL4
ENSG00000204183	1.987560474	0.036682908	GDF5OS
ENSG00000182333	4.863870367	0.036682908	LIPF
ENSG00000183648	1.148788736	0.036682908	NDUFB1
ENSG00000143869	1.619252374	0.036682995	GDF7
ENSG00000137501	1.294730828	0.036694278	SYTL2
ENSG00000095397	1.904562276	0.036766881	WHRN
ENSG00000102401	1.05400663	0.036945209	ARMCX3
ENSG00000181013	3.67172236	0.036949515	C17orf47
ENSG00000197006	0.879956492	0.036949515	METTL9
ENSG00000134339	1.801396643	0.036949515	SAA2
ENSG00000163755	1.246644829	0.036983192	HPS3
ENSG00000177191	1.649357135	0.036997243	B3GNT8
ENSG00000168418	1.337078355	0.037085237	KCNG4
ENSG00000088812	0.919314644	0.037127463	ATRN
ENSG00000180992	1.485632174	0.037193154	MRPL14
ENSG00000151176	1.188139166	0.037322133	PLBD2
ENSG00000115762	1.105317736	0.037322133	PLEKHB2
ENSG00000167487	1.213171677	0.037370469	KLHL26
ENSG00000106554	1.074995988	0.037373522	CHCHD3
ENSG00000182326	1.214697026	0.037435474	C1S
ENSG00000162604	0.963706871	0.037440201	TM2D1
ENSG00000183779	1.946243746	0.037448794	ZNF703
ENSG00000235173	1.647211622	0.037458402	HGH1
ENSG00000107187	2.470356639	0.037519514	LHX3
ENSG00000148702	3.228549776	0.037639362	HABP2
ENSG00000007908	2.911320149	0.037744939	SELE
ENSG00000204655	4.5355328	0.03776758	MOG
ENSG00000056972	0.967526752	0.037773888	TRAF3IP2
ENSG00000175793	2.450229958	0.037781112	SFN
ENSG00000138769	3.330366326	0.037828105	CDKL2
ENSG00000134255	0.925964646	0.037919719	CEPT1
ENSG00000100422	1.116386756	0.037919719	CERK
ENSG00000135747	1.161524454	0.037919719	ZNF670 ZNF695
ENSG00000102554	1.992466671	0.037921293	KLF5
ENSG00000159199	1.445275685	0.037921625	ATP5G1

ENSG00000167103	2.115365579	0.037921625	PIP5KL1
ENSG00000174945	1.48782619	0.03793898	AMZ1
ENSG00000106829	0.829791494	0.037964254	TLE4
ENSG00000103326	0.814294853	0.038003468	CAPN15
ENSG00000078967	1.00516806	0.038073272	UBE2D4
ENSG00000138675	1.811274525	0.038076619	FGF5
ENSG00000232062	5.470338737	0.038076619	HLA DQA1
ENSG00000263163	1.210857842	0.038076619	SLC27A3
ENSG00000138162	1.312088012	0.038089178	TACC2
ENSG00000179915	1.547638786	0.038119143	NRXN1
ENSG00000070367	1.011295669	0.038122173	EXOC5
ENSG00000172771	1.276604427	0.038231753	EFCAB12
ENSG00000143107	3.03009921	0.038231753	FNDC7
ENSG00000142798	1.271806654	0.038231753	HSPG2
ENSG00000163599	3.272455762	0.038445006	CTLA4
ENSG00000198837	0.724317378	0.038445006	DENND4B
ENSG00000135835	1.60015162	0.038445006	KIAA1614
ENSG00000099250	1.451481829	0.038445006	NRP1
ENSG00000128271	1.794042331	0.038547984	ADORA2A
ENSG00000152234	1.057768355	0.038668932	ATP5A1
ENSG00000224531	1.43576971	0.038673161	SMIM13
ENSG00000112367	1.4212673	0.038679306	FIG4
ENSG00000165125	1.640956644	0.038734343	TRPV6
ENSG00000099814	2.059674348	0.038806181	CEP170B
ENSG00000154237	1.029630244	0.038806181	LRRK1
ENSG00000157064	1.907889252	0.038806181	NMNAT2
ENSG00000233917	6.173738341	0.038806181	POTEB
ENSG00000081870	1.10281087	0.03888565	HSPB11
ENSG00000162643	4.093058081	0.03888565	WDR63
ENSG00000183018	0.970697316	0.038912299	SPNS2
ENSG00000174358	2.914571012	0.038917892	SLC6A19
ENSG00000126088	0.95443833	0.039072656	UROD
ENSG00000198576	2.00168387	0.039091125	ARC
ENSG00000106331	2.304031456	0.039091125	PAX4
ENSG00000112511	1.719004372	0.039213829	PHF1
ENSG00000139973	1.46685091	0.039216824	SYT16
ENSG00000243649	2.127187182	0.03928032	CFB
ENSG00000228253	1.030835825	0.039310753	ATP8
ENSG00000146376	1.472396961	0.039330893	ARHGAP18
ENSG00000170248	0.955552046	0.039350208	PDCD6IP
ENSG00000166803	1.097937698	0.039457697	PCLAF
ENSG00000151320	1.53626998	0.039540497	AKAP6
ENSG00000132199	0.952255316	0.039540497	ENOSF1
ENSG00000268869	2.441903673	0.039540497	ESPNP
ENSG00000102383	1.099431707	0.039540497	ZDHHC15
ENSG00000102962	1.320278399	0.039583555	CCL22
ENSG00000095139	0.981336038	0.039648174	ARCN1
ENSG00000175455	0.938726038	0.039648174	CCDC14
ENSG00000275395	2.757472483	0.039648174	FCGBP
ENSG00000134324	1.243706991	0.039648174	LPIN1
ENSG00000146007	1.120023588	0.039648174	ZMAT2
ENSG00000152082	1.074744965	0.039684472	MZT2B
ENSG00000114446	0.920355308	0.039685977	IFT57
ENSG00000140478	2.072544111	0.039710526	GOLGA6D
ENSG00000141371	3.421972636	0.039713397	C17orf64
ENSG00000189337	1.265769081	0.039757266	KAZN
ENSG00000166292	3.334551732	0.039757266	TMEM100
ENSG00000166682	2.002699118	0.039768919	TMPRSS5
ENSG00000185347	1.420680978	0.039779781	TEDC1
ENSG00000150779	1.828946567	0.039978482	TIMM8B
ENSG00000163872	0.738619142	0.039995771	YEATS2
ENSG00000135446	1.132483846	0.04004944	CDK4
ENSG00000146221	2.402738502	0.040066101	TCTE1
ENSG00000151148	1.142705327	0.040066101	UBE3B
ENSG00000163468	1.086926685	0.040144465	CCT3
ENSG00000160888	1.457903241	0.040176237	IER2
ENSG00000145912	1.03072328	0.040176237	NHP2

ENSG00000146757	1.435055049	0.040176237	ZNF92
ENSG00000105366	1.223308855	0.040180732	SIGLEC8
ENSG00000160058	1.352476149	0.040232361	BSDC1
ENSG00000180376	0.816091977	0.040232361	CCDC66
ENSG00000234487	1.184098146	0.040249495	HLA F
ENSG00000225691	5.931218442	0.04025259	HLA C
ENSG00000276155	2.389483489	0.040269355	MAPT
ENSG00000138892	2.89618309	0.040269355	TTLL8
ENSG00000258429	1.803049683	0.040286188	PDF
ENSG00000178741	1.192539057	0.040420599	COX5A
ENSG00000123143	0.794003771	0.040420599	PKN1
ENSG00000132953	0.786646817	0.040425119	XPO4
ENSG00000055163	0.983378092	0.040425134	CYFIP2
ENSG00000205629	1.169293169	0.040425134	LCMT1
ENSG00000131236	0.982944555	0.040425594	CAP1
ENSG00000189108	3.304714383	0.040425594	IL1RAPL2
ENSG00000176946	1.104978391	0.040425594	THAP4
ENSG00000126814	1.312215349	0.040532131	TRMT5
ENSG00000100024	1.745767775	0.040580535	UPB1
ENSG00000088205	0.916099694	0.040583122	DDX18
ENSG00000116132	2.161769807	0.040583122	PRRX1
ENSG00000100504	0.819193479	0.040600626	PYGL
ENSG00000136099	3.301165988	0.040636941	PCDH8
ENSG00000095752	1.963128156	0.040669548	IL11
ENSG00000075975	0.93950992	0.040669548	MKRN2
ENSG00000143036	4.600821704	0.04067249	SLC44A3
ENSG00000172247	1.163620837	0.040684507	C1QTNF4
ENSG00000198909	0.972207892	0.040684507	MAP3K3
ENSG00000257150	2.656735078	0.040883688	PGAM1P5
ENSG00000145777	4.426256838	0.040883688	TSLP
ENSG00000130054	2.171316838	0.040914884	FAM155B
ENSG00000172209	2.243762534	0.040914884	GPR22
ENSG00000102935	1.222428761	0.040914884	ZNF423
ENSG00000084652	0.887650583	0.040966735	TXLNA
ENSG00000106258	0.951544934	0.040971282	CYP3A5
ENSG00000156453	2.502785776	0.04101911	PCDH1
ENSG00000140612	0.92109645	0.041043175	SEC11A
ENSG00000135763	1.644187646	0.041068501	URB2
ENSG00000110871	1.026705806	0.041111414	COQ5
ENSG00000165271	0.883867188	0.041157147	NOL6
ENSG00000149262	0.757952935	0.041182629	INTS4
ENSG00000163431	2.421339874	0.041182629	LMOD1
ENSG00000087269	1.016857677	0.041182629	NOP14
ENSG00000091651	0.882485356	0.041182629	ORC6
ENSG00000175274	1.004998509	0.041182629	TP53I11
ENSG00000102901	0.768178934	0.041249707	CENPT
ENSG00000124767	1.356180563	0.041249707	GLO1
ENSG00000108946	0.734880395	0.041249707	PRKAR1A
ENSG00000160208	0.855890304	0.041249707	RRP1B
ENSG00000112983	1.026642227	0.041393655	BRD8
ENSG00000169062	0.87430424	0.041446522	UPF3A
ENSG00000077498	2.966378037	0.041542168	TYR
ENSG00000169035	2.457947329	0.041543208	KLK7
ENSG00000174738	0.983997688	0.041554763	NR1D2
ENSG00000088451	1.795992009	0.041554763	TGDS
ENSG00000164983	0.804780315	0.041613801	TMEM65
ENSG00000105185	1.13569801	0.041658657	PDCD5
ENSG00000007264	0.980163062	0.041704588	MATK
ENSG00000139914	3.208978319	0.041716072	FITM1
ENSG00000197982	1.659331266	0.041882292	C1orf122
ENSG00000072803	0.97123175	0.041882292	FBXW11
ENSG00000132109	1.251506765	0.041895107	TRIM21
ENSG00000137699	2.230544254	0.041895107	TRIM29
ENSG00000112576	1.014071319	0.042035262	CCND3
ENSG00000278224	2.569856059	0.042050717	PRICKLE4
ENSG00000105392	1.623194857	0.042106408	CRX
ENSG00000140259	1.002571307	0.042152321	MFAP1

ENSG00000112697	0.901256136	0.042152321	TMEM30A
ENSG00000198053	0.913535025	0.042191569	SIRPA
ENSG00000100336	0.909594582	0.04223799	APOL4
ENSG00000174059	0.99109874	0.04223799	CD34
ENSG00000176809	1.051299563	0.04223799	LRRC37A3
ENSG00000131242	1.362446834	0.04223799	RAB11FIP4
ENSG00000226858	4.268413393	0.04223799	ZFP57
ENSG00000187951	0.948386565	0.042355328	ARHGAP11B
ENSG00000149557	1.864292931	0.042371142	FEZ1
ENSG00000128191	1.066281157	0.042536178	DGCR8
ENSG00000138678	1.703641613	0.042536178	GPAT3
ENSG00000160593	1.223955932	0.042536178	JAML
ENSG00000116288	1.145449525	0.042536178	PARK7
ENSG00000183632	4.501980644	0.042536178	TP53TG3
ENSG00000166793	1.434149709	0.042536178	YPEL4
ENSG00000146858	1.380027186	0.042536178	ZC3HAV1L
ENSG00000155714	1.409921694	0.042569856	PDZD9
ENSG00000064886	1.693156971	0.042611323	CHI3L2
ENSG00000138780	1.008690202	0.042634077	GSTCD
ENSG00000184381	0.997335313	0.042634077	PLA2G6
ENSG00000101307	1.246088534	0.042666218	SIRPB1
ENSG00000237763	2.2090687	0.042668394	AMY1A
ENSG00000205835	3.811582076	0.042736615	GMNC
ENSG00000149451	1.787351344	0.042757631	ADAM33
ENSG00000100890	0.993484805	0.042817411	KIAA0391
ENSG00000100416	0.747467604	0.042817411	TRMU
ENSG00000146909	0.887458522	0.042907697	NOM1
ENSG00000164975	1.274121966	0.042907697	SNAPC3
ENSG00000148200	1.2792292	0.042914045	NR6A1
ENSG00000001497	0.807226774	0.042968075	LAS1L
ENSG00000110200	1.023991372	0.043004879	ANAPC15
ENSG00000276068	1.516442213	0.043005345	NAIP
ENSG00000160613	0.897518385	0.043005345	PCSK7
ENSG00000162430	0.840329755	0.043005345	SELENON
ENSG00000197275	1.585618543	0.043036063	RAD54B
ENSG00000100014	0.75796346	0.043162154	SPECC1L
ENSG00000108509	0.906402098	0.043183816	CAMTA2
ENSG00000171916	2.401370762	0.043183816	LGALS9C
ENSG00000140992	1.037284314	0.043183816	PDPK1
ENSG00000221878	2.63089403	0.043183816	PSG7
ENSG00000048028	1.727887345	0.043183816	USP28
ENSG00000130713	1.033695811	0.043237151	EXOSC2
ENSG00000185332	2.404988668	0.043237151	TMEM105
ENSG00000166558	3.651973399	0.04333001	SLC38A8
ENSG00000184497	1.822974907	0.04335022	TMEM255B
ENSG00000124541	1.108286002	0.043511259	RRP36
ENSG00000007001	1.457226483	0.043540198	UPP2
ENSG00000100216	1.031382415	0.043565911	TOMM22
ENSG00000172927	1.976775677	0.043597847	MYEOV
ENSG00000179846	1.541189622	0.043679868	NKPD1
ENSG00000143942	1.761290813	0.043759936	CHAC2
ENSG00000169239	1.049572188	0.043763915	CA5B
ENSG00000128262	1.686270731	0.043763915	POM121L9P
ENSG00000157224	1.180389884	0.043785519	CLDN12
ENSG00000177082	0.794904155	0.04385949	WDR73
ENSG00000101935	1.7821161	0.043946829	AMMECR1
ENSG00000213923	0.794497731	0.043946829	CSNK1E
ENSG00000186526	1.427748051	0.043946829	CYP4F8
ENSG00000197653	1.704470168	0.043946829	DNAH10
ENSG00000070785	1.016476201	0.043985066	EIF2B3
ENSG00000116191	0.877247172	0.04400198	RALGPS2
ENSG00000114374	3.890337233	0.044010765	USP9Y
ENSG00000184206	1.52799376	0.044219114	GOLGA6L4
ENSG00000108433	0.855367581	0.044221567	GOSR2
ENSG00000138378	1.488912057	0.044233269	STAT4
ENSG00000180998	1.193426026	0.044391163	GPR137C
ENSG00000100883	0.778785219	0.044407459	SRP54

ENSG00000144749	0.903526926	0.04441918	LRIG1
ENSG00000106003	1.483544361	0.044501689	LFNG
ENSG00000112290	1.047790361	0.044505912	WASF1
ENSG00000182795	2.601351485	0.044550761	C1orf116
ENSG00000090686	0.731689477	0.044566871	USP48
ENSG00000152669	3.745074136	0.044668121	CCNO
ENSG00000145626	2.353881628	0.044717299	UGT3A1
ENSG00000099875	1.324970256	0.044730864	MKNK2
ENSG00000150676	1.727218692	0.044766599	CCDC83
ENSG00000115919	1.111482644	0.044766599	KYNU
ENSG00000177879	0.993660922	0.044827184	AP3S1
ENSG00000222011	1.425489166	0.045022648	FAM185A
ENSG00000163291	0.967832779	0.045117998	PAQR3
ENSG00000169220	0.960721298	0.045117998	RGS14
ENSG00000072756	0.83798732	0.045117998	TRNT1
ENSG00000123836	1.289740063	0.045130231	PFKFB2
ENSG00000138100	2.395389164	0.045154648	TRIM54
ENSG00000162105	1.310888415	0.04515517	SHANK2
ENSG00000171992	1.070535449	0.04515517	SYNPO
ENSG00000213937	1.493508399	0.045175834	CLDN9
ENSG00000053372	1.13505346	0.045175834	MRTO4
ENSG00000174669	1.106627793	0.045175834	SLC29A2
ENSG00000273274	0.958003015	0.045175834	ZBTB8B
ENSG00000106688	3.143209566	0.045184342	SLC1A1
ENSG00000234616	0.865165222	0.045206147	JRK
ENSG00000149115	0.946124448	0.045206147	TNKS1BP1
ENSG00000150938	1.072608786	0.045249605	CRIM1
ENSG00000158769	0.944984749	0.045249605	F11R
ENSG00000164347	0.938837524	0.045249605	GFM2
ENSG00000109320	1.158140494	0.045249605	NFKB1
ENSG00000143653	1.06536146	0.045249605	SCCPDH
ENSG00000117153	1.352524427	0.045349699	KLHL12
ENSG00000162437	0.809314089	0.045349699	RAVER2
ENSG00000111728	1.149159976	0.045349699	ST8SIA1
ENSG00000104219	1.303370336	0.045349699	ZDHHC2
ENSG00000180616	1.062788046	0.045372352	SSTR2
ENSG00000131848	1.324400967	0.045372352	ZSCAN5A
ENSG00000151748	1.049620374	0.045392413	SAV1
ENSG00000162599	1.312704571	0.045429524	NFIA
ENSG00000110237	1.177333769	0.045563249	ARHGEF17
ENSG00000158717	1.437267802	0.045597581	RNF166
ENSG00000188613	1.870140595	0.045627298	NANOS1
ENSG00000116685	1.069767788	0.04568842	KIAA2013
ENSG00000186951	0.961908849	0.04568842	PPARA
ENSG00000177398	1.730156191	0.04568842	UMODL1
ENSG00000164465	1.608223159	0.045718511	DCBLD1
ENSG00000105676	1.043761645	0.045729808	ARMC6
ENSG00000125633	0.899612563	0.045816833	CCDC93
ENSG00000019169	2.759151942	0.045816833	MARCO
ENSG00000135074	1.200173159	0.04585921	ADAM19
ENSG00000180259	4.131787766	0.04585921	PRNT
ENSG00000143195	1.836159049	0.04590415	ILDR2
ENSG00000243927	1.615587622	0.045954634	MRPS6
ENSG00000145331	2.064733286	0.045954634	TRMT10A
ENSG00000116039	2.988037076	0.046003216	ATP6V1B1
ENSG00000265190	2.318869428	0.046188816	ANXA8
ENSG00000099795	1.201594681	0.046239629	NDUFB7
ENSG00000221955	1.166952045	0.046239629	SLC12A8
ENSG00000179542	1.420095758	0.046271638	SLITRK4
ENSG00000124279	1.883932139	0.046283078	FASTKD3
ENSG00000125731	1.184335003	0.046283078	SH2D3A
ENSG00000067646	8.493173659	0.046310515	ZFY
ENSG00000172530	1.124437073	0.046311185	BANP
ENSG00000240230	0.890126273	0.046422012	COX19
ENSG00000062822	1.133123499	0.046458162	POLD1
ENSG00000150907	1.096006525	0.046472196	FOXO1
ENSG00000073712	1.780718409	0.046475811	FERMT2

ENSG00000196172	1.19274966	0.046475811	ZNF681
ENSG00000277322	1.534060923	0.046480345	GOLGA6L6
ENSG00000153237	1.231959284	0.046486122	CCDC148
ENSG00000105855	1.277410606	0.046576256	ITGB8
ENSG00000185888	3.54101345	0.046583363	PRSS38
ENSG00000066735	2.027011832	0.04662363	KIF26A
ENSG00000172772	3.03040407	0.04662363	OR10W1
ENSG00000099960	4.324051414	0.04662363	SLC7A4
ENSG00000117408	1.489749685	0.046685691	IPO13
ENSG00000013297	1.204247738	0.046716864	CLDN11
ENSG00000185101	1.221074049	0.046777958	ANO9
ENSG00000180720	2.73156167	0.046777958	CHRM4
ENSG00000146857	3.22535644	0.046818662	STRA8
ENSG00000151572	2.550636287	0.04683329	ANO4
ENSG00000069275	1.008405748	0.04683329	NUCKS1
ENSG00000117448	1.056925757	0.046896744	AKR1A1
ENSG00000166415	1.68720554	0.046944757	WDR72
ENSG00000106714	1.948213634	0.046951958	CNTNAP3
ENSG00000110344	0.785465118	0.046966832	UBE4A
ENSG00000162704	1.205042241	0.046973115	ARPC5
ENSG00000153574	1.283488154	0.046992881	RPIA
ENSG00000139438	2.002638704	0.047005096	FAM222A
ENSG00000060982	0.84339132	0.047022136	BCAT1
ENSG00000104093	0.912934167	0.047022136	DMXL2
ENSG00000278463	1.608307253	0.047095342	HIST1H2AB
ENSG00000125995	1.303628275	0.047095342	ROMO1
ENSG00000166546	1.496054121	0.047100044	BEAN1
ENSG00000196338	1.666693098	0.047133092	NLGN3
ENSG00000120094	2.970917969	0.047156413	HOXB1
ENSG00000127774	1.377133915	0.047203049	EMC6
ENSG00000128016	1.637821925	0.047263648	ZFP36
ENSG00000198798	2.947891821	0.047273329	MAGEB3
ENSG00000198899	1.001114261	0.047277617	ATP6
ENSG00000168702	2.577547346	0.047277617	LRP1B
ENSG00000125863	1.751518239	0.047277617	MKKS
ENSG00000108179	1.295542934	0.047378449	PPIF
ENSG00000197894	1.306293736	0.047387542	ADH5
ENSG00000127445	1.250906071	0.047387542	PIN1
ENSG00000262406	4.403885164	0.047459983	MMP12
ENSG00000070778	1.876181639	0.047523738	PTPN21
ENSG00000154719	1.192241214	0.047542578	MRPL39
ENSG00000163376	1.302606788	0.047595766	KBTBD8
ENSG00000212907	0.914587608	0.047620115	ND4L
ENSG00000114956	1.241823725	0.04788175	DGUOK
ENSG00000140395	1.064285817	0.048002855	WDR61
ENSG00000140522	2.704259618	0.048006185	RLBP1
ENSG00000132300	0.806864384	0.048015041	PTCD3
ENSG00000169826	1.102590556	0.048031897	CSGALNACT2
ENSG00000128891	0.982154797	0.048094633	CCDC32
ENSG00000180329	1.152348386	0.048094633	CCDC43
ENSG00000213218	3.940399569	0.048094633	CSH2
ENSG00000170345	1.683373177	0.048094633	FOS
ENSG00000090674	1.345222977	0.048094633	MCOLN1
ENSG00000185960	1.175678045	0.048094633	SHOX
ENSG00000164051	1.349706885	0.048276591	CCDC51
ENSG00000145113	4.898061385	0.048276591	MUC4
ENSG00000196290	1.263794303	0.048296379	NIF3L1
ENSG00000176623	0.820577838	0.048319176	RMDN1
ENSG00000117597	1.154562449	0.048431485	DIEXF
ENSG00000129353	0.9562368	0.048431485	SLC44A2
ENSG00000204983	2.240567858	0.048477584	PRSS1
ENSG00000159905	1.21178015	0.048477584	ZNF221
ENSG00000101412	1.141434467	0.048518178	E2F1
ENSG00000151322	1.412671172	0.048518178	NPAS3
ENSG00000154065	2.234521998	0.048625093	ANKRD29
ENSG00000173846	1.236706277	0.048661647	PLK3
ENSG00000125520	1.30419339	0.048690483	SLC2A4RG

ENSG00000258644	1.751007019	0.048775315	SYNJ2BP COX16
ENSG00000183092	1.339182195	0.048793018	BEGAIN
ENSG00000188641	0.803061747	0.048794344	DPYD
ENSG00000005022	0.996698927	0.048813554	SLC25A5
ENSG00000130559	0.816941503	0.048864708	CAMSAP1
ENSG00000163006	1.296211376	0.048973369	CCDC138
ENSG00000164484	1.414541988	0.049033794	TMEM200A
ENSG00000121236	1.246434149	0.049033794	TRIM6
ENSG00000130638	0.862619089	0.049093057	ATXN10
ENSG00000181804	1.663327322	0.04912198	SLC9A9
ENSG00000083168	0.941737544	0.049147909	KAT6A
ENSG00000132475	0.846088316	0.049225916	H3F3B
ENSG00000154262	1.735476758	0.049298105	ABCA6
ENSG00000151338	0.950485503	0.049306676	MIPOL1
ENSG00000163785	0.938539459	0.049336803	RYK
ENSG00000278570	2.583703193	0.049418948	NR2E3
ENSG00000055130	0.812187633	0.049455096	CUL1
ENSG00000144824	0.949257717	0.049569554	PHLDB2
ENSG00000152583	2.562813361	0.049569554	SPARCL1
ENSG00000198965	4.686111907	0.049571566	OR10R2
ENSG00000131620	2.265181292	0.049657774	ANO1
ENSG00000129562	1.117042192	0.049657774	DAD1
ENSG00000184207	1.466020626	0.049657774	PGP
ENSG00000197901	2.285067329	0.04967704	SLC22A6
ENSG00000011083	2.204729015	0.049681986	SLC6A7
ENSG00000136840	1.030992813	0.049681986	ST6GALNAC4
ENSG00000185905	0.920184847	0.049714471	C16orf54
ENSG00000198937	1.510709787	0.049714471	CCDC167
ENSG00000164933	0.916816159	0.049884179	SLC25A32
ENSG00000197841	1.429385205	0.049884179	ZNF181
ENSG00000106477	1.14388551	0.049897365	CEP41
ENSG00000158623	1.065205895	0.049924384	COPG2
ENSG00000125703	1.883209719	0.049980073	ATG4C
ENSG00000106346	1.050257746	0.049980073	USP42
ENSG00000177628	1.146802051	0.049996334	GBA
ENSG00000010256	0.94146421	0.049996334	UQCRC1

10.4 Appendix 4

List of genes differentially expressed between human foetal liver HSC/MPPs and LMPPs (positive log fold represents genes upregulated in the foetal liver derived LMPPs), described in chapter 4.

Ensemb ID	og2 Fo d Change	padj	Gene Name
ENSG00000132744	4.020106581	2.76E 36	ACY3
ENSG00000042062	3.019266039	5.37E 27	RIPOR3
ENSG00000108924	2.664283841	2.41E 23	HLF
ENSG00000261150	3.377185123	5.80E 22	EPPK1
ENSG00000165168	5.24237647	1.10E 21	CYBB
ENSG00000182557	2.217434516	7.94E 21	SPNS3
ENSG00000128322	3.268381421	4.85E 20	IGLL1
ENSG00000142185	3.218521912	1.04E 19	TRPM2
ENSG00000164946	3.848039262	1.52E 19	FREM1
ENSG00000109684	2.514816778	6.94E 18	CLNK
ENSG00000005381	3.476677198	8.81E 17	MPO
ENSG00000196159	2.980044081	2.63E 16	FAT4
ENSG00000076641	2.742002584	4.20E 16	PAG1
ENSG00000037280	2.85987931	6.55E 16	FLT4
ENSG00000198752	3.148331961	9.53E 16	CDC42BPB
ENSG00000000971	2.448074128	1.44E 15	CFH
ENSG00000130396	2.783856733	1.63E 15	AFDN
ENSG00000005844	1.887775641	5.18E 15	ITGAL
ENSG00000142173	2.733756749	5.51E 15	COL6A2
ENSG00000049323	2.759982987	3.48E 14	LTBP1
ENSG00000134755	3.112116776	4.43E 14	DSC2
ENSG00000154783	1.897973373	1.77E 13	FGD5
ENSG00000186469	2.378779793	1.77E 13	GNG2
ENSG00000140968	3.494688823	3.93E 13	IRF8
ENSG00000120093	1.562145338	7.88E 13	HOXB3
ENSG00000171791	1.866847601	1.03E 12	BCL2
ENSG00000120156	3.153135366	1.20E 12	TEK
ENSG00000005379	2.361585043	2.53E 12	TSPOAP1
ENSG00000133026	1.83377913	4.94E 12	MYH10
ENSG00000165092	2.174486874	1.39E 11	ALDH1A1
ENSG00000141756	2.012888007	6.74E 11	FKBP10
ENSG00000010327	2.02174646	7.05E 11	STAB1
ENSG00000164125	1.958470525	8.08E 11	FAM198B
ENSG00000171843	2.247920751	1.05E 10	MLLT3
ENSG00000086730	1.685989284	2.32E 10	LAT2
ENSG00000164330	2.921033266	3.17E 10	EBF1
ENSG00000134871	3.364446401	5.12E 10	COL4A2
ENSG00000133800	3.772481826	6.08E 10	LYVE1
ENSG00000198879	1.658989128	6.82E 10	SFMBT2
ENSG00000249751	8.242045336	3.43E 09	ECSCR
ENSG00000131477	2.909727366	4.32E 09	RAMP2
ENSG00000079337	1.177387984	4.32E 09	RAPGEF3
ENSG00000177469	2.055525648	5.07E 09	CAVIN1
ENSG00000130635	1.53925645	5.07E 09	COL5A1
ENSG00000113389	1.302010418	7.56E 09	NPR3
ENSG00000127507	1.571422648	8.04E 09	ADGRE2
ENSG00000143995	1.323646128	8.83E 09	MEIS1
ENSG00000162367	1.170090071	1.46E 08	TAL1
ENSG00000132669	2.601975985	1.62E 08	RIN2
ENSG00000068724	1.599004666	1.62E 08	TTC7A
ENSG00000120278	3.35958562	1.80E 08	PLEKHG1
ENSG00000105374	2.947615417	1.95E 08	NKG7
ENSG00000182578	1.836969726	2.67E 08	CSF1R
ENSG00000120279	3.928282531	3.25E 08	MYCT1
ENSG00000135048	2.494366543	4.08E 08	TMEM2
ENSG00000117480	2.074920135	6.70E 08	FAAH

ENSG00000106236	3.501264372	8.52E 08	NPTX2
ENSG00000179776	2.861119168	8.73E 08	CDH5
ENSG00000170476	1.650341174	9.25E 08	MZB1
ENSG00000117069	4.665256604	1.27E 07	ST6GALNAC5
ENSG00000266074	1.265778674	1.36E 07	BAHCC1
ENSG00000167483	1.554200429	1.38E 07	FAM129C
ENSG00000066056	1.095431615	1.38E 07	TIE1
ENSG00000031081	1.409213605	1.39E 07	ARHGAP31
ENSG00000154133	1.924207339	1.39E 07	ROBO4
ENSG00000142611	1.90334699	1.61E 07	PRDM16
ENSG00000147862	2.985501308	2.10E 07	NFIB
ENSG00000124507	3.942054354	2.10E 07	PACSIN1
ENSG00000157510	2.193428809	2.29E 07	AFAP1L1
ENSG00000196684	1.299332088	2.80E 07	HSH2D
ENSG00000102755	2.973628212	2.88E 07	FLT1
ENSG00000109452	1.317338754	2.91E 07	INPP4B
ENSG00000154479	1.740821856	2.98E 07	CCDC173
ENSG00000132465	5.739898503	3.05E 07	JCHAIN
ENSG00000125733	2.176721561	3.26E 07	TRIP10
ENSG00000135709	2.548914741	3.86E 07	KIAA0513
ENSG00000169398	1.296349706	4.91E 07	PTK2
ENSG00000161544	3.291261866	4.94E 07	CYGB
ENSG00000100968	1.879757475	5.82E 07	NFATC4
ENSG00000003147	1.663159731	5.97E 07	ICA1
ENSG00000274267	1.159163286	7.68E 07	HIST1H3B
ENSG00000119919	3.28005373	7.68E 07	NKX2 3
ENSG00000121966	2.412780229	8.93E 07	CXCR4
ENSG00000160339	3.922635274	9.29E 07	FCN2
ENSG00000181444	1.713384675	9.67E 07	ZNF467
ENSG00000172889	0.932089324	9.94E 07	EGFL7
ENSG00000184557	2.585209102	1.30E 06	SOCS3
ENSG00000205978	1.414093145	1.33E 06	NYNRIN
ENSG00000168497	1.507052417	1.53E 06	CAVIN2
ENSG00000115085	1.858483191	1.92E 06	ZAP70
ENSG00000197879	2.860577855	2.04E 06	MYO1C
ENSG00000214193	1.331401518	2.28E 06	SH3D21
ENSG00000143507	1.098339716	2.59E 06	DUSP10
ENSG00000169291	2.210986951	2.65E 06	SHE
ENSG00000102302	1.778409747	2.72E 06	FGD1
ENSG00000107807	4.714337071	2.87E 06	TLX1
ENSG00000169992	1.296343999	3.47E 06	NLGN2
ENSG00000107281	2.602033096	3.49E 06	NPDC1
ENSG00000011454	1.417217113	3.50E 06	GPR21
ENSG00000120594	1.572137413	3.55E 06	PLXDC2
ENSG00000181409	2.144582505	4.33E 06	AATK
ENSG00000117519	1.579909554	4.44E 06	CNN3
ENSG00000066735	2.858413861	4.44E 06	KIF26A
ENSG00000260314	2.435246205	4.61E 06	MRC1
ENSG00000169184	1.641018858	4.69E 06	MN1
ENSG00000196839	1.506458553	5.46E 06	ADA
ENSG00000144218	1.317287338	6.43E 06	AFF3
ENSG00000179348	1.258392317	6.77E 06	GATA2
ENSG00000151718	1.371626306	7.32E 06	WWC2
ENSG00000148400	0.899377551	7.46E 06	NOTCH1
ENSG00000203883	1.984147261	7.58E 06	SOX18
ENSG00000130592	1.523994018	7.62E 06	LSP1
ENSG00000101000	1.945729747	7.77E 06	PROCR
ENSG00000170873	1.474510329	7.79E 06	MTSS1
ENSG00000120280	1.218486308	7.88E 06	CXorf21
ENSG00000162909	1.448295196	8.85E 06	CAPN2
ENSG00000090097	2.815880704	1.07E 05	PCBP4
ENSG00000169575	3.954741928	1.08E 05	VPREB1
ENSG00000130300	2.051293373	1.16E 05	PLVAP
ENSG00000186642	2.78505211	1.28E 05	PDE2A
ENSG00000137834	2.490268506	1.30E 05	SMAD6
ENSG00000128052	4.823405869	1.31E 05	KDR
ENSG00000166349	2.241817612	1.37E 05	RAG1

ENSG00000177398	2.403109299	1.45E 05	UMODL1
ENSG00000245848	1.475690597	1.52E 05	CEBPA
ENSG00000118257	2.066976187	1.63E 05	NRP2
ENSG00000126217	1.607573208	1.66E 05	MCF2L
ENSG00000135047	3.423678435	1.73E 05	CTSL
ENSG00000134709	1.816268527	1.80E 05	HOOK1
ENSG00000215252	1.204185365	2.00E 05	GOLGA8B
ENSG00000046889	1.270900046	2.26E 05	PREX2
ENSG00000138449	1.960584002	2.36E 05	SLC40A1
ENSG00000143889	1.770566975	2.42E 05	HNRNPLL
ENSG00000171115	1.846122182	2.50E 05	GIMAP8
ENSG00000100368	1.316829148	3.00E 05	CSF2RB
ENSG00000135838	2.440465521	3.00E 05	NPL
ENSG00000137726	1.516773696	3.21E 05	FXYD6
ENSG00000122642	1.524137206	3.45E 05	FKBP9
ENSG00000198851	2.466208709	3.57E 05	CD3E
ENSG00000109756	1.097519297	3.74E 05	RAPGEF2
ENSG00000065054	1.586129198	3.79E 05	SLC9A3R2
ENSG00000187837	1.041296605	3.94E 05	HIST1H1C
ENSG00000137198	1.997149199	4.48E 05	GMPR
ENSG00000100068	1.096878958	5.01E 05	LRP5L
ENSG00000108511	2.391090222	5.20E 05	HOXB6
ENSG00000169418	3.035178331	5.22E 05	NPR1
ENSG00000198729	4.459955583	5.22E 05	PPP1R14C
ENSG00000165810	2.575753178	5.46E 05	BTNL9
ENSG00000121858	1.788417033	5.59E 05	TNFSF10
ENSG00000125968	2.546160431	5.64E 05	ID1
ENSG00000131067	1.629349269	5.70E 05	GGT7
ENSG00000122224	1.771399583	6.98E 05	LY9
ENSG00000197409	1.050862458	7.07E 05	HIST1H3D
ENSG00000116016	2.79405711	7.21E 05	EPAS1
ENSG00000276053	1.100561488	7.30E 05	LAIR1
ENSG00000135318	3.31043106	7.33E 05	NT5E
ENSG00000151838	1.994641421	7.53E 05	CCDC175
ENSG00000167780	4.579325415	7.96E 05	SOAT2
ENSG00000136011	4.487830526	8.03E 05	STAB2
ENSG00000163513	0.8763236	8.03E 05	TGFBR2
ENSG00000134278	1.229813739	8.27E 05	SPIRE1
ENSG00000183166	1.388932765	8.84E 05	CALN1
ENSG00000184357	1.12666166	8.84E 05	HIST1H1B
ENSG00000244242	2.69872112	8.84E 05	IFITM10
ENSG00000141293	1.712900709	9.06E 05	SKAP1
ENSG00000050820	3.435805675	9.72E 05	BCAR1
ENSG00000174944	2.113552736	9.82E 05	P2RY14
ENSG00000176105	1.421772497	9.82E 05	YES1
ENSG00000149564	1.091935349	9.83E 05	ESAM
ENSG00000138795	1.354336052	0.00010083	LEF1
ENSG00000133636	4.918016934	0.00010101	NTS
ENSG00000134817	2.826288483	0.00010171	APLNR
ENSG00000095637	1.916610284	0.00010221	SORBS1
ENSG00000138411	3.684423354	0.00011293	HECW2
ENSG00000185010	2.729386424	0.00011378	F8
ENSG00000153253	2.240067727	0.00012363	SCN3A
ENSG00000181804	2.334304079	0.00012752	SLC9A9
ENSG00000147168	1.418216699	0.00013234	IL2RG
ENSG00000008311	1.662928875	0.00013284	AASS
ENSG00000074660	1.099596572	0.00015409	SCARF1
ENSG00000159640	1.50621142	0.00017102	ACE
ENSG00000185499	2.329362505	0.00019402	MUC1
ENSG00000149557	3.090357856	0.00019758	FEZ1
ENSG00000085733	2.76382851	0.00020582	CTTN
ENSG00000100234	1.103595751	0.00020582	TIMP3
ENSG00000173269	1.546870929	0.00021103	MMRN2
ENSG00000074047	2.496089882	0.00021271	GLI2
ENSG00000130940	1.428802104	0.00022311	CASZ1
ENSG00000111261	1.92429303	0.00022937	MANSC1
ENSG00000281818	1.92429303	0.00022937	MANSC1

ENSG00000125266	3.057531769	0.0002345	EFNB2
ENSG00000075240	1.286397588	0.00023541	GRAMD4
ENSG00000152128	1.480257497	0.00023541	TMEM163
ENSG00000215788	1.362680674	0.00023541	TNFRSF25
ENSG00000064042	2.064655769	0.00023653	LIMCH1
ENSG00000070882	1.277782674	0.00024321	OSBPL3
ENSG00000091409	1.288418125	0.00025874	ITGA6
ENSG00000130158	1.974124008	0.0002641	DOCK6
ENSG00000184867	1.848108551	0.00027048	ARMCX2
ENSG00000042493	1.314898081	0.00027048	CAPG
ENSG00000105974	2.739047029	0.00027663	CAV1
ENSG00000204186	1.128391983	0.00029537	ZDBF2
ENSG00000105810	1.062031752	0.00030437	CDK6
ENSG00000030419	1.300435137	0.00031092	IKZF2
ENSG00000169744	1.877935724	0.00031092	LDB2
ENSG00000161647	2.122174485	0.00031092	MPP3
ENSG00000073712	2.735773818	0.00032737	FERMT2
ENSG00000250722	1.902730924	0.0003455	SELENOP
ENSG00000157873	1.545604558	0.00035197	TNFRSF14
ENSG00000196628	1.02234501	0.00036427	TCF4
ENSG00000173166	2.373905526	0.00038242	RAPH1
ENSG00000129946	3.1040011	0.00038242	SHC2
ENSG00000136114	1.852932528	0.00039414	THSD1
ENSG00000159674	1.632341306	0.00040213	SPON2
ENSG00000158528	1.394058635	0.00040281	PPP1R9A
ENSG00000101439	1.514138545	0.00040962	CST3
ENSG00000100242	0.841739024	0.00040962	SUN2
ENSG00000073849	0.854028944	0.00043966	ST6GAL1
ENSG00000068078	2.21075181	0.00044028	FGFR3
ENSG00000147206	3.121395872	0.00044207	NXF3
ENSG00000182568	1.256244433	0.00046421	SATB1
ENSG00000198825	0.782709885	0.00047186	INPP5F
ENSG00000198873	1.037491356	0.00049295	GRK5
ENSG00000276043	1.367410465	0.00049295	UHRF1
ENSG00000273936	1.504812546	0.0004951	TNFRSF14
ENSG00000163519	4.73395632	0.00049646	TRAT1
ENSG00000074219	2.680458179	0.00050089	TEAD2
ENSG00000111057	1.657837434	0.00050658	KRT18
ENSG00000198842	1.39841366	0.00052812	DUSP27
ENSG00000117983	3.06606667	0.00053214	MUC5B
ENSG00000144476	1.496628218	0.00053763	ACKR3
ENSG00000204681	2.507183001	0.00053886	GABBR1
ENSG00000107186	1.242614995	0.00054492	MPDZ
ENSG00000114115	2.501356503	0.00054492	RBP1
ENSG00000131016	3.296314586	0.00054794	AKAP12
ENSG00000185386	1.091178258	0.00057504	MAPK11
ENSG00000166856	2.313977843	0.00059201	GPR182
ENSG00000143369	2.715424217	0.00061829	ECM1
ENSG00000151176	1.446904089	0.0006308	PLBD2
ENSG00000102362	1.020170903	0.00067584	SYTL4
ENSG00000178498	1.072144832	0.00068124	DTX3
ENSG00000198585	0.835853509	0.0007135	NUDT16
ENSG00000197822	2.365280729	0.00073019	OCLN
ENSG00000103489	1.185508319	0.00074386	XYLT1
ENSG00000177685	2.820438435	0.00077182	CRACR2B
ENSG00000163687	3.63548447	0.00079381	DNASE1L3
ENSG00000143153	1.418346525	0.00081803	ATP1B1
ENSG00000183735	0.85059981	0.00088714	TBK1
ENSG00000118946	2.48493249	0.00090058	PCDH17
ENSG00000157570	2.132397819	0.00090437	TSPAN18
ENSG00000111961	2.216276349	0.0009123	SASH1
ENSG00000175899	1.542207812	0.00095199	A2M
ENSG00000250510	1.932393789	0.00096802	GPR162
ENSG00000163069	2.477955265	0.00096802	SGCB
ENSG00000172037	1.417130501	0.00097136	LAMB2
ENSG00000111676	0.76463735	0.00099901	ATN1
ENSG00000137804	0.791202735	0.00099901	NUSAP1

ENSG00000168056	1.081610416	0.00102939	LTBP3
ENSG00000069702	2.509713405	0.00102939	TGFBR3
ENSG00000153113	0.990377587	0.00106935	CAST
ENSG00000278463	0.870671713	0.00109281	HIST1H2AB
ENSG00000159216	0.85055811	0.00109379	RUNX1
ENSG00000165030	1.452538147	0.00116044	NFIL3
ENSG00000171680	2.2946288	0.00116044	PLEKHG5
ENSG00000172493	1.049653148	0.00116588	AFF1
ENSG00000196460	2.027472492	0.00116588	RFX8
ENSG00000153162	2.09988576	0.00122732	BMP6
ENSG00000036448	1.646406664	0.00122732	MYOM2
ENSG00000137831	1.453662595	0.00122732	UACA
ENSG00000069188	1.328029547	0.00123523	SDK2
ENSG00000102575	2.268142104	0.00124019	ACP5
ENSG00000140678	1.350902587	0.00131365	ITGAX
ENSG00000005249	1.564904803	0.00141872	PRKAR2B
ENSG00000026508	0.952635138	0.00143138	CD44
ENSG00000049089	1.526629619	0.00143138	COL9A2
ENSG00000174804	2.393912982	0.00143138	FZD4
ENSG00000134107	3.167021532	0.00145786	BHLHE40
ENSG00000153904	1.54745227	0.00146429	DDAH1
ENSG00000188580	1.664286259	0.00146429	NKAIN2
ENSG00000003393	0.789420189	0.00149435	ALS2
ENSG00000138678	2.246229739	0.00149435	GPAT3
ENSG00000117643	1.963856891	0.00156318	MAN1C1
ENSG00000198589	0.895673112	0.00158164	LRBA
ENSG00000152952	1.285043806	0.00163188	PLOD2
ENSG00000274618	0.866833272	0.00163214	HIST1H4F
ENSG00000174482	4.156368369	0.00174868	LINGO2
ENSG00000112799	2.871349176	0.00175237	LY86
ENSG00000227507	1.77875787	0.00181666	LTB
ENSG00000157933	1.154218748	0.00185691	SKI
ENSG00000180530	1.01737319	0.00186101	NRIP1
ENSG00000124440	1.0664472	0.00190612	HIF3A
ENSG00000120318	2.321100904	0.0019319	ARAP3
ENSG00000134202	1.336586109	0.00198466	GSTM3
ENSG00000160145	2.038879714	0.00201355	KALRN
ENSG00000165682	3.641485881	0.00204777	CLEC1B
ENSG00000142798	1.750129929	0.00204777	HSPG2
ENSG00000141503	0.727790729	0.00208556	MINK1
ENSG00000132321	1.554087388	0.00210975	IQCA1
ENSG00000185101	1.650800916	0.00211932	ANO9
ENSG00000205755	1.571911054	0.00211932	CRLF2
ENSG00000148468	2.26170929	0.00218221	FAM171A1
ENSG00000276368	0.960221747	0.00218221	HIST1H2AJ
ENSG00000187800	1.184329313	0.00219641	PEAR1
ENSG00000197992	2.514342471	0.0022425	CLEC9A
ENSG00000041353	1.635704955	0.00231568	RAB27B
ENSG00000130598	1.264235493	0.00231568	TNNI2
ENSG00000106789	1.09108688	0.00235363	CORO2A
ENSG00000165125	2.009690114	0.00240539	TRPV6
ENSG00000096433	2.282310286	0.00241792	ITPR3
ENSG00000007968	0.898461139	0.00242058	E2F2
ENSG00000143469	1.457597587	0.00242338	SYT14
ENSG00000076706	2.030899831	0.0024338	MCAM
ENSG00000163637	3.873793049	0.0024338	PRICKLE2
ENSG00000196632	1.511691532	0.0024338	WNK3
ENSG00000278828	0.848996551	0.00247333	HIST1H3H
ENSG00000132359	0.978685099	0.00247333	RAP1GAP2
ENSG00000182866	1.517217527	0.00258769	LCK
ENSG00000167703	1.138195703	0.00267273	SLC43A2
ENSG00000072163	2.772333678	0.00269329	LIMS2
ENSG00000134986	0.756000537	0.0027058	NREP
ENSG00000101871	2.352623591	0.00276431	MID1
ENSG00000092929	0.74260802	0.00276431	UNC13D
ENSG00000177303	1.391855138	0.00281019	CASKIN2
ENSG00000135540	1.062893243	0.00290796	NHSL1

ENSG00000277401	3.281383535	0.00297056	TJP1
ENSG00000185630	1.004253685	0.0029744	PBX1
ENSG00000203852	0.815067631	0.00299006	HIST2H3A
ENSG00000203811	0.815067631	0.00299006	HIST2H3C
ENSG00000177374	1.556108546	0.00301525	HIC1
ENSG00000148773	0.761912288	0.00301525	MKI67
ENSG00000117586	0.923970013	0.00306916	TNFSF4
ENSG00000163661	1.65810892	0.00315191	PTX3
ENSG00000116962	2.877716701	0.00318629	NID1
ENSG00000176083	2.068465556	0.00337635	ZNF683
ENSG00000162430	0.817487422	0.0034414	SELENON
ENSG00000168421	0.928183342	0.00349696	RHOH
ENSG00000101333	1.182625763	0.00356031	PLCB4
ENSG00000091592	0.872215474	0.00359557	NLRP1
ENSG00000274750	1.314435953	0.00371685	HIST1H3E
ENSG00000186583	1.737537225	0.00371685	SPATC1
ENSG00000135476	0.935346642	0.00395106	ESPL1
ENSG00000169403	1.507488243	0.00395106	PTAFR
ENSG00000120693	1.662070874	0.00395106	SMAD9
ENSG00000181631	1.740613691	0.00401134	P2RY13
ENSG00000274137	2.773655599	0.00407083	MYOM2
ENSG00000215126	1.485121333	0.00422623	CBWD2
ENSG00000082438	1.354800846	0.00430114	COBLL1
ENSG00000170482	1.441583989	0.00430114	SLC23A1
ENSG00000138722	1.080940834	0.00431164	MMRN1
ENSG00000100055	1.324142935	0.00434538	CYTH4
ENSG00000064393	0.81492074	0.00434538	HIPK2
ENSG00000138315	3.977965604	0.00434538	OIT3
ENSG00000167994	2.207617674	0.00434538	RAB3IL1
ENSG00000146674	2.846913899	0.00439704	IGFBP3
ENSG00000170542	1.07916359	0.00439904	SERPINB9
ENSG00000204197	0.838015864	0.00441044	KIFC1
ENSG00000101200	2.76810155	0.00441383	AVP
ENSG00000171703	0.798547752	0.0044334	TCEA2
ENSG00000198467	0.915411802	0.0044334	TPM2
ENSG00000070778	2.027628931	0.00443837	PTPN21
ENSG00000010610	1.788650489	0.0047221	CD4
ENSG00000198844	2.363042899	0.00492595	ARHGEF15
ENSG00000164741	1.855899543	0.00492595	DLC1
ENSG00000136286	0.79587199	0.00509648	MYO1G
ENSG00000173548	1.297425432	0.00509674	SNX33
ENSG00000124019	1.055307006	0.00513736	FAM124B
ENSG00000197536	0.796970571	0.00522435	C5orf56
ENSG00000104081	1.229399238	0.00524816	BMF
ENSG00000165591	2.083680268	0.00524816	FAAH2
ENSG00000082074	0.944112961	0.00524816	FYB1
ENSG00000197061	0.852748499	0.00524816	HIST1H4C
ENSG00000198053	0.903927721	0.00544013	SIRPA
ENSG00000141753	1.998511789	0.00545646	IGFBP4
ENSG00000110811	1.176174802	0.00555177	P3H3
ENSG00000132613	0.669901891	0.00563437	MTSS1L
ENSG00000142627	3.192884249	0.00563573	EPHA2
ENSG00000196923	0.766442815	0.0056527	PDLIM7
ENSG00000164877	0.917923689	0.00572897	MICALL2
ENSG00000105472	1.222745906	0.00577277	CLEC11A
ENSG00000133574	1.5129269	0.00582916	GIMAP4
ENSG00000066382	1.143615174	0.00585647	MPPED2
ENSG00000116833	2.03283586	0.00592996	NR5A2
ENSG00000099250	1.776031517	0.00605101	NRP1
ENSG00000176907	4.575879013	0.00612859	TCIM
ENSG00000135218	3.098017829	0.00630926	CD36
ENSG00000142089	1.092476529	0.0065896	IFITM3
ENSG00000197355	1.157574142	0.00666022	UAP1L1
ENSG00000198835	1.701583945	0.0066859	GJC2
ENSG00000130783	1.341039766	0.00686218	CCDC62
ENSG00000145708	2.799203461	0.00686218	CRHBP
ENSG00000134874	1.472297621	0.00686218	DZIP1

ENSG00000112715	1.234290358	0.00686218	VEGFA
ENSG00000080200	0.996072182	0.00688273	CRYBG3
ENSG00000142552	2.217940418	0.00688273	RCN3
ENSG00000110841	0.805407456	0.00698431	PPFIBP1
ENSG00000277157	1.13404813	0.00703419	HIST1H4D
ENSG00000203814	0.616421003	0.00703419	HIST2H2BF
ENSG00000188130	0.898978738	0.00735305	MAPK12
ENSG00000271605	1.59325899	0.00745284	MILR1
ENSG00000105251	2.602201109	0.00747592	SHD
ENSG00000166963	1.228314448	0.00754852	MAP1A
ENSG00000258102	2.782460807	0.00757357	MAP1LC3B2
ENSG00000189007	0.745941789	0.00758038	ADAT2
ENSG00000008277	1.28940099	0.00769947	ADAM22
ENSG00000100596	0.848549389	0.00788316	SPTLC2
ENSG00000090530	1.698877759	0.00799595	P3H2
ENSG00000133246	0.808880251	0.00799595	PRAM1
ENSG00000173762	1.542304179	0.00810547	CD7
ENSG00000276966	0.845996018	0.00814811	HIST1H4E
ENSG00000168067	0.739483259	0.00830828	MAP4K2
ENSG00000153246	1.870811827	0.00845422	PLA2R1
ENSG00000198722	1.073831039	0.0085074	UNC13B
ENSG00000135655	0.682280556	0.00855699	USP15
ENSG00000082458	1.405741	0.00860811	DLG3
ENSG00000182247	0.877822424	0.00861175	UBE2E2
ENSG00000155629	0.95600993	0.00863687	PIK3AP1
ENSG00000167460	0.808028383	0.00869448	TPM4
ENSG00000157978	1.033390748	0.00871964	LDLRAP1
ENSG00000111077	2.006194362	0.00888739	TNS2
ENSG00000166165	1.603132511	0.00918807	CKB
ENSG00000277075	0.758540472	0.00918807	HIST1H2AE
ENSG00000124575	0.788431954	0.00919852	HIST1H1D
ENSG00000149212	0.923203725	0.00919852	SESN3
ENSG00000126787	0.806655368	0.00923119	DLGAP5
ENSG00000142748	4.008318466	0.00925999	FCN3
ENSG00000163492	1.394539124	0.00931436	CCDC141
ENSG00000139289	3.177309845	0.0095025	PHLDA1
ENSG00000111879	1.179529604	0.0095089	FAM184A
ENSG00000181218	1.375623197	0.0095089	HIST3H2A
ENSG00000127124	0.945300029	0.0095089	HIVEP3
ENSG00000056998	1.46439594	0.00960115	GYG2
ENSG00000076555	0.93076214	0.00962699	ACACB
ENSG00000277564	1.60140258	0.00965853	RBFOX2
ENSG00000168758	1.174765552	0.00965853	SEMA4C
ENSG00000115252	1.211225507	0.00975376	PDE1A
ENSG00000107742	0.974399289	0.00975376	SPOCK2
ENSG00000278550	3.976103006	0.00977482	SLC43A2
ENSG00000101255	1.686735999	0.00977482	TRIB3
ENSG00000273703	0.935084003	0.00977964	HIST1H2BM
ENSG00000151917	1.217860041	0.00980151	BEND6
ENSG00000182255	2.744114597	0.00997658	KCNA4
ENSG00000125347	0.737308876	0.010056	IRF1
ENSG00000234876	2.170588739	0.010056	NOTCH4
ENSG00000124788	0.96795496	0.01016429	ATXN1
ENSG00000107518	2.296610749	0.01034405	ATRNL1
ENSG00000117724	0.684383506	0.01046694	CENPF
ENSG00000100503	0.598684147	0.0105954	NIN
ENSG00000185737	2.439374011	0.01061855	NRG3
ENSG00000242732	1.136803489	0.01072517	RTL5
ENSG00000002586	1.012496936	0.01080788	CD99
ENSG00000104870	0.929643106	0.01080788	FCGRT
ENSG00000172340	1.564131305	0.01080788	SUCLG2
ENSG00000187498	3.255851954	0.01132641	COL4A1
ENSG00000167286	2.171307525	0.0114575	CD3D
ENSG00000122122	1.038065713	0.01155414	SASH3
ENSG00000118200	1.529351172	0.01158139	CAMSAP2
ENSG00000196422	0.82845191	0.01178152	PPP1R26
ENSG00000174233	0.89969839	0.01204009	ADCY6

ENSG00000182742	0.988398487	0.01235191	HOXB4
ENSG00000163462	1.028135005	0.01235997	TRIM46
ENSG00000141542	1.234048515	0.0125977	RAB40B
ENSG00000078596	0.978243676	0.01264111	ITM2A
ENSG00000127329	2.521092969	0.01273162	PTPRB
ENSG00000137801	2.77530638	0.01273162	THBS1
ENSG00000123094	1.119277467	0.0128626	RASSF8
ENSG00000099864	1.331647036	0.01287122	PALM
ENSG00000142583	0.837567825	0.01289638	SLC2A5
ENSG00000146021	0.837076604	0.01300542	KLHL3
ENSG00000026652	0.945737188	0.01306965	AGPAT4
ENSG00000164035	1.470558422	0.01306965	EMCN
ENSG00000179862	3.466424818	0.01368675	CITED4
ENSG00000184270	0.789114047	0.01374522	HIST2H2AB
ENSG00000141622	1.452821994	0.01374522	RNF165
ENSG00000177663	1.104996807	0.01387989	IL17RA
ENSG00000149948	0.631257261	0.01394561	HMGA2
ENSG00000092421	1.148202829	0.01412102	SEMA6A
ENSG00000143344	1.857549119	0.01474199	RGL1
ENSG00000278677	0.803993535	0.01485477	HIST1H2AM
ENSG00000198155	1.137051225	0.01489893	ZNF876P
ENSG00000157456	0.764398168	0.01510585	CCNB2
ENSG00000230143	1.228900068	0.01510585	FLOT1
ENSG00000119411	1.121762129	0.01510744	BSPRY
ENSG00000112419	0.761238566	0.01518796	PHACTR2
ENSG00000198796	1.820970805	0.01537228	ALPK2
ENSG00000173917	1.1126937	0.01537228	HOXB2
ENSG00000156049	2.984184052	0.01575409	GNA14
ENSG00000162415	1.359639267	0.01593229	ZSWIM5
ENSG00000198908	1.094992266	0.01593891	BHLHB9
ENSG00000142733	1.37138841	0.01593891	MAP3K6
ENSG00000101017	1.574708965	0.01604283	CD40
ENSG00000134352	1.114380306	0.01604283	IL6ST
ENSG00000137509	0.829621545	0.01631121	PRCP
ENSG00000183963	1.271691998	0.0163198	SMTN
ENSG00000137507	2.296987854	0.01635228	LRRC32
ENSG00000156738	2.80239281	0.01675353	MS4A1
ENSG00000139679	1.134627118	0.01687196	LPAR6
ENSG00000214140	2.200621325	0.01687196	PRCD
ENSG00000174032	0.838175116	0.01687196	SLC25A30
ENSG00000211584	0.80658172	0.01687196	SLC48A1
ENSG00000232632	2.935651406	0.01697946	GABBR1
ENSG00000172824	1.121865283	0.01698962	CES4A
ENSG00000165475	1.058032782	0.01730444	CRYL1
ENSG00000182195	1.283741139	0.01730444	LDOC1
ENSG00000153933	0.926425361	0.01740892	DGKE
ENSG00000104833	1.364361508	0.01745286	TUBB4A
ENSG00000179588	1.209209951	0.01745286	ZFPM1
ENSG00000184992	0.683911301	0.01749903	BRI3BP
ENSG00000172568	1.826472292	0.01754062	FNDC9
ENSG00000237112	2.854928397	0.017625	GABBR1
ENSG00000198865	0.812354995	0.01776273	CCDC152
ENSG00000206466	2.85260006	0.01776273	GABBR1
ENSG00000174099	0.97052275	0.01795164	MSRB3
ENSG00000131069	0.945877889	0.01813248	ACSS2
ENSG00000145555	1.620672839	0.0183811	MYO10
ENSG00000143382	1.073441852	0.01845393	ADAMTSL4
ENSG00000133106	1.083920204	0.01868143	EPSTI1
ENSG00000166147	0.989152905	0.01882868	FBN1
ENSG00000196935	1.459434972	0.01912895	SRGAP1
ENSG00000158406	0.98794617	0.01964309	HIST1H4H
ENSG00000151651	0.922346937	0.0199834	ADAM8
ENSG00000163751	1.789664594	0.0199834	CPA3
ENSG00000106123	0.970725312	0.0199834	EPHB6
ENSG00000130508	0.731653239	0.02001998	PXDN
ENSG00000259207	2.451484301	0.02004146	ITGB3
ENSG00000110092	1.441920381	0.02041688	CCND1

ENSG00000185551	3.383726191	0.02041688	NR2F2
ENSG00000067606	1.261573212	0.02051084	PRKCZ
ENSG00000178573	1.752526701	0.02052871	MAF
ENSG00000183918	3.319336552	0.02055578	SH2D1A
ENSG00000107331	0.84403877	0.02065111	ABCA2
ENSG00000080503	0.701211142	0.0209492	SMARCA2
ENSG00000148841	1.362162987	0.02126323	ITPRIP
ENSG00000167487	0.976074641	0.02126323	KLHL26
ENSG00000129007	0.799603672	0.02131388	CALML4
ENSG00000160883	3.670263793	0.02131388	HK3
ENSG00000144824	1.028915808	0.02131388	PHLDB2
ENSG00000132819	0.966969965	0.02131388	RBM38
ENSG00000174130	1.200368186	0.02131388	TLR6
ENSG00000146856	1.33197498	0.02147248	AGBL3
ENSG00000181104	0.858124247	0.02147248	F2R
ENSG00000151240	2.341962219	0.02156264	DIP2C
ENSG00000166396	3.745033991	0.02188618	SERPINB7
ENSG00000126353	2.796281752	0.02197274	CCR7
ENSG00000115271	0.820955968	0.02241177	GCA
ENSG00000131378	0.633102399	0.02242289	RFTN1
ENSG00000183579	1.273929105	0.02242289	ZNRF3
ENSG00000040608	1.278612743	0.02245122	RTN4R
ENSG00000198517	0.668729027	0.02251869	MAFK
ENSG00000136630	1.650197239	0.02261039	HLX
ENSG00000090776	1.245723444	0.02290445	EFNB1
ENSG00000154380	1.278983737	0.02290445	ENAH
ENSG00000153071	1.460315712	0.02302634	DAB2
ENSG00000162407	2.670792367	0.02302634	PLPP3
ENSG00000168994	1.524469471	0.02303755	PXDC1
ENSG00000071246	1.011032282	0.0232328	VASH1
ENSG00000120549	2.868654568	0.02329218	KIAA1217
ENSG00000169908	2.485377412	0.02329218	TM4SF1
ENSG00000168615	0.884469442	0.02332229	ADAM9
ENSG00000118276	0.689470482	0.02332229	B4GALT6
ENSG00000121068	2.398186833	0.02362811	TBX2
ENSG00000275379	0.752600312	0.02387794	HIST1H3I
ENSG00000154277	1.361453927	0.024231	UCHL1
ENSG00000106327	1.187024982	0.0242371	TFR2
ENSG00000277632	2.885687933	0.02435385	CCL3
ENSG00000113971	0.800731319	0.02435385	NPHP3
ENSG00000148154	2.227104131	0.02437889	UGCG
ENSG00000101405	2.051141871	0.02439048	OXT
ENSG00000143776	0.797207661	0.02484114	CDC42BPA
ENSG00000204136	1.608280626	0.02484114	GGTA1P
ENSG00000123066	0.72348715	0.02494541	MED13L
ENSG00000175063	0.764708509	0.02494822	UBE2C
ENSG00000197496	1.269737243	0.02515348	SLC2A10
ENSG00000116128	1.489534932	0.02528229	BCL9
ENSG00000206511	2.792328807	0.02555351	GABBR1
ENSG00000072694	1.947524446	0.02575314	FCGR2B
ENSG00000091262	1.033050337	0.02622041	ABCC6
ENSG00000151687	0.931861476	0.02622041	ANKAR
ENSG00000234289	0.747390185	0.02622041	LOC102724334
ENSG00000181192	0.617909349	0.02663675	DHTKD1
ENSG00000198010	2.430231966	0.02682173	DLGAP2
ENSG00000184515	3.463692789	0.02692445	BEX5
ENSG00000197629	1.475787087	0.02723554	MPEG1
ENSG00000160712	0.918420786	0.02735361	IL6R
ENSG00000123146	0.992402326	0.02749539	ADGRE5
ENSG00000105552	0.807888218	0.02749539	BCAT2
ENSG00000278705	0.837140175	0.02771098	HIST1H4B
ENSG00000007237	0.809180094	0.02779634	GAS7
ENSG00000148908	1.054420946	0.02788656	RGS10
ENSG00000131747	0.695627254	0.02788656	TOP2A
ENSG00000129467	1.521393007	0.02788712	ADCY4
ENSG00000145349	1.184129465	0.02822727	CAMK2D
ENSG00000126759	1.007773149	0.02875508	CFP

ENSG00000183049	0.665514536	0.02893247	CAMK1D
ENSG00000128596	0.680803047	0.02893247	CCDC136
ENSG00000106080	0.79734989	0.02905318	FKBP14
ENSG00000212747	2.315203252	0.02919076	RTL8B
ENSG00000256069	1.823018861	0.02996615	A2MP1
ENSG00000140450	0.966447933	0.0299811	ARRDC4
ENSG00000064989	0.661340455	0.0299811	CALCRL
ENSG00000101665	1.940663267	0.0299811	SMAD7
ENSG00000103056	0.852032189	0.0299811	SMPD3
ENSG00000188486	0.75441724	0.03012787	H2AFX
ENSG00000129993	0.662802804	0.03013946	CBFA2T3
ENSG00000100077	0.862046345	0.03033122	GRK3
ENSG00000053918	1.581420048	0.03129698	KCNQ1
ENSG00000010671	0.719624917	0.03159227	BTK
ENSG00000170485	1.80855278	0.03234712	NPAS2
ENSG00000167100	0.917175939	0.03240218	SAMD14
ENSG00000276644	0.714381039	0.03245803	DACH1
ENSG00000108773	0.516475308	0.03245803	KAT2A
ENSG00000149573	1.055697666	0.03288176	MPZL2
ENSG00000120832	1.099406269	0.03303032	MTERF2
ENSG00000206282	1.081265167	0.033132	RGL2
ENSG00000134061	1.269331477	0.03337543	CD180
ENSG00000266338	0.772594303	0.03360352	NBPF15
ENSG00000169413	1.933867446	0.03375688	RNASE6
ENSG00000136982	0.667189243	0.03443169	DSCC1
ENSG00000198435	1.023074764	0.03443169	NRARP
ENSG00000153404	1.1574279	0.0344874	PLEKHG4B
ENSG00000188643	2.370659958	0.03465398	S100A16
ENSG00000077782	1.126619519	0.03469929	FGFR1
ENSG00000224103	1.749963862	0.03476704	HLA DPA1
ENSG00000130958	1.247022263	0.03476704	SLC35D2
ENSG00000178999	0.654592702	0.03512909	AURKB
ENSG00000167371	2.035337192	0.03513883	PRRT2
ENSG00000180596	0.717258638	0.03532078	HIST1H2BC
ENSG00000273983	0.730025002	0.03532078	HIST1H3G
ENSG00000148655	0.822850728	0.03532078	LRMDA
ENSG00000151503	0.581779792	0.03532078	NCAPD3
ENSG00000204301	3.366577621	0.03532078	NOTCH4
ENSG00000182957	0.903305698	0.03532078	SPATA13
ENSG00000188906	2.491583844	0.03540966	LRRK2
ENSG00000161013	0.799799978	0.03550967	MGAT4B
ENSG00000089159	0.715236345	0.03550967	PXN
ENSG00000139687	0.532202444	0.03646247	RB1
ENSG00000100979	0.905289811	0.03647612	PLTP
ENSG00000205309	0.84484608	0.03650395	NT5M
ENSG00000070190	0.759905482	0.03665458	DAPP1
ENSG00000167419	1.393309378	0.03665458	LPO
ENSG00000161981	0.85139453	0.03716069	SNRNP25
ENSG00000033627	0.752451191	0.03718008	ATP6V0A1
ENSG00000138346	0.709811694	0.03718008	DNA2
ENSG00000137414	0.901934255	0.03718008	FAM8A1
ENSG00000258405	1.286366623	0.03746862	ZNF578
ENSG00000042980	0.844754131	0.03795474	ADAM28
ENSG00000164181	1.309768972	0.03850767	ELOVL7
ENSG00000105997	0.73893985	0.03850767	HOXA3
ENSG00000166927	1.417303793	0.03850767	MS4A7
ENSG00000105426	0.976543129	0.03853874	PTPRS
ENSG00000133169	1.876715851	0.03903923	BEX1
ENSG00000166341	0.82349782	0.0392117	DCHS1
ENSG00000004866	1.171546226	0.039393	ST7
ENSG00000278634	1.483853168	0.03942255	LILRA2
ENSG00000197956	1.160697699	0.03950682	S100A6
ENSG00000053747	1.536754502	0.03961134	LAMA3
ENSG00000135919	1.212977919	0.04021224	SERPINE2
ENSG00000242361	1.301942756	0.04030331	HLA DMA
ENSG00000137501	1.033422313	0.04030331	SYTL2
ENSG00000187815	1.161089279	0.04034202	ZFP69

ENSG00000176624	0.737142777	0.04046278	MEX3C
ENSG00000165795	0.990519762	0.04075135	NDRG2
ENSG00000136160	2.155891009	0.04086214	EDNRB
ENSG00000198959	1.633704447	0.04086214	TGM2
ENSG00000117877	1.063823921	0.04119215	CD3EAP
ENSG00000263961	1.125365709	0.04119215	RHEX
ENSG00000166510	2.163392184	0.04131026	CCDC68
ENSG00000110077	3.134639694	0.0415144	MS4A6A
ENSG00000183580	2.530841048	0.0421005	FBXL7
ENSG00000187513	3.007582275	0.0423309	GJA4
ENSG00000141698	0.755157635	0.0423309	NT5C3B
ENSG00000274429	1.141317478	0.0427901	DLG5
ENSG00000189057	0.806322001	0.04297813	FAM111B
ENSG00000162711	0.730099958	0.04302265	NLRP3
ENSG00000116604	0.703665484	0.04317401	MEF2D
ENSG00000172380	2.322482308	0.0435403	GNG12
ENSG00000069020	0.814557868	0.04358929	MAST4
ENSG00000274891	0.82946935	0.04358929	TRAPPC12
ENSG00000120217	2.108709341	0.04410523	CD274
ENSG00000184113	1.505584845	0.04441531	CLDN5
ENSG00000157927	1.007265073	0.04451401	RADIL
ENSG00000082269	0.668880496	0.04460489	FAM135A
ENSG00000128567	1.329657839	0.04476735	PODXL
ENSG00000189337	0.939513436	0.04529112	KAZN
ENSG00000177511	2.466032159	0.04529112	ST8SIA3
ENSG00000198948	1.554200216	0.04600396	MFAP3L
ENSG00000100320	0.789992909	0.04610085	RBFOX2
ENSG00000020181	0.64149706	0.04677559	ADGRA2
ENSG00000118971	0.600808316	0.0467928	CCND2
ENSG00000090006	0.620077237	0.04679458	LTBP4
ENSG00000162825	0.885126071	0.04679458	NBPF20
ENSG00000168016	0.755141741	0.04679458	TRANK1
ENSG00000277059	1.315204439	0.04683475	FAM30A
ENSG00000151062	0.916395914	0.04790017	CACNA2D4
ENSG00000130037	3.199893797	0.04815773	KCNA5
ENSG00000140400	0.624369493	0.0484206	MAN2C1
ENSG00000117400	0.918704441	0.04866367	MPL
ENSG00000159335	1.178887773	0.04866367	PTMS
ENSG00000175189	3.243698341	0.04908682	INHBC
ENSG00000137727	1.432397173	0.04910205	ARHGAP20
ENSG00000149782	0.633298868	0.04910205	PLCB3
ENSG00000198734	2.065996588	0.04914069	F5
ENSG00000157445	2.46603193	0.04920567	CACNA2D3
ENSG00000198286	0.841900712	0.04928243	CARD11
ENSG00000136574	2.42088932	0.04997034	GATA4

10.5 Appendix 5

List of genes commonly upregulated in foetal liver and neonatal/adult derived populations in humans and mice, described in chapter 5.

FL human FL Mouse	CB human BM mouse
DDX3Y	NLRC5
AKAP12	ITPR2
LIN28B	SLC44A2
CCNB1	SLC4A8
ASPM	DACH1
KIF20A	ARMCX3
KIF15	IRF7
BUB1B	CSGALNACT2
DLK1	CSGALNACT1
LMNB1	CYTIP
AURKA	RNF125
CENPE	SUN2
PLK1	GATA2
RBP1	SETD7
ENC1	TNFAIP3
CD33	CHST11
UBE2C	NRXN1
CENPF	PNRC1
TPX2	SIAH2
RGL1	IRS2
HMMR	RASA4
KIF2C	SMIM3
IGF2BP1	PDE4B
SKA2	ABHD4
SUV39H2	IRAK2
TNNI2	SLC28A2
CHCHD1	CDKN1B
DYNLL1	IQSEC2
CACYBP	CYTH1
COTL1	OPTN
DLAT	LGALS3BP
GINS2	SRGN
HSPD1	NR4A2
SLC9A9	VLDLR
DHCR24	FBXO33
NASP	KLF13
DNMT3B	SLC16A11
KIF23	ANXA1
GIMAP8	MAP3K8
MYCN	FAAH
CCNF	GADD45B
HMGA1	HIP1R
NUTF2	OSM
EGFL7	COL23A1
TTLL12	PIK3IP1
TOMM40	SELE
PHGDH	PER1
GTF2H3	NR4A3
MRPL19	GBP2
ELOVL1	SCN1B
PLD4	ZC3H12A
STOML2	KCNA3
KIF22	HK3
IGSF10	BCL6
UQCC2	IER3
SNRPC	
SELENOH	
FASTKD2	

CBX5	
CEP41	
ACAT2	
TTLL4	
APEX1	
CKAP5	
DNMT3A	
MARCKS	
ITGA4	
IFT57	
SIRPA	
PTCD3	